

**GEOLOGY OF THE EASTERN TEHACHAPI MOUNTAINS AND LATE
CRETACEOUS - EARLY CENOZOIC TECTONICS OF THE SOUTHERN
SIERRA NEVADA REGION, KERN COUNTY, CALIFORNIA**

Thesis by
David Judson Wood

In Partial Fulfillment of the Requirements
for the Degree of
Doctor of Philosophy

California Institute of Technology
Pasadena, California

1997

(Submitted December 12, 1996)

© 1997

David J. Wood

All rights reserved

ACKNOWLEDGMENTS

I would like to thank my thesis advisor Dr. Jason B. Saleeby for his support, encouragement, and guidance of my work. He taught me to expand my mind to see the big picture of things, and he also taught me what a peperite is. I want to thank Dr. Leon T. Silver for his support and interest in my work, for his generosity with his time, for teaching me to see what the rocks have to say, and for sharing his excitement about the complexities of California geology. I would also like to thank the members of my thesis committee, Dr. Hugh Taylor, Dr. Jason Saleeby, Dr. Lee Silver, Dr. Brian Wernicke, and Dr. Robert Clayton for reading my thesis and participating in my thesis defense.

I would like to acknowledge the financial support for this study which has come from a National Science Foundation grant awarded to J. B. Saleeby, an NSF Graduate Student Fellowship, a Geological Society of America Penrose grant, and a Koons Field Fellowship at Caltech. This study would not have been possible without the permission and interest of the many private landowners in the Tehachapi area including Ted Wyman, Dave Eckert, John Broome, Bob Scott, Bill Schulgen, Frank Williams, Steve and Mahonna Arnds, Doug Kurfess, the members of the Old West Ranch Property Owners Association, and many others. I would like to thank the Kern County Department of Parks for reduced rates on camping at Tehachapi Mountain Park and I would also like to thank Stuart Etherton at Tehachapi Mountain Park for his help and for providing me with useful information about the area. Other people in the study area who have been helpful and hospitable are Jack Ford, Dick Mays, Stan Cramer, Dale Hendrickson, Steve Palmer, Diana Belles, and Glen Mueller.

I would like to give special acknowledgment to the work of T. W. Dibblee Jr. and D. C. Ross in the southern Sierra Nevada. The results of their extensive regional studies provided the inspiration for many of the ideas in this study. I would like to thank John Crowell and Tom Anderson for their interest in and encouragement of my work in the

Tehachapi Mountains. In the course of my work I have enjoyed and benefited from discussions with many graduate students at Caltech including John Nourse, Greg Holk, Doug Yule, and Carey Gazis. I would like to thank Eleanor Dixon for providing unpublished thermobarometric and geochronologic data from the southern Sierra Nevada area and for discussions about the thermobarometric and cooling history of the southern Sierra Nevada. I also wish to thank Charlie Lough for providing me with his unpublished mapping of the Tehachapi and San Emigdio Mountains and also for his interest in my work. Thanks are due to John Sharry for sharing his perspective on the complex geology of the Tehachapi Mountains and for giving me copies of his maps. I would also like to thank the participants of the October 1995 Penrose Conference held in Tehachapi for their insightful questions and helpful comments during the field trip to the eastern Tehachapi Mountains. The stereonet plots in this study were prepared with the aid of the Stereonet computer program, version 4.9.5., from R. W. Allmendinger.

I owe special thanks to Donna Sackett, Jan Haskell, and Kathy Lima for going beyond the call of duty in helping me to make all of the necessary arrangements for the submission and defense of my thesis from long-distance. I would like to thank Jan Mayne for her help and advice on drafting the maps and figures in my thesis. I appreciate the assistance of Mahmood Chaudhry in preparing mineral separates for many of the samples collected in this study. I would like to thank Brian and Karen at Burnham Petrographics for the high quality of the thin sections they made of the samples that were examined in this study. I would like to thank Gregory Dubois-Felsmann and Aaron "Luc" Melman for accompanying me in the field, and more importantly for their friendship and support while I was at Caltech. And last but not least, I owe a great debt of thanks to my wife Cathy for her encouragement, support, and patience during the writing of this thesis, and also for her help on numerous trips with me in the field.

ABSTRACT

Many geologic studies have inferred that the California continental margin in the vicinity of the western Mojave Desert was tectonically disrupted after emplacement of the Cretaceous Cordilleran batholith and prior to Neogene displacements on the San Andreas fault system. The causes of this regional deformation, however, are poorly understood. Located along the northern margin of this disrupted region at the southern end of the comparatively little deformed Sierra Nevada batholith, the eastern Tehachapi Mountains are ideally situated to study the possible mechanisms of this disruption. In view of this, the geology and structure of the eastern Tehachapi Mountains were investigated using geologic field mapping at scales of 1:6,000 through 1:24,000, detailed petrographic studies, and structural and kinematic analysis of deformation fabrics and structures in the field and in the lab. The study area is divided by a generally N trending shallowly SE dipping ductile-cataclastic fault zone called the Blackburn Canyon fault into the eastern Tehachapi gneiss complex in the footwall and the Oak Creek Pass complex in the hangingwall.

The eastern Tehachapi gneiss complex is composed of two different sequences of metasedimentary rocks that have been intruded by three generations of plutonic rocks. The Brite Valley group metasedimentary rocks consist largely of pelites and graphitic quartzite with subordinate marble. The Antelope Canyon group metasedimentary rocks consist of a lower section composed mostly of thinly laminated dirty quartzite overlain by an upper section of marble. The earliest intrusive rocks in the area (group I orthogneisses) are lithologically diverse and include granite augen gneiss, garnetiferous hornblende diorite gneiss, and hornblende biotite quartz diorite gneiss. Both groups of paragneiss and the group I orthogneisses are intruded by group II plutons of the Tehachapi Intrusive Complex. The Tehachapi Intrusive Complex is composed of comagmatic gabbro, quartz diorite, and tonalite and it is inferred to be continuous with the large ~100 Ma Bear Valley

Springs tonalite pluton exposed to the west. The group III intrusives are small bodies and thin sheets of leucocratic biotite granite which intrude all of the other lithologies.

The rocks in the gneiss complex have had a complex deformational history. The metasedimentary rocks are folded into map-scale N to NW trending SW vergent isoclinal F1 folds. Later (?) intrusion of the group I orthogneisses was accompanied (?) and followed by amphibolite facies metamorphism and the localized formation of NE trending shallow plunging open to tight F2 folds. During (?) and after intrusion of the ~100 (?) Ma Tehachapi Intrusive Complex the gneiss complex was metamorphosed at amphibolite facies and deformed by map-scale open to tight NW trending SW vergent F3 folds. After much of the F3 folding the basement rocks in the Tehachapi Valley area appear to have been folded into a regional dextral-sense convex-west F4 oroclinal fold. In the later stages of F4 folding part of the southwest limb of the Tehachapi Valley orocline is inferred to have been transposed into a NW trending shallow NE dipping noncoaxial ductile shear zone called the eastern Tehachapi shear zone. The shear zone has a structural thickness of ~1 km, top to the S-SW shear sense, and most shearing appears to have occurred during greenschist facies retrograde metamorphism. The shear zone appears to continue to the north across Tehachapi Valley where it is inferred to merge with the steeply E dipping dextral-slip proto-Kern Canyon fault. Motion on the shear zone is inferred to have ended at about the time when the Late Cretaceous (?) group III leucogranites intruded. Following shear zone activity rocks in the gneiss complex locally were folded in gentle NE trending subhorizontal F5 folds. Late top to the NE shearing in the upper structural levels of the gneiss complex suggests that a normal fault may be concealed beneath the alluvium of Tehachapi Valley.

The lithologies and deformation history of the Oak Creek Pass complex are very different from the eastern Tehachapi gneiss complex. The Oak Creek Pass complex is composed mostly of granodioritic plutonic rocks (group IV intrusives) which commonly are cataclastically deformed and metamorphosed at greenschist and lower grade. Arkosic

sandstones and conglomerates of the Late Cretaceous (?)–Eocene (?) Witnet Formation locally are unconformable above the granodiorite. Emplacement of the Oak Creek Pass complex above the eastern Tehachapi gneiss complex along the Blackburn Canyon fault took place after most of the activity along the eastern Tehachapi shear zone. Shear sense along the Blackburn Canyon fault is top to the S or SE. The Oak Creek Pass complex is divided into a number of structural plates by low-angle (?) ductile-cataclastic fault zones one of which is the NE trending Mendiburu Canyon fault. Synclinal F6 folding of the Witnet Formation and NW vergent overthrusting of the Witnet Formation by granitic rocks along the Mendiburu Canyon fault are interpreted to postdate motion along the Blackburn Canyon fault. Deformation of the Witnet Formation is inferred to be pre-Miocene in age based on correlation with a similar deformation event across Tehachapi Valley.

The Brite Valley group metasedimentary rocks are suggested to correlate with the western facies of the Triassic–Jurassic age Kings sequence and the Antelope Canyon group rocks may correlate with the eastern facies of the Kings sequence or possibly with Late Proterozoic–Cambrian age rocks of the miogeocline. Juxtaposition of the two groups of metasedimentary rocks may have been along a cryptic structure that was active prior to intrusion of some of the group I plutons which are inferred to be mid-Cretaceous in age. Formation of the NE trending F2 folds between ~117 Ma and ~100 Ma is suggested to have resulted from the local reorientation of the regional stress field in the vicinity of a weak strike-slip (?) fault such that the direction of maximum compressive stress during the deformation was oriented subparallel to the trend of the Sierra Nevada batholith. The F3 folds, F4 folds, and the eastern Tehachapi shear zone are interpreted to have formed more or less sequentially during a protracted period of contractional deformation in the middle to lower crust of the southern Sierra Nevada batholith from ~100 Ma to ~80 Ma. Top to the S–SW motion along the shear zone may reflect the underthrusting of Rand schist beneath the batholith at lower structural levels during low-angle Laramide subduction.

The Blackburn Canyon fault and a number of other previously identified low-angle faults in the southern Sierra Nevada region are suggested to be extensional faults along which part of the southern Sierra Nevada batholith was unroofed. The source region for the out of place Oak Creek Pass complex and other inferred allochthonous rocks is suggested to be the area in the Sierra Nevada east of the proto-Kern Canyon fault and south of South Fork Valley. Exposures of Witnet Formation may be the remnants of a syn-extensional sedimentary deposit that accumulated in a supradetachment basin. This inferred extensional exhumation of the southeastern Sierra Nevada may have begun as early as ~85-90 Ma and ended at ~80 Ma or later based on data from previous studies in the region. Thus, contractional deformation in the middle crust of the southern Sierra Nevada region may have been coeval with upper crustal extensional deformation in Late Cretaceous time.

Correlation of the Cretaceous structural histories of the eastern Tehachapi gneiss complex and the northern Salinian block in the Coast Ranges of central California supports previous suggestions that the two areas may have evolved in close proximity to one another. The relative westward offset of the Salinian block from the Sierra Nevada prior to the Neogene may in part be the result of Late Cretaceous-early Cenozoic (?) westward extrusion of wedges of middle to lower crust bounded by thrust faults below and E dipping extensional faults above in a manner analogous to recent models for deformation in the Himalayas. The upper plate rocks of the Blackburn Canyon fault appear to be rotated about 90° clockwise relative to their inferred source region and the F4 folds in the Tehachapi area appear to have dextral vergence. The vergence of the folding and the sense of rotation both are consistent with Late Cretaceous dextral-oblique convergence indicated by plate motion models and with the presence of Late Cretaceous synbatholithic dextral transpressional and strike-slip shear zones in the Sierra Nevada to the north.

TABLE OF CONTENTS

ACKNOWLEDGMENTS.....	iii
ABSTRACT	v
TABLE OF CONTENTS.....	ix
LIST OF FIGURES	xiv
LIST OF TABLES	xiv
LIST OF PLATES	xiv
CHAPTER I: INTRODUCTION.....	1
REGIONAL GEOLOGIC SETTING	1
OBJECTIVES OF THIS STUDY	7
LOCATION AND DESCRIPTION OF THE STUDY AREA	9
PREVIOUS WORK IN THE STUDY AREA	12
METHODS OF INVESTIGATION	14
CHAPTER II: TECTONOSTRATIGRAPHY AND LITHOLOGIC DESCRIPTIONS.....	16
OVERVIEW.....	16
EASTERN TEHACHAPI GNEISS COMPLEX.....	21
METASEDIMENTARY ROCKS	21
Antelope Canyon Group Metasedimentary Rocks	25
Unit WW	33
Unit XX.....	34
Unit YY.....	34
Unit ZZ.....	35
Unit A.....	35
Unit B.....	36
Unit C.....	36
Brite Valley Group Metasedimentary Rocks.....	37
Unit 1	37
Unit 2	40
Unit 3	40
Unit 4	40
Rand Schist.....	41
INTRUSIVE ROCKS AND ORTHOGNEISS.....	42
Group I Orthogneisses	42
Mixed tonalite gneiss.....	43
Antelope Canyon biotite garnet hornblende diorite gneiss.....	47

No Name Canyon augen gneiss	48
Paradise Valley granite gneiss	49
Biotite hornblende quartz diorite gneiss	50
Group II Intrusives	51
Tehachapi Intrusive Complex.....	51
Gabbro of the Tehachapi Intrusive Complex	52
Tonalite of the Tehachapi Intrusive Complex.....	55
Pine Tree tonalite.....	58
Highline olivine gabbro.....	62
Group III Intrusives	64
Brushy Ridge granite and other leucocratic granites	64
OAK CREEK PASS COMPLEX.....	65
METAVOLCANIC ROCKS.....	67
Oaks Metavolcanic Rocks.....	67
INTRUSIVE ROCKS	68
Group IV Granitic Rocks	68
Bootleg Canyon granodiorite	68
Mendiburu Canyon granodiorite.....	71
Old West Ranch monzogranite.....	73
WITNET FORMATION	74
TERTIARY VOLCANIC ROCKS	75
CHAPTER III: DEFORMATION AND METAMORPHISM	78
STRUCTURAL ELEMENTS.....	78
FOLIATIONS	78
LINEATIONS.....	80
KINEMATIC INDICATORS.....	82
FOLDS	83
DEFORMATION PRIOR TO THE EASTERN TEHACHAPI SHEAR ZONE	83
EARLY FOLDING (F1) AND FAULTING.....	83
DEFORMATION AND METAMORPHISM OF THE GROUP I	
ORTHOGNEISS AND F2 AND F3 FOLDING	87
DEFORMATION AND F3 FOLDING OF THE GROUP II INTRUSIVE	
ROCKS.....	93
REGIONAL-SCALE F4 FOLDING - THE TEHACHAPI VALLEY AND	
WALKER BASIN OROCLINES	102
THE EASTERN TEHACHAPI SHEAR ZONE.....	103
SHEAR ZONE FABRICS AND METAMORPHISM.....	104
MOUNTAIN PARK FAULT.....	111
TACO SADDLE FAULT.....	111
POSSIBLE LARGE SCALE SHEATH FOLD AT ASTRONOMY RIDGE	112
SHEAR ZONE NORTH OF TEHACHAPI VALLEY	113
MAGNITUDE OF SHEAR ZONE DISPLACEMENT	123
LATE TO POST-EASTERN TEHACHAPI SHEAR ZONE DEFORMATION.....	126
DEFORMATION OF THE BRUSHY RIDGE GRANITE AND NEARBY	
ROCKS.....	126

NORTHEAST TRENDING CREULATION CLEAVAGE AND F5 FOLDS	131
BLACKBURN CANYON FAULT.....	132
MENDIBURU CANYON FAULT AND F6 FOLDING	140
STRUCTURES OF UNCERTAIN RELATIVE AGE AND SIGNIFICANCE	149
WATER CANYON FAULT	149
OAK CREEK MYLONITE ZONE.....	151
QUAIL CANYON AND SOUTH RIDGE FAULT ZONES	153
SLIVER OF GNEISS COMPLEX ABOVE BLACKBURN CANYON FAULT	155
TEJON CANYON FAULT	159
METAMORPHISM	159
SUMMARY OF METAMORPHIC HISTORY	159
GARNET BEARING VEINS, MIGMATITES, AND OTHER MOBILIZATES	161
THERMOBAROMETRIC STUDIES IN THE TEHACHAPI MOUNTAINS REGION.....	165
STRUCTURAL CROSS SECTIONS	166
CHAPTER IV: DISCUSSION AND INTERPRETATION	172
INFERRED AGE AND SEQUENCE OF TECTONIC EVENTS.....	172
METASEDIMENTARY ROCKS: POSSIBLE CORRELATION, INFERRED AGE, AND PRE-INTRUSIVE DEFORMATION	172
BRITE VALLEY GROUP	175
ANTELOPE CANYON GROUP	177
METASEDIMENTARY ROCKS AT MONOLITH	178
PRE-INTRUSIVE DEFORMATION OF THE METASEDIMENTARY ROCKS.....	179
JUXTAPOSITION OF THE METASEDIMENTARY ROCK GROUPS.....	180
AGE AND NORTHWARD CONTINUATION OF THE WATER CANYON FAULT.....	183
LATE EARLY CRETACEOUS NW-SE DIRECTED INTRA-ARC SHORTENING.....	184
STYLE AND AGE OF NW-SE SHORTENING IN THE STUDY AREA.....	184
POSSIBLE CORRELATIVE DEFORMATIONS IN THE SOUTHWEST CORDILLERA	186
A MODEL FOR ARC-PARALLEL SHORTENING DEFORMATION	190
PROTRACTED MID- TO LATE CRETACEOUS CONTRACTIONAL DEFORMATION IN THE MIDDLE TO LOWER CRUSTAL LEVELS OF THE SOUTHERN SIERRA NEVADA BATHOLITH	195
CONTRACTIONAL DEFORMATION IN THE STUDY AREA.....	195
AGE OF THE CONTRACTIONAL DEFORMATION IN THE EASTERN TEHACHAPI MOUNTAINS	200

POSSIBLE REGIONAL CORRELATION OF DEFORMATIONS IN THE EASTERN TEHACHAPI GNEISS COMPLEX.....	203
Southernmost Sierra Nevada Region.....	203
Central Sierra Nevada and White-Inyo Mountains Region	206
DISCUSSION AND INTERPRETATION OF THE MID- TO LATE CRETACEOUS AGE DEFORMATION.....	207
SIGNIFICANCE OF RETROGRADE METAMORPHISM DURING CONTRACTION.....	210
REGIONAL LOW-ANGLE DUCTILE-CATACLASTIC FAULTS IN THE SOUTHERN SIERRA NEVADA - POSSIBLE LATE CRETACEOUS-PALEOCENE AGE EXTENSIONAL STRUCTURES	211
EXPOSURE DEPTH OF ROCKS IN THE SOUTHERN SIERRA NEVADA.....	212
EXTENSIONAL ORIGIN FOR THE BLACKBURN CANYON FAULT	215
AGE OF THE BLACKBURN CANYON FAULT.....	216
REGIONAL CORRELATION OF THE BLACKBURN CANYON FAULT	218
POSSIBLE SOURCE LOCATION FOR ALLOCHTHONOUS ROCKS IN THE SOUTHERN SIERRA NEVADA REGION	228
REGIONAL SIGNIFICANCE OF THE WITNET FORMATION.....	234
OVERVIEW OF INFERRED REGIONAL EXTENSIONAL FAULTING.....	239
Age of Extensional Faulting	239
Regional Extension Direction.....	241
Apparent Rotation of Hangingwall Rocks.....	242
Rate of Extensional Faulting.....	243
POSSIBLE COEVAL LATE CRETACEOUS AGE EXTENSION AND CONTRACTION.....	244
OTHER POSSIBLE EXTENSIONAL FAULTS IN THE STUDY AREA.....	245
Inferred Tehachapi Valley Fault.....	245
Oak Creek Mylonite Zone.....	248
Possible Late Extension Along the Mountain Park and Taco Saddle Faults.....	249
APPARENT DEXTRAL-SENSE OFFSET AND WESTWARD DISPLACEMENT OF PRE-CENOZOIC GEOLOGIC FEATURES IN THE SOUTHERN SIERRA NEVADA-MOJAVE DESERT REGION.....	249
PREVIOUSLY DOCUMENTED DISPLACEMENTS AND DEXTRAL DEFLECTIONS.....	252
STRUCTURAL CORRELATION OF THE EASTERN TEHACHAPI MOUNTAINS WITH THE NORTHERN SALINIAN BLOCK	254
Northeast Trending Shallow Plunging Folds.....	255
Northwest Trending Shallow Plunging Folds.....	256
Steep-axis Folds	258
Late Recrystallized and Mylonitic Fabrics	259
POSSIBLE MECHANISMS FOR WESTWARD/DEXTRAL OFFSETS.....	260
CENOZOIC DEFORMATION IN THE SOUTHERN SIERRA NEVADA REGION.....	264
MENDIBURU CANYON FAULT AND POSSIBLE RELATED STRUCTURES	264

POSSIBLE MIOCENE EXTENSION AND CRUSTAL ROTATIONS IN THE SOUTHERN SIERRA NEVADA	265
GARLOCK FAULT	267
CHAPTER V: SUMMARY AND CONCLUSIONS	268
REFERENCES	270

LIST OF FIGURES

Figure 1.....	2
Figure 2.....	10
Figure 3.....	17
Figure 4.....	22
Figure 5.....	26
Figure 6.....	28
Figure 7.....	38
Figure 8.....	53
Figure 9.....	84
Figure 10.....	89
Figure 11.....	94
Figure 12.....	97
Figure 13.....	106
Figure 14.....	115
Figure 15.....	118
Figure 16.....	127
Figure 17.....	133
Figure 18.....	137
Figure 19.....	142
Figure 20.....	145
Figure 21.....	157
Figure 22.....	167
Figure 23.....	173
Figure 24.....	198
Figure 25.....	219
Figure 26.....	226

LIST OF TABLES

TABLE 1.....	30
TABLE 2.....	44
TABLE 3.....	56
TABLE 4.....	59
TABLE 5.....	66
TABLE 6.....	70
TABLE 7.....	76

LIST OF PLATES

(Plates are located in the pocket at the back of the thesis)

- Plate 1. Geologic map of the eastern Tehachapi Mountains (1:24,000 scale)
- Plate 2. Explanation for geologic map (Plate 1) and cross sections (Plate 3)
- Plate 3. Geologic cross sections of the eastern Tehachapi Mountains
- Plate 4. Geologic map of the eastern Tehachapi Mountains, patterned (1:48,000 scale)
- Plate 5. Location map for rock samples collected in this study

CHAPTER I: INTRODUCTION

The subject of this study is the geologic and tectonic evolution of the eastern Tehachapi Mountains region which is located in the southern part of the Sierra Nevada in California (Figure 1). Ever since the study of Locke et al. (1940) who pointed out that the southernmost part of the Sierra Nevada, now referred to as the Tehachapi Mountains, has an anomalous east-west trend relative to the contiguous north-northwest trending Sierra Nevada to the north, the Tehachapi Mountains have attracted the attention of geologists in California. While the present-day uplift and exposure of the rocks in the Tehachapi Mountains most likely is partially the result of a component of convergence associated with strike-slip activity along the Neogene age San Andreas and related faults, the igneous and metamorphic rocks exposed in the Tehachapi Mountains preserve evidence of earlier Cretaceous age deformations which are the focus of this study.

In the parts of this chapter which follow the regional geology of southern California and the southern Sierra Nevada area is summarized and the objectives of this study are outlined. The area examined in this study is described, the previous work done in the area is reviewed, and finally the methods used in this investigation are outlined. In Chapter II tectonostratigraphy of the study area is reviewed and lithologic descriptions of all of the rock units are given. In Chapter III the structural data are presented, and in Chapter IV the different phases of the deformation history of the study area are discussed and put into regional tectonic context.

REGIONAL GEOLOGIC SETTING

The Sierra Nevada in central California and the Peninsular Ranges in southern California both are composed of largely continuous exposures of mostly Cretaceous age plutonic rocks and they are part of the exhumed root zone of an Andean-type continental margin magmatic arc of Cretaceous age (Figure 1). With ~300 km of right-lateral

Figure 1.

Index map of southern and central California showing the location of the study area in the southernmost Sierra Nevada, the location of features discussed in the text, the distribution of Cretaceous age plutonic rocks (exclusive of the eastern Mojave Desert region), and areas of syn- to post-emplacement ductile deformation of the Cretaceous plutonic rocks. Outlined but unpatterned areas in the figure are pre-Cretaceous age basement rocks. The figure is modified in part after Plate 1 of Powell (1993) which is a recent comprehensive compilation map of the pre-late Cenozoic geology bordering the San Andreas fault in California. Silver et al. (1979) documented a distinct age boundary within the Peninsular Ranges batholith with plutons having U-Pb zircon ages ~105 Ma and older found to the west of the boundary. For comparison a boundary of the same age is shown for the Sierra Nevada batholith based on U-Pb zircon age data from Saleeby and Sharp (1980), Stern et al. (1981), Chen and Moore (1982), Saleeby et al. (1987), Tobisch et al. (1989), Busby-Spera and Saleeby (1990), and Saleeby et al. (1990). Other sources of geologic and geochronologic data for the figure include (by region): Sierra Nevada (Ross, 1989b; Ross, 1990; Bateman, 1992; Saleeby, 1990b), Salinian block (Ross, 1984; Mattinson, 1990; James, 1992), Mojave Desert (Karish et al., 1987; Silver and Nourse, 1991; Glazner et al., 1994), Transverse Ranges (May and Walker, 1989), Peninsular Ranges (Silver and Hill, 1986; Todd et al., 1988). Sources of data for the shear zones are discussed in the text. Abbreviations are BC, Bench Canyon shear zone; BCP, Birch Creek pluton; BF, Banning fault; BH, Bodega Head; BL, Ben Lomond Mountain; CLMSZ, Cuyamaca-Laguna Mountains shear zone; CM, Chocolate Mountains; CMZ, Cucamonga mylonite zone; CW, Courtright-Wishon shear zone; EP, El Paso Mountains; EPRMZ, eastern Peninsular Ranges mylonite zone; ETSZ, eastern Tehachapi shear zone; FI, Farallon Islands; FM, Funeral Mountains; GL, Gem Lake shear zone; GR, Gabilan Range; KP, Kaiser Peak shear zone; LC, Leidy Creek pluton; LI, Lake Isabella; LP, La

Panza Range; MM, Montara Mountain; MP, Mount Pinos; OM, Orocochia Mountains; PF, Papoose Flat pluton; PKCFZ, proto Kern Canyon fault zone; PM, Panamint Mountains; PR, Point Reyes; PRR, Portal-Ritter Ridge; QM, Quartz Mountain shear zone; RF, Rosy Finch shear zone; RM, Rand Mountains; RRKCF, Rinconada-Reliz-King City fault zone; SAICF, San Antonio-Icehouse Canyon fault zone; SBM, San Bernardino Mountains; SGF, San Gabriel fault; SGHF, San Gregorio-Hosgri fault; SGM, San Gabriel Mountains; SJF, San Jacinto fault; SL, Santa Lucia Mountains; SP, Sierra Pelona; TM, Tehachapi Mountains; VCF, Vasquez Creek fault; WHF, Waterman Hills detachment fault.

displacement removed along the Neogene San Andreas fault in central California (Hill and Dibblee, 1953) and in southern California (Dillon and Ehlig, 1993) it is apparent that the continuity of the Cretaceous batholith in southern California is disrupted in the vicinity of the Mojave Desert and the palinspastically restored Salinian block (Burchfiel and Davis, 1981; Silver, 1982; Silver, 1983; May, 1989; Malin et al., 1995). Coextensive with this disrupted area are scattered exposures of gneissic and mylonitic Cretaceous age plutonic rocks (compiled in Powell (1993)) many of which appear to have been deformed in the Late Cretaceous (summarized in May (1989)). In the same region there are a number of fault bounded exposures of metamorphosed graywacke and basalt, the Rand, Pelona, and related schists, which are thought to have been thrust beneath the continental margin during the Late Cretaceous (Malin et al., 1995; Jacobson et al., 1996). A number of different models have been proposed to account for this apparent regional tectonic disruption of the continental margin including a proto-San Andreas fault (Suppe, 1970; Howell, 1975; Nilsen, 1978), oroclinal folding (Burchfiel and Davis, 1981), west-vergent thrust faulting (Silver, 1982; Silver, 1983; May, 1989; Hall, 1991), and west-directed extension (Malin et al., 1995).

Located to the north of this tectonically disrupted region is the N-NW trending Sierra Nevada batholith. The Sierra Nevada batholith is an excellent exposure of the root zone of a subduction-related magmatic arc, and it offers a continuous exposure from high level calderas in the central Sierra Nevada down to deep levels of the batholith in the Tehachapi Mountains of the southernmost Sierra Nevada (Saleeby, 1990b). The deformed and metamorphosed host rocks of the batholith locally are preserved in discontinuous generally N-NW trending scattered screens and pendants. The Sierra Nevada batholith exhibits a marked transverse (west to east) zonation in its petrology, geochemistry, isotopic properties, and age. From west to east the batholith becomes less mafic and more potassic with dominantly gabbroic to tonalitic plutons in the west side of the batholith and quartz

monzonites and granites localized along the eastern side of the batholith (Lindgren, 1915; Moore, 1959; Bateman and Dodge, 1970; Kistler, 1974; Ross, 1990; Bateman, 1992). The initial $^{87}\text{Sr}/^{86}\text{Sr}$ ratios of plutons along the west side of the batholith are less than 0.706 while plutons in central and eastern parts of the batholith generally have initial Sr ratios greater than 0.706 (Kistler and Peterman, 1973; Kistler and Peterman, 1978; Kistler and Ross, 1990). The Cretaceous age plutons in the Sierra Nevada batholith exhibit a regular trend of decreasing ages from west to east with U-Pb zircon ages of 120 to 130 Ma on the west side of the batholith ranging to ~83 Ma on the east side (Saleeby and Sharp, 1980; Stern et al., 1981; Chen and Moore, 1982; Saleeby et al., 1987).

Most areas of the Sierra Nevada batholith are largely undeformed although there are a number of localized longitudinal strike-slip and reverse ductile shear zones within the batholith (summarized in Tobisch et al. (1995)) and parts of the southernmost end the batholith are extensively ductilely deformed and cut by low-angle faults (Figure 1). A growing body of evidence suggests that the site of the Sierra Nevada batholith has been the locus of repeated sinistral and dextral strike-slip fault dislocations of the continental margin both prior to and during emplacement of the batholith as summarized by Saleeby and Busby-Spera (1992) and Saleeby and Busby (1993). Recognition of the pre-batholithic dislocations is difficult because framework rocks of the batholith that may have hosted these faults or that may have been displaced by these faults are preserved only as discontinuous and scattered screens and pendants. Several Late Cretaceous age N to N-NW trending dextral-sense synbatholithic shear zones have been documented in the Sierra Nevada including the proto-Kern Canyon fault zone (Busby-Spera and Saleeby, 1990), the Rosy Finch shear zone (Tikoff and Teyssier, 1992), and the Gem Lake shear zone (Greene and Schweickert, 1995) (Figure 1).

In the southernmost Sierra Nevada deep-crustal levels of the batholith are exposed and the rocks there are pervasively ductilely deformed and also cut by low-angle ductile and

cataclastic faults. Geobarometric studies in the southern part of the Sierra Nevada and in the Tehachapi Mountains indicate that the rocks were intruded and/or deformed at depths of 20-30 km in Late Cretaceous time (Sharry, 1981; Ague and Brimhall, 1988a; Pickett and Saleeby, 1993; Dixon et al., 1994; Dixon, 1995). Parts of the southernmost Sierra Nevada and Tehachapi Mountains are penetratively deformed and display high temperature gneissic fabrics (Sams and Saleeby, 1988; Ross, 1989b), and the rocks locally are cut by low-angle mylonitic and cataclastic fault zones active in Late Cretaceous and early Cenozoic time (Silver, 1986; Nourse, 1989; Silver and Nourse, 1991; Saleeby et al., 1993; Wood et al., 1993; Malin et al., 1995). Late Cretaceous-early Cenozoic deformation in the southern Sierra Nevada is inferred to have been accompanied by local clockwise-sense vertical-axis rotations of the batholithic crust (Burchfiel and Davis, 1981; Kanter and McWilliams, 1982; McWilliams and Li, 1985). Geologic, isotopic, and geochronologic studies of the southern Sierra Nevada region and the Salinian block of coastal central California reveal that the two areas are similar in many respects and the studies have suggested that the two areas were tectonically displaced from one another (Silver, 1982; Ross, 1984; Silver and Mattinson, 1986; James, 1992).

OBJECTIVES OF THIS STUDY

The study area in the eastern Tehachapi Mountains is located in the southernmost Sierra Nevada between continuous exposures of largely undeformed Cretaceous age plutonic rocks of the Sierra Nevada batholith to the north and scattered exposures of tectonically disrupted Cretaceous age plutonic rocks in the Mojave Desert region to the south. The study area lies in the region where the N trending dextral strike-slip proto-Kern Canyon fault zone (Busby-Spera and Saleeby, 1990) projects to an intersection with NE trending low-angle ductile-cataclastic faults that are exposed immediately to the north of the Garlock fault along the southeastern margin of the southern Sierra Nevada (Silver, 1986). As such the study area is ideally situated to investigate the relationship between dextral-

sense synbatholithic strike-slip faulting in the Sierra Nevada and probable Late Cretaceous age low-angle faulting in the southernmost Sierra Nevada and Mojave Desert areas. Since the study area is located on the north margin of the tectonically disrupted area in southern California as described above a better understanding of the geology of the area is also crucial for regional palinspastic reconstructions for Late Cretaceous time. It is also important to understand the Late Cretaceous-early Cenozoic age deformation in southern California so that inferred pre-Late Cretaceous age strike-slip truncations of the continental margin (e.g. Burchfiel and Davis, 1972; Silver and Anderson, 1974; Walker, 1988; Schweickert and Lahren, 1990; Saleeby and Busby, 1993)) as well as other postulated major regional deformation events of Triassic-Jurassic age (Miller et al., 1995) and Permian age (Snow, 1992) can be better evaluated.

The major objectives of this study are summarized as follows. The first is to determine the structural and temporal relationship between synbatholithic strike-slip faulting in the Sierra Nevada batholith and low-angle faulting in the southernmost Sierra Nevada through detailed geologic mapping and a synthesis of the available regional data. The second is to characterize the stratigraphy and pre-intrusive deformation history of the batholith framework rocks in order to evaluate whether or not pre-batholith tectonic dislocations may exist in the area. The third is to look for structures that might have been involved in the possible tectonic exhumation of the deep-level rocks in the southern Sierra Nevada. The fourth is to determine the overall structural history of the batholithic rocks and framework rocks in order to compare it with the deformation history of the Salinian block which has been suggested to correlate with the southern Sierra Nevada based on composition, age, and isotopic data. The fifth is to try to reconcile the evidence that suggests the rocks in the southernmost Sierra Nevada were deformed in Late Cretaceous-early Cenozoic time by both oroclinal folding and low-angle faulting.

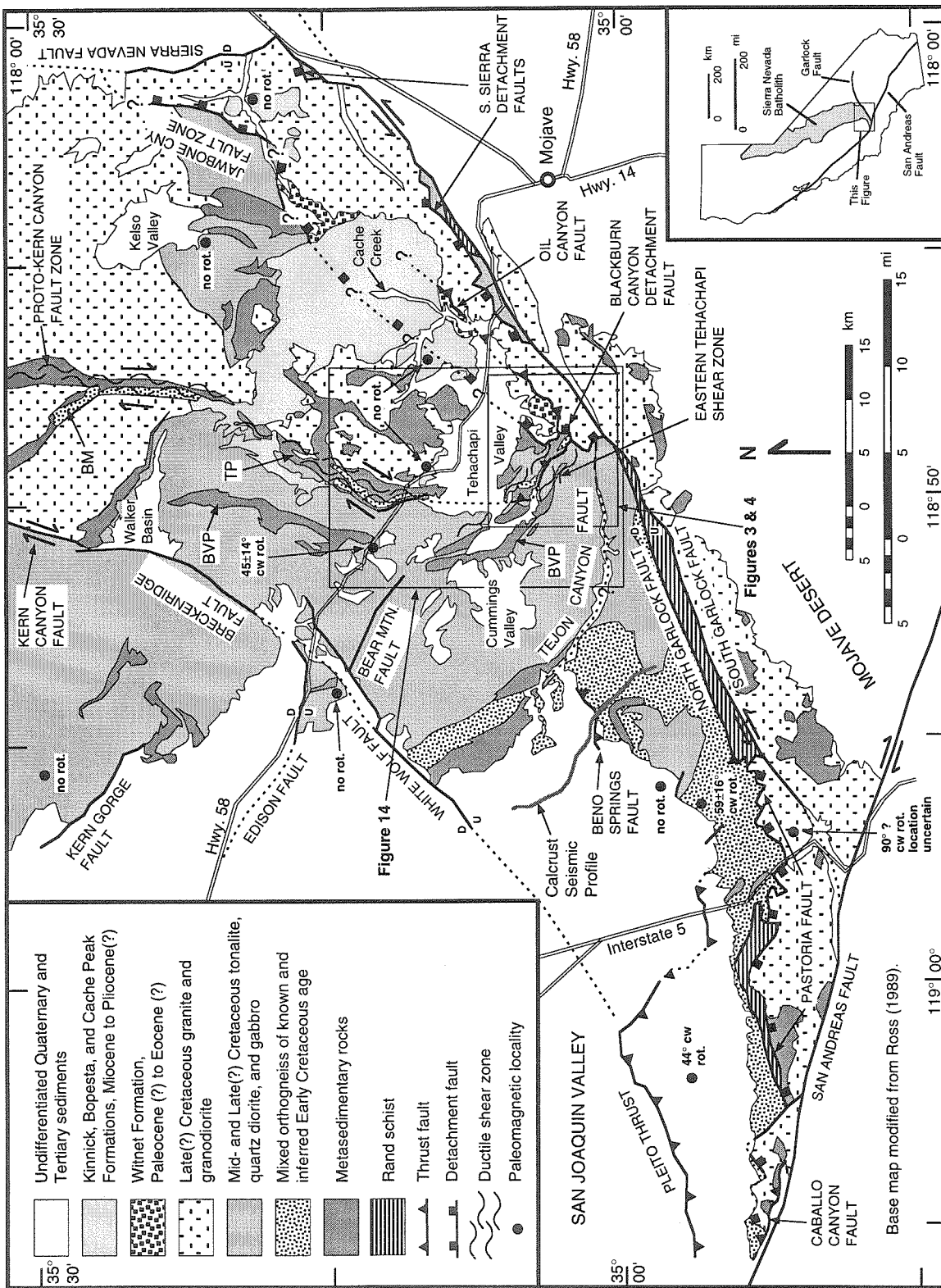
LOCATION AND DESCRIPTION OF THE STUDY AREA

The study area encompasses the eastern end of the Tehachapi Mountains which are an E-NE trending range of mountains located northeast of the San Andreas fault at the southwestern end of the N-NW trending Sierra Nevada (Figure 1). Physiographically the Tehachapi Mountains are bounded on the east by Tehachapi Valley, on the north by Cummings Valley and the southern San Joaquin Valley, and on the south by the Mojave Desert (Figure 2). To the west the Tehachapi Mountains are continuous with the San Emigdio Mountains and Interstate 5 (Grapevine Canyon) is generally considered to be the approximate boundary between the two ranges. The Tehachapi Mountains are split, almost axially, by the NE trending Garlock fault, and they are also divided in their eastern part by the arcuate W to NW trending Tejon Canyon fault (Figure 2). In this study the mountains south of the Garlock fault are referred to as the southern Tehachapi Mountains, the mountains north of the Garlock fault and west of the Tejon Canyon fault are referred to as the western Tehachapi Mountains, and the mountains east of the Tejon Canyon fault are referred to as the eastern Tehachapi Mountains.

The area mapped in this study includes about 40 square miles south of Tehachapi Valley and north of the Garlock fault, and about 10 square miles along the north side of Tehachapi Valley were also examined (Figures 4 and 14). All of the land in the study area is privately owned except for Tehachapi Mountain Park which is a Kern County public park located near the center of the study area south of Tehachapi Valley (Figure 4). The elevation of the study area ranges from ~4000' at Tehachapi Valley to ~7900' at the tops of the highest peaks which include Tehachapi Mountain, Double Mountain, and Bison Peak. The higher elevations in the western and central parts of the study area are underlain by resistant gneissic rocks into which creeks have cut steep-sided canyons resulting in a generally rugged topography. The eastern part of the area is underlain by deeply weathered granitic rocks which have eroded to form a more gentle rolling topography. On the north

Figure 2.

Regional geology and index map for the southernmost Sierra Nevada and Tehachapi Mountains region. The eastern Tehachapi Mountains are bounded by Tehachapi Valley, the Tejon Canyon fault, and Cummings Valley; the southern Tehachapi Mountains are located between the south Garlock fault and the Mojave Desert; the western Tehachapi Mountains are bounded by the Tejon Canyon fault, the San Joaquin Valley, Interstate 5, and the south Garlock fault; the San Emigdio Mountains are bounded by the San Joaquin Valley and the San Andreas fault and are located west of Interstate 5. The geology is modified from Ross (1989b) and Smith (1964). Rocks of the granite and granodiorite map unit have $Sr_i \geq 0.706$ and rocks of the tonalite, quartz diorite, and gabbro map unit have $Sr_i < 0.706$ except for the exposures south of Kelso Valley where rocks of the tonalite and gabbro unit have $Sr_i \geq 0.706$ (Kistler and Ross, 1990). Locations where paleomagnetic data (sources discussed in text) have been collected on rocks of the batholith as well as on Miocene sedimentary and volcanic rocks are shown by black circles. Modifications of geology southwest of Cummings Valley and east of Interstate 5 from Sharry (1981), Sams (1988), and Pickett and Saleeby (1993). Location of the Pastoria fault in the vicinity of the west end of the north Garlock fault from Peters (1972) and west of Interstate 5 and east of Rand schist exposure from C. Lough (written communication, 1993). Geology of the Tehachapi Valley region from this study, Dibblee and Louke (1970), Dibblee and Warne (1970), and Sams (1986). Location of the Oil Canyon fault from Smith (1951) and Michael (1960). Location of the proto-Kern Canyon fault zone from Busby-Spera and Saleeby (1990) and Gazis and Saleeby (1991). Location of southern Sierra detachment faults from Silver (1986) and Silver (personal communication, 1991). Location of the Jawbone Canyon fault zone from Samsel (1962) and Dibblee (1967). Easternmost exposure of the Witnet Formation from Dibblee (1959, 1967). Abbreviations are BM, Brown Meadow augen gneiss; BVP, Brite Valley pendants; TP, Tehachapi pendant.



side of the mountains at the higher elevations the vegetation consists of coniferous forests while the lower elevations are covered by dense brush and Pinyon Pine trees on the slopes, and Oak trees in the Canyon bottoms. The south side of the mountains, which face the Mojave Desert, are sparsely forested at high elevation and the lower slopes are covered by chaparral, Pinyon Pine trees, and Juniper trees.

PREVIOUS WORK IN THE STUDY AREA

Some of the earlier references to the geology of the study area consist of abbreviated descriptions of several gold mines and limestone quarries found south of Tehachapi Valley (Goodyear, 1888; Tucker, 1929; Troxel and Morton, 1962). The first extensive study of the geology of the Tehachapi area was made by Lawson (1906) who was drawn to the area by the geomorphic discordance and unusual drainage of Tehachapi Valley and several other relatively large, broad, and high valleys found in the southern part of the Sierra Nevada. Lawson (1906) studied the sedimentary and volcanic rocks in and around Tehachapi Valley, and based on the depositional and deformation histories of these rocks in conjunction with geomorphic observations he described the formation and evolution of Tehachapi Valley.

Most of the detailed geologic studies in the vicinity of Tehachapi Valley have focused on the sedimentary and volcanic rocks exposed immediately to the northeast of the valley in the Cache Creek area (Figure 2). Some of these sedimentary rocks were identified as Miocene in age on the basis of mammal fossils by Buwalda (1916), and in a later study Buwalda (1934) divided the sedimentary and volcanic rocks exposed northeast of Tehachapi Valley rocks into three formations, the pre-Miocene Witnet Formation, the Lower Miocene Kinnick Formation, and the Upper Miocene Bopesta Formation. Buwalda (1920; 1935; 1954) noted that these sedimentary and volcanic rocks had been deformed at least twice during the Tertiary. In the first deformation prior to deposition of the Kinnick Formation granitic basement rocks were thrust to the northwest over the Witnet Formation,

and in the second deformation the Kinnick and Bopesta Formations were folded about NE trending axes. The first detailed map of part of the Witnet, Kinnick, and Bopesta Formations in the Cache Creek area was made by Smith (1951) who also documented their stratigraphy and suggested that the Tertiary deformation in the area was related to activity along the nearby Garlock fault. In a subsequent study of the same region Michael (1960) refined part of the existing stratigraphy, defined a new volcanic unit called the Cache Peak Formation which appears to be Pliocene in age, and he suggested that the Witnet Formation might correlate with the Goler Formation mapped by Dibblee (1952) in the El Paso Mountains to the east. Dibblee (1967) and Dibblee and Louke (1970) also mapped these Tertiary rocks and Dibblee (1967) recognized that Witnet Formation was also present south of Tehachapi Valley in the area of the current study. The Bopesta Formation has been studied in detail by Quinn (1987) who also summarized recent estimates for the ages of the Tertiary formations.

The crystalline basement rocks of the study area have been examined by a number of different workers, but most of the mapping has been in reconnaissance. Dibblee (1967) mapped part of the current study area and shows the basement rocks as being quartz diorite on the west and quartz monzonite on the east. In more detailed later studies Dibblee and Louke (1970) and Dibblee and Warne (1970) mapped the Tehachapi and Cummings Mountain 15' quadrangles, respectively, at a scale of 1:62,500. The area of this study is located in the southwest corner of the Tehachapi 15' quadrangle and in the southeast corner of the Cummings Mountains 15' quadrangle. Dibblee and Louke (1970) showed the study area as being composed of three major lithologic units, metasedimentary rocks and hornblende biotite quartz diorite to the west and quartz monzonite to the east, and they provided the first detailed lithologic descriptions of the crystalline basement rocks in the region. They also noted that the metasedimentary rocks are intruded by the hornblende biotite quartz diorite, which is commonly foliated with a NW trending NE dipping fabric,

and they suggested that the quartz monzonite intrudes the quartz diorite along a sinuous but generally north dipping contact that dips shallowly to the west. In a study of the basement rocks in the vicinity of the Garlock fault Sharry (1981) identified the presence of hypersthene in quartz dioritic rocks north of the fault, and locally north of and adjacent to the fault he mapped a severely deformed hornblende diorite gneiss unit called the White Oak diorite.

Ross (1989b) integrated the previous mapping of many different workers in the southern Sierra Nevada-Tehachapi Mountains region with his own primarily petrologic and petrographic studies of the basement rocks in the region into a relatively coherent picture of the regional geology. In the area covered by the current study Ross (1989b) grouped the hornblende biotite quartz diorite of earlier studies into the regional-scale Bear Valley Springs tonalite batholith, and he identified the local presence of hypersthene-bearing amphibolitic rocks in the tonalite. Ross (1989b) recognized that parts of the tonalite in the study area were severely deformed and he also mapped a small body of deformed quartzofeldspathic gneiss. The quartz monzonitic rocks on the east side of the study area were considered by Ross (1989b) to be part of the regionally extensive Claraville granodiorite. Some of the rocks in the study area were examined in reconnaissance by Sams (1986), and Sams (1986) and Saleeby et al.(1987) in regional geochronologic and isotopic studies determined a ~100 Ma U-Pb zircon age for the Bear Valley Springs tonalite west of Tehachapi Valley.

METHODS OF INVESTIGATION

The geology of the eastern Tehachapi Mountains was mapped at scales of 1:24,000, 1:12,000, and 1:6,000 and then compiled at 1:24,000 scale as shown in Plate 1. The study area is located in the Tehachapi South and Cummings Mountain U.S. Geological Survey 7.5' quadrangles in Kern County, California. The U. S. Geological Survey 1966 version (photorevised 1973) topographic maps for those quadrangles were used as base maps for

the geologic mapping in this study. Most of the study area is covered by either forest at higher elevations or dense brush on the lower mountain slopes making it difficult to locate oneself on the map. A barometric altimeter was used during mapping as a location aid and its accuracy is estimated to be about ± 20 -40 feet elevation during stable weather conditions. Access to most of the study area is on well maintained dirt ranch roads. Many of the ranch roads are not shown on the original topographic base maps and since many of the best rock exposures are in roadcuts along these roads the road locations were mapped out with the aid of the altimeter.

The different map units and structures in the study area have been characterized using both field and laboratory observations. Over 500 rock samples were collected in this study for petrographic and structural analysis. Thin sections were prepared for more than half of these samples to study their petrography, characterize their deformation fabrics, and determine their sense of shear. Techniques for the determination of shear sense from kinematic indicators in rocks are well established and the methods used in this study are discussed in the chapter on the structural history of the study area. Combined structural and kinematic analysis of both the microstructural and field structural data was used to investigate the deformation history of the study area. Ten rock samples were collected for radiometric age determinations using the U-Pb method on zircons. Zircons were extracted from the samples using standard mineral separation techniques in preparation for future geochronologic studies. Plate 4 shows the locations of the samples collected for dating.

CHAPTER II: TECTONOSTRATIGRAPHY AND LITHOLOGIC DESCRIPTIONS

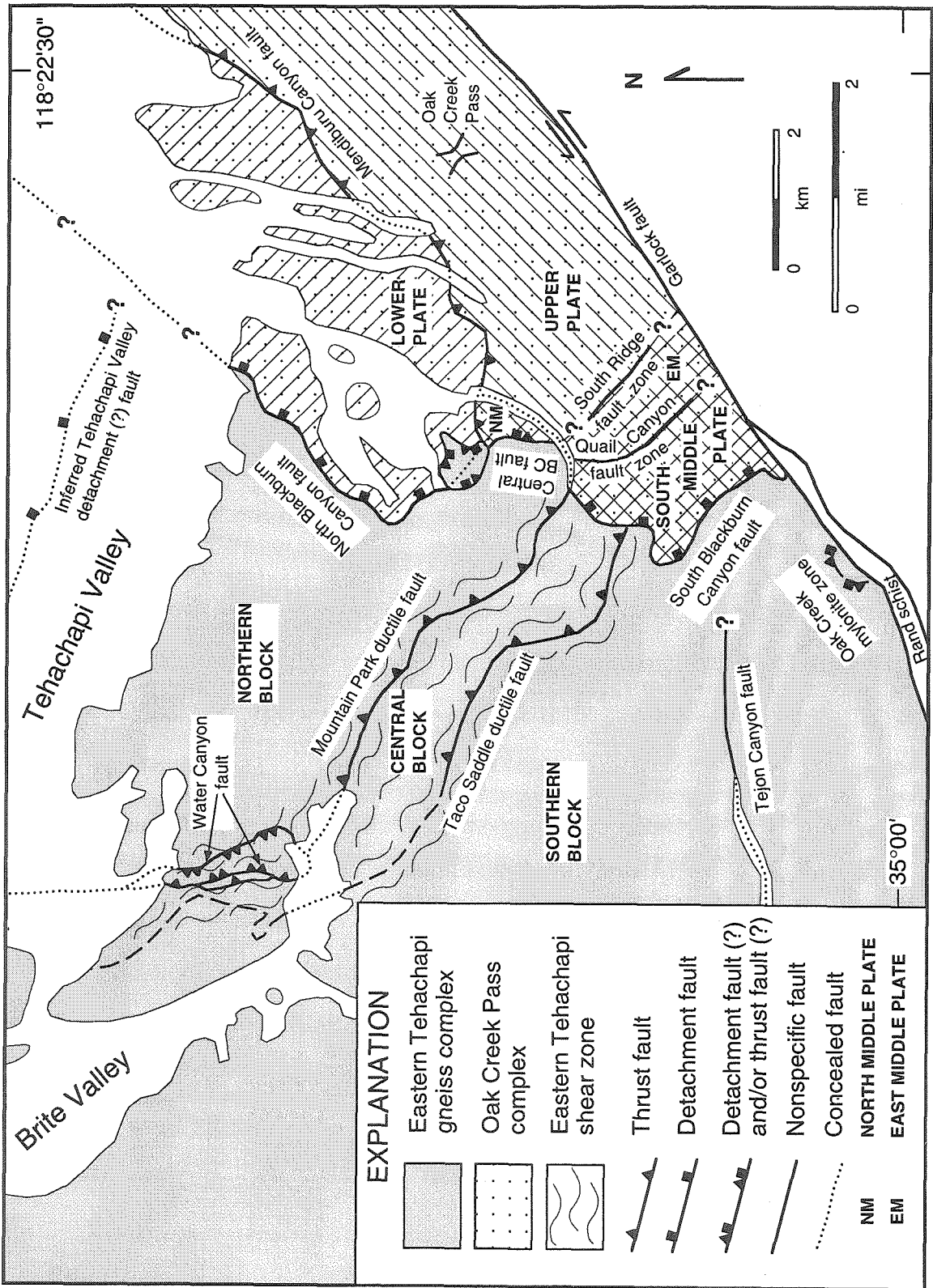
OVERVIEW

The study area in the eastern Tehachapi mountains consists of a high grade poly-deformed and metamorphosed gneiss terrane on the west that is overlain to the east along a gently undulating shallowly SE dipping fault by a complex of low grade cataclastically deformed granitic rocks that locally have conglomeratic and arkosic sediments deposited on top of them. The footwall gneiss terrane is called the eastern Tehachapi gneiss complex, the hangingwall granitic and sedimentary complex is called the Oak Creek Pass complex, and the intervening ductile-brittle fault is called the Blackburn Canyon detachment fault (Figure 3). The intrusive, deformation, and metamorphic histories of the two complexes prior to their final juxtaposition along the Blackburn Canyon fault are different. The major structures that subdivide each complex are outlined below in order to provide a framework for the location of the different metasedimentary and intrusive units described later in this section. Both complexes and many of the structures in them are intruded by swarms of volcanic dikes of inferred Tertiary age.

The eastern Tehachapi gneiss complex is divided into three structural blocks by two subparallel, NW trending, moderate to shallow NE dipping ductile faults with mylonitic fabrics. The northeastern ductile fault is called the Mountain Park fault and the ductile fault to the southwest is called the Taco Saddle fault (Figure 3). From northeast to southwest the structural blocks are informally named Pine Tree, Astronomy Ridge, and Double Mountain, respectively, based on prominent geographic features in each block. In this paper for the sake of clarity the three structural blocks of the eastern Tehachapi gneiss complex will be referred to as the northern, central, and southern blocks (Figure 3). The Taco Saddle fault appears to die out along strike to the northwest. Northwest of the

Figure 3.

Map showing tectonic stratigraphy, fault locations and names, and structural domains for the study area in the eastern Tehachapi Mountains. The eastern Tehachapi gneiss complex comprises the footwall of the Blackburn Canyon detachment fault and the Oak Creek Pass complex comprises the hangingwall of that fault. The gneiss complex is divided into three structural blocks by the Mountain Park and Taco Saddle ductile faults. The structural blocks are termed the northern, central, and southern blocks. The Taco Saddle fault appears to die out along strike to the northwest. Northwest of the termination of the Taco Saddle fault the southwest boundary of the central structural block is defined by the northeast margin of the Brite Valley pendant and is shown by the heavy dashed line. The Water Canyon fault is indicated by double thrust teeth and it is inferred to be synformally folded as discussed in the text. Three segments of the Blackburn Canyon fault are defined by intersections with the Mendiburu Canyon and Quail Canyon faults of the Oak Creek Pass complex. See the text for descriptions of the faults in the Oak Creek Pass complex. The southern part of the north Blackburn Canyon fault is inferred to be concealed beneath a fault-bounded sliver of the gneiss complex. The lower plate, upper plate, and middle plates of the Oak Creek Pass complex are indicated by northwest trending hatching, northeast trending hatching, and cross hatching, respectively.



disappearance to the northwest of the Taco Saddle fault the southwest boundary of the central structural block is defined to be the northeast margin of a metasedimentary pendant and the boundary is shown by the heavy dashed line in Figure 3.

The gneiss in the central structural block and in the adjacent margins of the northern and southern blocks frequently exhibits solid-state shear fabrics. This zone of ductile shear that traverses the gneiss complex, and which includes both the Mountain Park and Taco Saddle faults, is called the eastern Tehachapi shear zone (ETSZ) (Wood et al., 1993). The E dipping west limb of the synformally folded Water Canyon fault (double teeth in Figure 3) in the northern block of the gneiss complex locally appears to be coincident with the Mountain Park fault, but the two faults are considered to be separate structures as will be discussed later.

The Oak Creek Pass complex hosts several fault zones that project to intersections with the Blackburn Canyon detachment fault at the western end of the complex. These faults are the Mendiburu Canyon fault, the South Ridge fault zone, the Quail Canyon fault zone, and an unnamed inferred fault concealed beneath the alluvium of Blackburn Canyon. The region where these faults appear to converge is complicated and poorly exposed. The Mendiburu Canyon fault is a NE trending fault along which arkosic sediments deposited on granitic rock appear to have been overridden from the southeast by other granitic rocks. The termination of the west end of the Mendiburu fault at the Blackburn Canyon fault is obscured by a small sliver of gneiss that is part of the eastern Tehachapi gneiss complex, a complication to be discussed later. The Quail Canyon and South Ridge fault zones are NW to N trending zones of extensive cataclasis with local areas of protomylonitic foliation. These two fault zones appear to juxtapose different plutonic lithologies and complicated deformation fabrics in the fault zones generally are eastward dipping. The Quail Canyon and South Ridge fault zones were not studied in detail and the precise location, regional extent, and sense of motion of these fault zones are not well defined.

Three segments of the Blackburn Canyon fault are defined based on the projected intersections of the Mendiburu Canyon fault and the Quail Canyon fault with the Blackburn Canyon fault. North of the intersection with the Mendiburu Canyon fault is the north segment of the Blackburn Canyon fault, between the Mendiburu Canyon fault and Quail Canyon fault intersections is the central segment, and south of the Quail Canyon fault intersection is the south segment of the Blackburn Canyon fault. The southern part of the north Blackburn Canyon fault is inferred to be concealed beneath a fault bounded sliver of the gneiss complex.

In order to elucidate the geology of the structurally complicated Oak Creek Pass complex the rocks have been separated into five fault bounded groups (Figure 3) which are referred to as plates in part to differentiate them from the structural "blocks" of the eastern Tehachapi gneiss complex, but also because regional structural relations (Silver, 1986; Silver and Nourse, 1991) suggest that some of the fault bounded domains are thin relative to their areal extent. The lower plate of the Oak Creek Pass complex constitutes the footwall of the Mendiburu Canyon fault and the hangingwall of the north Blackburn Canyon fault. The upper plate of the Oak Creek Pass complex is part of the hangingwall of the Mendiburu Canyon fault and it is lithologically distinct from the lower plate. The upper plate is bounded on the north by the Mendiburu Canyon fault, on the west by a fault inferred to be concealed beneath the alluvium of Blackburn Canyon, on the southwest by the South Ridge fault zone, and on the southeast by the Garlock fault.

Three additional plates, which map relations suggest are structurally lower than the upper plate, are called the north, south, and east middle plates. However, as will be discussed later, it is unclear whether all of the middle plates are structurally above the lower plate because there are a number of different interpretations of fault relationships in the Oak Creek Pass complex. The north middle plate is bounded by the Mendiburu Canyon fault on the north, the central Blackburn Canyon fault on the west, and an unnamed fault

inferred to be concealed under the alluvium to the east. The south middle plate is bordered by the south Blackburn Canyon fault to the north and west, the Quail Canyon fault to the east, and the Garlock fault to the south. The east middle plate is bounded by the central Blackburn Canyon fault to the north, the Quail Canyon fault zone to the west, the South Ridge fault zone to the east, and the Garlock fault to the south.

EASTERN TEHACHAPI GNEISS COMPLEX

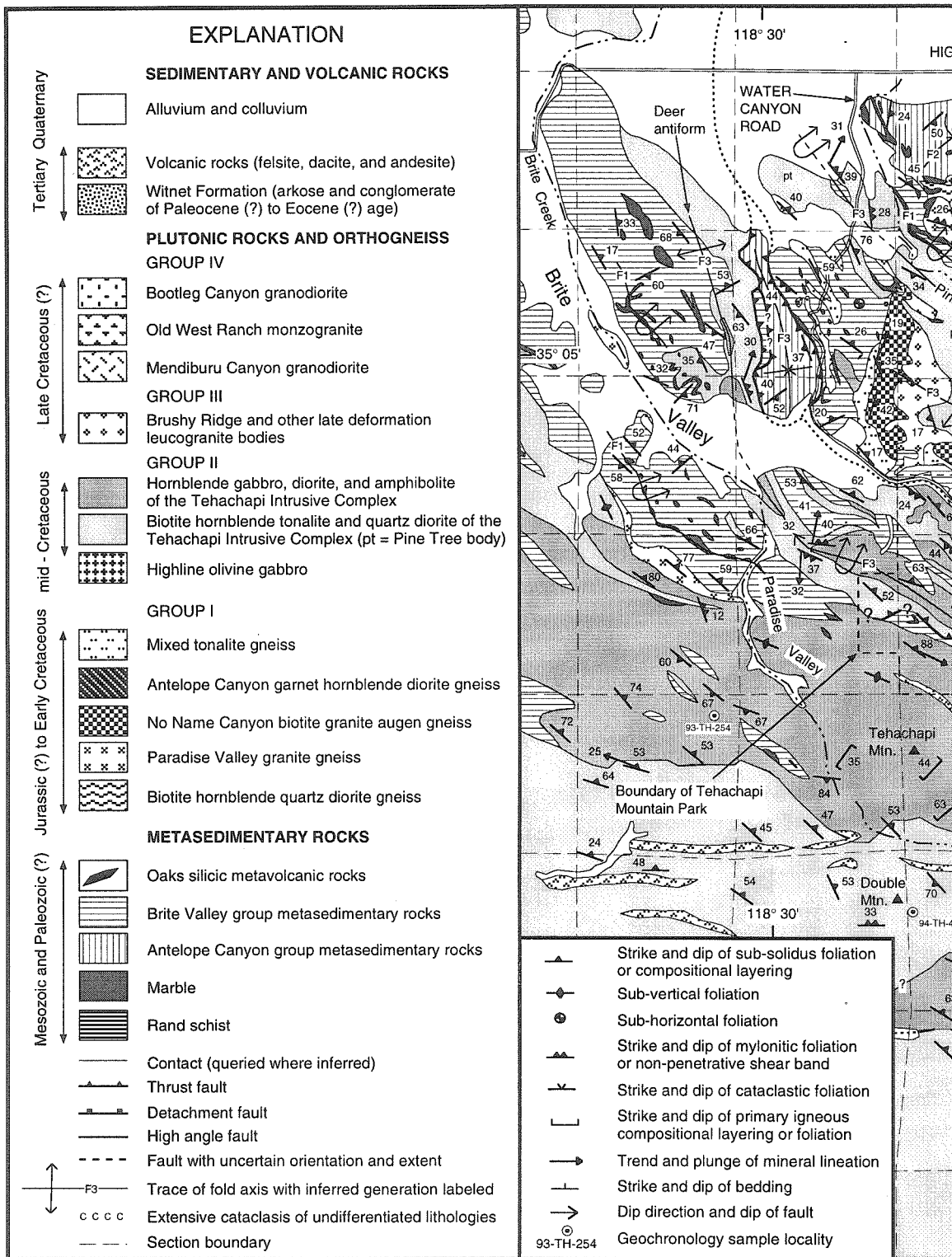
The eastern Tehachapi gneiss complex consists of a framework of metasedimentary rocks intruded by several generations of plutonic rocks of the Sierra Nevada batholith. Figure 4 and Plates 1 and 4 are geologic maps of the study area showing the location of the lithologic units discussed in this section. The pre-batholith metasedimentary rocks are divided into two groups that have different sequences of lithologies. The intrusive rocks are divided into three groups, groups I, II, and III, based on composition, crosscutting relations, and deformation fabrics. Group I intrusive rocks are orthogneisses of different compositions that have a high temperature gneissic fabric that frequently is concordant to fabrics in the adjacent metasedimentary rocks. Group II intrusive rocks, the most voluminous in the study area, are gabbroic to tonalitic plutons that locally intrude members of the group I orthogneisses and have well developed gneissic and mylonitic fabrics where they are deformed in the eastern Tehachapi shear zone. The group III intrusives are leucogranite plutons that intrude both group I and group II intrusive rocks.

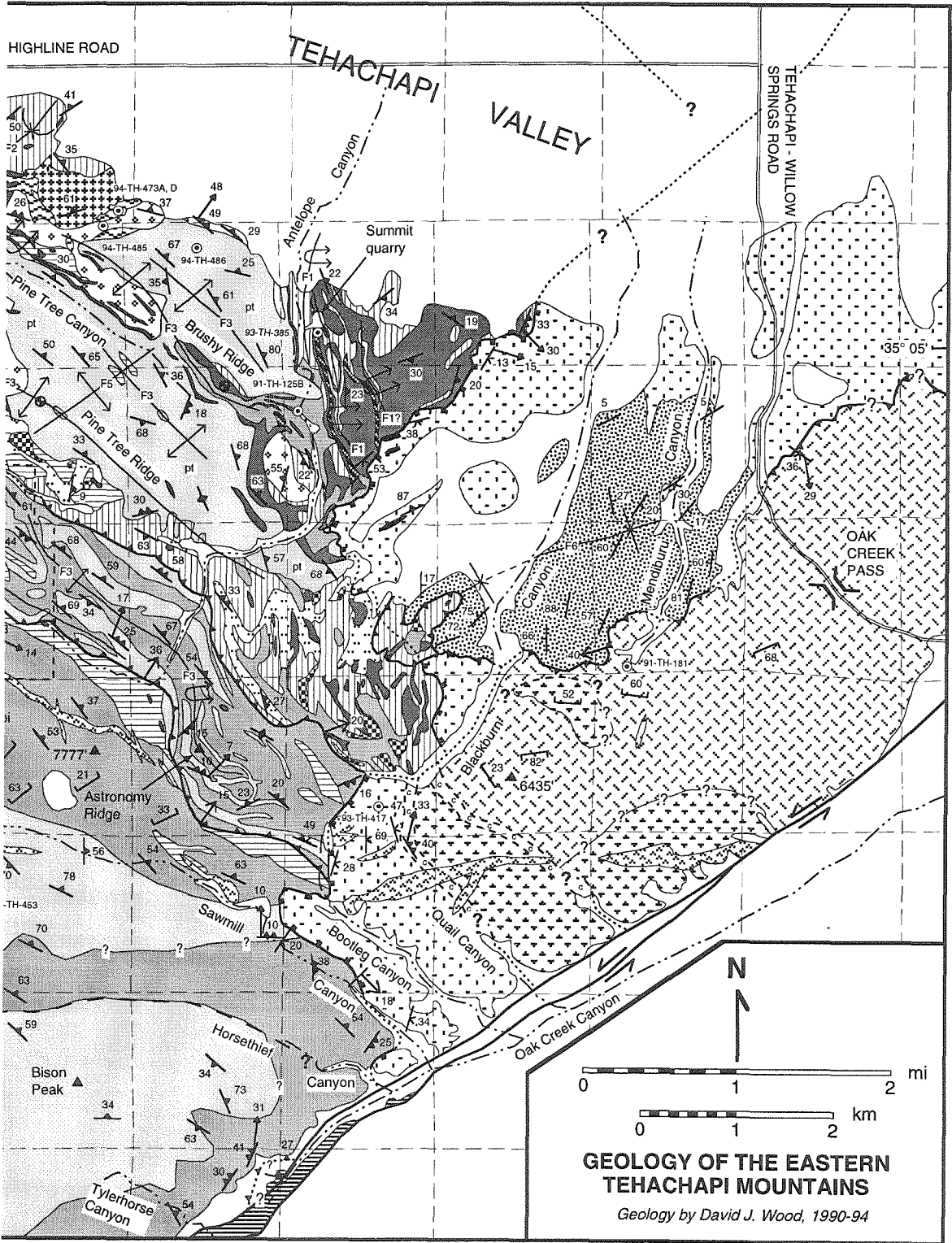
METASEDIMENTARY ROCKS

The eastern Tehachapi gneiss complex contains two sequences of metasedimentary rocks, the Antelope Canyon group and the Brite Valley group. The boundary between the two metasedimentary rock sequences approximately coincides with the eastern Tehachapi shear zone and both sequences are deformed in the shear zone (see Figures 3 and 4). The Antelope Canyon group rocks are found mostly to the northeast of the eastern Tehachapi shear zone and most of the Brite Valley metasedimentary rocks are found to the southwest.

Figure 4.

Geologic map of the study area in the eastern Tehachapi Mountains. A larger unsplit version of this figure is reproduced at a scale of 1:48,000 in Plate 4.





Some Brite Valley group rocks do occur in the northern structural block, north of the Mountain Park fault.

Antelope Canyon Group Metasedimentary Rocks

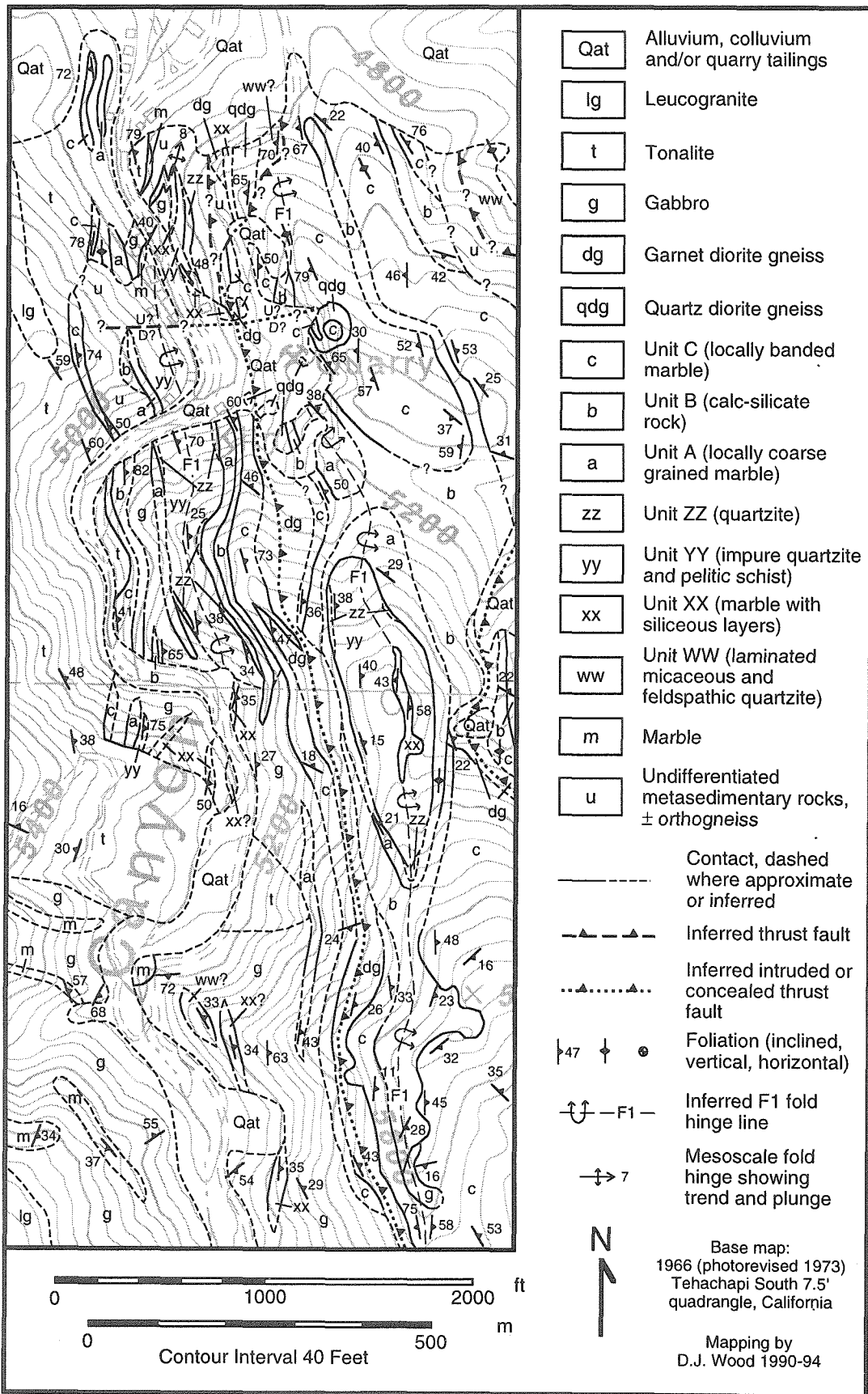
The Antelope Canyon group consists of a structurally lower portion dominated by metamorphosed siliciclastic rocks and a structurally higher part that consists largely of metamorphosed carbonate rocks. The sequence has been deformed, metamorphosed and intruded by batholith rocks multiple times. Overall fabrics range from gneissic to schistose in the quartzofeldspathic lithologies and coarsely crystalline to well foliated in the carbonate lithologies. Most of the lithologies are compositionally banded to some degree at both outcrop and thin section scale and the dominant foliation usually is subparallel to this compositional layering. Some of this compositional banding may reflect original bedding.

The best exposures of the Antelope Canyon group are located along the east side of lower Antelope Canyon and also along the ridge-top north of the uppermost part of Blackburn Canyon (Figure 4). The type locality of the Antelope Canyon group rocks is located in lower Antelope Canyon and a detailed map of this area is shown in Figure 5. The Antelope Canyon group rocks are folded into map-scale tight to isoclinal folds that have N to NW trending subhorizontal to shallow N plunging hinges and limbs that dip to the E. These antiformal and synformal folds in some cases appear to be separated by pre-batholithic thrust (?) faults between their limbs. A few of these folds are observed to close, and sequences of distinctive lithologies are repeated in adjacent folds and apparently overturned across some of the folds. Based on these observations a lithologic sequence consisting of seven mappable units has been compiled for the Antelope Canyon group rocks and is shown in Figure 6. The modal mineralogy of each of the units is shown in Table 1.

The sequence as shown in Figure 6 is composite since a complete and continuous section is not exposed along a single section. Unequivocal protolith sedimentary structures

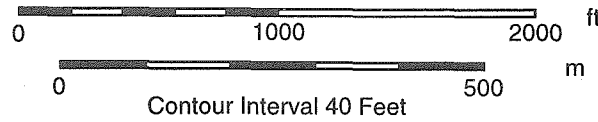
Figure 5.

Detailed geologic map of the type locality for the Antelope Canyon group metasedimentary rocks. The garnet diorite gneiss unit is inferred to have intruded along prebatholithic thrust faults.



- Qat Alluvium, colluvium and/or quarry tailings
- lg Leucogranite
- t Tonalite
- g Gabbro
- dg Garnet diorite gneiss
- qdg Quartz diorite gneiss
- c Unit C (locally banded marble)
- b Unit B (calc-silicate rock)
- a Unit A (locally coarse grained marble)
- zz Unit ZZ (quartzite)
- yy Unit YY (impure quartzite and pelitic schist)
- xx Unit XX (marble with siliceous layers)
- ww Unit WW (laminated micaceous and feldspathic quartzite)
- m Marble
- u Undifferentiated metasedimentary rocks, ± orthogneiss

- Contact, dashed where approximate or inferred
- Inferred thrust fault
- Inferred intruded or concealed thrust fault
- Foliation (inclined, vertical, horizontal)
- Inferred F1 fold hinge line
- Mesoscale fold hinge showing trend and plunge



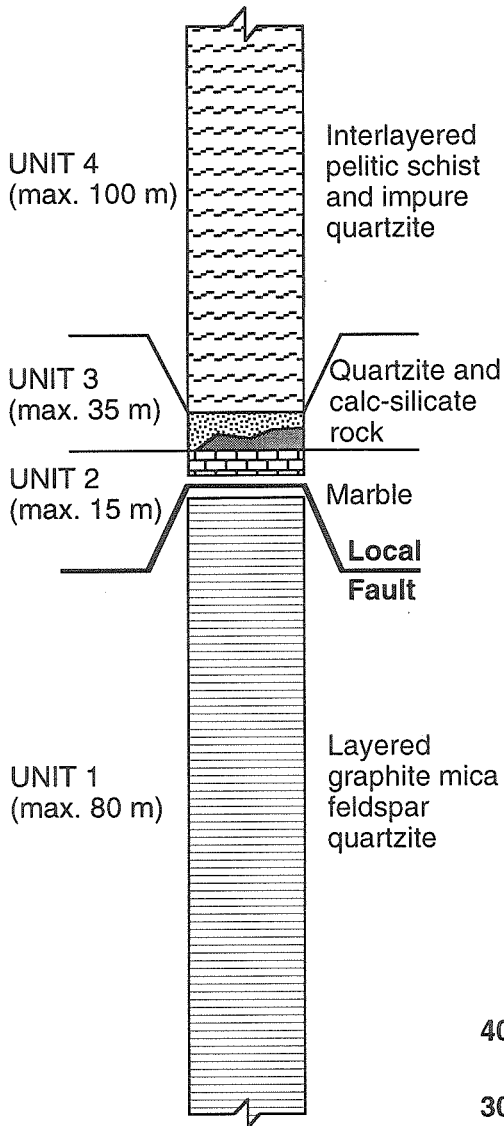
Base map:
1966 (photorevised 1973)
Tehachapi South 7.5'
quadrangle, California

Mapping by
D.J. Wood 1990-94

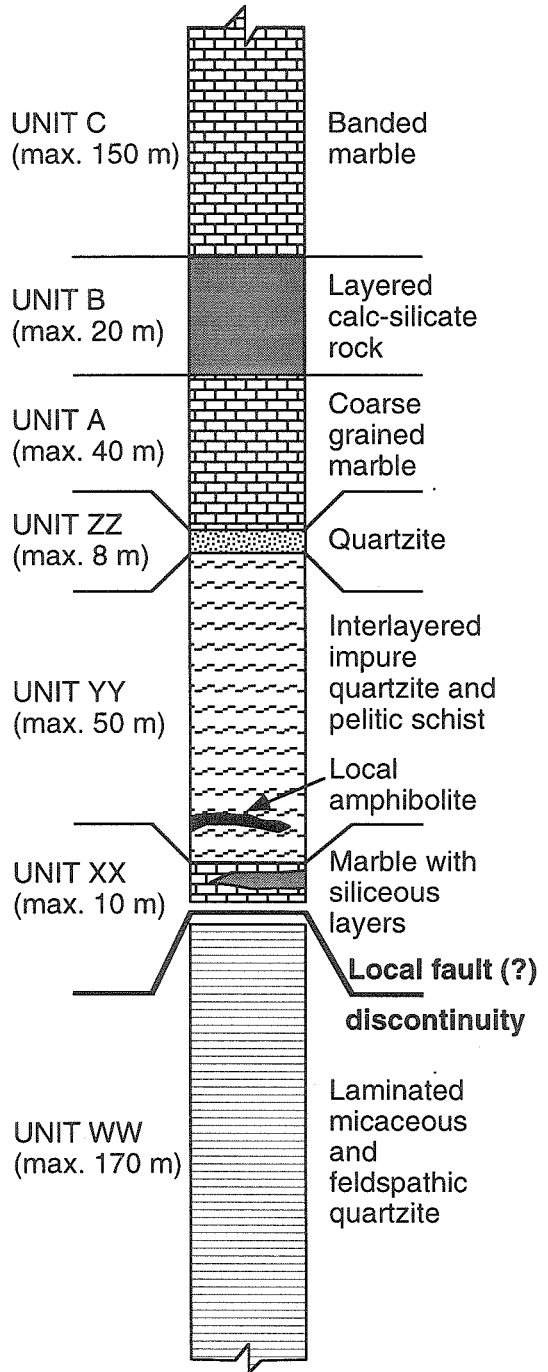
Figure 6.

Pre-intrusive composite stratigraphy for the two groups of metasedimentary rocks found in the eastern Tehachapi mountains study area. The thickness of lithologic units is tectonic and was estimated from field observations or measured from the geologic map. The stratigraphy and relative thickness of units shown in the figure for the Brite Valley group rocks are from the area south of the south end of Brite Valley. The stratigraphy and relative thickness of units shown in the figure for the Antelope Canyon group rocks are from exposures east of the lower part of Antelope Canyon. The estimated maximum thickness observed in the entire study area for each unit is shown in parentheses below the unit name.

BRITE VALLEY GROUP COMPOSITE STRATIGRAPHY



ANTELOPE CANYON GROUP COMPOSITE STRATIGRAPHY



SCALE (meters)

Thickness of units is tectonic thickness

indicating stratigraphic up were not observed, but there is a consistent structural succession of lithologic units from the cores to the outer limbs of antiforms throughout the area, with the structurally lowest units located in the cores of the antiforms. The thickness of a given unit commonly varies widely throughout the area because of folding and tectonic attenuation. In some places a unit may be absent, possibly because of incomplete exposure, boudinage, or unrecognized fault removal. The relative thicknesses of the units shown in the lithologic column in Figure 6 are for the most complete and continuous section located south of the Summit quarry in lower Antelope Canyon (Figure 5). The estimated maximum tectonic thickness of each unit in the entire study area is shown in parentheses after the unit name.

Unit WW

The siliciclastic dominated lower part of the Antelope Canyon sequence is divided into four units and from lowest to highest structural level they are sequentially labeled unit WW through unit ZZ. Unit WW is a rusty weathering, light gray colored, fine grained, well foliated and compositionally laminated, micaceous and feldspathic gneissic quartzite that locally is interlayered with lenses and layers of medium grained vitreous quartzite. The distinct compositional laminations are composed of thin (<1 millimeter) biotite rich layers alternating with 1 to 2 millimeter thick layers of quartz and plagioclase and potassium feldspar. The quartzite tends to split along mica rich laminations and fine grained flakes of graphite commonly are visible on the split surfaces. Where deeply weathered the quartzite has a light tan color and it is friable, readily disintegrating along the closely spaced mica rich laminations.

The quartzite commonly hosts concordant layers consisting of medium to coarse grained quartz and feldspar. The layers are several millimeters to several centimeters thick and they pinch and swell. Multiple generations of mafic to felsic and concordant to discordant, dikes, sills, and transposed bodies of inferred orthogneiss are hosted by unit

WW. The apparent abundance of intrusions in unit WW in contrast to the other paragneiss units may in part be attributable to its low structural position. The lower contacts of unit WW are intrusive or tectonic. The contact between unit WW and the structurally higher unit XX is not well defined because of intervening intrusions, structural complexities, and lack of exposure. Based on map relations, however, unit WW everywhere appears to be structurally the lowest member of the Antelope Canyon group rocks.

Unit XX

Located structurally above unit WW, unit XX consists of one or two marble layers interlayered with reddish weathering calc-silicate rock and quartzite. The marble layers range from ~1 meter to several meters in thickness and they commonly contain numerous contorted and boudinaged millimeter to ~10 centimeter thick layers and lenses of siliceous material. The marble typically has a grayish white color that locally is tinged with pink. In addition to calcite other minerals present in the marble and calc-silicate rock of unit XX include wollastonite, diopside, garnet, sphene, epidote, phlogopite, plagioclase, potassium feldspar, and quartz. No dolomite was observed in the thin sections examined, but the presence of Mg-bearing calc-silicate minerals suggests the protolith may have been slightly dolomitic. The contact between unit XX and the overlying unit YY is not well defined and in most areas only the marble portion of unit XX is exposed. The calc-silicate rock and quartzite of the upper part of unit XX appear to grade upward into unit YY.

Unit YY

Unit YY consists of fine to medium grained quartzite and biotite quartzofeldspathic gneiss interlayered with discontinuous pelitic layers ranging from several millimeters to tens of centimeters thick. The pelitic intervals contain biotite, plagioclase, and quartz, \pm muscovite, \pm sillimanite, \pm garnet. The paragneiss of unit YY is light grayish brown to green in color and it weathers to produce a reddish brown soil. The green color comes

from the common presence of retrograde chlorite. The contact of unit YY with the overlying unit ZZ is sharp.

Unit ZZ

Unit ZZ is a white to gray metaquartzarenite that ranges from 2 to 8 meters thick where it is best exposed in lower Antelope Canyon. It consists of 95-100% quartz in recrystallized grains up to 1 centimeter in diameter, and locally it contains up to ~5% of very fine grained deep reddish colored biotite that is homogeneously disseminated throughout the rock and imparts a dark gray color to the quartzite. There are no clear relict sedimentary structures in the quartzite although there are layers and lens-shaped regions of different color or grain size. Coarser grained parts of the quartzite are massive, generally light colored, and vitreous, while finer grained areas sometimes appear to have millimeter-scale laminations defined by differing shades of gray. In the thickest and best exposure unit ZZ is composed of two quartzite subunits separated by a 10 centimeter to 1 meter thick interval of pelitic material that occurs about two thirds of the way up from the base of the unit.

Unit A

The carbonate dominated upper part of the Antelope Canyon group is composed of two marble layers, units A and C, separated by an interval of calc-silicate rock. Unit A, structurally above unit ZZ, is gray dolomitic marble that ranges texturally from massive and coarsely crystalline to medium grained and compositionally banded. In the coarsely crystalline part of unit A rhombohedral crystals of calcite up to 2-3 centimeters in length locally are present. In the compositionally banded marble 1-4 millimeter thick yellow-orange and greenish-gray bands of silicate and calc-silicate minerals alternate with 5-15 millimeter wide intervals of medium grained gray dolomitic marble. Flakes of graphite and amber colored phlogopite commonly are visible in hand specimen. Other minerals present in the marble include dolomite, forsterite, garnet, diopside, tremolite, sphene, and opaques.

Locally present at the bottom of unit A is a narrow interval of calc-silicate rock with a thin (~1 meter thick) marble layer at the base.

Unit B

Structurally above unit A, unit B consists of layers of red-orange weathering calc-silicate rock interlayered with marble layers containing contorted calc-silicate layers. The layers of calc-silicate rock and marble range in thickness from several centimeters to tens of centimeters. Locally present in unit B are layers and lenses of mafic gneiss that have the composition of a biotite hornblende diorite. The contacts of the mafic gneiss are mostly transposed and the foliation in the gneiss is concordant with the foliation present in the other lithologies in unit B. Locally, however, the contacts of the mafic gneiss appear to cross lithologic layering in unit B at a low angle which suggests the gneiss intruded the calc-silicate rocks. The calc-silicate rock is grayish-green colored when unweathered, fine grained and compositionally laminated on a submillimeter-scale. The mineral assemblage in the calc-silicate rock includes potassium feldspar, diopside, epidote, sphene, and opaques, \pm quartz, \pm calcite, \pm garnet, \pm wollastonite, \pm hornblende.

Unit C

The upper marble, unit C, is generally fine grained and white in color and it commonly contains millimeter-scale gray colored bands, spaced millimeters to centimeters apart, which give the rock a distinctive banded or zebra-striped appearance. The dark color in the bands may be from finely disseminated graphite since scattered flakes of graphite are visible in hand specimens of the marble and fine grained opaque grains with a distinct platy habit are visible in thin section. On weathered surfaces the marble has a cream color which may in part be due to staining resulting from the oxidation of submillimeter size grains and cubes of pyrite scattered through the marble. Troxel and Morton (1962) also noted the graphite and pyrite in this marble. The banded marble of unit C locally contains seams of

quartz and calc-silicate minerals and dolomite was observed in one thin section. Scattered flakes of phlogopite in some samples also suggest the marble is slightly dolomitic.

Brite Valley Group Metasedimentary Rocks

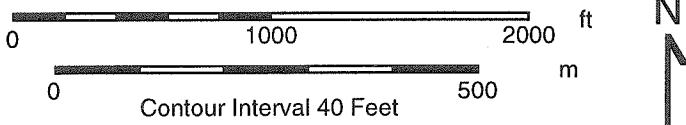
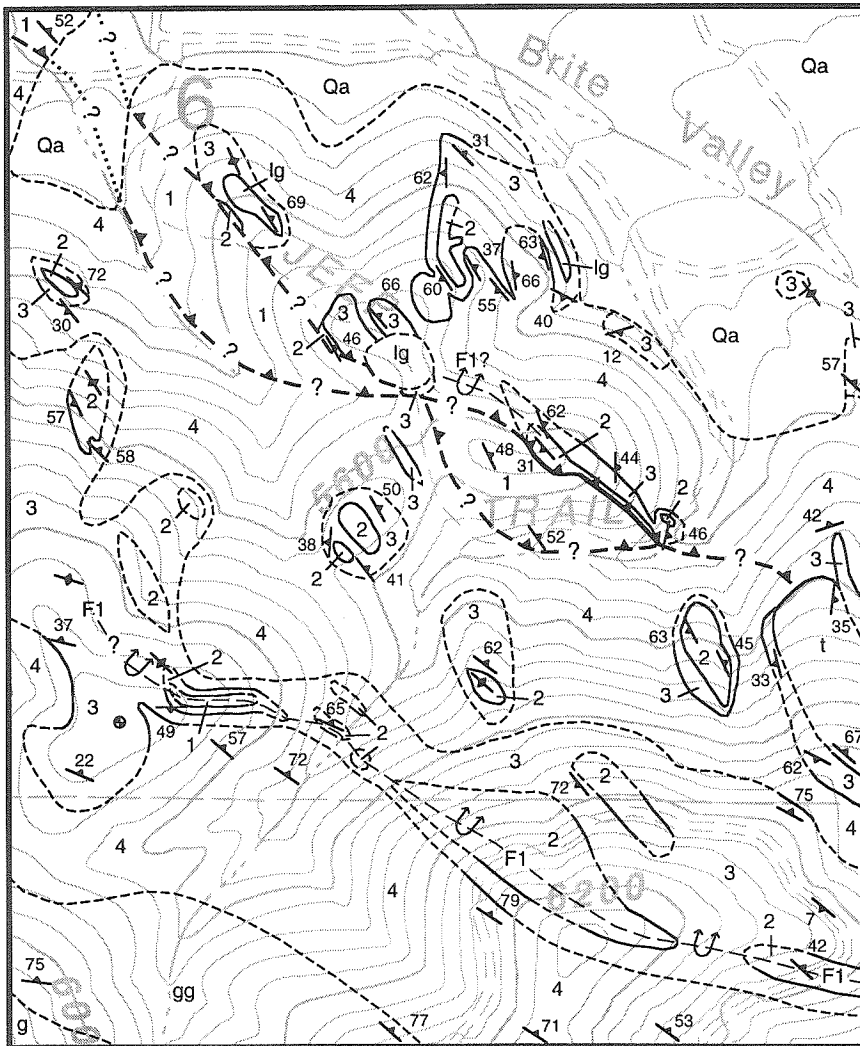
The Brite Valley group rocks are best exposed in the western end of the study area to the north and south of the southern end of Brite Valley (Figure 4). The type locality for the Brite Valley group rocks is found immediately south of Brite Valley and Figure 7 is a detailed map of this area. Like the Antelope Canyon sequence the metasedimentary rocks of the Brite Valley group have been deformed and metamorphosed several times, and invaded by different generations of intrusions. The Brite Valley group is not as well exposed as the Antelope Canyon group. On the grass and brush-covered slopes surrounding Brite Valley marble and massive quartzite frequently are the only lithologies that crop out. Based on field observations and map relations (Figure 7) a lithologic sequence has been compiled for the Brite Valley metasedimentary rocks (Figure 6). The Brite Valley group is divided into four units, sequentially numbered 1 through 4, with unit 1 occupying the structurally lowest position. The modal mineralogy of the different lithologic units is shown in Table 1.

Unit 1

Unit 1 consists of graphitic quartzite and quartzofeldspathic gneiss that locally is calcareous or micaceous, and it appears to be the structurally lowest lithology in the Brite Valley sequence because it is exposed in the core of antiformal folds of unit 2 marble at several locations. When fresh the quartzite is white to dark gray in color, locally vitreous, and it invariably weathers to a yellowish or rusty-red color that may result from the oxidation of pyrite. The quartzite of unit 1 is compositionally banded with dark gray graphite rich seams 1 millimeter or less in thickness alternating with white to light gray quartz rich bands up to several centimeters thick. Quartz comprises 75-95% of the rock and the remainder may include diopside, potassium feldspar, plagioclase, graphite, biotite,

Figure 7.

Detailed geologic map of the type locality for the Brite Valley group metasedimentary rocks. Intrusion of the small tonalite body along the east margin of the map and intrusion of a small gabbro body just outside of the northwest corner of the map may have been localized along prebatholithic thrust faults that are inferred to be present within the metasedimentary rocks.



Qa	Alluvium	-----	Contact, dashed where approximate or inferred
lg	Leucogranite	-----▲-----	Fault (queried and dashed where inferred)
t	Tonalite	┆47 ┆ ●	Foliation (inclined, vertical, horizontal)
g	Gabbro	↕ — F1 —	Inferred F1 fold hinge line
gg	Granite gneiss		
4	Unit 4 (pelitic gneiss)		
3	Unit 3 (quartzite and calc-silicate rock)		
2	Unit 2 (marble)		
1	Unit 1 (graphitic dirty quartzite)		

Base map: 1966 (photorevised 1973)
Tehachapi South 7.5' quadrangle, California

Mapping by D.J. Wood 1990-94

and muscovite. The graphite is prominently visible on foliation surfaces and comprises up to about 2% of the rock.

Unit 2

Overlying unit 1 is a marble layer, unit 2, that ranges in thickness from less than 1 meter to about 10 meters. Local exposures of the marble are thicker but these occur in areas where the marble layer appears to be repeated because of folding or because the marble is thickened in the hinge region of folds. The marble is white, medium grained, and usually contains scattered flakes of graphite. It weathers to a light gray color and locally contains fractures that are stained orange. Parts of the marble are dolomitic and phlogopite is present locally.

Unit 3

Structurally above the unit 2 marble is unit 3 which consists of up to several meters of layered calc-silicate rock capped by a massive quartzite layer 1-2 meters thick. The calc-silicate rock is light gray to yellow-green in color and it weathers to a rusty-red color. The mineralogy of the calc-silicate is variable and it contains quartz, clinozoisite, and sphene, \pm actinolite, \pm diopside, \pm biotite, \pm epidote, \pm hornblende, \pm potassium feldspar, \pm plagioclase, \pm wollastonite, \pm garnet, \pm calcite, \pm forsterite, \pm muscovite. The quartzite at the top of unit 3 is light gray in color, commonly vitreous, and usually contains a few percent biotite and/or muscovite that define a weak foliation. The calc-silicate rock is rarely exposed between outcrops of the unit 2 marble and unit 3 quartzite.

Unit 4

Unit 4 consists of well foliated interlayered pelitic and psammitic schist and gneiss with a medium to coarse grained lepidoblastic texture. Phyllonitic fabrics locally are developed in the pelite in the vicinity of the eastern Tehachapi shear zone. The primary metamorphic mineral assemblage in most samples of the pelitic schist examined includes garnet, sillimanite, muscovite, biotite, plagioclase, and quartz. Locally migmatitic textures

are present with millimeter to several centimeter thick leucocratic layers, stringers, and lenses of medium grained quartz and feldspar, \pm garnet, concordantly interlayered with sillimanite and biotite rich layers. Distinctive features of the metapelitic lithology commonly visible in the field include abundant red garnets up to ~2 centimeters in diameter, and coarse grained pale-blue colored elongate aggregates of prismatic sillimanite crystals. The garnets poikilitically enclose biotite, quartz, and sillimanite, and sillimanite occurs both as prismatic crystals and as fibrolitic masses.

All of the pelitic schist samples examined exhibit evidence of retrograde metamorphism. Chlorite and epidote growing around the margins and in the cleavage surfaces of biotite grains are interpreted to be replacing the biotite. Muscovite grains that have grown at high angle to the main foliation in some samples are interpreted to be of secondary origin. Much of the sillimanite in the pelitic samples is replaced by a "shimmer aggregate" of fine grained white mica. The overall color of the schist varies from gray in minimally retrograded areas to dark grayish-green where abundant secondary chlorite is present. The schist weathers to a reddish brown color and it decomposes to a dark brown soil.

Rand Schist

The Rand schist is part of a regionally extensive terrane in southern California of graywacke, basalt, and chert metamorphosed at relatively high P and moderate T and usually exposed beneath low angle faults (Ehlig, 1968; Silver and Nourse, 1986; Jacobson et al., 1988). At the southern edge of the study area Rand schist is exposed between the north and south branches of the high-angle Garlock fault (Sharry, 1981). Small exposures of the Rand schist in the alluvium between Tylerhorse and Horsethief Canyons, however, may be located north of the north branch of the Garlock fault (Figure 4), as will be discussed later. There the schist has a blue-gray color and thin quartzite (metachert ?) layers are interlayered locally with the schist. The single sample of the schist examined in

thin section for this study contains sphene, biotite, muscovite, epidote, quartz, chlorite, and albite, with a small amount of interstitial calcite. The albite is poikilitic, enclosing quartz and what may be graphite, and the biotite appears to be breaking down to chlorite.

INTRUSIVE ROCKS AND ORTHOGNEISS

Plutonic rocks and orthogneiss in the eastern Tehachapi gneiss complex are subdivided into three groups (I, II, and III) based on their composition, fabric, cross-cutting relations, metamorphism, style and degree of deformation, and habit of intrusion. The intrusions within each group appear to have experienced similar deformation and metamorphic histories. Group I consists of a number of small orthogneiss bodies with different compositions, group II consists of voluminous variably deformed plutons ranging in composition from gabbro to tonalite, and group III consists of several intrusions of leucocratic granite (color index ≤ 5). The petrographic names of the plutonic rocks in this study are based on the classification of Streckeisen (1973).

Group I Orthogneisses

The orthogneisses of group I consist of a number of small, strongly deformed, generally tabular shaped intrusive bodies with gneissic fabrics that have compositions ranging from gabbro to granite. The five group I orthogneisses shown in the geologic map (Figure 4) are the mixed tonalite gneiss, the Antelope Canyon garnet hornblende diorite gneiss, the No Name Canyon biotite granite augen gneiss, the Paradise Valley granite gneiss, and the biotite hornblende quartz diorite gneiss. The contacts and foliations of the group I orthogneiss bodies generally are concordant with fabrics in adjacent metasedimentary wallrocks, but locally apophyses of the orthogneiss bodies clearly intrude and crosscut the compositional layering in the adjacent paragneiss. The tabular shape of some of the orthogneiss bodies may be the result of localized intrusion along preexisting structures within the metasedimentary rocks and it also may be the result of subsequent deformation as will be discussed later.

Members of the group I orthogneisses are intruded locally by group II and group III plutons. In contrast to the group II and group III intrusives, the group I orthogneisses everywhere possess well developed gneissic fabrics. Another distinctive feature of the group I orthogneisses is that they generally exhibit in thin-section much less evidence of the retrograde alteration that is ubiquitous in the metasedimentary rocks and in the other intrusive rocks of the study area. The modal mineralogies of the five group I orthogneiss units discussed below are shown in Table 2.

Mixed tonalite gneiss

Scattered exposures of the mixed tonalite gneiss are found in a narrow zone along the southwest margin of the northern structural block, north of the Mountain Park fault. In this area mixed tonalite gneiss intrudes both groups of metasedimentary rocks. The tonalite gneisses consist of well-foliated gray-colored, tan-weathering, medium-grained biotite tonalite that has a granolepidoblastic texture. Variable amounts of hornblende, garnet, cummingtonite, and muscovite locally are present in the tonalite gneiss. The color index of the mixed tonalite gneiss ranges from 4 to 25. Biotite in the gneiss has a deep reddish brown color, and when present, hornblende is brown to green in color. Plagioclase, ranging in composition from An₂₅ to An₃₈, usually is antiperthitic. Subhedral poikilitic garnets enclose biotite, plagioclase and quartz. Some of what has been mapped as the mixed tonalite gneiss unit (Figure 4) may be tonalite that is part of the group II intrusive rocks. In the vicinity of the eastern Tehachapi shear zone (Figure 3) the group II tonalite is severely deformed and it is sometimes difficult to differentiate it from the group I mixed tonalite gneiss.

The tonalite gneiss locally hosts leucocratic veins consisting of medium grained plagioclase and quartz as well as veins that have a granitic composition. The leucocratic veins tend to be more concordant than discordant to the gneissic fabric in the tonalite, and sometimes they form diffuse, irregular patches. These veins frequently host garnets up to

TABLE 2 (CONTINUED). MODAL MINERALOGY OF GROUP I ORTHOGNEISSES IN THE EASTERN TEHACHAPI MOUNTAINS

Sample Number	Primary/Prograde Mineral Assemblage											Secondary/Retrograde Mineral Assemblage															
	C	Qz	Kf	Pl	A	Hb	Bt	Op	Cm	Cx	Ox	Ga	Mu	Sp	Ap	Al	Zr	Ac	Ch	Ep	Sp	Sr	Ca	Sa	Other		
	I																										
Fine grained biotite granite gneiss																											
94-TH-440A	9	30	30	30	nd		9	x			1					x	x	x								x	
94-TH-450	3	32	30	35	nd		3	x								x	x	x								x	

Notes: Cl= color index, AN = anorthite content of plagioclase feldspar estimated using method of Michel-Lévy and/or Carlsbad-albite method, nd = no data.

Mineral name abbreviations: Qz = quartz, Kf = potassium feldspar, Pl = plagioclase feldspar, Hb = hornblende, Bt = biotite, Op = opaques, Cm = cummingtonite, Cx = clinopyroxene, Ox = orthopyroxene, Ga = garnet, Mu = muscovite, Sp = sphene, Ap = apatite, Al = allanite, Zr = zircon, Ac = actinolite, Ch = chlorite, Ep = epidote, Sp = sphene, Sr = sericite, Ca = calcite, Sa = saussuritization of plagioclase feldspar, Pr = prehnite, Cz = clinozoisite, Tr = tremolite, Ab = albite, Gr = graphite, Mo = monazite.

Table entry abbreviations: numbers = modal percentage mineral in sample estimated using percentage diagrams for estimating composition by volume, x = mineral present in amount less than 1 %, xx = present in significant amounts but too fine grained and disseminated or cataclased to reliably estimate modal percentage, r = remnants of formerly more abundant mineral now largely replaced by other minerals, p = primary/prograde mineral in amount less than 1 %, ? = mineral identification equivocal.

~1 centimeter in diameter, and aggregations of millimeter-size garnets commonly are found in the center of the diffuse leucocratic patches. Clumps of subhedral garnets also occur in the tonalite in the vicinity of the veins. The concordance of many of the garnet bearing veins with the foliation in the biotite tonalite gneiss contrasts with the mostly discordant leucocratic veins that frequently host undeformed garnets in the group II dioritic plutons as will be discussed later.

Antelope Canyon biotite garnet hornblende diorite gneiss

The Antelope Canyon diorite gneiss is found on both sides of lower Antelope Canyon (Figure 4) where it intrudes the Antelope Canyon group metasedimentary rocks and is intruded by group II gabbro. The diorite gneiss forms long narrow bodies localized between the limbs of adjacent antiformal folds in the Antelope Canyon group paragneiss which suggests the diorite may have intruded along preexisting structural weaknesses such as faults. The rock is a dark-gray colored moderately-foliated medium-grained biotite hornblende diorite gneiss that hosts abundant garnets (5-20% of the rock) that grow across the fabric in the gneiss. The garnets, up to 7 centimeters in diameter, are found within veins of plagioclase and quartz or in the matrix of the rock surrounded by haloes of plagioclase and quartz. The large garnets commonly have a sieve-like texture and enclose blebs of quartz as well as some grains of hornblende, biotite, plagioclase, and accessory minerals. The gneiss has a foliation defined by the alignment of biotite and hornblende, and in thin section the rock frequently displays a well developed granoblastic polygonal texture with numerous 120° triple junctions among the grains.

The color index of the gneiss ranges from 35 to 45 with hornblende comprising 17-40% of the rock, garnet 5-20% of the rock, and biotite 1-5% of the rock. Hornblende, with olive-tan to dark brown pleochroism, contains abundant inclusions of apatite and opaque minerals. Biotite has tan to deep red-brown pleochroism and it commonly has opaque minerals and lozenges of potassium feldspar growing along its cleavage. Quartz

(1-5% of the rock) is rare in the matrix of the rock, but occurs within the garnets and in the leucocratic haloes surrounding the garnets. Most of the plagioclase has a composition ranging from An17 to An38. Accessory minerals in the diorite gneiss include apatite, allanite, and abundant zircon. Retrograde alteration in this gneiss is relatively minor and consists of local chlorite growth along cracks in the garnets, minor sericitization and saussuritization of plagioclase located preferentially along fractures, and local growth of blue-green colored actinolite around the margins of hornblende crystals.

No Name Canyon augen gneiss

The augen gneiss of No Name Canyon is found in scattered exposures along the southwest part of the northern structural block, northeast of the Mountain Park fault. The largest body of the augen gneiss (0.3 by 1.8 km) is north trending, east dipping, and is located east of Water Canyon road (Figure 4). The No Name Canyon augen gneiss is a strongly deformed gray to tan colored medium to coarse grained biotite (\pm hornblende) granite that is characterized by distinctive augen of white to pink colored potassium feldspar or oligoclase that are up to ~3 centimeters in length. The overall texture of the gneiss is anhedral granular. The large body of augen gneiss east of Water Canyon road is extensively intruded by leucocratic biotite (\pm garnet) granite dikes and sills that are inferred to be from the adjacent group III leucogranite intrusion. The best exposures of contact relations of the augen gneiss are on the mountain slopes just north of the intersection of the Mountain Park fault with the Blackburn Canyon fault. In this area the augen gneiss intrudes the Antelope Canyon group paragneiss and it is intruded by group II gabbro. North of Tehachapi Valley in the Tweedy Creek area there is a biotite granite augen gneiss very similar to the No Name Canyon augen gneiss in composition and structural position. The Tweedy Creek augen gneiss is dated at 113 Ma using the U/Pb method on zircon (Saleeby et al., 1987).

The color index of the No Name canyon augen gneiss ranges from 3 to 20 and biotite is the only mafic mineral in most of the samples examined. The potassium feldspar exhibits Carlsbad and microcline twinning and local myrmekite is preferentially developed along the grain margins of the feldspar that are oriented parallel to the foliation. Antiperthitic plagioclase has a composition that ranges from An₂₁ to An₃₁. In the vicinity of the Mountain Park fault the augen gneiss exhibits extensive retrograde alteration and biotite is replaced by epidote and chlorite and plagioclase is extensively saussuritized. There appear to be two generations of biotite present in some thin sections, one generation is oriented parallel to the main gneissic fabric in the granite and the other is oriented at a high angle to that fabric.

Paradise Valley granite gneiss

The Paradise Valley granite gneiss is a long narrow body of white to tan colored, fine to medium grained muscovite, garnet, biotite granite gneiss located along the south margin of the Brite Valley pendant west of Paradise Valley. A few small scattered bodies of similar appearing granite gneiss too small to show at the scale of the map in Figure 4 are found within the paragneiss along strike to the southeast and are inferred to be part of the unit. Contacts showing crosscutting relationships of this unit with adjacent paragneiss and group II gabbro were not observed, but the orientation and intensity of the deformation fabrics in the gneiss suggest it was deformed along with the paragneiss prior to intrusion of the adjacent group II gabbro, and thus belongs with the group I orthogneisses. The granite has a well defined gneissic foliation defined by the alignment of flattened and recrystallized biotite, quartz, and feldspar grains.

The rock shows evidence of recrystallization and new mineral growth after development of the strong gneissic fabric. Undeformed subhedral reddish colored garnets 1 to 4 millimeters in diameter clearly grow across the fabric of the gneiss which is defined by the parallel alignment of red-brown colored biotite and flattened aggregates of

recrystallized quartz and feldspar. Some of the garnet crystals enclose kinked biotite grains. Locally, secondary muscovite grains grow at a high angle to the main foliation. Quartz grains, some containing minute needles of an opaque mineral (rutile ?), commonly exhibit a polygonal texture with 120° grain boundary triple junctions. Biotite has a red-brown color except in the vicinity of garnet crystals where it sometimes has a green color. Locally ragged biotite grains are surrounded by muscovite and opaque minerals suggesting it is breaking down.

Biotite hornblende quartz diorite gneiss

Small bodies of quartz diorite gneiss are found in the Antelope Canyon group metasedimentary rocks throughout the study area, but the only exposures large enough to show in Figure 4 are found in the northern part of the study area, 1 to 2 km southeast of the intersection of Highline and Water Canyon roads. Contacts of the quartz diorite gneiss unit with the Antelope Canyon group paragneiss are tectonically transposed and a clear intrusive relationship is not evident, but the quartz diorite gneiss is intruded by group II gabbro and group III leucogranite. The rock is a dark gray colored (color index of 33 to 50) fine to medium grained biotite hornblende (\pm cummingtonite, \pm clinopyroxene, \pm orthopyroxene) quartz diorite to diorite gneiss. Olive to brown colored hornblende is locally cored by cummingtonite or clinopyroxene, and biotite has a reddish brown color. The composition of the plagioclase ranges from An₃₅ to An₄₇.

In most areas the quartz diorite gneiss has a prominent foliation defined by the alignment of biotite, hornblende, and plagioclase grains, but locally the gneiss has a well developed granoblastic texture without an obvious foliation. In some areas the gneiss is intruded by dikes and sills of biotite tonalite that both share and crosscut the fabric in the gneiss, and in some cases the dikes appear to have been completely transposed into the fabric of the gneiss. Secondary alteration in the gneiss includes growth of blue-green

colored actinolite on the hornblende, replacement of the biotite by chlorite, and growth of fine grained sericite in the plagioclase.

Group II Intrusives

The group II intrusives of the eastern Tehachapi gneiss complex consist of a large igneous complex composed of gabbro, diorite, and tonalite, called the Tehachapi Intrusive Complex, and a small body of olivine gabbro called the Highline gabbro. The group II plutons intrude the orthogneisses of group I and they are intruded by the leucogranites of group III. The group II plutons are not as pervasively deformed as are the group I orthogneisses. A modest high temperature solid-state foliation is developed throughout much of the study area in the group II plutons, and intense gneissic and mylonitic fabrics in the group II rocks are developed within and adjacent to the eastern Tehachapi shear zone and in the lowest structural levels of the southern structural block in the vicinity of the Oak Creek mylonite zone (Figure 3).

Tehachapi Intrusive Complex

The Tehachapi Intrusive Complex is composed of two major groups of lithologies, hornblende gabbro, diorite, and quartz diorite (hereafter referred to as gabbro), and biotite hornblende tonalite and quartz diorite (hereafter referred to as tonalite). The gabbro and tonalite of the Tehachapi Intrusive Complex comprise the largest part of the eastern Tehachapi gneiss complex, and they intrude both groups of metasedimentary rocks and the group I orthogneisses in all three structural blocks of the study area, as shown in Figure 4. In the more deformed parts of the Tehachapi Intrusive Complex igneous textures are largely obliterated and gabbro is recrystallized into a locally foliated fine grained amphibolite gneiss and tonalite exhibits a penetrative gneissic to mylonitic fabric. The amphibolite and tonalite gneiss are continuous, however, with less deformed parts of the Tehachapi Intrusive Complex where inferred primary igneous textures are preserved.

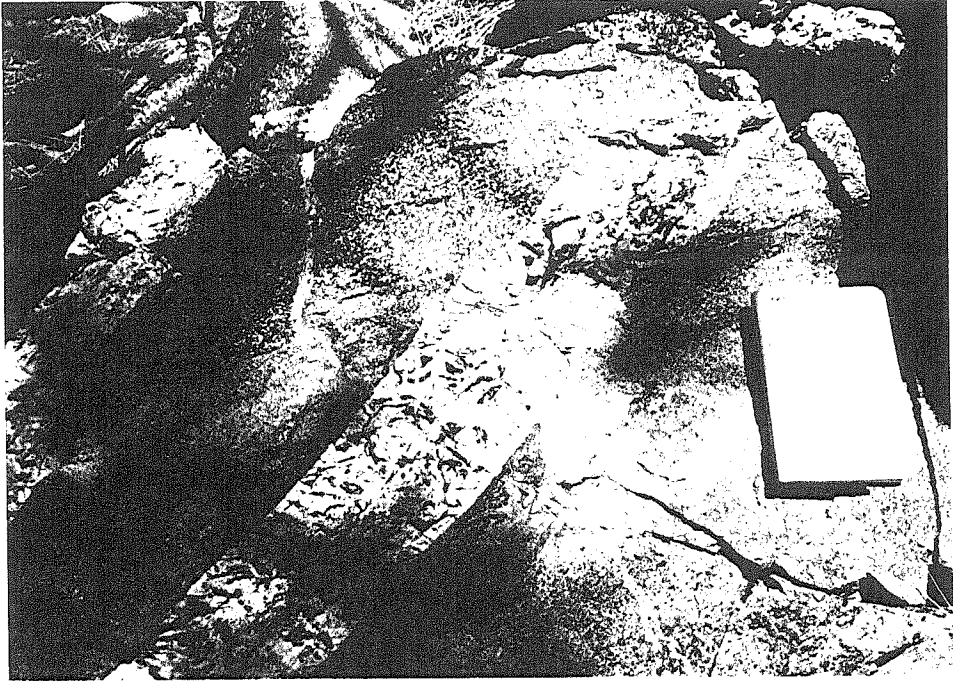
Contact relationships between the gabbro and tonalite are variable. In some areas both units are intimately intermingled over a wide interval and in other locations the contacts are sharp with veins of tonalite intruding the gabbro or undeformed gabbro enclosing gneissic tonalite. Veins of tonalite are both concordant and discordant to the fabric in the gabbro. Fine grained mafic-rich enclaves and schlieren of gabbroic composition also are ubiquitous in the tonalite. Contacts between the two units tend to become better defined within the more deformed parts of the gneiss complex because the quartz bearing tonalite generally exhibits a stronger gneissic fabric than does the gabbro. Many of the contacts between the gabbro and tonalite south of the eastern Tehachapi shear zone are gradational in character and the contacts in that area shown in Figure 4 are approximately located between regions dominated by gabbro and areas dominated by tonalite. Throughout most of the area the gabbro appears to structurally underlie the tonalite. The mutual crosscutting relations and the close association of the gabbro with the tonalite suggests that the two units may be comagmatic.

Gabbro of the Tehachapi Intrusive Complex

The gabbroic portion of the Tehachapi Intrusive Complex consists of dark gray colored, fine to coarse grained, equigranular hornblende (\pm cummingtonite, \pm clinopyroxene, \pm orthopyroxene, \pm biotite) gabbro, diorite, and local quartz diorite with an anhedral to subhedral granular texture. The intensity of fabric development in the gabbro is variable. In some areas the gabbro is massive with no discernible fabric, in other areas a weak to moderate foliation is defined by the alignment of mafic minerals (Figure 8A), and in some areas within the eastern Tehachapi shear zone the gabbro has a strong gneissic fabric and leucocratic veins have been transposed into parallelism with the fabric (Figure 8B). South of the eastern Tehachapi shear zone in the vicinity of Tehachapi Mountain and Peak 7777' (Figure 4) textural features inferred to be of primary igneous origin, such as comb layering and the rhythmic alternation of hornblende and plagioclase-rich

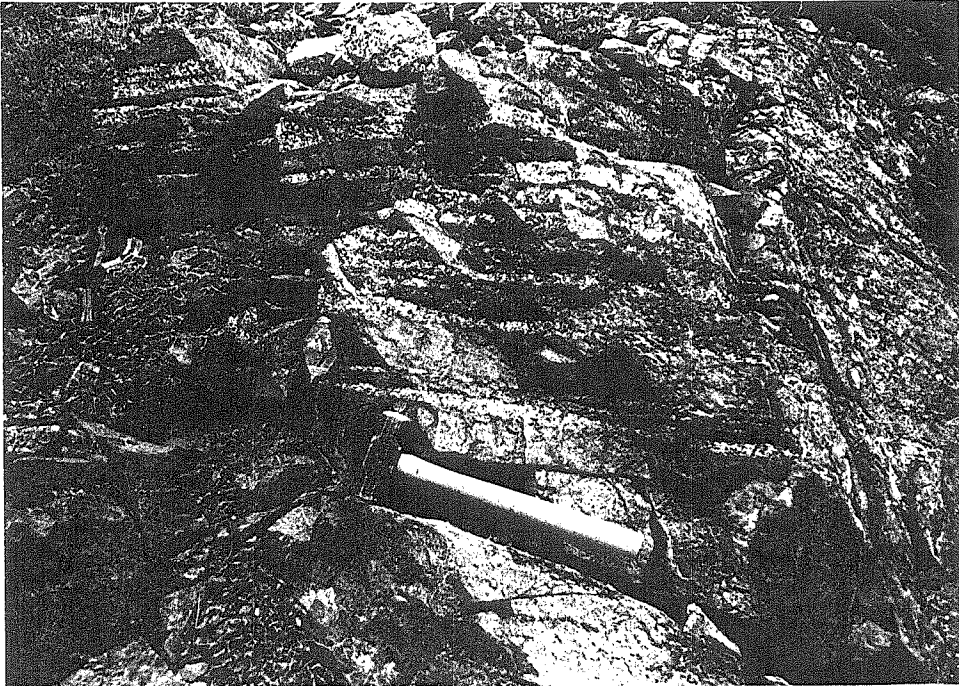
Figure 8.

A) Photograph of moderately deformed gabbro of the Tehachapi Intrusive Complex from a locality south of the eastern Tehachapi shear zone near Peak 7777'. View is towards the E-NE. Field notebook is resting on medium grained hornblende gabbro which has a high temperature subsolidus foliation (running from middle upper right to middle lower left in the photo) that dips moderately to the NE. Left of the field notebook are two crosscutting hornblende tonalite pegmatitic dikes (running from upper right to lower left in the photograph). Aligned hornblende grains in the dikes define a weak foliation that is subparallel to the foliation in the host gabbro suggesting some foliation development occurred after emplacement of the dikes. Field notebook is 19 centimeters tall. B) Photograph of severely deformed gabbro of the Tehachapi Intrusive Complex from a locality in the eastern Tehachapi shear zone on Astronomy Ridge. View is towards the N. The rock is composed of dark gray layers of fine grained amphibolite gneiss alternating with light colored layers of medium grained hornblende tonalite gneiss (layering runs left to right across the photo). The gneissic foliation dips shallowly towards the NE and the hornblende in this rock is extensively altered to chlorite and epidote. The tonalitic layers in the gneiss are interpreted to be dikes similar to the ones in Figure 8A that have been transposed into parallelism with the low-angle shear zone fabric. The length of the hammer head is 13 centimeters and the length of the hammer is 40 centimeters.



A

B



compositional layers that is suggestive of cumulate layering, are present in the gabbro. The large exposure of gabbro south of the Taco Saddle fault in the study area appears to be continuous to the northwest with a belt of amphibolite and hypersthene bearing mafic-rich rocks mapped within the Bear Valley Springs tonalite east and south of Cummings Valley by Ross (1989b).

The gabbroic rocks are distinguished from the tonalite by their color indices which range from ~30 to 50, the low abundance or absence of biotite, and the generally low abundance of quartz (usually less than 10%) which is mostly interstitial. See Table 3 for the modal mineralogy of the gabbroic rocks of the Tehachapi Intrusive Complex. Hornblende, comprising 15-45% of the gabbro, is pleochroic in shades of brown, commonly contains a patchy distribution of opaque minerals and locally is intergrown with, or surrounds cummingtonite. Orthopyroxene and clinopyroxene are both found as skeletal cores in hornblende and cummingtonite grains. In the least deformed or altered sample of the gabbro examined exsolution textures are preserved in the pyroxenes with lamellae of clinopyroxene present in the orthopyroxene and lamellae of hornblende present in the clinopyroxene. Biotite, when present, is irregularly distributed and generally is not found inside hornblende suggesting it may be a late crystallizing phase. Plagioclase ranges from andesine through labradorite in composition and in the least deformed samples the plagioclase exhibits normal zoning.

Tonalite of the Tehachapi Intrusive Complex

The tonalitic part of the Tehachapi Intrusive Complex consists of medium to light gray colored, medium grained, well-foliated biotite hornblende (\pm cummingtonite, \pm clinopyroxene, \pm orthopyroxene) tonalite, and quartz diorite that has an anhedral to subhedral granular texture. In the less deformed parts of the eastern Tehachapi gneiss complex the tonalite contains abundant fine-grained mafic enclaves and schlieren that are concordant with the foliation. The tonalite of the Tehachapi Intrusive Complex in the study

TABLE 3 (CONTINUED). MODAL MINERALOGY OF GROUP II GABBRO, DIORITE, AND QUARTZ DIORITE IN THE EASTERN TEHACHAPI MOUNTAINS

Sample Number	Primary/Prograde Mineral Assemblage													Secondary/Retrograde Mineral Assemblage										
	C	Qz	Kf	Pl	A	Hb	Bt	Op	Om	Cx	Ox	Other	Sp	Ap	Zr	Ac/Cl	Ch	Ep	Cz	Sp	Sr	Ca	Sa	Other
92-TH-236	35	6	59	nd	15	r?	x						x	x	10	10	x		x	x		xx	Zl-x	
93-TH-254	30	3	67	38	20	x	x	x		10			x	x	x	x		x						
92-TH-261B	nd	10	xx	nd	xx		x					x			xx	xx	xx					xx	xx	Zl-xx
93-TH-343	20	3	71	56	15		1	5							x	3	2							Ab-xx
93-TH-378	45	3	52	13	20		x								x	10	15		x		x	xx		
93-TH-397	26	15	59	44	14	7	x	3		1				x	x	x					x	x		
94-TH-464A	50		50	71	15		x		20	15					x	x					x			

Leucocratic marginal tonalite phase of gabbro, diorite, and quartz diorite of Tehachapi Intrusive Complex

91-TH-108	13	46	40	27		1	x								x	x				x	x			Zo-x
91-TH-167	26	40	34	40	2	r	1	3							x	x	x							
93-TH-390A	15	40	45	32		x	x								x	x								
93-TH-390B	10	45	45	45	3	x	1	4							x	x								

Notes: Cl= color index, AN = anorthite content of plagioclase feldspar estimated using method of Michel-Lévy and/or Carlsbad-albite method. Mineral name abbreviations: Qz = quartz, Kf = potassium feldspar, Pl = plagioclase feldspar, Hb = hornblende, Bt = biotite, Op = opaques, Cm = cummingtonite, Cx = clinopyroxene, Ox = orthopyroxene, Ga = garnet, Ol = olivine, Sh = spinel, Mu = muscovite, Sp = sphene, Ap = apatite, Al = allanite, Zr = zircon, Ac/Cl = actinolite/calcic clinopyroxene, Ch = chlorite, Ep = epidote, Cz = clinozoisite, Sp = sphene, Sr = sericite, Ca = calcite, Sa = saussurization of plagioclase feldspar, Zl = zeolite, Pr = prehnite, Pm = pumpellyite, Cl = clay, Zo = zoisite, Ab = local albization of plagioclase, Se = serpentine.

Table entry abbreviations: numbers = modal percentage mineral in sample estimated using percentage diagrams for estimating composition by volume, x = present in amounts less than 1 %, xx = present in significant amounts but too fine grained and disseminated or cataclased to reliably estimate modal percentage, r = remnants of formerly more abundant mineral now largely replaced by other minerals, ? = mineral identification equivocal.

area appears to be continuous with the Bear Valley Springs tonalite to the north and west as well as with the hypersthene tonalite of Bison Peak to the south, both of which are well dated by the U-Pb method on zircons at about 100 Ma (Saleeby et al., 1987).

The tonalitic rocks are distinguished from the gabbro by their more moderate color index (15 to 35), the moderate abundance of biotite (typically 10-20%), and the abundance of quartz (15-30%). See Table 4 for the modal mineralogy of the Tehachapi Intrusive Complex tonalitic rocks. Green to brown colored hornblende comprises 10-25% of the tonalite and it poikilitically encloses quartz, biotite, and plagioclase, while clinopyroxene and orthopyroxene, when present, comprise only 1-2% of the rock. Orthopyroxene was found only in a few samples from the southern structural block consistent with the observations of hypersthene in the tonalite of Bison Peak by Sharry (1981). Antiperthitic plagioclase is andesine in composition. Accessory minerals in the tonalite include allanite that is frequently rimmed by epidote, sphene found in anhedral granular aggregates, apatite, and zircon. Euhedral, possibly primary, sphene appears to be present only in the tonalite of the north structural block as discussed below.

Pine Tree tonalite

The Tehachapi Intrusive Complex tonalite in the northern structural block is exposed over an area of about 12 square km yet it has an apparent thickness of no more than several hundred meters so it has the form of a relatively thin sheet with an overall shallow dip to the northeast. This sheet of tonalite, called the Pine Tree tonalite, is differentiated here from the other tonalite of the Tehachapi Intrusive Complex because locally it has a different composition and texture, and, as will be discussed later, its structural position in the gneiss complex and its sheetlike form may have been controlled by a preexisting structure. North of Tehachapi Valley in the Tweedy Creek area a narrow tonalite body that is correlated with the Pine Tree tonalite, for reasons to be discussed later, has been dated at 97 Ma using the U/Pb method on zircons (Saleeby et al., 1987).

TABLE 4 (CONTINUED). MODAL MINERALOGY OF GROUP II TONALITE IN THE EASTERN TEHACHAPI MOUNTAINS

Sample Number	Primary/Prograde Mineral Assemblage										Accessories					Secondary/Retrograde Mineral Assemblage											
	C	Qz	Kf	Pl	A	Hb	Bt	Op	Om	Cx	Ox	Al	Sp	Ap	Zr	Ac	Ch	Ep	Cz	Sp	Sr	Ca	Sa	Other			
93-TH-331A	20	25	x	55	nd	3	17	x			x		x	x	x	x	x	x	x	xx	x						
93-TH-331B	15	30		51	30	8	7	x					x	x	x	x				x	x						
93-TH-332	38	5	x	57	43	25	13	x	?				x	x	x				x	x							
93-TH-346	15	30		54	34	x	13	x			1		x	x	x				x	x							
93-TH-356B	nd	xx	x	xx	nd			x								xx	xx		x					Zl-x			
93-TH-365	27	25		48	42	16	8	x			x		x	x	x	1			x	1							
93-TH-373	27	16		57	23	23	2	x					x	2		x				x							
93-TH-393A	23	20	x	57	40	10	r				x		x	x	13	x			x	x							
93-TH-395	12	25	1	63	nd		r	x					?		10	2			x	xx							
93-TH-405A	23	20		55	28	1	1	x			x		x	x	20	1			x	x	1			Kf-x			
94-TH-452	30	15		55	44	22	7	x	1				x	x						x							
<u>South (Double Mountain) structural block tonalite of Tehachapi Intrusive Complex</u>																											
90-TH-27	30	15		54	43	20	9	x	1	1			x	x	x	x			x						x		
92-TH-213	25	17		58	43	15	10		r?	r?			x	x	x	x			x						Pr-?		
92-TH-240	30	18		52	nd	20	5						x	x	5	x									xx		
92-TH-243	35	7		58	38	29	2	x	x				x	x	2	x			x						Pr-2,Zl-?		
92-TH-251	40	15		40	38	25	r?	x					x	x	7	8			x						xx		
92-TH-252	33	7		60	43	26	3	x	3	1			x	x	x	x			x						Pr-x		
92-TH-253	30	6		64	45	23	3	x	1	x	1		x	x	2	x			x						x		
92-TH-256B	26	10	x	64	43	15	10	x	1	x			x	x													
93-TH-371	35	20		45	nd	10r	r	x			x		x	x	15	10			x	x					xx		
94-TH-453	35	17		42	42	18	10	x	r				x	x	7	x			x						Pr-x		

Notes: Cl= color index, AN = anorthite content of plagioclase feldspar estimated using method of Michel-Lévy and/or Carlsbad-albite method, nd = no data. Mineral name abbreviations: Qz = quartz, Kf = potassium feldspar, Pl = plagioclase feldspar, Hb = hornblende, Bt = biotite, Op = opaques, Cm = cummingtonite, Cx = clinopyroxene, Ox = orthopyroxene, Al = allanite, Sp = sphene, Ap = apatite, Zr = zircon, Ac = actinolite, Ch = chlorite, Ep = epidote, Cz = clinozoisite, Sr = sericite, Ca = calcite, Sa = saussurization of plagioclase feldspar, Zl = zeolite, Pr = prehnite.

Table entry abbreviations: numbers = modal percentage mineral in sample estimated using percentage diagrams for estimating composition by volume, x = present in amounts less than 1 %, xx = present in significant amounts but too fine grained and disseminated or cataclased to reliably estimate modal percentage, r = remnants of formerly more abundant mineral now largely replaced by other minerals, ? = mineral identification equivocal.

The composition of the Pine Tree tonalite locally ranges to granodiorite and it is the only intrusive rock in the eastern Tehachapi gneiss complex that contains primary (?) euhedral wedge-shaped sphene crystals (see Table 4). Aggregates of later crystallizing or secondary granular sphene are also present in the Pine Tree tonalite. The Pine Tree tonalite is also characterized by the local presence of relatively large (up to ~1 centimeter in length) euhedral phenocrysts of turbid milky white colored plagioclase and blue-green colored hornblende. The orientation of the foliation changes throughout the eastern end of the Pine Tree tonalite and commonly it is concordant to the wallrocks it intrudes and discordant to the regional trend of the foliation in the rest of the Tehachapi Intrusive Complex.

Veins and irregularly shaped patches of medium to coarse grained plagioclase and quartz (\pm hornblende, \pm garnet) occur locally in both the gabbro and tonalite of the Tehachapi Intrusive Complex. Some of the garnets growing in the gabbro are large, up to 6 centimeters in diameter. Many of these garnet bearing veins and patches appear to postdate much of the fabric development in the orthogneiss. In the study area the late tectonic veins and feldspathic patches with abundant garnets frequently are found within 100 to 200 meters on either side of the two ductile faults in the gneiss complex. The contact zone between the gabbro and the tonalite of the Tehachapi Intrusive Complex also seems to be a common location for the growth of these syn- to post-tectonic garnets. At some gabbro-tonalite contacts medium to coarse grained leucocratic veins of tonalite hosting euhedral centimeter size hornblende crystals also invade and crosscut the gabbro.

Almost all samples of the gabbro and tonalite of the Tehachapi Intrusive Complex examined petrographically contain retrograde alteration mineral assemblages. Within the eastern Tehachapi shear zone the alteration commonly is so severe that only relicts of the original mineralogy remain. Hornblende in the gabbro frequently is rimmed by pale green colored acicular actinolite. In the gabbro and tonalite the hornblende also is replaced by aggregates of chlorite and epidote. Much of the biotite is pseudomorphed by chlorite or

replaced by aggregates of granular epidote, sphene, and opaque minerals. Plagioclase usually hosts a fine grained aggregate of sericite and saussurite that frequently is concentrated in the cores of the grains. Locally, the plagioclase grains are mantled by light colored rims of albite, or the plagioclase is cracked and albite appears to line the cracks. Calcite is sometimes found in the interstices of the grains in the rock and also within plagioclase grains. Fractures developed at high angle to the fabric in the tonalite commonly are filled with potassium feldspar.

Highline olivine gabbro

The Highline gabbro is a small tabular shaped intrusion located southeast of the intersection of Highline and Water Canyon roads. The gabbro intrudes metasedimentary rocks of the Antelope Canyon group and group I quartz diorite gneiss, and it is intruded by the Brushy Ridge group III leucogranite. Most of the Highline gabbro lacks a discernible foliation and appears undeformed. A moderate gneissic fabric, however, is developed along the southwest margin of the intrusive where it is closest to the eastern Tehachapi shear zone. The Highline gabbro is a medium to coarse grained dark gray olivine orthopyroxene clinopyroxene gabbro with a subhedral inequigranular seriate texture. See Table 3 for the modal mineralogy of the gabbro. Parts of the gabbro are leucocratic and the color index of the gabbro ranges from 28 to 72. The minerals in the gabbro have well developed reaction textures. Where olivine grains (Fo85 composition) are adjacent to plagioclase the olivine is rimmed by a layer of pale brown colored orthopyroxene. The orthopyroxene, in turn, is rimmed by a layer of pale greenish brown colored hornblende intergrown with elongate blebs of pale green colored spinel that is adjacent to the plagioclase. Pale pink colored patchy clinopyroxene crystals are intergrown with hornblende and are surrounded by a rim of hornblende where adjacent to plagioclase.

The Highline gabbro differs from the gabbro in the Tehachapi Intrusive Complex in a number of respects. Olivine is relatively abundant in the Highline gabbro (3-18%), but

olivine was not observed in the Tehachapi Intrusive Complex gabbro. The plagioclase in the Highline gabbro is more calcic (An75 to An80) than the plagioclase of the gabbro of the intrusive complex (mostly An45 to An60). The Highline gabbro is also intruded by several N-NW trending subvertical plagiogranite dikes, and similarly oriented dikes are not present in the Tehachapi Intrusive Complex. The plagiogranite dikes are 1 to 2 meters thick and they are discontinuously exposed along the same trend across the full width of the exposed gabbro. The dikes also intrude the group I biotite hornblende quartz diorite orthogneiss and the paragneiss immediately adjacent to the gabbro, but the dikes appear to be truncated by the group III Brushy Ridge leucogranite.

The dikes are medium grained to pegmatitic and they are composed of sodic plagioclase (An18 to An27) and quartz. Small amounts of biotite, centimeter-scale books of muscovite, and pinhead sized garnets are present locally in the dikes which generally have a color index ≤ 5 (Table 3). The contact of the dikes with the gabbro is sharp and at the contact the texture of the dike is granoblastic. Immediately adjacent to the contact hornblende in the gabbro is locally replaced by sphene, and biotite is replaced by chlorite. The close spatial association of the dikes with the gabbro, the generally coarse grained nature of the dikes, the local presence of annealed textures in the dike margin as opposed to chilled margin textures, the presence of muscovite and biotite, and the localized alteration of the gabbro at the dike contact all suggest the plagiogranite may be a late volatile-rich differentiate of the gabbro that intruded while the gabbro was still relatively hot. Locally, the dikes are deformed and have a steeply dipping proto- to ultramylonitic foliation oriented subparallel to the dike walls with a subhorizontal to shallow NW plunging mineral lineation. The sense of shear of this mylonitic foliation is sinistral based on mica fish and the obliquity of recrystallized quartz grains relative to the mylonitic foliation.

Group III Intrusives

The group III intrusives of the eastern Tehachapi gneiss complex consist of several small bodies of leucocratic granite which intrude both groups of metasedimentary rocks and intrude group II orthogneisses and group III plutons. No other rocks intrude the leucocratic granites which suggests they are among the youngest plutonic rocks in the gneiss complex. Some of the leucogranite bodies appear undeformed while other bodies of the leucogranite possess fabrics that range from a very weak foliation to a well-developed penetrative protomylonitic foliation.

Brushy Ridge granite and other leucocratic granites

There are four bodies of group III leucocratic granite in the study area large enough to show at the scale of the map in Figure 4. The largest body, called the Brushy Ridge leucogranite, is exposed on a ridge in the northernmost part of the study area (Figure 4). The Brushy Ridge leucogranite has the form of a thin sheet and it intrudes between the Pine Tree tonalite below and mixed ortho- and paragneiss above (see cross sections in Plate 3). South of the Brushy Ridge granite another sheet of granite, called the Pine Tree leucogranite, intrudes between the Pine Tree tonalite above, and the No Name Canyon augen gneiss below. In the vicinity of these two sheets of leucogranite the Pine Tree tonalite is intruded by numerous subvertical northeast trending dikes of leucocratic granite that are inferred to be offshoots of the leucogranite in the sheets. The third body of group III granite intrudes the metasedimentary rocks just west of Antelope Canyon. The paragneiss at this locality dips into and beneath the granite suggesting that the granite is structurally above the metasedimentary rocks. The fourth body of granite is exposed in the center of the alluvium of Brite Valley and south of the valley where it intrudes paragneiss.

These group III granites are medium to coarse grained, leucocratic (color index ≤ 5), and contain plagioclase of oligoclase composition (13-30%), perthitic potassium feldspar exhibiting microcline and Carlsbad twinning (35-60%), quartz (24-40%), and biotite (1-

5%), \pm garnet, \pm muscovite. The modal mineralogies of the group III leucocratic granites are shown in Table 5. Part of the Pine Tree granite is pegmatitic and contains centimeter-size books of muscovite and subhedral red garnets 1-2 millimeters in diameter in addition to biotite. Biotite in the Pine Tree granite is inhomogeneously distributed and in some areas it is concentrated in scattered oval shaped patches that are flattened and smeared out in the plane of foliation. The granite in Brite Valley is distinctive locally because it contains flakes of graphite visible to the naked eye. The group III leucogranites are compositionally similar to the granite of Tehachapi Airport mapped by Ross (1989b) north of Tehachapi Valley. Miller et al. (1996) suggest that the granite of Tehachapi Airport may be part of a group of distinctive muscovite and garnet bearing granites found in the Mojave Desert region. The presence of graphite in some of the group III leucocratic granitic rocks also suggests that they may be part of a belt of "strongly contaminated and reduced" granites found in the Sierra Nevada to the north (Ague and Brimhall, 1987; Ague and Brimhall, 1988b).

Fabrics in the group III granites are variable. The Brushy Ridge granite has a pervasive penetrative gneissic to protomylonitic fabric. The Pine Tree granite is moderately foliated and is cut by non-penetrative shear planes. The Brite Valley granite is largely unfoliated.

OAK CREEK PASS COMPLEX

The Oak Creek Pass complex comprises the hangingwall of the Blackburn Canyon detachment fault and it consists of a number of fault bounded structural plates (Figure 3) composed of cataclastically deformed granitic rocks, local metavolcanic (?) rocks, and arkosic and conglomeratic sedimentary rocks (Figure 4 and Plates 1 and 4). The granitic rocks of the Oak Creek Pass complex are referred to as the group IV intrusive rocks to distinguish them from the intrusive rocks of groups I through III found in the eastern Tehachapi gneiss complex. The only wallrocks for the group IV intrusive rocks are several

TABLE 5. MODAL MINERALOGY OF GROUP III LATE DEFORMATION LEUCOGRANITES

Sample Number	Primary/Prograde Mineral Assemblage											Secondary/Retrograde Mineral Assemblage																	
	C	Qz	Kf	Pl	A	Hb	Bt	Op	Cm	Cx	Ox	Ga	Gr	Sp	Ap	Al	Zr	Ac	Ch	Ep	Mu	Sp	Sr	Ca	Sa	Other			
<u>Brushy Ridge leucogranite</u>																													
90-TH-3	2	25	60	13	nd		2	x							x	x	x												
90-TH-9	2	30	48	20	25		2	x							x	x	x												
92-TH-269	1	35	35	30	nd		1								x	x	x										Kf-x		
93-TH-306	1	34	45	20	nd		1	x							x	x	x												
93-TH-307	3	30	40	27	23		3	x							x	x	x												
94-TH-443	5	40	35	20	24		5	x							x	x	x												
94-TH-485	3	35	40	22	nd		3	x							x	x	x											Op-x	
94-TH-487	2	24	50	24	30		2								x	x	x												
<u>Pine Tree leucogranite</u>																													
90-TH-20	0	35	40	25	nd		x								x	x	x												x
91-TH-134	3	32	40	25	nd		r					3			x	x	x												
92-TH-222	1	30	50	19	32		1	x							x	x	x												
93-TH-323A	2	38	40	20	26		2	x							x	x	x												
93-TH-328	1	34	35	30	nd		1								x	x	x												
93-TH-414	1	25	50	24	nd		1								x	x	x												x
<u>Brite Valley graphite leucogranite</u>																													
94-TH-427	1	30	50	19	31		x	x				1	x		x	x	x												

Notes: **CI** = color index, **AN** = anorthite content of plagioclase feldspar estimated using method of Michel-Lévy and/or Carlsbad-albite method, **nd** = no data.

Mineral name abbreviations: Qz = quartz, Kf = potassium feldspar, Pl = plagioclase feldspar, Hb = hornblende, Bt = biotite, Op = opaques, Crn = cummingtonite, Cx = clinopyroxene, Ox = orthopyroxene, Ga = garnet, Sp = sphene, Ap = apatite, Al = allanite, Zr = zircon, Ac = actinolite, Ch = chlorite, Ep = epidote, Cz = clinzoisite, Sp = sphene, Sr = serfite, Ca = calcite, Sa = saussurization of plagioclase feldspar, Gr = graphite.

Table entry abbreviations: numbers = modal percentage mineral in sample estimated using percentage diagrams for estimating composition by volume, x = present in amounts less than 1 %, xx = present in significant amounts but too fine grained and disseminated or cataclased to reliably estimate modal percentage, r = remnants of formerly more abundant mineral now largely replaced by other minerals, ? = mineral identification equivocal.

very small pendants of metavolcanic (?) rocks. Arkosic sediments and conglomerate of the Witnet Formation locally deposited on top of the granitic rocks are treated as part of the Oak Creek Pass complex. The locations of these units are shown in Figure 4.

METAVOLCANIC ROCKS

There are no metasedimentary rocks in the Oak Creek Pass complex. There are, however, a few small northeast trending pendants of silicic metavolcanic rocks located in the granitic rocks of the lower plate of the Oak Creek Pass complex north of the Mendiburu fault (Figures 3 and 4). This third group of batholith wallrocks in the study area is called the Oaks metavolcanic rocks.

Oaks Metavolcanic Rocks

In the lower plate of the Oak Creek Pass complex there are several small exposures of inferred metavolcanic rocks that occur as northeast trending steeply dipping pendants in granodiorite. The largest exposure consists of a foliated compositionally banded greenish-gray colored aphanitic silicic rock that contains flattened light and dark colored lithic fragments as well as small phenocrysts of biotite and feldspar. Local thin streaks of quartz may be flattened quartz phenocrysts. At another locality close to the Blackburn Canyon detachment fault there is a similar appearing rock although there the rock is moderately tectonized. At one other exposure, however, the rock consists of a black colored aphanitic glassy appearing groundmass that contains abundant lozenge shaped lithic fragments, 1-5 centimeters long and 0.5-3 centimeters wide, of various lithologies, including quartzite, medium grained quartz and feldspar porphyry, and calc-silicate rock.

At all the localities the Oaks metavolcanic rocks exhibit a flattening fabric, evidenced by flattened phenocrysts and lithic fragments, that locally is overprinted with a hornfelsic texture presumably related to intrusion of the granodiorite. In thin section the microcrystalline matrix of the well foliated rock consists of a mosaic of 0.01 to 0.02 millimeter grains of quartz, potassium feldspar, plagioclase of oligoclase composition,

biotite, muscovite, and opaques, \pm garnet, \pm hornblende. Potassium feldspar and quartz each comprise ~35% of the rock, plagioclase 20%, and biotite 10%. Compositional layering is defined by layers richer in biotite or potassium feldspar and may be relict flow banding. The aphanitic groundmass, feldspar phenocrysts, flattened (?) quartz phenocrysts (?), lithic fragments, possible relict flow banding, and composition all suggest the protolith of this rock is a metamorphosed silicic (dacitic to rhyolitic) volcanic rock.

INTRUSIVE ROCKS

Group IV Granitic Rocks

The group IV intrusive rocks are found on the east side of the study area in the hangingwall of the Blackburn Canyon detachment fault and they comprise most of the Oak Creek Pass complex. Most of the group IV rocks are granodiorite to monzogranite (subfield 3b in the center of the QAP triangle of Streckeisen (1973)) in composition. These granitic rocks are deeply weathered and covered by a thick mantle of grus. The best exposures of the group IV rocks are found in roadcuts, the walls of deeply incised gullies, and in small outcrops immediately adjacent to resistant aplite dikes and Tertiary hypabyssal dikes. Most of the group IV rocks are cataclased and hydrothermally altered to some degree which may have contributed to the development of the deep zone of weathering. Three different igneous units are defined in the group IV rocks, the Bootleg Canyon granodiorite, the Mendiburu Canyon granodiorite, and the Old West Ranch monzogranite. All of these group IV granitic rocks are part of what Ross (1989b) maps as the Whiterock facies of the granodiorite of Claraville, and what Dibblee and Louke (1970) map as quartz monzonite.

Bootleg Canyon granodiorite

The Bootleg Canyon granodiorite is named after Bootleg Canyon in the southwestern part of the Oak Creek Pass complex. The best exposures of the granodiorite occur in Bootleg canyon and along the ridge-top north of the canyon. Ross (1989a)

originally mapped a granodiorite he named after Bootleg Canyon, but subsequently he included it with a unit he calls the "Whiterock" facies of the granodiorite of Claraville (Ross, 1989b). The lower structural plate and the north and south middle structural plates of the Oak Creek Pass Complex are composed solely of the Bootleg Canyon granodiorite (Figures 3 and 4). The Bootleg Canyon granodiorite of the lower plate is partly nonconformably overlain by the Witnet Formation. The southern contact of both units is the Mendiburu fault. The Bootleg Canyon granodiorite of the middle plates is bounded to the west by the Blackburn Canyon fault, to the north by the Mendiburu Canyon fault, to the south by the Garlock fault, and to the east by the Quail Canyon fault and an inferred fault buried beneath the alluvium of Blackburn Canyon.

The Bootleg Canyon granodiorite is a medium grained equigranular sphene hornblende biotite granodiorite with a color index of ~20. Locally the granodiorite has a distinctive appearance with prominent euhedral 1 to 3 millimeter size grains of black hornblende, black biotite, and amber sphene scattered throughout a matrix of feldspar and quartz that is markedly white in color. The whitish color of the leucocratic minerals may in part be due to saussuritization of the plagioclase and fine-scale fracturing and granulation of the quartz. The granodiorite is non- to poorly foliated, but most exposures of the rock exhibit evidence for cataclasis in the form of variably oriented fractures and shear planes that are greenish in color due to secondary chlorite and epidote mineralization. The ubiquitous brecciation of the granodiorite is consistent with the tectonic contacts with adjacent igneous and metamorphic rocks.

The modal mineralogy of the Bootleg Canyon granodiorite is shown in Table 6. Quartz (20-25%) and alkali feldspar (2-20%) generally are anhedral and interstitial. Plagioclase (40-60%) is oligoclase in composition, generally subhedral and it commonly exhibits normal zoning. Hornblende and biotite each comprise ~10% of the rock. The hornblende is blue-green in color, euhedral and it commonly forms boat-shaped crystals up

TABLE 6. MODAL MINERALOGY OF GROUP IV GRANITIC ROCKS IN THE OAK CREEK PASS COMPLEX

Sample Number	Primary Mineral Assemblage													Accessories										Secondary/Retrograde Assemblage									
	C	Qz	Kf	Pl	A	Hb	Bt	Op	Ox	Cx	Ox	Sp	Ap	Al	Zr	Ac	Ch	Ep	Cz	Sp	Sr	Ca	Sa	Zi	Other								
<u>Bootleg Canyon granodiorite</u>																																	
90-TH-49	22	25	10	43	25	10	11	x				1	x	x	x	x	x	x				xx			?	Pr-x							
92-TH-192	20	20	15	45	28	8	11	x				1	x	x	x	x	x	x							x	Pm-?							
92-TH-235	12	20	2	63	24	r	1						x			12	xx							x	2	Cl-xx							
92-TH-259	18	20	20	42	26	1	r	x				1	x	x	x	15	xx	x						x	xx	Op-x							
93-TH-349	13	25	20	42	23	4	9					1	x			x										Cl-?							
93-TH-383A	nd	xx	xx	xx	nd		xx					x		x		xx	xx								xx								
93-TH-417	20	25	10	45	27	7	12	x				1	x			xx	xx							xx	x								
<u>Old West Ranch monzogranite</u>																																	
90-TH-28	8	25	28	39	35	x	8	x				x	x	x	x	xx	xx	x							xx		Pr-x						
90-TH-35	15	18	22	45	28	2	13	x				x	x	x	x	xx	xx	x							x	xx	x						
90-TH-44	9	15	27	49	32	x	9	x				x	x	x	x	xx	x	x							xx		Pm-?						
92-TH-187	15	25	30	30	37	x	15	x				x	x	x	x	xx	xx								xx		Op-x						
92-TH-196	3	35	25	37	29	x	3	x				x	x	x	x	xx	xx								xx								
<u>Mendiburu Canyon granodiorite</u>																																	
90-TH-38B	14	20	25	41	33	x	14					x	x			x											x						
91-TH-181A	25	20	25	30	30	18	7					x	x	x		x											x						
91-TH-181B	10	15	15	60	nd	2	8	x				x	x			x											x						
92-TH-195	15	25	15	45	31	3	12					x	x	x	x	x	x	x									Kf-x						
94-TH-480A	5	35	20	40	26		5	x					x	x	x	x	x										Cl-xx						
<u>Mafic enclaves within Mendiburu Canyon granodiorite</u>																																	
91-TH-179	40	25	10	25	37	x	30	x	3	7		x	x	x	x	x									x		x						
92-TH-194	40	2	x	57	37	30	10	1				x	x			x									x		x						

Notes: Cl= color index, AN = anorthite content of plagioclase feldspar estimated using method of Michel-Lévy and/or Carlsbad-albite method, nd = no data.

Mineral name abbreviations: Qz = quartz, Kf = potassium feldspar, Pl = plagioclase feldspar, Hb = hornblende, Bt = biotite, Op = opaques, Cm = cummingtonite, Cx = clinopyroxene, Ox = orthopyroxene, Sp = sphene, Ap = apatite, Al = allanite, Zr = zircon, Ac = actinolite, Ch = chlorite, Ep = epidote, Cz = clinzoisite, Sp = sphene, Sr = sericite, Ca = calcite, Sa = saussurization of plagioclase feldspar, Zi = zeolite, Pr = prehnite, Pm = pumpellyite, Cl = clay.

Table entry abbreviations: numbers = modal percentage mineral in sample estimated using percentage diagrams for estimating composition by volume, x = present in amounts less than 1 %, xx = present in significant amounts but too fine grained and disseminated or cataclitized to reliably estimate modal percentage, r = remnants of formerly more abundant mineral now largely replaced by other minerals, ? = mineral identification equivocal.

to 5 millimeters long. The biotite is brown and occurs as distinct hexagonal shaped books up to several millimeters across. Wedge shaped amber sphene crystals up to several millimeters in length are an ubiquitous accessory mineral in the granodiorite, commonly constituting 1% or more of the rock.

Virtually all the samples examined are moderately to severely altered and most display cataclastic fabrics with shattered mineral grains. The mafic minerals commonly are replaced by chlorite and epidote, plagioclase is extensively saussuritized, zeolite overgrowths occur in biotite and chlorite and within fractures, prehnite lozenges occur along the cleavage of biotite, and fracture networks are locally filled with aggregates of an extremely fine grained whitish mineral that may be a clay. One sample contains a single grain of a mineral growing within chlorite that is tentatively identified as pumpellyite. The mineral may be epidote but it has pale yellow to pale brownish green pleochroism and a crystal shape that resembles an oak leaf, both characteristics of pumpellyite (MacKenzie and Guilford, 1980).

Mendiburu Canyon granodiorite

The Mendiburu Canyon granodiorite is present in the upper plate of the Oak Creek Pass complex along with the Old West Ranch monzogranite. Contact relationships between the two units are complex and poorly exposed. Most of the contacts appear to be tectonic and are marked by a diffuse zone of cataclasis. One contact east of Blackburn Canyon, however, appears to be intrusive. The contact is difficult to locate precisely, but in roadcut exposures dikes of the Old West Ranch monzogranite clearly intrude the Mendiburu Canyon granodiorite. The thickness and number of the dikes increase as the contact is approached until the granodiorite disappears and the monzogranite is the only unit present. Dikes of the Old West Ranch monzogranite are also scattered throughout the Mendiburu Canyon granodiorite supporting the inference that the granodiorite is older than the monzogranite. The cataclastic contacts may be former intrusive contacts that were

disrupted by later tectonism. The Mendiburu Canyon granodiorite is rarely exposed since it readily weathers to a grus composed of granule-size grains. The most prominent outcrops in the area underlain by the granodiorite commonly are dikes of the more resistant Old West Ranch monzogranite. The best exposures of the Mendiburu Canyon granodiorite are located in the upper end of Mendiburu Canyon and in roadcuts north of the top of Hill 6435' east of Blackburn Canyon (Figure 4).

The Mendiburu Canyon granodiorite is a medium to coarse grained, locally porphyritic, hornblende biotite granodiorite with a color index that generally ranges from 15 to 25. In places the granodiorite has a modest inferred primary igneous foliation defined by aligned biotite and elongate mafic pods, but more commonly it has a cataclastic fabric characterized by discrete shear planes and fractures. The granodiorite hosts abundant mafic enclaves ranging in size from a few centimeters to more than 10 meters across. The composition of these mafic pods ranges from granodiorite to diorite and they typically have a color index of ~40. The mafic minerals in the enclaves consist mostly of biotite and hornblende, but one sample contained 3% cummingtonite and 7% clinopyroxene (Table 6).

Quartz constitutes 15-35% of the Mendiburu Canyon granodiorite and it exhibits modest undulatory extinction and fracturing. Pale pink alkali feldspar, 15-25% of the rock, occurs as subhedral to euhedral phenocrysts up to ~1.5 centimeter in length and exhibits both Carlsbad and microcline twinning. Subhedral and occasionally antiperthitic plagioclase constitutes 30-60% of the rock. The plagioclase ranges in composition from An₂₆ to An₃₃ and locally exhibits oscillatory zoning. Subhedral brown biotite and green poikilitic hornblende are present in a ratio of about 4:1 in most samples. Accessory minerals present in the granodiorite include sphene, apatite, allanite, and zircon (Table 6). Biotite grains commonly are kinked and replaced by chlorite, and feldspar and quartz locally are shattered and the fractures filled with chlorite or sericite suggesting the cataclastic deformation was accompanied by or followed by an influx of aqueous fluid.

Old West Ranch monzogranite

The Old West Ranch monzogranite is found in both the upper plate and the east middle plate of the Oak Creek Pass complex. In the upper plate it intrudes and is in tectonic contact with the Mendiburu Canyon granodiorite. Dikes of the monzogranite, ranging from several centimeters to tens of meters thick intrude the granodiorite, and a small plug of the monzogranite intrudes the granodiorite north of Hill 6435'. The monzogranite is also found immediately north of the Garlock fault in the upper plate, but the nature of the contact with the granodiorite to the north is not known. The Old West Ranch monzogranite in the east middle structural plate of the Oak Creek Pass complex is tectonically bounded on all sides, the Quail Canyon fault to the west, the Blackburn Canyon fault to the north, the South Ridge fault zone to the east, and the Garlock fault to the south.

The Old West Ranch monzogranite is a medium grained, equigranular to slightly porphyritic biotite monzogranite with a color index of 3 to 15. Quartz comprises 15-35% of the rock and it is commonly fractured. Alkali feldspar, 22-30% of the rock, occurs in anhedral poikilitic grains that enclose biotite, quartz, and plagioclase. The potassium feldspar commonly contains strings of microperthite and it exhibits both microcline and Carlsbad twinning. Subhedral to euhedral plagioclase grains exhibit normal zoning and range in composition from An₂₅ to An₃₇. Fine to medium grained biotite, 3-15% of the rock, occurs in irregular aggregates up to several millimeters in size. Hornblende is present in trace amounts (Table 6).

The monzogranite locally displays a weak inferred igneous foliation and it is extensively cataclasized. The monzogranite weathers to a grus with sand-size particles. The least weathered exposures of the Old West Ranch monzonite are light to medium gray in color. A distinctive feature of some samples is the presence of sharply rectangular phenocrysts, up to 2 centimeters in length, of poikilitic whitish plagioclase that host prominent rectangular-shaped zones of fine-grained dark mineral inclusions. In contrast to

the Mendiburu Canyon granodiorite, the Old West Ranch monzogranite does not contain abundant mafic enclaves.

WITNET FORMATION

In the lower plate of the Oak Creek Pass complex arkosic and conglomeratic sedimentary rocks locally are deposited on top of the Bootleg Canyon granodiorite. These sedimentary rocks were first mapped by Dibblee (1967) and Dibblee and Louke (1970) who, on the basis of lithologic similarity, correlated them with the Witnet Formation exposed immediately northeast of Tehachapi Valley in the vicinity of lower Cache Creek and Oil Canyon, see Figure 2. The age of the Witnet Formation is unknown because no fossils have been found in it, but it is older than the Early Miocene Kinnick Formation (Quinn, 1987) which unconformably overlies the Witnet Formation in the Cache Creek area (Dibblee and Louke, 1970). In the study area the Witnet Formation is synformally folded about a northeast trending axis and appears to be overridden from the southeast along the Mendiburu Canyon fault as will be discussed later.

The Witnet Formation consists of light gray to olive-tan fine to medium grained arkosic immature sandstone interbedded with scattered brown to black shaley layers and layers and lenses of conglomerate containing well-rounded pebble to cobble size clasts. Beds in the sandstone range from several centimeters to several meters in thickness and sedimentary structures such as cross bedding and channel scours are common. The arkosic sandstone has the composition of granodiorite and in many outcrops where sedimentary features are not obvious the sandstone may be mistaken for weathered granodiorite. Located in the lower part of the Witnet Formation is a prominent layer of conglomerate composed of rounded and polished pebbles and cobbles of quartzite, volcanic porphyry, granitic aplite and pegmatite, and granitic rocks. Clasts of gabbro or tonalite composition are conspicuously absent in the conglomerate. In the vicinity of the contact with the underlying granodiorite the Witnet Formation contains rounded to subrounded cobble to

boulder size clasts of granodiorite and monzogranite unsupported in a poorly bedded matrix of arkosic sandstone of similar composition. Locally near the contact with the Witnet Formation the granodiorite is weathered into spheroidally shaped rusty red-stained hummocks that are more resistant than the granodiorite below. The stained granodiorite may represent an old weathering profile.

The composition of the arkosic sandstone in the Witnet Formation is close to the composition of granodiorite. The sandstone generally is fine grained and the grain size ranges from ~4 millimeters down to much less than 1 millimeter. The samples of arkosic sandstone examined in thin section are composed of quartz (35%), potassium feldspar (20-25%), plagioclase (30-41%), biotite (4-10%). One sample also contains a trace of hornblende. See Table 7 for the modal mineralogy of sandstone from the Witnet Formation. Green biotite grains are kinked and crumpled, and they are replaced locally by epidote and chlorite. Turbid plagioclase grains locally contain small grains of sericite, and angular shards of quartz are fractured but not recrystallized. At thin section scale the samples examined do not display a strong planar fabric. The sandstone is grain supported and the mineral grains are packed tightly together with very little interstitial space. Calcite and zeolite minerals fill cracks and the interstices between the grains and appear to cement the sandstone. Scattered throughout fractured plagioclase and forming thin films along some of the grain boundaries are very small elongate grains (~0.0025 x 0.025 millimeters in size) with a pale green color and low birefringence that may be crystals of smectitic clay. The lack of grain size sorting, the angularity of the mineral grains, the well preserved biotite grains, and the abundance of feldspar in these samples all suggest that the sources for the arkosic sandstone in the Witnet Formation were close by.

TERTIARY VOLCANIC ROCKS

Dikes of mostly light colored aphanitic sub-volcanic rocks intrude the eastern Tehachapi gneiss complex and the Oak Creek Pass complex in the southern part of the

study area. Most of the dikes are subvertical to steeply dipping with a general E-W trend. Individual dikes range from tens of centimeters to tens of meters in thickness and commonly intrude close to or adjacent to one another forming semicontiguous transverse exposures up to several hundred meters wide. The dikes crosscut the Quail Canyon and South Ridge fault zones in the Oak Creek Pass complex and crosscut mylonitic rocks of the eastern Tehachapi shear zone. No dikes could be followed across the Blackburn Canyon detachment fault, but undeformed dikes intrude the cataclastic granitic rocks in the hangingwall immediately adjacent to the fault.

Many of the dikes are light tan to pinkish colored felsite and they commonly contain small phenocrysts of quartz and/or plagioclase. The felsite dikes commonly exhibit intricate concentric or dendritic patterns of rusty-red stains along fracture surfaces. The margins of some of the felsite dikes are composed of vitreous black material that has a perlitic structure. Other dikes of possible basaltic or andesitic composition are dark olive-green to gray in color and contain phenocrysts of plagioclase, biotite, and either pyroxene or hornblende. The compositions of the volcanic dikes in the study area were not studied in detail. The ages of the dikes in the study area are not directly known, but they are inferred to be Miocene in age based on correlation with similar volcanic rocks which intrude and are interlayered with the nearby Miocene age sedimentary rocks of the Kinnick and Bopesta Formations (Dibblee, 1967; Dibblee and Louke, 1970).

CHAPTER III: DEFORMATION AND METAMORPHISM

The rocks in the study area preserve evidence for a complex deformation history that includes multiple generations of folding, the regional and local formation of both high and low temperature deformation fabrics, and the development of both ductile and brittle low-angle fault zones. Most of the deformation episodes were accompanied by localized or regional metamorphic recrystallization. The first section of this chapter summarizes the different types of structural data collected including several different types of foliations and lineations, information on shear sense, and the orientation and style of folds. In the following three sections the structural and metamorphic data are presented and discussed in relative age sequence from oldest to youngest. Since the eastern Tehachapi shear zone is the most prominent structural feature in the area the three sections cover the pre-, syn-, and post-shear zone deformation and metamorphic history. Section five discusses several structures that have an unknown or ambiguous relative age. Section six summarizes the metamorphic history of the study area and discusses several aspects of the metamorphic evolution not covered in the earlier sections. The final section of this chapter discusses the geologic cross sections of the study area shown in Figure 22 and Plate 3.

STRUCTURAL ELEMENTS

FOLIATIONS

Primary planar fabrics such as bedding in the metasedimentary rocks and magmatic foliation in the igneous rocks are absent or rare in the rocks of the eastern Tehachapi gneiss complex. The dominant fabric of the metasedimentary rocks is a penetrative gneissic to schistose foliation defined by the planar alignment of tabular and platy minerals. The orientation of this foliation usually is subparallel to compositional layering in the paragneiss. The compositional layering in the metasedimentary rocks most likely

represents transposed sedimentary bedding. Unequivocal primary sedimentary structures were not observed in the metasedimentary rocks.

The primary foliation in the group I orthogneisses is gneissic. Most of the group I orthogneisses exhibit some evidence of annealing in thin section. The gneissic foliation is defined by either the planar alignment of inequigranular minerals in the rock or, where the texture of the rock is granoblastic and the minerals more equigranular or by the alternation of millimeter-scale compositional layers of light and dark minerals. Quartz in the tonalite gneiss characteristically forms lenticular shaped grains.

Foliations and textures that may have a primary igneous origin are present locally in the gabbro and tonalite of the Tehachapi Intrusive Complex and in the granitic rocks of the Oak Creek Pass complex. An important criterion for a primary magmatic foliation is the preferred alignment of igneous minerals that show no evidence of plastic deformation or recrystallization (Paterson et al., 1989). Even though most samples from the Tehachapi Intrusive Complex show extensive evidence of plastic deformation in thin section, elongate plagioclase grains typically have a preferred alignment and their twin planes are oriented parallel to the long axis of the grains. These observations suggest that a solid state fabric has been superimposed on a magmatic foliation (Paterson et al., 1989). Fine-grained mafic enclaves and schlieren are abundant in the tonalite of the Tehachapi Intrusive Complex and they show a preferred alignment that usually is subparallel to the subsolidus foliation in the tonalite, again suggesting superposition of a deformation fabric on a magmatic fabric.

A cataclastic foliation is the most prominent fabric in the granitic rocks of the Oak Creek Pass complex. In thin section the cataclastic foliation is characterized by brittle shear planes along which the minerals of the rock are fractured and broken with little evidence for recrystallization. Commonly the plagioclase is cracked and quartz commonly has a granulated or shattered appearance. The cataclastic foliation has a strong preferred orientation adjacent to the faults bounding the various structural plates, but away from the

faults the fractures and shears appear to be randomly oriented and the rock has an overall shattered appearance.

In this study the term mylonitic foliation is used in the sense of Wise et al. (1984) for a foliation resulting from the reduction in average grain size of the rock to less than ~0.5 millimeters by syntectonic crystal-plastic mechanisms. The terms protomylonite, orthomylonite, and ultramylonite refer to a penetratively deformed rock where the relict unrecrystallized porphyroclasts constitute more than 50%, 10 to 50%, and less than 10% of the rock, respectively (Wise et al., 1984). Many of the rocks in the study area that have an overall gneissic foliation locally are cut by discrete oblique mylonitic shear surfaces (typically < 1 millimeter wide) or narrow zones (on the scale of centimeters wide) along which dynamic recrystallization and grain size reduction has occurred. These shear surfaces and zones are referred to as shear bands. Where the discrete shear surfaces are penetrative a composite fabric resembling an S-C fabric is produced. In this study, however, the term S-C fabric is reserved for those instances where the foliation and shear surfaces appear to have formed coevally as will be discussed later.

LINEATIONS

Linear fabric elements found in the rocks of the study area include mineral lineations, slickenside striae, and hingelines to meso- and micro-scale folds. The fold hingelines and slickensides need little discussion, but the mineral lineations require some explanation. The mineral lineations are found within foliation or shear surfaces where they are defined by the preferred alignment of the long axes of inequant mineral grains, elongate aggregates of mineral grains, or streaks and smears of minerals. Some of the mineral lineations are associated with deformation fabrics that exhibit clear evidence for a preferred sense of shear when viewed in sections oriented parallel to the mineral lineation and perpendicular to the foliation. Other mineral lineations are associated with metamorphic or igneous fabrics that lack evidence for simple shearing along the direction of the mineral

lineation. Based on these observations two types of mineral lineations were defined in this study.

Type 1 mineral lineations generally are localized within the foliation surface of the rock and are characterized by the preferred alignment of the long axis of elongate minerals such as sillimanite and hornblende as well as by the preferred alignment of elongate aggregates of more equigranular mineral grains such as biotite, feldspar, and quartz. In thin sections and outcrop exposure planes oriented parallel to type 1 mineral lineations and perpendicular to the host foliation a preferred sense of shear generally is not evident in the rock. The type 1 lineations are inferred to parallel the long axis of the finite strain ellipsoid and are interpreted to be stretching lineations. Hingelines to mesoscale and map-scale folds commonly are oriented subparallel to the type 1 mineral lineations.

Type 2 mineral lineations, found within shear surfaces of deformed rocks, are defined by trains of extended and fractured mineral grains such as feldspar or hornblende, and also by smeared aggregates of quartz, biotite, chlorite, or epidote. Since the type 2 mineral lineations are measured in shear surfaces instead of foliation surfaces they are not, strictly speaking, stretching lineations (Lin and Williams, 1992a). Many of the type 2 mineral lineations appear to result from intersection of the shear surfaces in the rock with minerals elongated along the stretching direction contained in the foliation. Thus, the type 2 mineral lineations represent a projection of the stretching lineation onto the shear surfaces as has been noted before by Berthé et al. (1979) for lineations in sheared granites. In thin sections and outcrop exposures oriented parallel to type 2 mineral lineations and perpendicular to the shear surfaces in the host rock a preferred sense of shear usually is observed. The type 2 mineral lineations are inferred to parallel the slip direction of the shear surfaces because they have an orientation that is subparallel to ridge-in-groove striations also found in the shear surfaces (Lin and Williams, 1992b).

KINEMATIC INDICATORS

Shear sense in the deformed rocks was determined from structures suitable for kinematic analysis present in outcrops and in oriented thin-sections. Micro- and mesoscale structures found in the study area which yield sense of shear information include composite foliations such as S-C fabrics (Berthé et al., 1979; Lister and Snoke, 1984) and shear bands (White et al., 1986; Simpson, 1986), asymmetric σ and δ porphyroclasts (Passchier and Simpson, 1986), mica fish (Lister and Snoke, 1984), the oblique alignment of elongate recrystallized quartz grains (Simpson and Schmid, 1983; Lister and Snoke, 1984), the asymmetry of intrafolial folds (White et al., 1986), and the orientation of tension gashes and arrays of en echelon veins (Ramsay and Graham, 1970; McClay, 1987).

Many of the deformed rocks in the study area have composite S-C fabrics consisting of a schistose or gneissic foliation that is crosscut by a second foliation composed of discrete shear surfaces. Simpson (1986) suggests that use of the term S-C mylonite should be used only in the case where development of S (schistosity) and C (shear) surfaces can be demonstrated to have been synchronous or almost so. Where composite fabrics with S and C surfaces are developed in the study area it commonly appears that the shear planes were superimposed on rocks possessing a previously developed schistosity or gneissosity.

The clearest example of the inferred non-coeval formation of foliation and shear surfaces in the study area is in the augen gneiss of No Name Canyon. The augen gneiss possesses a well developed gneissic foliation which has a variable orientation because the gneiss appears to have been folded. In contrast, a family of discrete shear surfaces which crosscut the gneissic fabric of the augen gneiss have a similar orientation throughout the gneiss. There is no systematic relationship between the orientation of the gneissic foliation and the shear surfaces as might be expected in the development of coeval S and C surfaces as proposed by Berthé et al. (1979). The main foliation in the augen gneiss is interpreted to

have developed during an earlier and separate deformation than the deformation that produced most of the shear surfaces in the augen gneiss. Because of the coeval development of S and C surfaces implied by the term S-C fabric, the shear fabrics in the augen gneiss and in most of the other deformed rocks of the study area will hereafter be referred to as shear band fabrics.

FOLDS

All of the metasedimentary rocks and most of the igneous rocks in the eastern Tehachapi gneiss complex have been folded multiple times by folds that range from regional to microscopic in scale. Most of the deformation episodes in the study area were accompanied by an episode of folding that has a distinctive orientation and style. These different generations of folds are important elements in the sequence of deformation in the study area, so most of the deformation events described below are referenced to one of the generations of folding. The terminology used in the following sections to describe the tightness and other features of the folds in this study is from Fleuty (1964).

DEFORMATION PRIOR TO THE EASTERN TEHACHAPI SHEAR ZONE

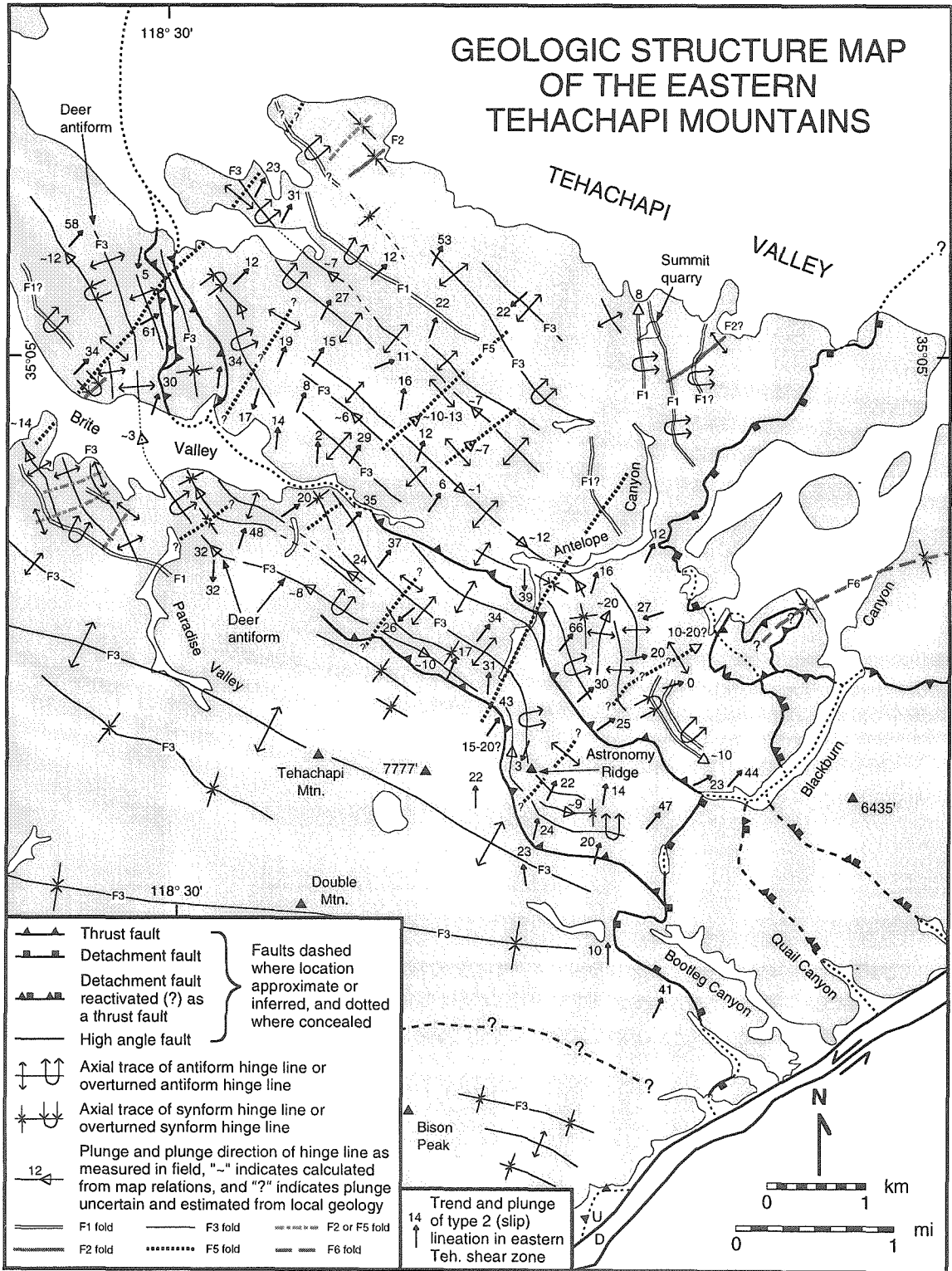
EARLY FOLDING (F1) AND FAULTING

The earliest deformation recognized involves faulting and map-scale folding of the lithologic layering in both groups of metasedimentary rocks. This early folding event is designated F1 and the axial traces of F1 hingelines are shown in a structure map of the area (Figure 9) and also in Figures 4, 5, and 7. The early folds in the Antelope Canyon group metasedimentary rocks (F1_{AC}) are tight to isoclinal antiforms and synforms with N trending subhorizontal to shallow N plunging axes and shallowly to moderately E dipping limbs. The Summit marble quarry east of lower Antelope Canyon is located in the thickened hinge region of one of these folds (Figure 5). Marble exposed in the walls of the quarry hosts layers of well foliated fine grained biotite hornblende (\pm quartz) diorite gneiss that are subconcordant to the compositional layering in the folded marble. It is not obvious

Figure 9.

Geologic structure map of the eastern Tehachapi Mountains region. Note the systematic changes in the trends and/or plunges of the F3 fold hinge lines. The $\sim 45^\circ$ change in the trend of the F3 folds in the vicinity of Brite Valley is inferred to be the result of F4 oroclinal folding as discussed in the text. The plunge changes of the F3 fold hinge lines on either side of upper Antelope Canyon are interpreted to be the result of folding in an F5 synform that has a shallow plunge to the NE. The change in trend of the F3 hinge lines on either side of upper Antelope Canyon may be the result of F4 oroclinal folding prior to the F5 folding. Alternatively, the F3 fold hinge lines may have been rotated in a large sheath fold during eastern Tehachapi shear zone deformation as discussed in the text.

GEOLOGIC STRUCTURE MAP OF THE EASTERN TEHACHAPI MOUNTAINS



whether the biotite hornblende diorite gneiss intruded prior to the F1_{AC} folding or after the folding because the contacts are severely transposed by later deformation and metamorphism. The Antelope Canyon garnet diorite gneiss intrudes between the limbs of adjacent F1_{AC} antiformal folds in the lower Antelope Canyon area. Marble in the vicinity of the garnet diorite gneiss locally appears to have been fractured and subsequently recrystallized. The localization of these garnet diorite gneiss bodies between adjacent folds, their inferred thin tabular shape in cross section, and the nearby presence of fractured marble suggests they may have intruded along faults between the folds.

In a number of places west of upper Blackburn Canyon there are abrupt lithologic breaks between adjacent F1_{AC} folds. Where marble is present next to these discontinuities it commonly is stained orange, brecciated, and dolomitized. Although the fractured marble was not observed to be intruded by any plutons the fractured zone does not continue along strike into nearby group II gabbro. This suggests that the marble was brecciated prior to intrusion of the gabbro. Also in the region west of upper Blackburn Canyon tabular bodies of the No Name Canyon augen gneiss appear to have been emplaced into lithologic discontinuities between adjacent F1_{AC} folds. These lithologic discontinuities are interpreted as thrust faults that developed during W vergent F1_{AC} folding and prior to the intrusion of the No Name Canyon augen gneiss.

The earliest recognized folds in the Brite Valley group metasedimentary rocks (F1_{BV}) are map-scale, isoclinal, locally recumbent, SW vergent, and have hinge lines that trend to the NW and plunge very shallowly to the NW (Figures 7 and 9). Thrust (?) faulting also may have accompanied the F1 folding of the Brite Valley group paragneiss. South of Brite Valley the lower contact of a discontinuously exposed marble layer locally is sheared along what is inferred to be a fault contact (Figure 7). Small bodies of group II tonalite and gabbro found along strike from the location of the sheared marble locality may have intruded along the inferred fault.

The structural and intrusive relations described above suggest the F1 folds may have formed in conjunction with thrust faulting localized between the limbs of adjacent folds. The first deformation recognized in the Antelope Canyon paragneiss appears to have occurred prior to intrusion of both the Antelope Canyon garnet diorite gneiss and the No Name Canyon augen gneiss. The early deformation in the Brite Valley paragneiss is inferred to have occurred before intrusion of group II gabbro and tonalite. The localized fracturing and dolomitization of the marble in the vicinity of the inferred thrust faults suggests the initial folding and faulting took place at relatively low temperatures before metamorphism and intrusion of the section. It is not known if metamorphism accompanied or closely followed the F1 folding because of later high-grade metamorphic events.

DEFORMATION AND METAMORPHISM OF THE GROUP I ORTHOGNEISS AND F2 AND F3 FOLDING

Metamorphic mineral assemblages, deformation fabrics, and folds present in the group I orthogneisses and both groups of metasedimentary rocks suggest that all these rocks experienced two episodes of deformation under amphibolite facies metamorphic conditions prior to development of the eastern Tehachapi shear zone. The group II intrusive rocks were involved in the second of these two high temperature deformation episodes, but they show little evidence of being affected by the first event. Greenschist facies retrograde metamorphism accompanied the eastern Tehachapi shear zone deformation, but relicts of earlier mineral assemblages in the rocks of the gneiss complex indicate prior amphibolite facies metamorphism.

Paragneiss of pelitic composition found throughout the area has a pre-retrograde mineral assemblage consisting of garnet, biotite, sillimanite, muscovite, quartz, potassium feldspar, and plagioclase. This assemblage is indicative of amphibolite facies metamorphic conditions (Bucher and Frey, 1994). The presence of recrystallized brown hornblende, recrystallized plagioclase of andesine composition, and local dark reddish brown biotite in

the mafic dioritic, gabbroic, and amphibolitic group I orthogneisses also indicates amphibolite facies conditions. While all of the paragneiss and group I orthogneiss lithologies do not contain mineral assemblages diagnostic of metamorphic grade, the general concordance of gneissic foliation and type 1 mineral lineations among the different lithologies suggests they were deformed and metamorphosed together.

Equal area stereonet plots of poles to the compositional layering and gneissic foliation of the Brite Valley group paragneiss, the Antelope Canyon group paragneiss, and the group I orthogneisses are shown in A, B, and C of Figure 10, respectively. The poles to foliation plotted in Figure 10 do not cluster in a single well-defined maximum or girdle, but they do cluster in several distinct groups. The simplest interpretation of the foliation orientation data is that the gneissic foliation is folded by more than one set of folds. Assuming cylindrical folding the pattern of poles to foliation for each set of folds should define a great circle girdle in the stereonet plot. If each plot is considered without reference to the other plots a number of different great circles could be drawn through the data in each plot. The general concordance of foliation and contacts among the different gneiss units observed at any given location in the field, however, suggests that the different units were deformed together and that girdles having similar orientations might be present in all of the plots.

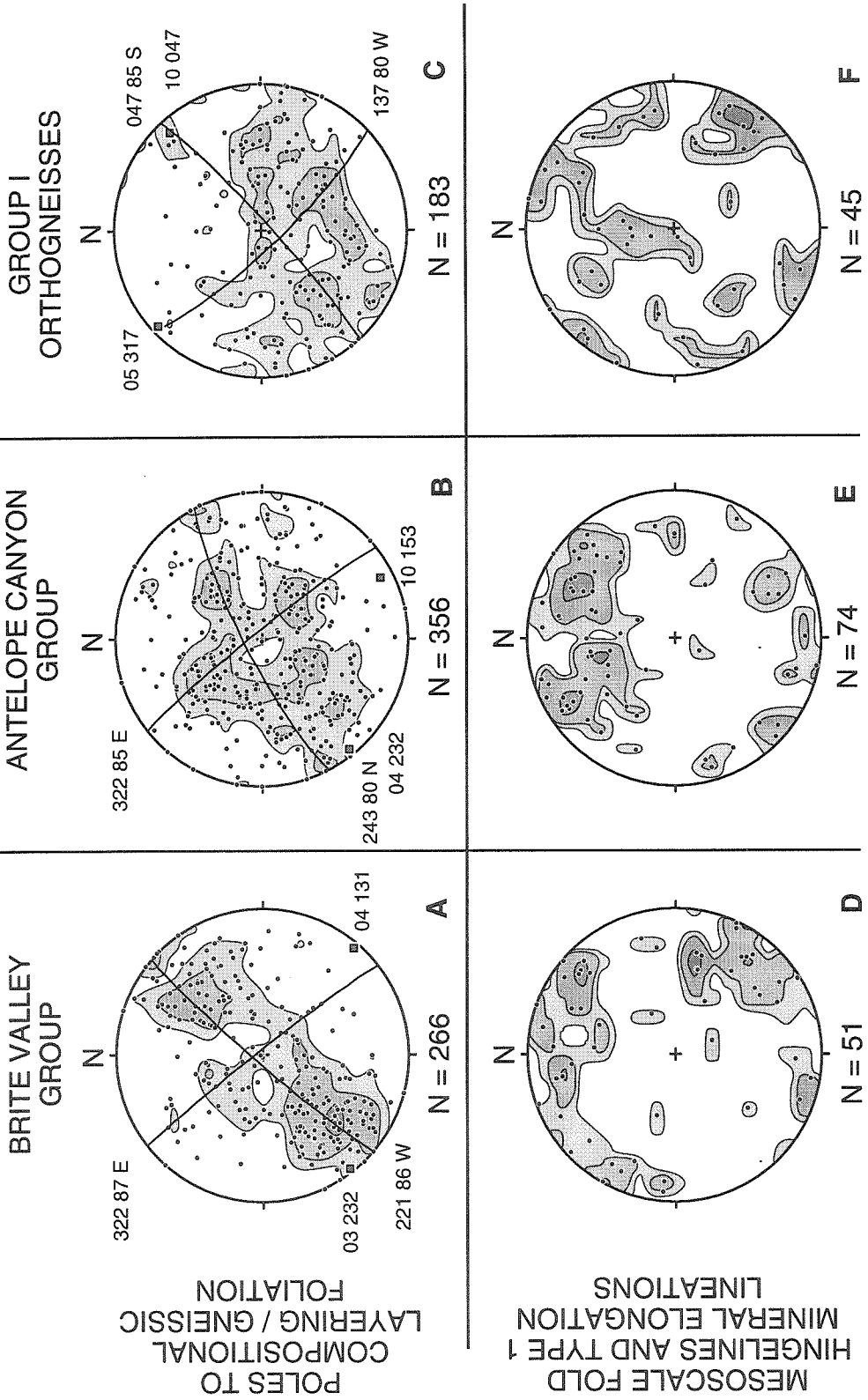
Based on this reasoning the great circles shown in plots 10A, B, and C were drawn by visual estimation. The most regular and symmetrical distribution of poles occurs in plot B and a possible interpretation of the pattern is that it results from two poorly defined girdles crossing at high angle. Two girdle patterns are less obvious in the data shown in plots A and C, but the great circles shown pass through most of the data and have similar trends to the ones in plot B. The small gray-shaded squares in the plots are the poles to the planes represented by the great circles, and the poles are interpreted to represent the approximate orientation of axes to two different sets of folds that deform the gneisses. The

Figure 10.

Structural data for paragneiss groups and group I orthogneiss in the eastern Tehachapi mountains. The data are plotted on lower hemisphere equal area stereonet projections and contoured at 1%, 2%, and 5% per 1% area. **A**, **B**, and **C** are plots of poles to compositional layering or gneissic foliation in the Brite Valley group metasedimentary rocks, the Antelope Canyon group metasedimentary rocks, and the group I orthogneisses, respectively. The great circles shown are visually estimated best fits to maxima in the distribution of plotted poles and the small shaded gray boxes are the poles to the planes represented by the great circles. The labels are the numeric values for the strike and dip of the great circles and the trend and plunge of the poles. **D**, **E**, and **F** are plots of mesoscale fold hinge lines and type 1 mineral lineations in the Brite Valley group metasedimentary rocks, the Antelope Canyon group metasedimentary rocks, and the group I orthogneisses, respectively. Type 1 mineral lineations include the preferred alignment of the long axis of elongate minerals such as sillimanite and hornblende, as well as the long axis of elongate aggregates of platy minerals such as biotite. In thin sections and outcrop exposure surfaces oriented parallel to type 1 mineral lineations and perpendicular to the host foliation a preferred sense of shear generally is not evident in the rock.

**STRUCTURAL DATA FOR PARAGNEISS GROUPS AND GROUP I ORTHOGNEISS
IN THE EASTERN TEHACHAPI MOUNTAINS**

(Lower hemisphere equal area projections. Contours = 1%, 2%, and 5% per 1% area.)



data in plots A, B, and C of Figure 10 suggest that the gneisses are folded about two sets of folds having nearly orthogonal subhorizontal axes, with one set trending NE and the other set trending NW. The two sets of nearly orthogonal folds in the high grade gneisses inferred from the foliation data are consistent with the orientation of two sets of mesoscale and map-scale folds present in the gneisses that are discussed below.

Type 1 mineral lineations present in the plane of the foliation in both the paragneiss and the orthogneiss are subparallel to the axes of mesoscale folds (Figure 10D, E, and F). The mineral lineations in the paragneiss (plotted in Figure 10D and E) are defined by the preferred alignment of sillimanite needles and elongate aggregates of feldspar grains, biotite, and muscovite; in the group I orthogneisses the mineral lineations (plotted in Figure 10F) are defined by the preferred alignment of the long axis of hornblende grains and elongate aggregates of feldspar and quartz. The lineations are defined by minerals of the amphibolite facies assemblage indicating they formed during the high grade metamorphism. Mesoscale folds are rare in the group I orthogneiss, but close to tight folds of the compositional layering in the paragneiss are common. The metamorphic mineral assemblage in the folds is the same as elsewhere in the paragneiss and in thin section the texture of the paragneiss in the fold hinge regions is granoblastic which suggests the folding was synchronous with the regional high temperature metamorphism. The folds generally do not possess an axial planar foliation. The type 1 mineral lineations and fold axes are somewhat scattered in orientation, but they appear to cluster into two groups, a NW-SE trending group and a NE-SW trending group. The NE trending mesoscale folds tend to have SE dipping axial surfaces while the NW trending folds usually have axial surfaces that dip to the NE.

Most of the NE trending folds and mineral lineations in the paragneiss and the group I orthogneiss appear to be older than the NW trending structures for the following reasons. First, rocks of the younger group II intrusives lack NE trending folds and type 1

mineral lineations, but they contain well developed NW trending folds and type 1 mineral lineations which are coaxial with the NW trending folds and lineations in the paragneiss and the group I orthogneisses. Second, NE trending fabric elements are uncommon in the metasedimentary rocks in the central part of the study area where the NW trending high temperature fabrics are best developed which suggests that they were transposed during the subsequent high temperature deformation which produced the NW trending fabrics. Third, in the hinge regions where map-scale NE and NW trending folds intersect the NW trending fabrics usually predominate. Lastly, the NE trending type 1 mineral lineations in the group I orthogneisses (Figure 10F) have a wide range in plunges which suggests they may be folded about younger NW trending folds.

The structural evidence outlined above suggests that the metasedimentary rocks and the older intrusive rocks of the study area were deformed twice at high temperature and that the NE trending folds and mineral lineations were overprinted and locally transposed by the NW trending folds and mineral lineations. The earlier NE trending folds deform metasedimentary rocks previously folded by F1 folds so they are designated F2 folds. The later NW trending folds are designated F3 folds. There is some indication, however, that a few NW trending folds formed prior to the F2 folds. Brite Valley group paragneiss with mesoscale NW trending folds locally is intruded by less deformed group II gabbro and tonalite of the Tehachapi Intrusive Complex. The NW trending folds could be from an unrecognized deformation event between the F1 and F2 folding events, the evidence for which is now mostly overprinted by later deformation, or these scattered folds might be small secondary folds that formed during F1 folding.

The F2 generation folds in the study area are generally upright, open to close map-scale and mesoscale folds with NE trending and shallowly NE plunging hinge lines. F2 folds are best preserved and most easily visible along the north margin of the study area in the metasedimentary rocks adjacent to the Highline gabbro (Figures 4 and 9) and also in the

metasedimentary rocks north of Brite Valley (Figure 11A). The F2 folds do not have an axial planar cleavage associated with them and there does not appear to be any unique metamorphic mineral growth associated with them.

Superposition of subhorizontal NE trending and NW to N trending map-scale folds in the metasedimentary rocks of study area locally appears to have produced "dome and basin" or "egg-carton" style fold interference patterns that correspond to the type 1 fold interference pattern of Ramsay (1967). These inferred interference patterns are best developed in the Brite Valley group paragneiss south of Brite Valley (Figure 4). The scattered exposures of marble south of Brite Valley appear to occur where NW trending F1 and F3 antiformal folds intersect NE trending antiformal folds that may be F2 folds.

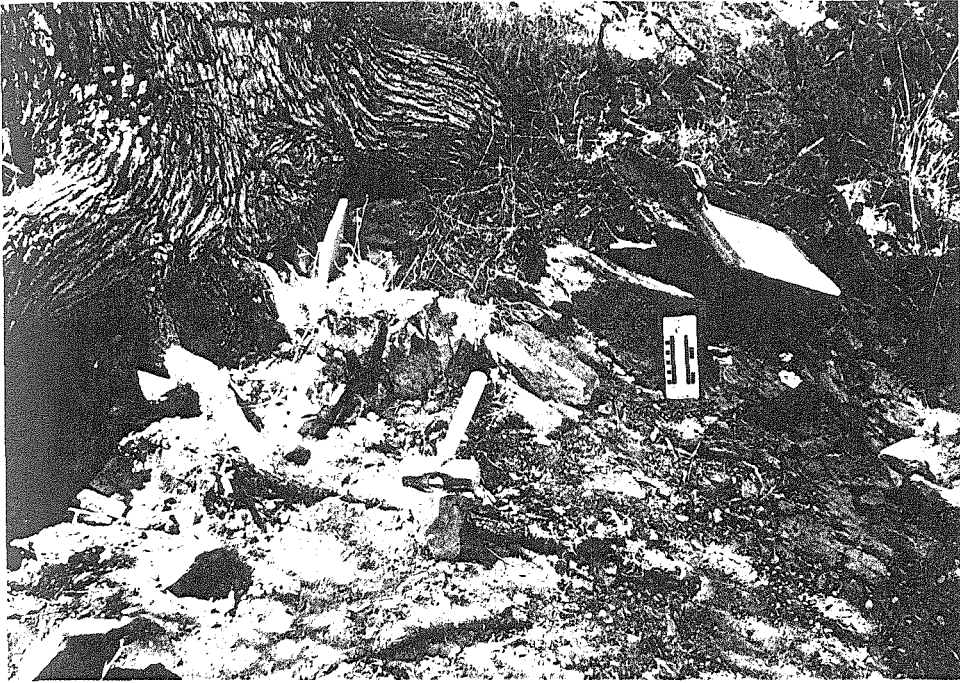
There is limited evidence suggesting that the later stages of the high-temperature deformation and F2 folding may have been accompanied by a small component of simple shear. At a number of locations in the group I orthogneisses shallowly plunging NW trending type 2 mineral lineations are present within the high temperature foliation of the orthogneisses. In thin-sections and outcrop faces oriented parallel to these type 2 lineations and perpendicular to the high temperature foliation microstructures indicate that the rocks were sheared top to the NW along the lineation direction prior to being annealed at high temperature. The significance of the sparse evidence for simple shear in the group I orthogneisses is not clear since the original orientation of the fabrics is uncertain.

DEFORMATION AND F3 FOLDING OF THE GROUP II INTRUSIVE ROCKS

The earliest deformation recognized in the group II gabbro and tonalite plutons of the Tehachapi Intrusive Complex produced high temperature solid-state gneissic fabrics as well as map-scale folds in the plutons. The mineralogy and textures of the gneisses indicate they were deformed under amphibolite facies conditions. In the central most deformed part of the area, coextensive with the later, lower temperature eastern Tehachapi shear zone (Figure 3), the gabbroic rocks are dynamically recrystallized to a fine grained

Figure 11.

A) Mesoscale F2 antiformal fold in pelitic gneiss located immediately north of Brite Valley. The view is towards the N. The hammer parallels the hinge line which has a plunge and trend of 11 200. The field notebook at the base of the tree located above and to the left of the hammer is parallel to the NW limb of the fold and the map board in the upper right of the photo is parallel to the SE limb of the fold. Scale with centimeters on left and inches on right is located between the hammer and the map board. B) Hinge of the F3 Deer antiform located ~1 km SE of Brite Valley in the central structural block. The view in the photo is towards the SE. The hammer lies along the fold hinge line (plunge and trend of 32 325) and the head points down plunge. The folded rock in the photo is mylonitic tonalite of the Tehachapi Intrusive Complex. Gabbro, which structurally underlies the tonalite in this area, is exposed immediately behind the rock outcrops visible in the photo. The length of the hammer head is 13 centimeters.



A



B

amphibolite gneiss consisting of plagioclase of andesine composition and brown hornblende. Plagioclase in the tonalite commonly is dynamically recrystallized into a fine grained polygonal mosaic which suggests that this deformation occurred at temperatures greater than about 500°C (Tullis and Yund, 1977; Simpson, 1985). In many areas this high temperature subsolidus foliation appears to be superimposed on a similarly oriented foliation having magmatic characteristics, as discussed earlier, which suggests that the deformation of the gabbro and tonalite plutons of the Tehachapi Intrusive Complex may have been synchronous with their emplacement and then continued after they crystallized.

In the Tehachapi Intrusive Complex the high-temperature subsolidus foliation in the gabbroic rocks is defined by the planar alignment of hornblende and plagioclase grains or by the parallel alignment of compositional layers dominated alternately by light or dark minerals. The foliation in the tonalite is best defined by the preferred alignment of biotite and lenticular shaped quartz grains. Figure 12A is a stereonet plot of poles to the gneissic foliation in both the gabbro and tonalite of the Tehachapi Intrusive Complex. From Figure 12A it is clear that most of the foliation strikes to the NW and dips moderately to the NE. The shaded gray square in the center of the highest concentration of poles to foliation is the pole to the NW trending great circle which represents the most common orientation of the foliation. The scattering of poles in the northeast quadrant suggests the foliation is folded about NW trending axes. The NE trending great circle represents the best fit plane to the data calculated using Bingham axial distribution analysis (Allmendinger, 1995). The small gray box in the northwest quadrant of Figure 12A is the pole to that plane and it is interpreted to approximate the average orientation of large-scale fold axes in the Tehachapi Intrusive Complex.

Figure 12B is a plot of type 1 mineral lineations and the hingelines of mesoscale folds in the Tehachapi Intrusive Complex. Most of the mineral lineations are defined by the long axis of aligned elongate hornblende grains. The fold axis orientation estimated from

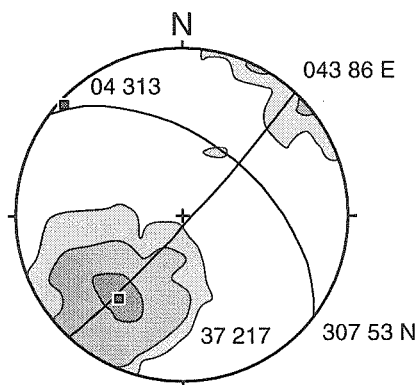
Figure 12.

Structural data for the Tehachapi Intrusive Complex and the eastern Tehachapi shear zone. The data are plotted on lower hemisphere equal area stereonet projections and contoured at 1%, 2%, 5%, and 7% per 1% area. **A** is a plot of poles to high temperature subsolidus foliation in the gabbro, quartz diorite, and tonalite of the Tehachapi Intrusive Complex. **B** is a plot of type 1 mineral lineations and hinge lines of mesoscale folds in the Tehachapi Intrusive Complex. **C** is a plot of poles to mylonitic foliation and shear bands of the eastern Tehachapi shear zone that are found in the group I orthogneisses, the Tehachapi Intrusive Complex (the group II intrusives), and the group III leucogranite intrusives. **D** is a plot of type 2 mineral lineations and linear grooves and striae associated with mylonitic and shear band fabrics of the eastern Tehachapi shear zone (data from same units as in **C**). The NE striking great circles in **A** and **C** are the best fit planes to the distribution of poles calculated using Bingham axial distribution analysis of the data. Assuming the girdle distribution of poles to foliation in **A** and **C** results from cylindrical folding, then the poles to the NE striking best fit planes, shown as small shaded gray boxes, represent the orientations of the best fit fold axes to the data. The NW striking great circles in **A** and **C** are the planes to poles that, based on visual estimation, plot in the center of the highest concentration of poles to foliation. The labels are the numeric values for the strike and dip of the great circles and the trend and plunge of the poles. Type 2 mineral lineations include the long axis of elliptically shaped mineral grains, trains of extended and locally fractured mineral grains, and minerals streaked out on shear surfaces. In thin sections and outcrop exposures oriented parallel to type 2 mineral lineations and perpendicular to the host foliation a preferred sense of shear commonly is observed.

STRUCTURAL DATA FOR THE TEHACHAPI INTRUSIVE COMPLEX AND THE EASTERN TEHACHAPI SHEAR ZONE

POLES TO SUB-SOLIDUS FOLIATION

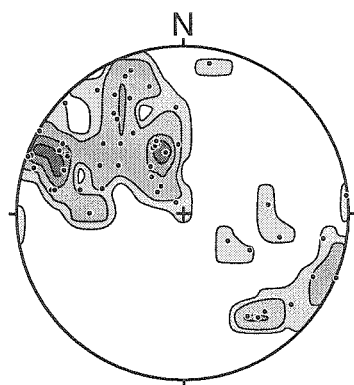
TEHACHAPI INTRUSIVE COMPLEX FABRICS



Number of points = 842

A

TYPE 1 MINERAL LINEATIONS AND HINGELINES OF MESOSCALE FOLDS

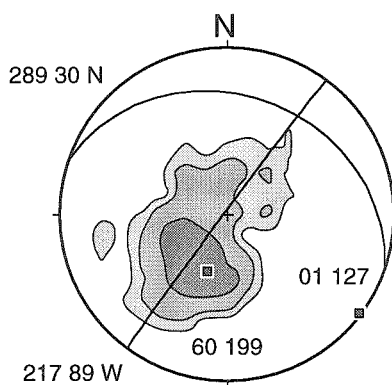


Number of points = 55

B

EASTERN TEHACHAPI SHEAR ZONE FABRICS

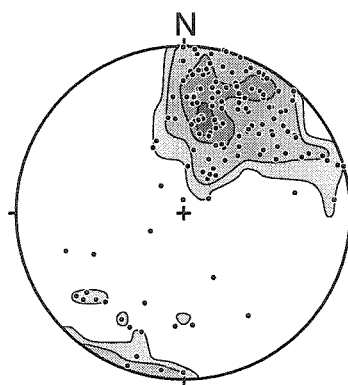
POLES TO MYLONITIC FOLIATION AND SHEAR BANDS



Number of points = 270

C

TYPE 2 MINERAL LINEATIONS AND STRIAE ASSOCIATED WITH SHEAR ZONE FABRICS



Number of points = 151

D

Lower hemisphere equal area projections.
Contours = 1%, 2%, 5%, and 7% per 1% area.

the distribution of foliation pole data in Figure 12A is similar to the orientations of type 1 mineral lineations and mesoscale folds shown in Figure 12B as well as to the orientation of map-scale folds which are discussed later. The high concentration of NW plunging lineations and fold axes suggests that structurally deeper levels of the Tehachapi Intrusive Complex are exposed to the southeast.

The first major deformation of the Tehachapi Intrusive Complex described above is inferred to be the same deformation as the second amphibolite facies deformation of the group I orthogneisses and the metasedimentary rocks for the reasons outlined below. First, the younger NW trending foliation and NW plunging lineations in the paragneiss and group I orthogneiss are mostly concordant to the high temperature subsolidus foliation and lineations in the Tehachapi Intrusive Complex, compare Figure 10 with Figure 12A and Figure 12B. Second, the first deformation of the Tehachapi Intrusive Complex and the second deformation of the group I orthogneisses both are accompanied by amphibolite facies metamorphism. Third, F3 folds in the paragneiss and map-scale folds in the Tehachapi Intrusive Complex both typically are tight to close and have axial surfaces that dip moderately to the NE. Based on the above observations the NW trending folds developed in the Tehachapi Intrusive Complex are inferred to be F3 folds. F3 folds and associated high temperature deformation fabrics in the Tehachapi Intrusive Complex are present in all three structural blocks of the gneiss complex.

Tonalite of the Tehachapi Intrusive Complex in the north structural block, called the Pine Tree tonalite sheet, is folded about subhorizontal NW trending axes into open to close F3 folds (Figures 4 and 9). The larger folds have a wavelength of several hundred meters and they have steeply NE dipping axial surfaces. The southwesternmost margin of the Highline olivine gabbro is deformed and folded in a small F3 synform. The biotite hornblende quartz diorite gneiss adjacent to the gabbro is also folded in this synform, but the nearby Brushy Ridge granite is not deformed in the fold suggesting it postdates the F3

folding. Enveloping surfaces tangent to the fold hinge regions in the Pine Tree tonalite, terminology of Hobbs et al. (1976), are subparallel to the local topography and dip shallowly to the NE. Foliation in most of the Pine Tree tonalite is moderately to steeply NE dipping except in fold hinge regions where subhorizontal to SW dips are observed. The structurally underlying gabbro in most areas of the north block is generally massive, medium grained, and weakly foliated.

The gabbro and tonalite in the central structural block between the Mountain Park and Taco Saddle ductile faults are the most deformed rocks of the Tehachapi Intrusive Complex (Figure 3). These units form a tectonic stratigraphy with the Brite Valley group metasedimentary rocks which from lowest to highest structural levels consists of gabbro, tonalite, and metasedimentary rocks, respectively. The tonalite gneiss in this block appears to be part of a formerly more or less continuous sheet that has been tectonically thinned and folded with portions removed by erosion and/or later faulting. Thickness of the tonalite layer that remains ranges from a few meters to about 200 meters. The major structure in the central block is a map-scale, asymmetric, SW vergent F3 antiform of tonalite gneiss cored by gabbro gneiss and named the Deer antiform (Figures 4 and 9). Folded tonalite in the hinge region of the Deer antiform is shown in Figure 11B.

The hinge line of the Deer antiform is NW trending and plunges shallowly to the NW or SE throughout most of the study area (Figure 9). In the northwest part of the central block north of Brite Valley, however, it plunges gently to the N and the gabbro core of the antiform disappears (Figure 4). South of Brite Valley the southwest limb of the antiform is overturned and dips steeply to moderately to the NE. The tonalite in the overturned limb is moderately to well foliated while the tonalite in the upright limb generally has a more intense gneissic fabric. Mylonitic and shear band fabrics found throughout the central structural block commonly crosscut the gneissic foliation in the tonalite and are inferred to be part of the eastern Tehachapi shear zone as will be discussed

later. The tonalite in the northeast limb of the Deer antiform appears to have several smaller second order F3 folds with NW trending axes superimposed on it (Figures 4 and 9). The tonalite appears to be preserved in synformal culminations of the second order F3 folds and former continuity of the tonalite is inferred. The intensity of the high temperature solid-state fabric development, the tightness of the Deer antiform, and the amount of attenuation and secondary folding of the limbs of the antiform all appear to increase from northwest to southeast in the central block, reaching a peak in the vicinity of Astronomy Ridge.

The south structural block of the gneiss complex is less deformed than the north and central blocks. Like the adjacent central block to the north the south block contains an areally extensive three layered sequence consisting of gabbro overlain by tonalite which in turn is overlain by metasedimentary rocks of the Brite Valley group. This block encompasses the rocks of the high peaks of the eastern Tehachapi Mountains including Tehachapi Mountain, Double Mountain, and Bison Peak. The map pattern of alternating northwest trending bands of gabbro and tonalite in Figure 4 suggests the south block is traversed by several regional-scale antiforms and synforms (Figure 9). Quartz diorite exposed on the southwest flank of Tehachapi Mountain is characterized by the local presence of coarse grained blebs of quartz that resemble gumdrops (Plate 1). This "gumdrop" quartz diorite is transitional in composition and texture between the gabbro and the tonalite of the Tehachapi Intrusive Complex which suggests that the contact between those two units parallels the topography on the southwest flank of Tehachapi Mountain and dips shallowly to the SW on the flank of a regional antiform. The scale and trend of these inferred structures suggests they are F3 folds like the Deer Antiform discussed above, although these folds appear to be more open and upright. Throughout the south structural block the tonalite typically is moderately to well foliated while the gabbro is generally poorly to moderately foliated with local areas of preserved cumulate textures. On average the foliation in the south structural block dips moderately to the NE.

REGIONAL-SCALE F4 FOLDING - THE TEHACHAPI VALLEY AND WALKER BASIN OROCLINES

Following most of the F3 folding and the associated high-temperature subsolidus fabric development in the study area the rocks of the eastern Tehachapi gneiss complex locally appear to have been folded into a large open concave-NE map-view fold. The most noticeable effect of this folding is the change in trend of the Deer antiform hinge line in the vicinity of southern Brite Valley (Figures 4 and 9). North of Brite Valley the F3 Deer antiform hinge line has a trend of $\sim N15^{\circ}W$ while southeast of the valley the hinge line has a trend of $\sim N60^{\circ}W$. Other F3 fold hinge lines in the vicinity of Brite Valley show similar changes in trend (Figure 9). The foliation trends do not appear to change as dramatically as the trend of the fold hinge, but north of Brite Valley in the central structural block the foliation in the tonalite has a more northerly trend overall than it does southeast of Brite Valley. A progressive change in trend of the high temperature subsolidus foliation in the Tehachapi Intrusive Complex south to north across Tehachapi Valley appears to reflect this folding as well and will be discussed later.

This map-scale folding in plan-view is designated F4 since the hinge line of the F3 Deer antiform is folded. Estimation of the orientation of the F4 fold axis is difficult since the fold does not have a well defined hinge and the contacts deflected in the hinge region have varying orientations. The hinge line of the gabbro-tonalite contact in the F3 Deer antiform has an overall subhorizontal to shallow northwesterly plunge throughout most of the study area. The shallow northward plunge of the F3 Deer antiform hinge line does not appear to change significantly in the vicinity of Brite Valley where the trend changes by $\sim 45^{\circ}$ across the F4 fold. This suggests that the F4 axis has a steep to subvertical plunge and that the F4 folding is oroclinal. The curved F3 Deer antiform hinge line and the curving trend of the high temperature subsolidus foliation also might be interpreted as having formed in situ without rotation about a steeply plunging F4 fold axis by conforming

around a rigid block impinging from the east. However, the inferred regional extent of the F4 folds, as discussed below, and the lack of kinematic data in this study indicating westward vergent thrusting suggests this is not the case.

The open to gentle F4 fold in the southern Brite Valley area appears to be part of much larger dextral-sense regional-scale Z-shaped fold of the crystalline basement in the southern Sierra Nevada. This regional-scale folding is reflected by changes in the trends of metasedimentary pendants (Figure 2). North of the area shown in Figure 2 the pendants in the Sierra Nevada batholith have mostly N-NW trends. South of about latitude $35^{\circ} 30' N$ the pendants deviate from the N-NW trend and they define a large open Z-shaped fold. Walker Basin is located within the northern bend of the Z-fold and Tehachapi Valley occupies the southern bend of the Z-fold defined by the pendants. The foliation in the plutonic rocks around the folds is subparallel to the contacts with the adjacent metasedimentary screens and pendants and both appear to be moderately to steeply dipping (Dibblee and Chesterman, 1953; Louke, 1966; Dibblee and Louke, 1970; Dibblee and Warne, 1970; Gazis and Saleeby, 1991) which suggests these regional-scale folds have moderately to steeply plunging axes. For convenience the convex-east fold is called the Walker Basin orocline and the convex-west fold is called the Tehachapi Valley orocline. In the region where Highway 58 crosses the screen of metasedimentary rocks at the northwest corner of Tehachapi Valley (Figure 2) there are ten-meter-scale dextral-sense Z-folds and kinks with moderate to steep N plunging axes in the paragneiss. These folds are interpreted to be smaller secondary F4 folds that formed during the regional-scale basement folding event.

THE EASTERN TEHACHAPI SHEAR ZONE

The central part of the eastern Tehachapi gneiss complex is traversed by the eastern Tehachapi shear zone which is a 2 to 3 km wide NW trending shallow NE dipping ductile shear zone with top to the S-SW shear sense (Figure 3). Deformation in the shear zone

was accompanied by greenschist facies retrograde metamorphism although early activity may have occurred during amphibolite facies conditions. Penetrative protomylonitic fabrics are developed locally in quartz bearing rocks throughout the central structural block and in the adjacent margins of the north and south structural blocks. Non-penetrative shear bands deform quartz poor lithologies in the shear zone and are common in all lithologies adjacent to the shear zone. The shear zone as shown in Figure 3 encompasses the region where quartz bearing rocks of the gneiss complex commonly are deformed to protomylonites. The structural thickness of the eastern Tehachapi shear zone normal to its margins is about one km. The Mountain Park and the Taco Saddle ductile faults bound the central and most deformed part of the shear zone. A zone of oblique dextral-sense ductile shearing immediately north of Tehachapi Valley (Figure 2) is inferred to be the northward continuation of the eastern Tehachapi shear zone and may be continuous with the proto-Kern Canyon fault zone to the north, as will be discussed later. South of Tehachapi Valley the ductile faults in the eastern Tehachapi shear zone may have accommodated as much as 5 to 8 km of displacement based on the apparent telescoping of regional geologic features.

SHEAR ZONE FABRICS AND METAMORPHISM

In the shear zone the moderate to steeply NE dipping high temperature subsolidus fabric of the gneiss complex is crosscut and locally transposed by shallow NE dipping protomylonitic foliation and shear bands. The mylonitic foliation is defined by ribbons of dynamically recrystallized quartz grains, porphyroclasts of fractured, flattened, and elongate feldspar grains, and trains of mica strung out along shear planes. The shear band foliation is defined by discrete non-penetrative shear surfaces, generally less than 1 millimeter thick, which crosscut and deflect the preexisting fabrics. The primary distinction between the protomylonitic and the shear band foliations is that in the former the shear planes are penetrative at thin section scale and dominate the fabric of the rock while in the latter the shear planes are non-penetrative and the rock fabric is dominated by the

preexisting foliation. Figure 12C is a stereonet plot of poles to the mylonitic foliation and shear bands in the eastern Tehachapi shear zone. It shows that the shear zone fabrics dip more shallowly to the northeast than the high temperature fabrics in the gneiss complex shown in Figure 12A.

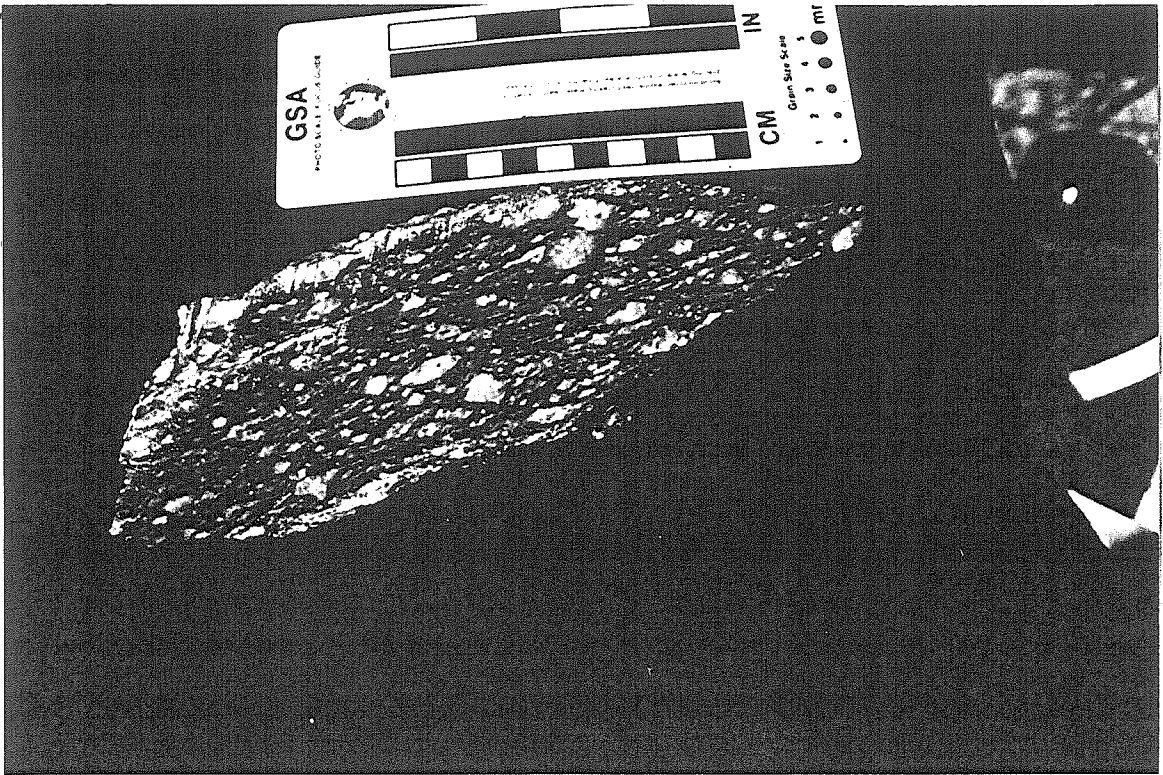
Lying within the protomylonitic foliation and the shear bands are N-NE trending type 2 mineral lineations and striations (Figure 12D). The type 2 mineral lineations are defined by elongate aggregates of quartz and feldspar, fractured and extended porphyroclasts of hornblende, feldspar, and garnet, and elongate smears of biotite, white mica, chlorite, or epidote. The striations are defined by fine-scale ridges and grooves that commonly are present on exposed shear surfaces, the "ridge-in-groove slickenside striae" of Lin and Williams (1992b). The type 2 mineral lineations and striations are interpreted to represent the transport direction (i.e. the "slip lineation") of the shear zone as opposed to the long axis of the finite strain ellipsoid (i.e. the "stretching lineation") since the lineations were measured in the shear surfaces and not in the schistosity surfaces as discussed earlier in this chapter. The orientations of type 2 mineral lineations and striations found in the gabbro and tonalite of the Tehachapi Intrusive Complex, the No Name Canyon augen gneiss, and group III leucocratic granite deformed in the shear zone are shown in Figure 12D. The majority of the type 2 mineral lineations and the striations are N-NE trending and plunge shallowly to the N-NE, although some of the lineations plunge shallowly to the S-SW.

Throughout the eastern Tehachapi shear zone kinematic indicators such as composite foliations, shear bands, mica fish, and asymmetric porphyroclasts viewed in surfaces perpendicular to the foliation and parallel to the type 2 mineral lineations and striations all consistently indicate top to the S-SW shear sense. An example of a kinematic indicator used in this study is shown in Figure 13A where a sample of augen gneiss displays a shear band fabric which indicates dextral (top to the S-SW) shear sense. Most

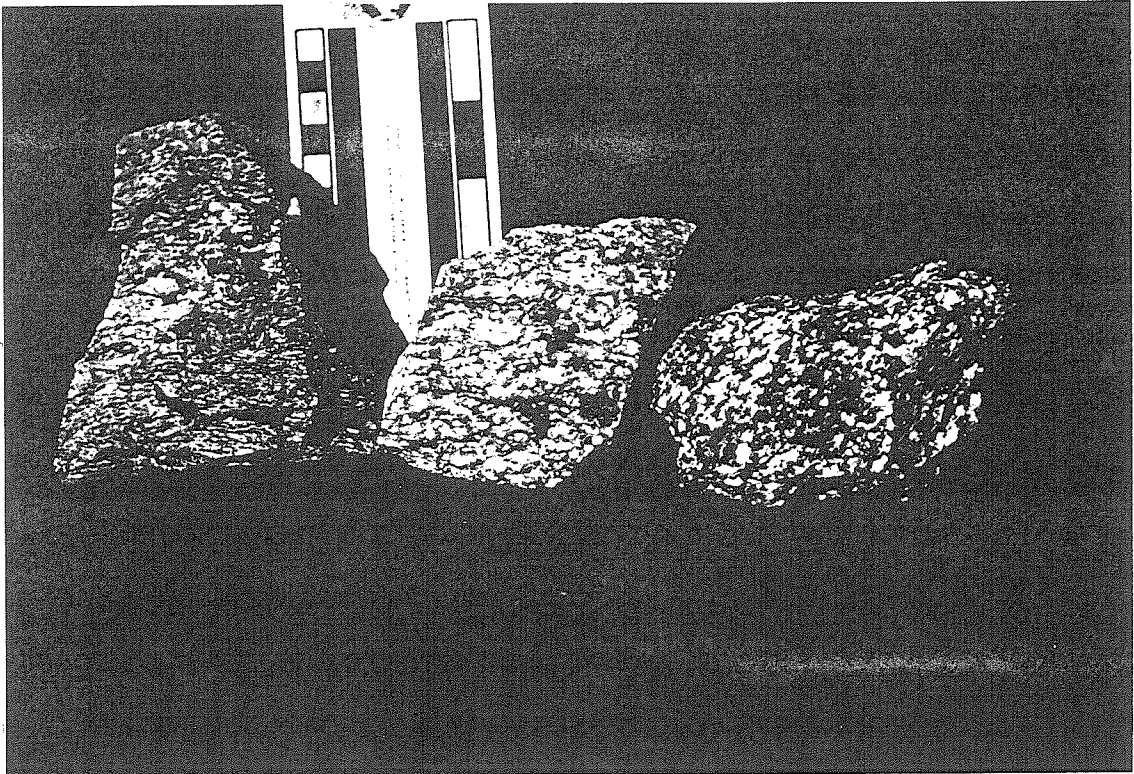
Figure 13.

A) Sample of augen gneiss of No Name Canyon with a composite fabric yielding sense of shear information. A penetrative foliation in the sample dips shallowly to the left in the photo and the foliation is crosscut by discrete shear surfaces which parallel the top and bottom margins of the photo. The sample has been cut perpendicular to the foliation and parallel to type 2 (slip) lineations found in the shear surfaces. Deflection of the foliation into the shear surfaces (most easily visible in upper right part of the cut sample) indicate dextral shearing which corresponds with top to the SSW shearing when the sample is in place in the field. B) Three samples of biotite hornblende tonalite from the Tehachapi Intrusive Complex showing changes visible in hand specimen resulting from deformation in the eastern Tehachapi shear zone. The tonalite on the right is from outside the shear zone in the south structural block and it is unaltered, it has a relatively high color index (dark minerals are hornblende and biotite and light minerals are plagioclase and quartz), and it has a moderately developed high temperature subsolidus foliation. The tonalite in the center is from the eastern Tehachapi shear zone in the central structural block and it has a strong gneissic to protomylonitic foliation. It also is substantially altered and has a lower color index than tonalite from outside the shear zone. The mafic minerals are partially replaced by chlorite and epidote and the plagioclase is saussuritized. The sample on the left is orthomylonitic tonalite from the Taco Saddle ductile fault which bounds the central structural block. The orthomylonitic tonalite is severely altered and almost all of the mafic minerals are replaced by chlorite and epidote. C) Photomicrograph of the orthomylonitic tonalite in B. The view in the photomicrograph is perpendicular to the mylonitic foliation and parallel to the mineral lineation. The width of the field of view is ~3 millimeters. The small lighter colored grains throughout the photo are recrystallized quartz and altered plagioclase. The dark lozenge-shaped mineral above and to the left of the center of the photomicrograph is chlorite. The asymmetric shape of the chlorite grain indicates that it has

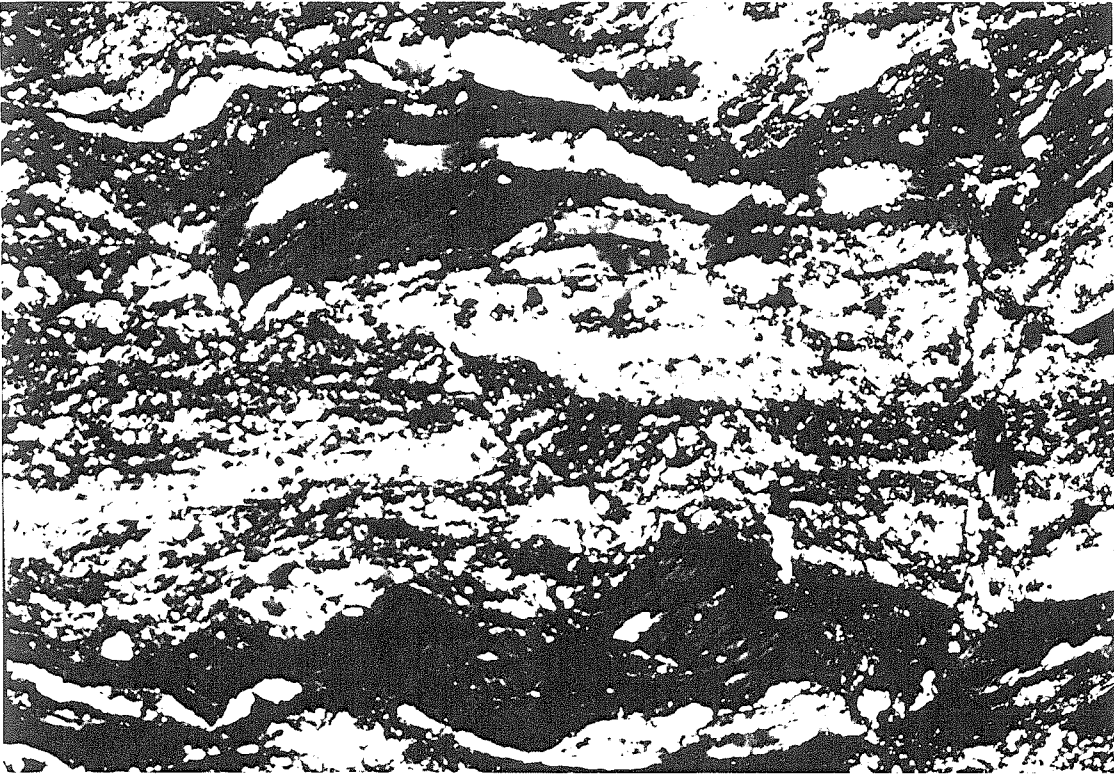
been sheared in a dextral sense. Along the bottom of the photomicrograph is another chlorite grain which is slivered by several synthetic dextral shears. The deformed secondary chlorite in this sample is evidence for fluid influx during shearing. D) Mylonitic tectonite with concordant quartz veins in the eastern Tehachapi shear zone. The gray colored layer beneath the top edge of the quarter is mylonitic marble. Below the quarter the white layers are quartz veins which are hosted by mylonitic tonalite.



A

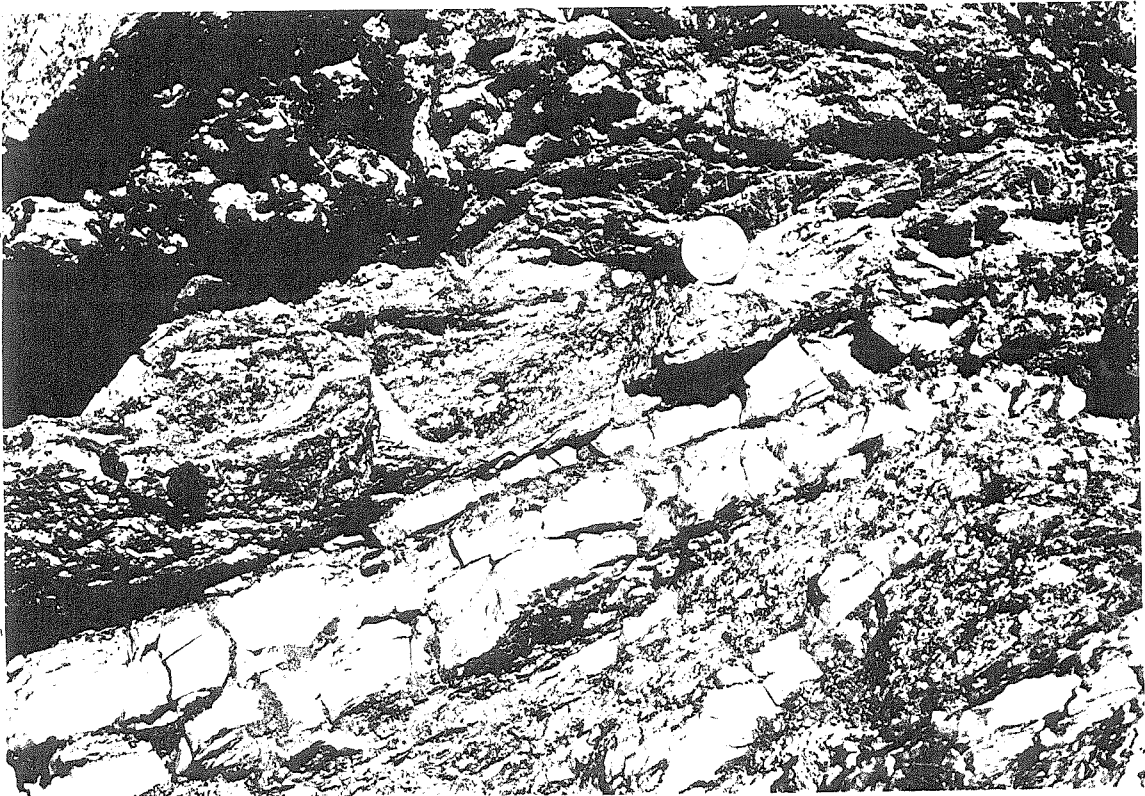


B



C

D



of the shallowly SW dipping shear surfaces and SW plunging lineations shown in Figure 12C and Figure 12D are from sheared tonalite gneiss on the southwest side of the hinge region of map-scale F3 folds. The shear sense in these local areas of SW dipping fabrics is also top to the S-SW which suggests that tightening of preexisting F3 folds during shear zone deformation may have slightly rotated early formed mylonitic and shear band fabrics through the hinge regions of the folds.

Deformation textures and retrograde greenschist facies mineral assemblages in the shear zone rocks suggest the deformation was accompanied by an influx of fluids and was continuous over an interval of waning temperature. Throughout the shear zone quartz is ribboned and dynamically recrystallized to polycrystalline aggregates composed of grains 0.1 to 0.5 millimeters in diameter. Most of the plagioclase and potassium feldspar in the mylonitic rocks is brittlely fractured, but sweeping or undulatory extinction and incipient subgrain development present in some feldspar grains indicates some deformation of feldspar occurred by crystal-plastic processes. The largely brittle deformation of feldspar in conjunction with the plastically deformed quartz suggests the rocks in the shear zone were deformed at a temperature of 400° to 500° C (Tullis and Yund, 1977).

Biotite and hornblende in the deformed rocks frequently are replaced by chlorite and epidote and the plagioclase is extensively saussuritized. The color index of the Tehachapi Intrusive Complex tonalite in the shear zone is consistently lower than it is in the tonalite outside the shear zone (see Figure 13B and compare the color index of the central block tonalite with the tonalite in the north and south blocks in Table 4). In the shear zone garnets growing across the earlier high temperature subsolidus fabric are fractured, locally extended in a direction parallel to the type 2 mineral lineations of the shear zone, and altered to chlorite. In some areas secondary epidote is clearly ductilely deformed and chlorite grains are deformed into "fish" along shear surfaces indicating that some of the deformation followed initial alteration of the rocks (Figure 13C). Quartz veins concordant to the

mylonitic fabric in the shear zone also suggest fluid influx during deformation (Figure 13D). In some of the samples from the shear zone that were examined quartz grains are fractured and tension gashes that crosscut the ductile fabric of the rock are filled with unstrained quartz. The orientation of the tension gashes is consistent with the top to the S-SW shear sense indicated by the ductile fabrics. The fracturing of quartz late in the evolution of the shear zone suggests temperatures on the order of 300° C (Tullis and Yund, 1977). Locally, in both the north and the central structural blocks veins of undeformed vitreous quartz up to several meters thick crosscut the ductilely deformed gneisses.

MOUNTAIN PARK FAULT

The Mountain Park ductile fault which separates the northern structural block from the underlying central block is a discontinuously exposed zone of localized intense ductile shearing. Where well exposed it is a several meter thick shallowly to moderately NE dipping zone of ortho- to ultramylonitic mixed gneisses that are extensively hydrothermally altered and retrograded. Ductile microstructures in the orthomylonite indicate top to the SW shear sense. In some areas a chloritic breccia is present in the fault zone and steeply NE dipping tension gashes filled with drusy quartz in adjacent orthogneisses suggest the ductile fault may have been reactivated later as a normal sense top to the NE brittle fault.

TACO SADDLE FAULT

The southwest boundary of the central structural block is the Taco Saddle ductile fault which is a locus of intense ductile shearing similar the Mountain Park fault zone along the northeast edge of the block (Figure 4). The Taco Saddle ductile fault is well developed only along the southernmost part of the Astronomy Ridge block where it is expressed by a zone of ortho- to ultramylonitic tonalite up to about 10 meters thick. The mylonite fabrics are shallowly to moderately NE dipping and kinematic indicators indicate top to the S-SW shear sense. Locally, the orthomylonite in the fault is shattered and forms light green colored cataclasite that has no discernible fabric. Thin section examination of less fractured

mylonite reveals incipient cataclasis and the fractures are filled with recrystallized quartz. The obliquity of recrystallized quartz grains in the fractures indicates the same top to the S-SW shear sense as the mylonite suggesting that top to the S-SW motion on this fault continued into the brittle regime. The trace of the Taco Saddle ductile fault to the northwest is less obvious, in part because exposures are limited. Orthomylonitic fabrics locally are developed along the contact between the southwest edge of the tonalite of the southwest limb of the Deer antiform and Brite Valley metasedimentary rocks in the underlying central block, but clear evidence for a discrete fault along strike to the northwest of Tehachapi Mountain Park is lacking.

POSSIBLE LARGE SCALE SHEATH FOLD AT ASTRONOMY RIDGE

There is some suggestion that a large-scale sheath fold may be partially developed in the vicinity of Astronomy Ridge at the southwest end of the central structural block (Figure 4). In map view the NW trending tonalite layers in the central block are deflected first to the south in the vicinity of Astronomy Ridge and then south and east of Astronomy Ridge the layers curve back around to an E trend, defining a southwestward protruding bulge. In addition, inferred F3 fold hingelines in the Astronomy Ridge area, although poorly defined because of tectonic attenuation, appear to be rotated in approximately the same sense as the lithologic layering (Figure 9). On the northwest flank of Astronomy Ridge both the gneissosity and the shear bands in the tonalite and gabbro locally are transposed and have N-NE strikes and shallow SE dips, but type 2 mineral lineations developed in the shear surfaces in this area still have the same N-NE trend and shallow NE plunge as they do elsewhere in the shear zone. Southeast of Astronomy Ridge the orientation of the gneissosity and shear surfaces locally mirrors the orientations observed northwest of Astronomy Ridge, having a similar NE strike, but having shallow NW dips instead of SE dips. The intensity of fabric development southeast of Astronomy Ridge, however, is not as great as it is to the northwest of Astronomy Ridge.

This apparent "bulge" to the southwest in the contacts and F3 fold hingelines exposed on Astronomy Ridge and the localized transposition of deformation fabrics on the northwest and southeast flanks of this deflection may represent the partial development of a large NE trending, shallowly NE plunging, but SW vergent sheath fold. This inferred sheath fold appears to have developed coevally with the eastern Tehachapi shear zone because type 2 mineral elongation lineations and slip lineations within this structure have the same orientation as similar lineations throughout the shear zone. In addition, even though shear surfaces on the flanks of this structure have NE trends, in contrast to the NW trends of shear surfaces throughout the rest of the shear zone, the sense of shear in both areas is the same, top to the S-SW. Development of this inferred large-scale open sheath fold with a generally NE trending axis subparallel to the regional orientation of mineral elongation lineations may have occurred by rotation of the previously existing NW trending F3 Deer antiform axis into the SW shear direction of the eastern Tehachapi shear zone. This type of mechanism has been proposed for the formation of sheath folds in high strain shear zones by Cobbold and Quinquis (1980). Development of this possible sheath fold at the southeast end of the central structural block may reflect greater strain in this part of the shear zone which is broadly consistent with the inferred southeastward increasing displacement along the Taco Saddle ductile fault discussed below and also with the observation that the thickness of tonalite layers appear to decrease to the southeast.

SHEAR ZONE NORTH OF TEHACHAPI VALLEY

The regional mapping of Ross (1989b) shows a relatively narrow zone of "cataclastic" deformation extending north of Tehachapi Valley centered along the continuous screen of metasedimentary rocks extending north from the northwest corner of Tehachapi Valley (Figure 2). In order to investigate the possible continuation of the eastern Tehachapi shear zone north of the main study area the geology of the area north and west of Tehachapi Valley to the latitude of Tweedy Creek was examined in reconnaissance and

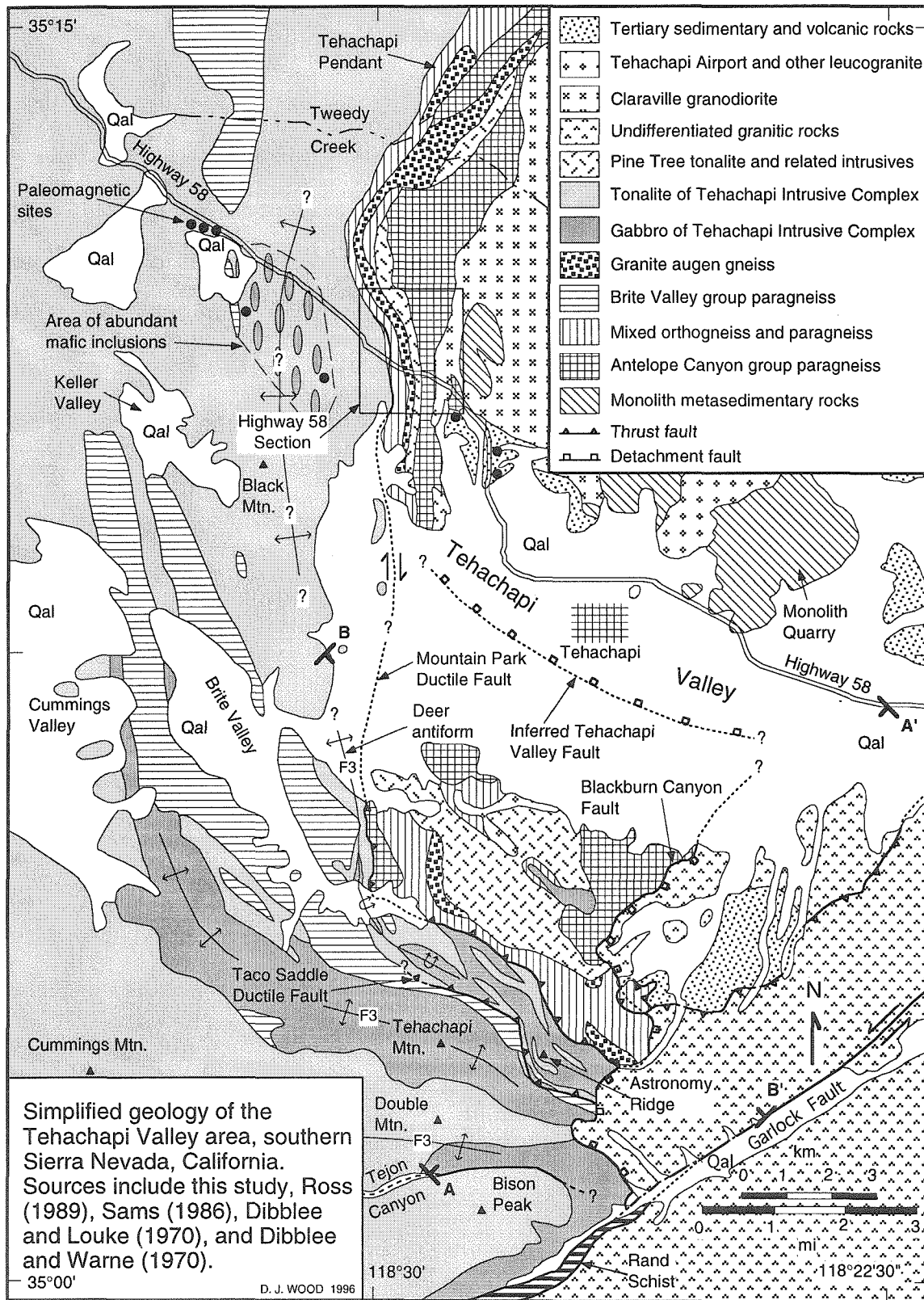
several square miles of the area in the vicinity of Highway 58 at the northwest corner of Tehachapi Valley was mapped at a scale of 1:12,000. Figure 14 is a simplified geologic map of the Tehachapi Valley area compiled from the mapping of this study south and north of Tehachapi Valley and a number of other sources listed in the figure caption. North of Tehachapi Valley there is a sequence of deformed metasedimentary rocks and intrusive units that is remarkably similar to the sequence of gneisses exposed south of Tehachapi Valley in the eastern Tehachapi gneiss complex (Figure 14).

The lithologies north of Tehachapi Valley which appear to have correlatives in the eastern Tehachapi gneiss complex south of Tehachapi Valley are from west to east: 1) biotite hornblende tonalite of the Tehachapi Intrusive Complex (i.e. Bear Valley Springs tonalite of Ross (1989b)) which hosts a pendant of metasedimentary rocks compositionally similar to the Brite Valley group rocks, 2) an interval of intimately mixed undifferentiated paragneiss, and tonalite orthogneiss that is similar to the group I tonalite gneiss south of the valley, 3) a long narrow tabular shaped body of the Tweedy Creek augen gneiss of Sams (1986) which is compositionally and texturally similar to the granite augen gneiss of No Name Canyon south of Tehachapi Valley, 4) two thin discontinuous sheetlike intrusions of biotite hornblende tonalite, one of which is the tonalite "cupola" of Saleeby et al. (1987), which are texturally and compositionally similar to the Pine Tree tonalite sheet south of Tehachapi Valley, and 5) a section of metasedimentary rocks with a sequence of lithologies similar the Antelope Canyon group paragneiss.

The lithologic sequences north and south of Tehachapi Valley are mostly similar, but there are two important differences. First, gabbroic rocks of the Tehachapi Intrusive Complex which are abundant south of Tehachapi Valley, are largely absent north of Tehachapi Valley. South of the valley gabbro is widely exposed in the cores of map-scale F3 antiformal folds and it is inferred to structurally underlie much of the tonalite of the Tehachapi Intrusive Complex. The only significant exposures of rocks of gabbroic

Figure 14.

Simplified geology of the Tehachapi Valley area showing that the distinctive sequence of lithologic units found south of Tehachapi Valley is also found to the north of Tehachapi Valley. The locations of several inferred map-scale F3 antiformal folds are shown in the figure. The Highway 58 section outlined in the figure is one of the domains for which structural data is shown in Figure 15. **A-A'** and **B-B'** are the locations of the geologic cross sections shown in Figure 22. The solid black circles are locations where paleomagnetic data were collected in the study of Kanter and McWilliams (1982). The area of abundant mafic inclusions is from Ross (1989b) and the sizes of the inclusions in the figure are schematic and not to scale. The sources for the geology in this figure are from this study, Ross (1989b), Dibblee and Louke (1970), Dibblee and Warne (1970), Sams (1986), and a compilation of student maps from a 1993 Caltech field class (led by J. B. Saleeby and L. T. Silver) held in the area north of Tehachapi Valley.



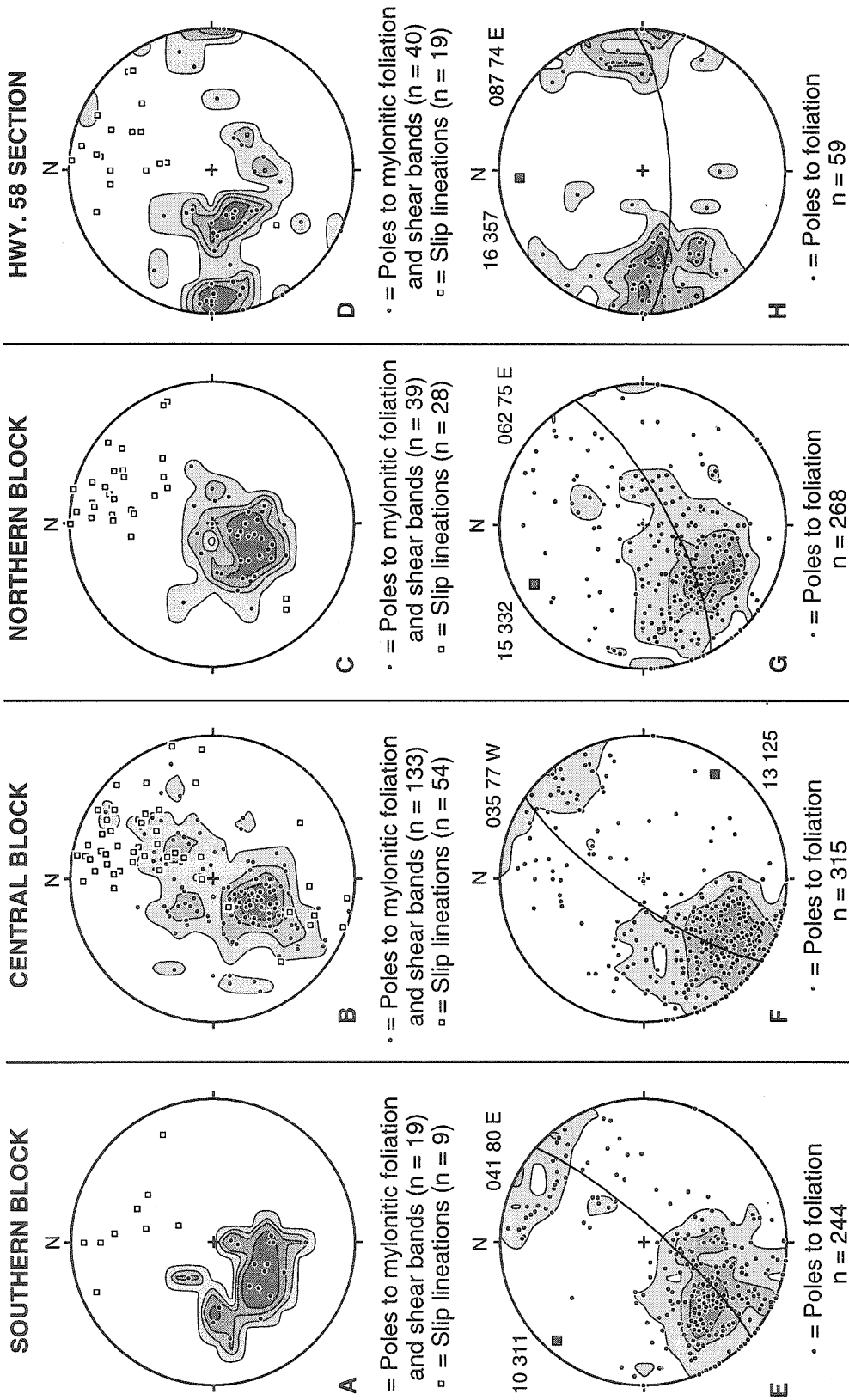
composition north of Tehachapi Valley are part of a small swarm of mafic inclusions in the tonalite northwest of Tehachapi Valley (Ross, 1989b). The abundance of gabbroic rocks south of Tehachapi Valley suggests that deeper levels of the batholithic crust may be exposed there than to the north which is consistent with the overall southward increase in depth of exposure of the southern Sierra Nevada batholith (Saleeby, 1990b). The second major difference between the lithologic sequences north and south of Tehachapi Valley is that the eastern margin of the sequence north of Tehachapi Valley is intruded by the biotite tonalite and granodiorite of Claraville (Saleeby et al., 1987; Sams and Saleeby, 1988) in contrast to the correlative boundary south of the valley where granodioritic rocks of the Oak Creek Pass complex overlie the gneiss complex along the Blackburn Canyon cataclastic fault zone. While the granodioritic rocks south of Tehachapi Valley in the hangingwall of the Blackburn Canyon fault do not appear to be significantly involved in the eastern Tehachapi shear zone there is a zone of dextral-oblique ductile deformation in the western margin of the Claraville granodiorite north of Tehachapi Valley that is inferred to be related to the eastern Tehachapi shear zone as will be discussed below.

The Tehachapi Intrusive Complex tonalite and Claraville granodiorite north of Tehachapi Valley both have an overall subhedral granular texture with a weak to moderate subsolidus foliation defined by the preferred alignment of plagioclase grains, mafic minerals, and flattened mafic enclaves. In the margins of those plutons adjacent to the N trending metasedimentary pendant where it crosses Highway 58 the solid-state foliation is more intensely developed and the texture of the rocks changes to become more anhedral granular. The foliations in the pluton margins are mostly N trending and steeply dipping (Figure 15H) and locally the rocks have a gneissic character defined by lenticular shaped quartz grains. The foliation in the deformed margins of the plutons is subparallel to the moderately to steeply dipping gneissic foliation in the intervening metasedimentary rocks, orthogneisses, and Pine Tree tonalite sheet. Superimposed on the gneissic fabric of the

Figure 15.

Structural data for the eastern Tehachapi shear zone plotted by structural domain. The locations of the southern, central, and northern structural blocks are shown in figure 3, and the location of the Highway 58 section is shown in Figure 14. The data are plotted on lower hemisphere equal area stereonet projections and poles to foliation are contoured at 1%, 3%, 5%, and 7% per 1% area. Lineations also are plotted in some of the stereonet plots, but the lineations are not contoured. **A**, **B**, and **C** are plots of poles to the eastern Tehachapi shear zone mylonitic and ductile shear band foliation in the Tehachapi Intrusive Complex from the southern, central, and northern structural blocks, respectively. **D** is a plot of poles to the shear zone mylonitic and ductile shear band foliation in the Tehachapi Intrusive Complex (including the Pine Tree tonalite) and the Claraville granodiorite in the Highway 58 section. The small squares plotted in **A**, **B**, **C**, and **D** are slip lineations (type 2 mineral lineations and slickenside striae) within the shear zone mylonitic and shear band foliation. The slip lineations are not contoured. **E**, **F**, **G**, and **H** are plots of pre-eastern Tehachapi shear zone high temperature gneissic foliation from the same units and structural domains as plots **A**, **B**, **C**, and **D** above, respectively. The great circles (with their associated poles represented by gray boxes) in **E**, **F**, **G**, and **H** represent best fit planes to the data calculated using Bingham axial distribution analysis. The labels are the numeric values for the strike and dip of the great circles and the trend and plunge of the poles. **I**, **J**, **K**, and **L** are plots of mineral stretching lineations (type 1 mineral lineations) associated with the high temperature gneissic foliation and mesoscale fold hinge lines from the same units and structural domains as above.

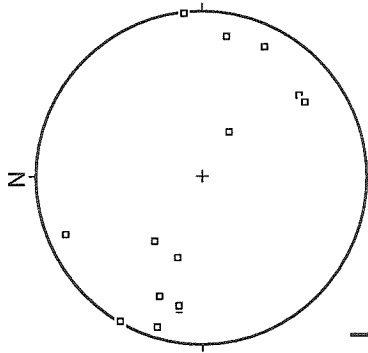
STRUCTURAL DOMAINS OF THE EASTERN TEHACHAPI SHEAR ZONE - DATA FROM THE TEHACHAPI INTRUSIVE COMPLEX AND THE CLARAVILLE GRANODIORITE
 (Lower hemisphere equal area projections, contours = 1%, 3%, 5%, and 7% per 1% area.)



STRUCTURAL DOMAINS OF THE EASTERN TEHACHAPI SHEAR ZONE

(Figures are lower hemisphere equal area stereonet projections)

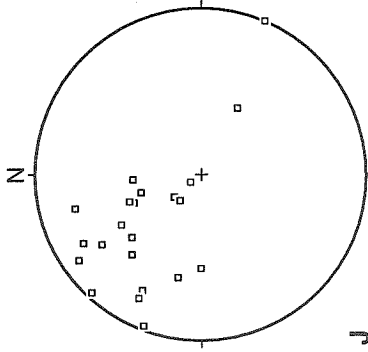
SOUTHERN BLOCK



I

Mineral elongation lineations
and fold hingelines
Number of points = 15

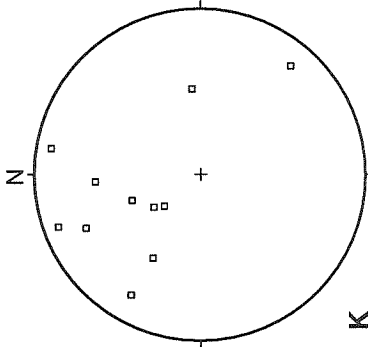
CENTRAL BLOCK



J

Mineral elongation lineations
and fold hingelines
Number of points = 24

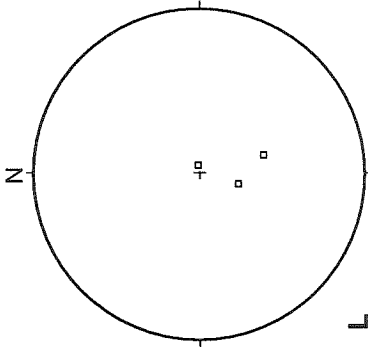
NORTHERN BLOCK



K

Mineral elongation lineations
and fold hingelines
Number of points = 11

HWY. 58 SECTION



L

Mineral elongation lineations
Number of points = 3

pendant rocks and pluton margins are non-penetrative ductile shear bands and locally a protomylonitic foliation. Some of the shear bands are steeply dipping and subparallel to the gneissic foliation, and some dip shallowly to the N and E and crosscut the gneissic foliation at high angle (Figure 15D).

In the shear bands quartz is dynamically recrystallized, feldspar is fractured, and biotite and hornblende are extensively altered and replaced by chlorite and epidote. Striations and type 2 mineral lineations defined by smeared micaceous minerals and elongate quartz-feldspar aggregates are present in the shear surfaces and plunge shallowly to the north-northeast (Figure 15D). In the Highway 58 area the shear sense of the subvertical shear bands is dextral and the shear sense of the N dipping shear bands is top to the S-SW. Even though there appears to be a bimodal distribution in the orientation of the shear bands around Highway 58 (Figure 15D) the similar orientation of striations and type 2 mineral lineations, the overall dextral oblique shear sense, and the greenschist facies mineral assemblages of all the shear bands suggest that the shear bands all formed during the same deformation event.

The shear bands developed in and around the Tehachapi pendant north of Tehachapi Valley are not as penetrative as the mylonitic fabrics and shear bands of the eastern Tehachapi shear zone south of Tehachapi Valley, but they have a similar orientation, shear sense, and metamorphic mineral assemblage which suggests that the eastern Tehachapi shear zone continues northward from Tehachapi Valley in this location. A correlative structure to the Mountain Park ductile fault also may be present in the Highway 58 area. The contact between the Tehachapi Intrusive Complex tonalite and the mixed orthogneiss and paragneiss north of Tehachapi Valley (Figure 14) commonly is the locus of intense mylonitic deformation and it occupies the same structural and lithostratigraphic position as the Mountain Park fault south of the valley which suggests it may be the northward continuation of that structure.

Structural data for the eastern Tehachapi shear zone north and south of Tehachapi Valley are plotted by structural domain in Figure 15. The locations of the southern, central, and northern structural blocks are shown in Figure 3 and the location of the Highway 58 section is shown in Figure 14. The structural data shown are from the Tehachapi Intrusive Complex, including the Pine Tree tonalite, and the Highway 58 section plot includes data from the Claraville granodiorite. The orientations of the mylonitic foliation and the slip lineations are similar in all four domains of the shear zone (Figures 15A, B, C, and D) with two exceptions. In the central block (Figure 15B) the mylonitic foliation locally dips to the SW and a few of the lineations plunge to the SW as well. As discussed earlier the SW dipping and plunging foliations and lineations are found in the hinge regions of F3 folds and they are inferred to have rotated to the southwest around the fold hinges as the shear zone evolved. The second difference in shear zone fabrics among the structural domains is that N trending subvertical shear bands with dextral shear sense are present in the Highway 58 domain (Figure 15D), but they are lacking in the other structural domains south of Tehachapi Valley. The presence of both shallow NE dipping and subvertical mylonitic foliation in the shear zone on the north side of Tehachapi Valley suggests that the shear zone in the Highway 58 structural domain is transitional between the N trending steeply dipping dextral-sense proto-Kern Canyon fault zone along strike ~15-20 km to the north (Busby-Spera and Saleeby, 1990) and the shallow NE dipping thrust-sense eastern Tehachapi shear zone to the south.

The moderate temperature shear zone fabrics have similar orientations in the different structural domains, but the high temperature solid-state foliation that is crosscut by the shear zone foliation varies systematically between some of the different domains. Figures 15E, F, G, and H are stereonet plots of poles to the high temperature subsolidus foliations in the different structural blocks. The great circle in each plot represents the best fit plane to the data calculated using Bingham axial distribution analysis (Allmendinger,

1995) and the shaded gray boxes are the poles to the planes and are inferred to represent the best fit cylindrical fold axis to the data. The overall foliation trend is to the northwest in the southern and central blocks, to the north-northwest in the northern block, and to the north in the Highway 58 domain. Relative to the foliation in the Highway 58 domain the high temperature foliation in the northern block is rotated counterclockwise by about 25° , and the foliations in the central and southern blocks are rotated counterclockwise by about 45° to 50° .

The apparent rotation in strike of the high temperature foliation suggested by the data shown in Figure 15 is inferred to have occurred during the regional F4 oroclinal folding. The change in foliation orientation between the central and northern blocks suggests that the Mountain Park ductile fault, the boundary between the two blocks, may have accommodated some differential rotation between the two domains. The systematically varying orientation of the high temperature foliation in the different domains coupled with the relatively constant orientation of the shear zone fabrics in the different domains suggests that regional F4 folding of the basement rocks in the study area occurred prior to much of the activity along eastern Tehachapi shear zone. Coeval development of the shear zone and the F4 folding cannot be ruled out, however, since earlier shear zone deformation fabrics may have been transposed by later activity.

MAGNITUDE OF SHEAR ZONE DISPLACEMENT

Estimation of the displacement across the eastern Tehachapi shear zone using quantitative strain measurements of the deformed rocks was not attempted in this study. Much of the displacement across the shear zone, however, appears to be accommodated along the Mountain Park and Taco Saddle ductile faults and consideration of the regional geology suggests a rough estimate can be made for the displacement across these faults as described below.

Along most of its length the Mountain Park ductile fault juxtaposes mixed paragneiss and group I orthogneiss in the hangingwall against tonalite and gabbro gneiss of the Tehachapi Intrusive Complex in the footwall block (Figure 14). At the northernmost end of the Mountain Park ductile fault, before it disappears beneath the alluvium of Tehachapi Valley, the metasedimentary rocks of the Brite Valley group in the footwall are almost in contact with Antelope Canyon group rocks in the hangingwall. North of Tehachapi Valley these two groups of rocks are found in two separate metasedimentary pendants/screens which trend approximately parallel to one another for over 20 km, maintaining a fairly regular separation of 4 to 6 km over that distance (Figure 2). The relatively constant spacing between the subparallel metasedimentary pendants could be due to a number of factors. Prebatholithic faults and folds in the metasedimentary rocks may have controlled and localized intrusion of the plutons along discrete zones. Alternatively, these exposures may be remnants of a formerly more or less continuous cover of metasedimentary rocks overlying the presently exposed levels of the batholith. As was discussed earlier there is evidence suggesting that a series of regional-scale F3 folds developed in the batholith during deformation and the metasedimentary rocks may be preferentially preserved in synformal culminations of these large-scale F3 folds. While these two groups of metasedimentary rocks may have converged before shearing along the Mountain Park fault zone, their apparent convergence south of Tehachapi Valley and the presence of the fault zone between them suggests they may have converged along the fault. If so, then the Mountain Park ductile fault may have accommodated 4 to 6 km of shortening normal to the trend of the two groups of metasedimentary rocks.

The Taco Saddle fault is defined by a localized zone of mylonitic deformation at the contact between gabbro and tonalite in the central structural block and Brite Valley group metasedimentary rocks in the southern structural block (Figure 14). The thickness and intensity of the mylonite developed along this fault contact, however, decreases along strike

to the northwest and in the vicinity of Brite Valley the contact is clearly intrusive and not a fault zone. These observations suggest that the displacement along the Taco Saddle ductile fault decreases to zero to the northwest, paralleling the general decrease in deformation intensity to the northwest observed in the overlying Astronomy Ridge block. It appears that the Taco Saddle fault zone does not extend north of Brite Valley and that it is a dislocation along which one flap of batholithic crust, the central structural block, has been thrust over another flap of crust, the southern structural block, in a scissor-like fashion with some of the convergence perhaps accommodated by ductile folding in the central block.

A screen of metasedimentary rocks that is continuous for many km pinches out in the vicinity of Astronomy Ridge and appears to have been overridden along the Taco Saddle fault zone. This metasedimentary screen has a width of about 1 km southwest of where the Taco Saddle fault has little or no displacement. Assuming the screen formerly was this wide along strike to the southeast, then that would suggest that about 1 km or more of map-view displacement has been accommodated along the Taco Saddle fault at Astronomy Ridge. A maximum displacement of about 2 km at the southeast end of the Taco Saddle fault is suggested by the apparent convergence of the Tehachapi Mountain F3 antiformal fold hinge line with the fault (Figure 14).

In summary, the sections of the Mountain Park and Taco Saddle ductile faults in the southeastern part of the gneiss complex together may have accommodated as much as 5 to 8 km of map-view shortening normal to their trends. Given that both faults in this area dip $\sim 30^\circ$ NE then the total displacement parallel to the fault surfaces equals the map-view displacement divided by the cosine of 30° which is about 6 to 9 km. Thus, since the shear strains in the gneisses are unknown, a minimum estimate for the total displacement along the eastern Tehachapi shear zone is about 6 to 9 km.

LATE TO POST-EASTERN TEHACHAPI SHEAR ZONE DEFORMATION DEFORMATION OF THE BRUSHY RIDGE GRANITE AND NEARBY ROCKS

The upper structural levels of the north block of the gneiss complex are intruded by three small bodies of leucocratic granite called the Brushy Ridge granite (Figure 4). The two westernmost granite bodies form relatively thin sheets oriented subparallel to the Pine Tree tonalite. Decimeter- to meter-scale subvertical northeast trending leucogranite dikes which intrude the tonalite in the vicinity of the leucogranite sheets are inferred to be part of the Brushy Ridge granite (Figure 16A). The granite has a well developed foliation defined by the subparallel alignment of discontinuous thin (less than 0.5 millimeters wide) biotite-rich seams that alternate with 2 to 3 millimeter thick tabular domains of feldspar and quartz. The foliation is subconcordant to the contacts of the granite bodies and has a NW trend with mostly moderate to shallow NE dips (Figure 16B). Locally, the granite sheets appear to be warped into very gentle NW trending upright folds. The hinges of these folds in some cases appear to be nearly coincident with the F3 fold hingelines in the adjacent Pine Tree tonalite, but the folds in the tonalite appear to be tighter than in the granite and are inferred to be older.

The leucogranite sheet southwest of Pine Tree Canyon appears to have been deformed in the eastern Tehachapi shear zone because shallow NE dipping shear surfaces with N-NE plunging slip lineations with top to the S-SW shear sense locally deform the granite. In contrast, the leucogranite sheet on Brushy Ridge, northeast of Pine Tree Canyon, is pervasively deformed by a moderate NE dipping shear band fabric that has almost the opposite shear sense, top down to the NE. Both the foliation and the shear surfaces in the Brushy Ridge granite body are NW trending, but the shear surfaces dip more steeply to the NE than the foliation in any given outcrop. In some areas the shear surfaces dominate the fabric of the granite and the rock is protomylonitic. Most quartz in the Brushy Ridge granite body is ribboned and dynamically recrystallized to aggregates of

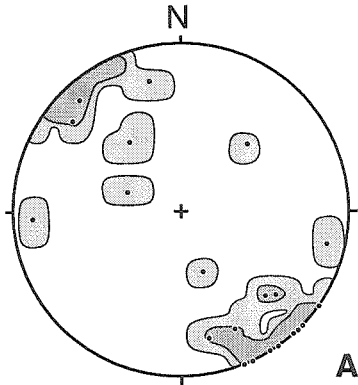
Figure 16.

Structural data for late to post eastern Tehachapi shear zone deformation events. The data are plotted on lower hemisphere equal area stereonet projections and contoured at 1% and 5% per 1% area. **A** is a plot of poles to dike walls of the Brushy Ridge leucogranite. **B** is a plot of poles to gneissic foliation of the Brushy Ridge leucogranite. The great circle (and associated pole) in **B** represent the best fit plane to the data using Bingham axial distribution analysis. The labels are the numeric values for the strike and dip of the great circle and the trend and plunge of the pole. **C** is a plot of poles to shear bands and mylonitic foliation in the northern block of the eastern Tehachapi gneiss complex that exhibit top down to the NE shear sense. **D** is a plot of type 2 mineral lineations and striae associated with the top down to the NE shear fabrics in **C**.

**STRUCTURAL DATA FOR LATE TO POST EASTERN
TEHACHAPI SHEAR ZONE DEFORMATION EVENTS**

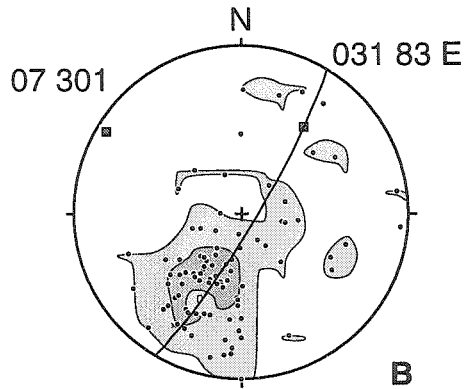
(Equal area lower hemisphere projections)

Poles to dike walls
of Brushy Ridge
leucogranite



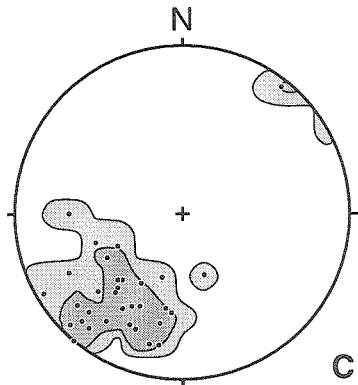
N = 21

Poles to foliation
of the Brushy Ridge
leucogranite



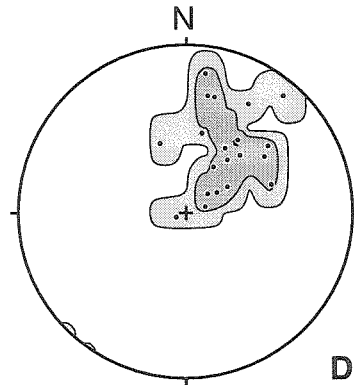
N = 94

Poles to shear band foliation
exhibiting top down to NE shear
sense in north block of ETGC



N = 32

Type 2 mineral lineations and
striations associated with top
down to NE shear bands



N = 21

Contours = 1% and 5% per 1% area.

0.1 to 0.2 millimeter grains. Recrystallization of the feldspar is uncommon although some of the potassium feldspar exhibits local subgrain development and minor recrystallization along fractures. Secondary fine grained white mica commonly is localized along and deformed in the shear surfaces and scattered larger grains of white mica with a "moth-eaten" appearance grow transversely to the main foliation in the granite. Striations and type 2 mineral lineations in the shear surfaces trend and plunge moderately to the NE. The top down to the NE sense of shear is based on thin section and outcrop observations of the deflection of S surfaces into C surfaces, the orientation of mica fish, the obliquity of recrystallized quartz grains, and the rotation of σ porphyroclasts.

The top down to the NE shear fabrics are not limited to the leucogranite on Brushy Ridge. At scattered locations in the north structural block of the gneiss complex west of Antelope Canyon and east of Water Canyon road non-penetrative shear bands with a similar orientation and shear sense as the C-surfaces in the Brushy Ridge granite are present in the Pine Tree tonalite, the No Name Canyon augen gneiss, and the group I quartz diorite gneiss. The poles to shear surfaces with top down to the NE shear sense in the Brushy Ridge granite and other rocks in the north block of the gneiss complex are plotted in Figure 16C and the striations and mineral lineations in the sheared rocks are plotted in Figure 16D. In the Pine Tree tonalite hornblende and biotite deformed in the shear surfaces are altered to chlorite and epidote and the epidote in the shear surfaces is ductilely deformed and recrystallized.

Crosscutting relations between shear bands with opposing shear sense are rare. At one outcrop of the No Name Canyon augen gneiss shear bands with top down to the NE shear sense clearly crosscut shallow NE dipping shear bands that have top verging to the S-SW shear sense, and in one thin section from a dike of the Brushy Ridge granite low-angle shear surfaces with top to the S-SW shear sense appear to be crosscut by more steeply dipping shear surfaces with the opposite shear sense. These observations suggest the top

down to the NE ductile deformation in the northern structural block may postdate the top to the S-SW shearing of the eastern Tehachapi shear zone although near synchronous deformation cannot be ruled out. The localization of the top down to the NE shear fabrics in the upper structural levels of the eastern Tehachapi gneiss complex immediately adjacent to Tehachapi Valley suggests the gneiss complex may comprise the footwall of a NE dipping normal fault buried beneath the alluvium of Tehachapi Valley (Figure 14). The implications of this inferred Tehachapi Valley fault will be discussed in Chapter 4.

The top down to the NE shear surfaces in the Brushy Ridge granite body are penetrative at thin section to hand sample scale; the spacing between the shear surfaces ranges from several millimeters to several centimeters. In contrast, the distribution and spacing of shear surfaces is heterogeneous in the adjacent Pine Tree tonalite, No Name Canyon augen gneiss, and quartz diorite gneiss. Penetrative top to the NE shear fabrics in the tonalite are only locally developed and restricted to areas close to the leucogranite, and in most areas of the north structural block the late top to the NE shear fabrics either are not evident or they occur as discrete shear bands ranging in width from several millimeters up to about one meter. The Brushy Ridge granite may have been deformed after its emplacement and the apparent localization of penetrative top to the northeast shear fabrics in the granite could be because it is weaker than the adjacent mafic quartz-poor rocks due to its high quartz content. Alternatively, the penetrative deformation of the granite relative to its wallrocks could be interpreted as indicating that the granite was deformed synchronous with its intrusion (Gapais, 1989). One possible way to test whether or not the granite was deformed during emplacement would be to date the white mica growing in the shear surfaces by the K-Ar or $^{40}\text{Ar}/^{39}\text{Ar}$ dating method and compare that age with the U-Pb zircon emplacement age of the granite.

NORTHEAST TRENDING CRENULATION CLEAVAGE AND F5 FOLDS

Development of the eastern Tehachapi shear zone appears to have been followed by a minor episode of NW-SE directed contractional deformation. Low-angle protomylonitic fabrics of the eastern Tehachapi shear zone and retrograde greenschist metamorphic fabrics in the metasedimentary rocks of the gneiss complex locally are deformed by a non-penetrative NE trending steeply to moderately dipping crenulation or kink band cleavage. In addition, rocks of the gneiss complex locally are folded into upright gentle folds that have NE trending hingelines that plunge shallowly to the NE. The wavelength of these folds ranges from several hundred meters for map scale folds to about 10 meters for outcrop scale folds. These post shear zone folds are designated F5 (Figure 9). Reversals in the plunge direction of some of the shallowly plunging F3 fold hingelines, from NW to SE or vice versa, are inferred to be the result of F5 folding. There are several structural windows through the Pine Tree tonalite sheet that appear to be located at the intersection of F3 and F5 antiformal folds, and the southwest contact of the Pine Tree tonalite in map-view locally has an embayed trace that may be an effect of the F5 folding (Figure 4). The small body of leucogranite immediately west of and adjacent to Antelope Canyon is inferred to be preserved in an F5 synformal culmination (Figures 4 and 9).

The NE trending cleavage and F5 folds appear to postdate the shear zone, but their minimum age is poorly constrained. Map-scale subhorizontal NE trending upright gentle folds and a subvertical NE trending crenulation cleavage are also present locally in the metasedimentary rocks north of Tehachapi Valley (D. J. Wood, unpublished mapping, 1993) in the vicinity of the Tehachapi Airport leucogranite of Ross (1989b) (Figure 14). Although the structures north of Tehachapi Valley were not studied in detail, their close association with the Tehachapi Airport leucogranite suggests their formation may be related to, and synchronous with, its intrusion. If the crenulation cleavage and F5 folds in the study area are coeval with the similar structures north of Tehachapi Valley, then they may

have formed when the Tehachapi Airport leucogranite intruded. Alternatively, the post-shear zone NE trending folds and crenulation cleavage in the study area may have formed during an episode of NW-SE directed contraction in early Tertiary (?) time when the Witnet Formation was folded, as will be discussed later.

BLACKBURN CANYON FAULT

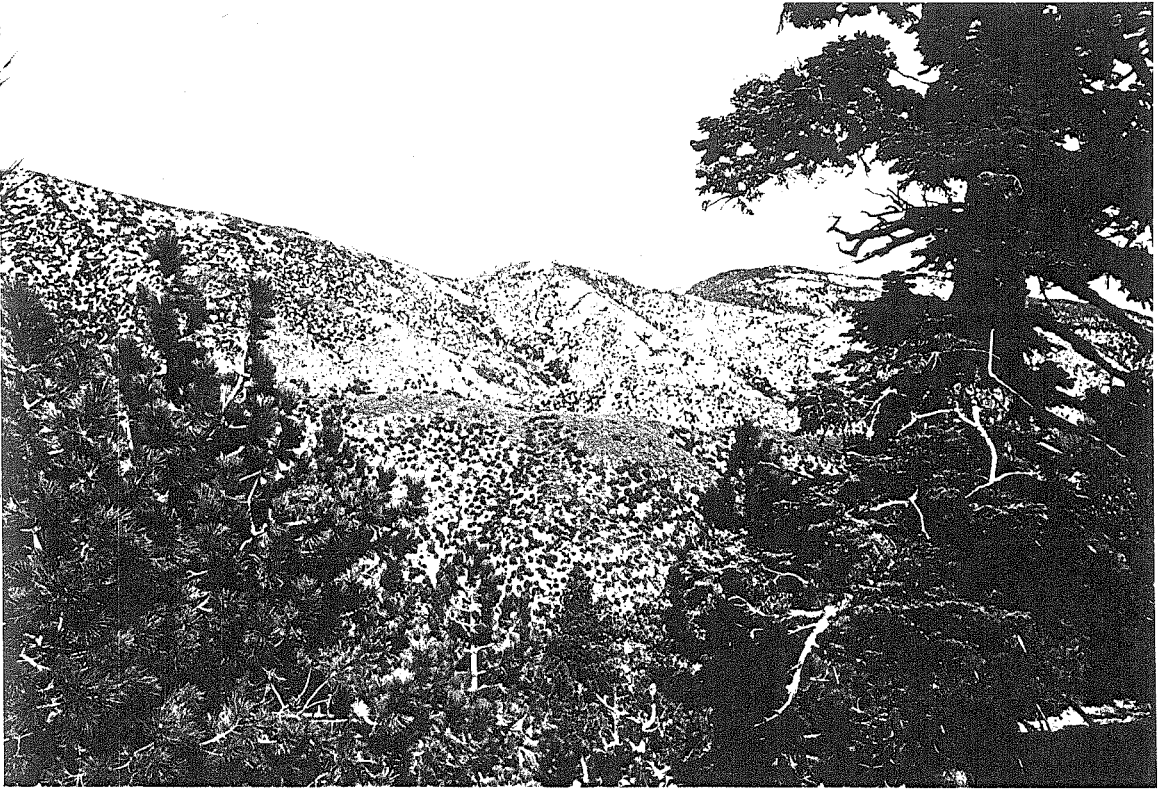
The high grade ductilely deformed rocks of the eastern Tehachapi gneiss complex are juxtaposed beneath cataclastically deformed and weakly metamorphosed granitic rocks of the Oak Creek Pass complex along the Blackburn Canyon fault which is a SE dipping low-angle detachment fault with a gently undulating surface (Figures 3, 4, and 17A). The fault is truncated to the south by the Garlock fault and to the north the fault is concealed by the alluvium of Tehachapi Valley. The Blackburn Canyon fault contact is sharp and the base of the hangingwall usually consists of ~3 to 10 meters of brownish green colored hackly-fracturing mostly fine grained granodiorite breccia that lies directly on the footwall. Locally, fractured but coherent gneiss in the upper part of the footwall grades upward into a crudely layered tectonic melange immediately adjacent to the fault. The melange may be several meters thick and it is composed of pebble to cobble size clasts of mylonitic marble and quartzite, angular fragments of gabbro, and occasionally pieces of what appear to be hangingwall granodiorite. At other locations in the footwall fracturing is comparatively minor and in the upper few meters of the footwall the compositional layering in the footwall gneisses is deflected into parallelism with the fault surface. South of Blackburn Canyon, where the footwall rocks are predominantly igneous a thin ≤ 1 meter thick layer of mylonitic marble locally overlies fractured gabbro in the footwall and directly underlies the upper plate granodiorite breccia (Figure 17B).

Deformation fabrics related the Blackburn Canyon detachment fault are both ductile and brittle in character although cataclastic fabrics are more common in the hangingwall and ductile fabrics are more common in the footwall (Figure 18). The hangingwall breccia

Figure 17.

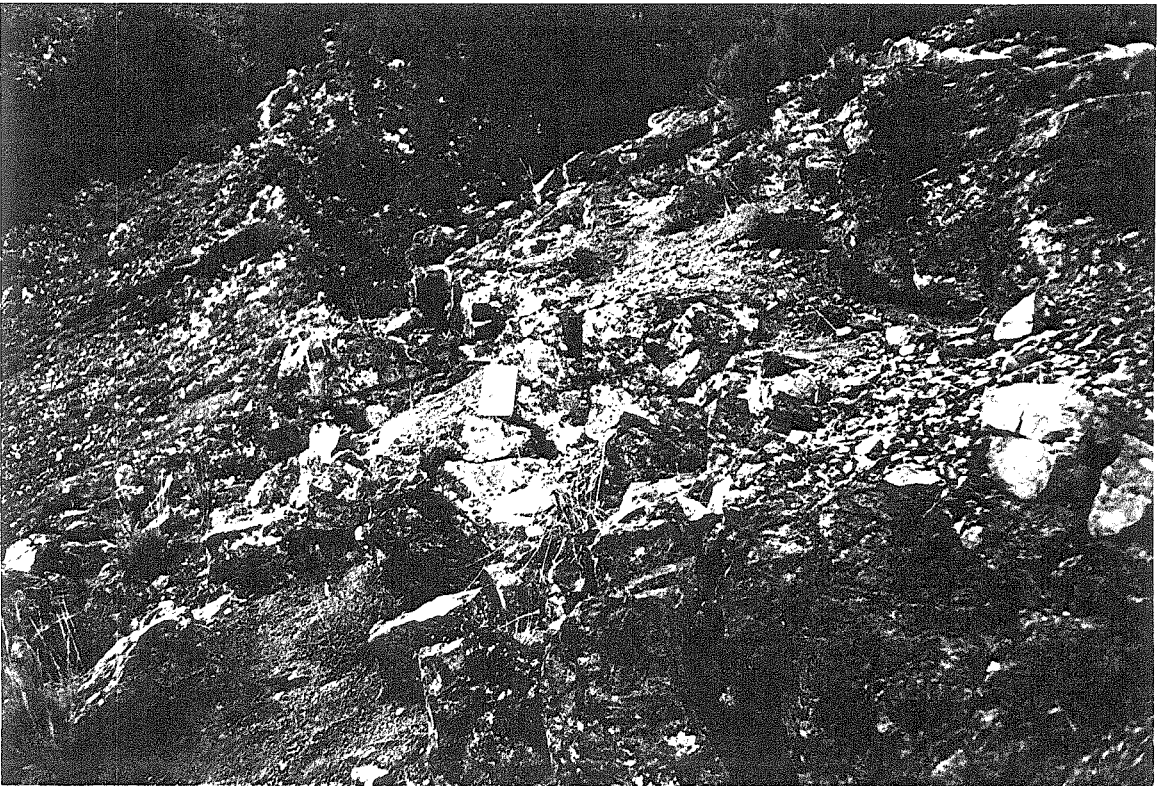
A) View from the east flank of Bison Peak looking towards the NE at the trace of the Blackburn Canyon detachment fault where it traverses the mountain slope. The skyline ridge at the left side of the photo leads up to Astronomy Ridge which is located outside of the photo. The Blackburn Canyon fault passes through the leftmost saddle on the skyline and the trace of the fault traverses the slope down and to the right just above the line of darker brush. The brush is growing in upper Bootleg Canyon. The lighter colored rocks to the right of the skyline saddle are granodioritic rocks in the upper plate of the fault. Between the ridge line in the foreground and the skyline ridge there is a small ridge behind which the trace of the fault disappears from view. Along this middle ridge there is a small saddle located in the center of the photo. The fault trace passes through this small saddle and drops down into Sawmill Canyon which lies behind the foreground ridge. The Blackburn Canyon detachment fault in the vicinity of Bootleg Canyon dips $\sim 18-27^\circ$ to the SE. B) Photo of the Blackburn Canyon detachment fault in lower Sawmill Canyon. View is towards the NW. The field notebook (19 centimeters tall) is resting on fractured gabbro in the footwall of the fault in the center of the photo. The light color of some of the gabbro is from calcite which is locally present in the fractures. The dark outcrop in the upper right part of the photo is a chloritic breccia of granodiorite that is found at the base of the hangingwall of the fault. The bench in the slope between the field notebook and chloritic breccia is the fault surface which dips shallowly to the SE at this locality. The angular white rock above the center of the right edge of the photo is a fragment of sheared marble that has broken loose from a thin layer of marble present along the fault surface (the marble layer is not visible in the photograph). C) Cataclastic Bootleg Canyon granodiorite in the hangingwall above the Blackburn Canyon fault in lower Sawmill Canyon. The dark lines are fractures and shears along which hornblende and biotite in the rock have been altered to chlorite and epidote. The lighter colored areas are veins and fractures filled with calcite and

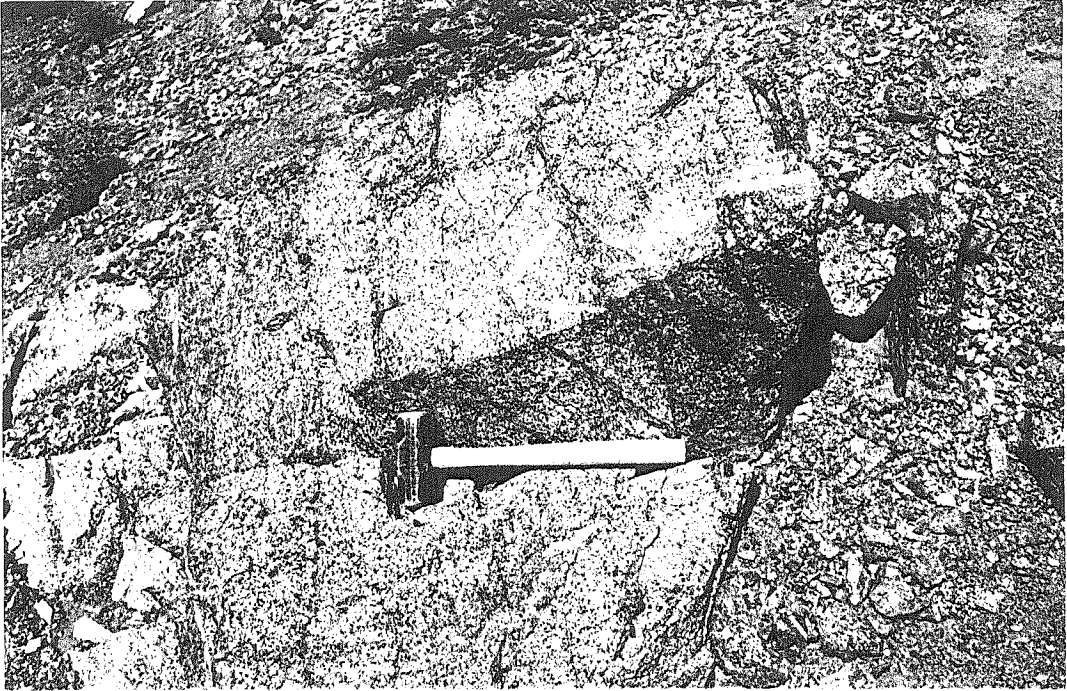
zeolite (?) minerals. The length of the hammer is 40 centimeters. D) Tehachapi Intrusive Complex tonalite with two different deformation fabrics in the footwall of the Blackburn Canyon fault in lower Sawmill Canyon. View in the photo is to the NE. To the left and below the bottom end of the hammer handle is an E-W trending 55° N dipping mylonitic shear band in the tonalite with top to the S shear sense which is inferred to be the result of shearing associated with the eastern Tehachapi shear zone. The hammer is leaning against tonalite deformed by brittle-ductile shear bands that have an orientation of $N35^{\circ}E 20^{\circ}SE$ and top down to the SE shear sense and which are inferred to result from shearing associated with the Blackburn Canyon fault. The crosscutting of the former shear band by the latter shear bands at the base of the hammer handle suggests that some deformation associated with the Blackburn Canyon fault post dates deformation associated with the eastern Tehachapi shear zone. The length of the hammer is 40 centimeters.



A

B





C



D

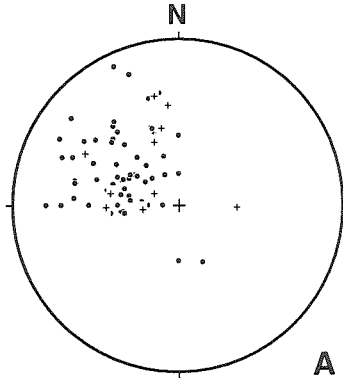
Figure 18.

Structural data for the Blackburn Canyon detachment fault. The data are plotted on lower hemisphere equal area stereonet projections. **A** is a plot of poles to cataclastic and mylonitic foliation in the footwall gneisses (solid circles) and hangingwall granitic rocks (crosses) adjacent to the Blackburn Canyon detachment fault. **B** is a plot of type 2 mineral lineations and striae (solid circles) and fold and boudin axes (crosses) associated with the Blackburn Canyon fault zone.

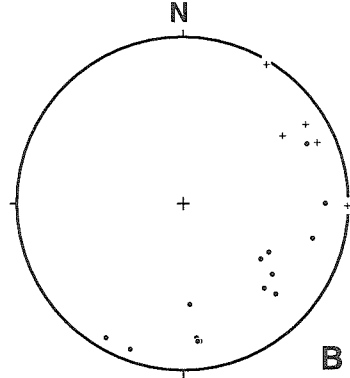
BLACKBURN CANYON DETACHMENT FAULT STRUCTURAL DATA

(Figures are lower hemisphere equal area stereonet projections)

Poles to cataclastic and mylonitic
foliation in the footwall and
hangingwall adjacent to
the detachment fault



Mineral lineations, striae
and axes of mesoscale folds
and boudins associated
with the fault zone



- | | |
|---|--|
| <ul style="list-style-type: none"> • = Poles to footwall foliations
Number of points = 61 + = Poles to hangingwall foliations
Number of points = 11 | <ul style="list-style-type: none"> • = Mineral lineations and striae
Number of points = 14 + = Fold and boudin axes
Number of points = 5 |
|---|--|

usually lacks a penetrative directional fabric although sometimes it has a faint compositional layering defined by alternating light and dark layers of comminuted mineral grains and locally this breccia is cut by discrete cataclastic shear surfaces that are subparallel to the underlying fault contact. Cataclastic foliation in the granodiorite is defined by shattered and granulated quartz, feldspar, sphene, and biotite grains 0.01 to 0.1 millimeters in size that are streaked out along shear surfaces. Lineations in the shear surfaces consist of smeared minerals and ridges and grooves. In less cataclastic samples incipiently recrystallized quartz suggests some of the deformation of the granodiorite occurred under ductile conditions. The feldspar is extensively saussuritized and much of the biotite and hornblende is replaced by chlorite and epidote. Late fractures in the cataclastic granodiorite sometimes are filled with calcite and a colorless low relief mineral that may be a zeolite mineral (Figure 17C).

In the footwall gneisses the high temperature fabrics of the gneiss complex are overprinted and locally transposed by moderate to shallow SE dipping ductile shear bands (Figure 18A). The shear bands are subparallel to the Blackburn Canyon fault and they are inferred to have formed during motion along the fault. The shear bands are defined by discrete shear surfaces, spaced several millimeters to several decimeters apart, along which preexisting foliation and leucocratic veins in the gneiss are offset. Along the ductile shear surfaces quartz and calcite are dynamically recrystallized while feldspars are fractured. Lineations present in the shear surfaces are defined by smears of chlorite, elongate quartzofeldspathic aggregates, and striations. The lineations trend to the SE and have shallow SE plunges (Figure 18B). Mesoscale folds with mostly NE trending subhorizontal hingelines are present in scattered locations within the Blackburn Canyon fault zone. The ductile fault zone fabrics commonly are overprinted by abundant brittle fractures filled with mostly unstrained calcite, quartz, or zeolites.

Shear sense in the ductilely deformed rocks of the Blackburn Canyon fault zone is consistently top down to the SE or S based on the orientation of mica fish, the obliquity of recrystallized quartz grains, the deflection of foliation into shear bands (Figure 17D), and the vergence of mesoscale folds. The shear sense in the cataclastic rocks is similar and was determined from the deflection of the cataclastic foliation into secondary shear surfaces.

The Blackburn Canyon fault appears to postdate the high temperature deformation in the gneiss complex because the trace of the fault is discordant to the regional NW trend of the high temperature deformation fabrics in the gneiss complex and greenschist facies deformation fabrics of the Blackburn Canyon fault are superimposed on the amphibolite facies fabrics of the gneiss complex. The Blackburn Canyon fault also appears to be younger than most of the eastern Tehachapi shear zone deformation since there is no evidence for a several km wide zone of greenschist facies top to the S-SW ductile shearing in the Oak Creek Pass complex east of the Blackburn Canyon fault. The Oak Creek Pass complex might, however, have been emplaced above the eastern Tehachapi gneiss complex along the Blackburn Canyon fault prior to the end of activity along the Mountain Park ductile fault. Both the Quail Canyon and the South Ridge fault zones in the Oak Creek Pass complex lie along strike from the Mountain Park fault and one or both of them might have been a continuation of the Mountain Park fault during the latest stages of its activity as will be discussed later.

MENDIBURU CANYON FAULT AND F6 FOLDING

The NE trending southeast contact of the lower plate of the Oak Creek Pass complex (Figure 3) is poorly exposed, but the evidence outlined below suggests the contact is a fault which, in this study, is called the Mendiburu Canyon fault. Between Tehachapi-Willow Springs road and Blackburn Canyon the fault juxtaposes Witnet Formation to the north against Mendiburu Canyon granodiorite of the upper plate of the Oak Creek Pass complex to the south (Figure 4). West of Blackburn Canyon the fault separates Witnet

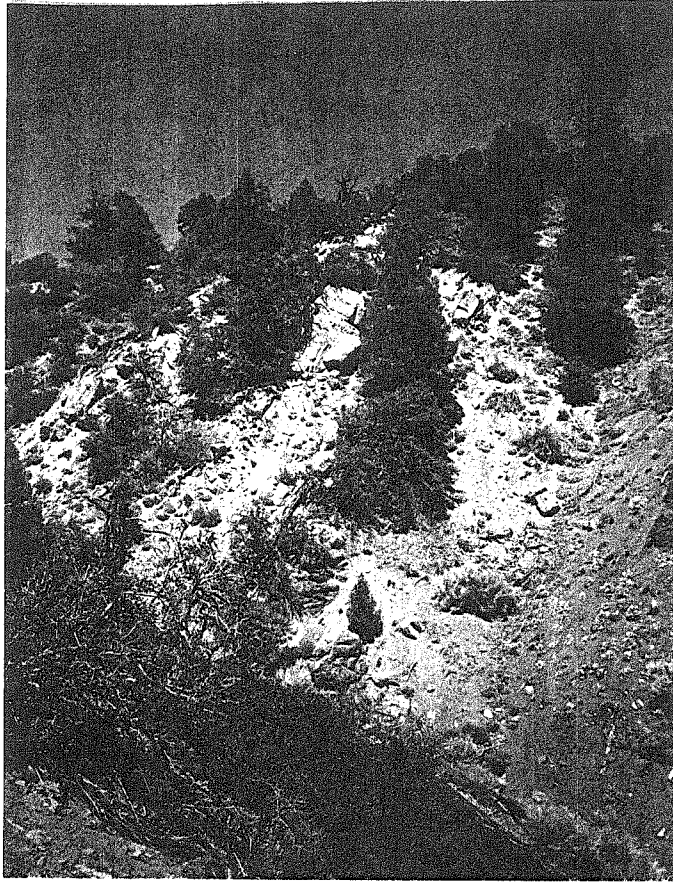
Formation to the north from Bootleg Canyon granodiorite to the south which is in the north middle plate of the Oak Creek Pass complex. At its western end the Mendiburu Canyon fault projects into a complicated and poorly exposed structural "knot", which will be discussed later, where a small fault bounded sliver of the gneiss complex appears to overlie the Blackburn Canyon fault. East of Tehachapi-Willow Springs road the trace of the Mendiburu Canyon fault is not well defined because the Witnet Formation is no longer present north of the fault and the granitic rocks on both sides of the fault are deeply weathered (Figure 4). A zone of cataclastic deformation and ground-water seeps between the Mendiburu Canyon granodiorite and the Bootleg Canyon granodiorite temporarily was exposed in a NW trending pipeline trench east of Tehachapi-Willow Springs road during the course of this study. Scattered SW dipping shear surfaces are present in the cataclastic rocks. This fractured zone is inferred to be the eastward continuation of the Mendiburu Canyon fault and the location of the fault on either side of the pipeline trench is estimated from local concentrations of vegetation which are inferred to be growing along the fault.

The best exposure of the Mendiburu Canyon fault zone is in upper Mendiburu Canyon (Figure 4) where both the Witnet Formation and the granitic rocks in the vicinity of the contact are hydrothermally altered and fractured and have a distinct light olive green color (Figure 19A). The olive green color appears to be due to the presence of an extremely fine grained pale yellow-green mineral, possibly a smectite clay, that is disseminated in fractures and grain interstices throughout the rocks. Zeolite minerals present in fractures and between grains in the Witnet Formation and in the Mendiburu Canyon granodiorite are fractured and broken in the Mendiburu Canyon fault zone in contrast to the rest of the Oak Creek Pass complex where secondary zeolite minerals generally are undeformed. Colluvium obscures the contact so it was not possible to determine whether or not any gouge material was present. The orientation of the fault contact measured in Mendiburu Canyon is N17°W 40°SW. The bedding in the adjacent

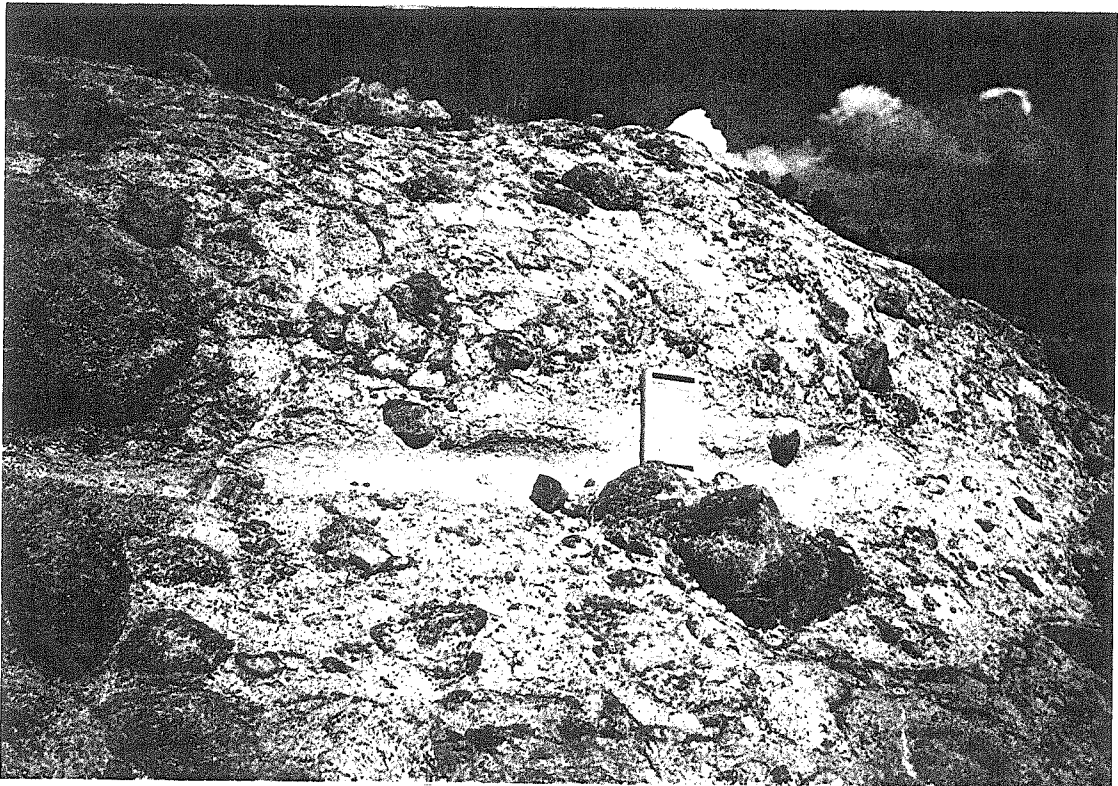
Figure 19.

A) View to the N of the Mendiburu Canyon fault in upper Mendiburu Canyon. The orientation of the fault surface at this locality is N17°W 40°SW. The fault passes between the two outcrops that are below and slightly to the left of the large bush in the center of the photo. The trace of the fault then passes through the large bush and into the tree at the head of the gully on the right side of the photo. The light colored soil to the left of the fault is underlain by Witnet Formation and the darker soil to the right of the fault is underlain by fractured granodiorite that has a greenish color due to clay (?) mineralization. The bush in the center of the photo is 2-3 meters high. B) Conglomeratic basal part of the Witnet Formation located within ~10-30 meters (stratigraphic thickness) of the contact with the underlying granodiorite. Cobbles and boulders of granodiorite are supported by a matrix of arkosic sandstone that resembles cemented grus. Bedding is defined by the light colored layer of arkosic sandstone parallel to the base of the field notebook. At this locality ~1 km away from the Mendiburu Canyon fault the bedding in the Witnet Formation dips ~17° to the NE. The field notebook is 19 centimeters tall.

A



B



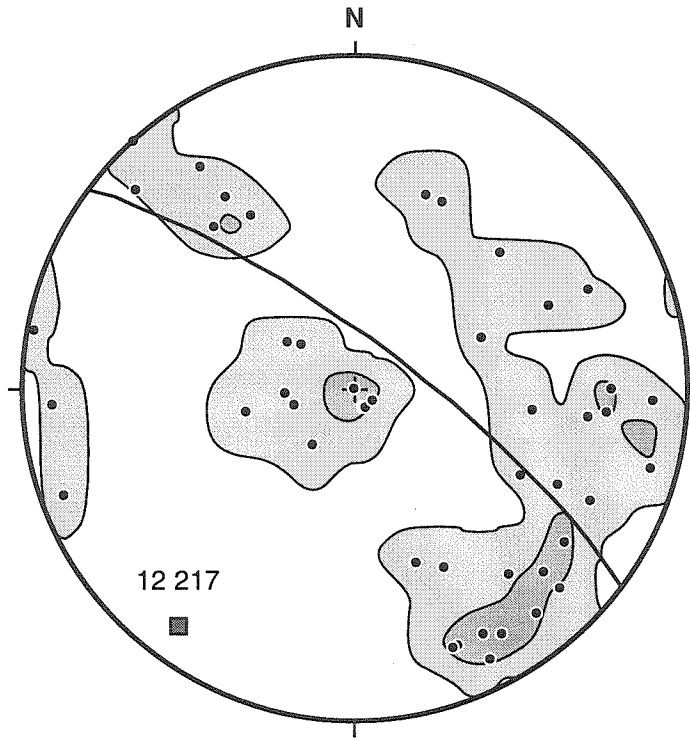
Witnet Formation is subparallel to the fault and cross-bedding indicates that it is not overturned. No features were observed which would indicate the sense of motion on the fault at this location. The attitude of the fault where it is exposed in Mendiburu Canyon is different, however, than what is suggested by the map pattern of the fault. The trace of the fault across the local topography suggests that the fault has an overall moderate dip to the SE.

The Witnet Formation in the lower plate of the Mendiburu Canyon fault is deposited on top of the Bootleg Canyon granodiorite and bedding in the Witnet Formation distal to the fault has N to NE trends and subhorizontal to shallow SE dips (Figure 19B). Adjacent to the Mendiburu Canyon fault the bedding in the Witnet Formation generally has a N to NE strike with moderate to steep dips to the W and NW, and the bedding locally is overturned towards the NW. The orientation of the bedding in the Witnet Formation (Figure 20) and the change from NW to SE dips along a NE trending axis (Figure 4) suggests the Witnet Formation is deformed into a synclinal fold having a NE trending subhorizontal axis. The steep southeast limb of the fold locally is overturned. The inferred axial trace of this fold is labeled F6 in Figures 4 and 9. The F6 folding and local northwestward overturning of the Witnet Formation adjacent to the Mendiburu Canyon fault and the local presence of shallow S dipping shear surfaces in the fault zone suggest the fault may be a SE dipping reverse fault. The granitic rocks of the north middle and upper plates of the Oak Creek Pass complex are inferred to have been thrust to the NW into and over the Witnet Formation along the fault.

The Mendiburu Canyon fault may correlate with a similar NE trending inferred fault contact exposed in Oil Canyon east Tehachapi Valley in the Cache Creek area (Figure 2). The Witnet Formation in the Oil Canyon area also is folded into a NE trending syncline and bedding in the southeast limb of the syncline dips steeply and locally is overturned to the NW (Dibblee and Louke, 1970). The contact between the Witnet Formation and granitic

Figure 20.

Plot showing poles to bedding of the Witnet Formation in the Oak Creek Pass complex. Data are plotted on a lower hemisphere equal area stereonet projection and contoured at 1% and 5% per 1% area. The great circle (and associated pole) represent the best fit plane to the data using Bingham axial distribution analysis. The label is the numeric value for the trend and plunge of the pole.

WITNET FORMATION - POLES TO BEDDING

Number of points = 48

(Lower hemisphere equal area projection)

Contours = 1% and 5% per 1% area

rocks to the southeast is interpreted by Smith (1951), Buwalda (1954), and Michael (1960) to be a shallowly SE dipping fault called the Oil Canyon fault, along which granitic rocks in the upper plate were thrust to the NW over the Witnet Formation. Their interpretation is based on the observations that the rocks along the contact are sheared and mineralized, the granitic rocks locally are structurally above the Witnet Formation along a shallow SE dipping contact, and the Witnet Formation adjacent to the contact locally is overturned. Dibblee and Louke (1970), in contrast, interpret the contact as a folded and upended depositional contact because the basal boulder conglomerate of the Witnet Formation appears to be deposited on the granitic rocks.

In the Cache Creek area the folding and possible overthrusting of the Witnet Formation is constrained to be pre-Early Miocene in age because Early Miocene Kinnick Formation (Quinn, 1987) is deposited in angular unconformity across the Witnet Formation and the Oil Canyon fault (Buwalda, 1954). The remarkable similarity between the folding of the Witnet Formation in the study area south of Tehachapi Valley and in the Cache Creek area suggests the two areas were deformed in the same event and that the Mendiburu Canyon fault may be pre-Miocene in age. The age of the Witnet Formation is unknown, but Dibblee and Louke (1970) note that it is lithologically similar to and may correlate with the Goler Formation in the El Paso Mountains. The upper part of the Goler Formation is Paleocene to Early Eocene in age on the basis of paleontologic data (Cox, 1987). This suggests that activity on the Mendiburu Canyon fault and folding of the Witnet Formation probably occurred between Early Eocene and Early Miocene time.

The northeast end of the Mendiburu Canyon fault is concealed beneath the alluvium of Tehachapi Valley, and as discussed above the fault is inferred to be continuous with the Oil Canyon fault east of Tehachapi Valley (Figure 2). It is not clear, however, what happens to the Mendiburu Canyon fault at its southwest end. The absence of the basal granodiorite boulder conglomerate of the Witnet Formation adjacent to the fault and the

projection of Witnet Formation bedding trends into the fault at high angle (Figure 4) both suggest the fault has accommodated some displacement and is not simply an unopened depositional contact. The amount of displacement along the Mendiburu Canyon fault is unknown. The presence of similar appearing granodiorite in both the footwall and hangingwall of the fault, the Bootleg Canyon granodiorite in Figure 4, suggests that large displacements on the order of tens of km are unlikely. If, as will be discussed later, the fault-floored sliver of the gneiss complex above the Witnet Formation is part of the hangingwall of the Mendiburu Canyon fault then the minimum amount of displacement along the southwest end of the fault appears to be on the order of ~1.5 to 2 km.

Assuming there has been some NW directed displacement of the upper plate of the Mendiburu Canyon fault it is not clear how this displacement is accommodated at the southwest end of the fault because a number of faults converge in that area and it is also a region of heavy brush and poor exposures (Figures 3 and 4). The Mendiburu Canyon fault does not appear to continue to the southwest into the eastern Tehachapi gneiss complex although a fault bounded sliver of the gneiss complex at the end of the Mendiburu Canyon fault may have been emplaced when the Mendiburu Canyon fault was active as will be discussed later. Most likely displacement along the Mendiburu Canyon fault was accommodated at its southwest end by local reactivation of the Blackburn Canyon fault and possibly the Quail Canyon and/or South Ridge fault zones as well (see Figure 21). There is some evidence that suggests more than one phase of activity along part of the Blackburn Canyon fault. Near the intersection of the Blackburn Canyon fault with the Quail Canyon fault zone gabbro adjacent to the Blackburn Canyon fault has a mylonitic fabric with top down to the SE shear sense that is crosscut by shallow E dipping non-penetrative shear surfaces that have SE trending and plunging slickenlines. Calcite and epidote are brittlely fractured along the later shears and the shear sense is top to the NW based on offset of the mylonitic fabric and leucocratic veins. The orientation, shear sense, and brittle character of

the late cross-cutting shears are consistent with the orientation and motion sense inferred for the Mendiburu Canyon fault.

The Mendiburu Canyon fault is inferred to have been active during the period when the Witnet Formation was deformed, but a fault in the same location as the Mendiburu Canyon fault may have existed prior to deposition of the Witnet Formation and the NW directed reverse motion along the Mendiburu Canyon fault may represent reactivation of a preexisting fault. The Oak Creek Pass complex originally may have been composed of two structural plates instead of the five plates shown in Figure 3. The three different plates that are composed of Bootleg Canyon granodiorite originally may have comprised a single lower plate and Mendiburu Canyon granodiorite intruded by Old West Ranch monzogranite together may have comprised the upper plate. These inferred original two plates may have been separated by a single low-angle fault that was subparallel to the structurally lower Blackburn Canyon fault and active at about the same time. Later deformation events then may have disrupted and reactivated different parts of the original detachment fault. Faults which are inferred to be preserved or reactivated segments of the original detachment fault between the two plates include, from south to north, the Quail Canyon fault zone, a short segment of an inferred unnamed fault buried beneath the alluvium of Blackburn Canyon, and the Mendiburu Canyon fault east of Blackburn Canyon. Reactivation of a previously existing fault also is suggested because the Witnet Formation appears to have been deposited on top of granodiorite that was previously cataclastically deformed.

STRUCTURES OF UNCERTAIN RELATIVE AGE AND SIGNIFICANCE

WATER CANYON FAULT

In the northwest part of the study area laminated quartzite gneiss of the Antelope Canyon group metasedimentary rocks structurally overlies metasedimentary rocks of the Brite Valley group along a poorly exposed W dipping tectonic contact called the Water Canyon fault (Figure 3). The best exposures of the fault are along the wall of upper Water

Canyon west of Water Canyon road (Figure 4). The fault is defined by scattered outcrops of mixed metasedimentary rocks with shallow to moderate westward dipping ortho- to ultramylonitic fabrics. In a few locations extremely fine grained greenish black colored waxy appearing material that fractures into lozenge shaped flakes is present along the fault. This material was not examined in thin section, but its fine grain size suggests it may be fault gouge or hydrothermally altered ultramylonite. Gneiss in the hangingwall and footwall adjacent to the Water Canyon fault commonly have a strongly sheared appearance and quartzite in outcrop locally appears to be mylonitic. In thin section, however, the texture in the gneisses is granoblastic to lepidoblastic with abundant triple junctions among the mineral grains which suggests the rocks were annealed at high temperature after and perhaps during deformation.

The fault projects southeastward across Water Canyon road immediately to the north of several massive outcrops of strongly deformed quartz rich paragneiss exposed in roadcuts on the east side of the road at the head of Water Canyon. The fault is not exposed, but in the area where the fault contact should be there are massive undeformed coarse grained white quartz veins that are up to several meters thick. The outcrop pattern of the quartz veins across the hill slope suggests that they occur along a surface that dips moderately to the SW and projects beneath the mylonitic quartzite exposed along the road. The location of the large quartz veins along the inferred projection of the fault and their position between the two different groups of metasedimentary rock suggests the quartz veins may have been deposited along the fault surface. The surface defined by the quartz veins is discordant to the fabric in the adjacent mylonitic gneisses which suggests the original fault contact may have been modified by later tectonism.

The trends of the Water Canyon fault and the nearby Mountain Park fault are similar and they dip towards each other (Figure 3), but the crosscutting relationship between the two faults is not known. The paragneiss between the two faults is folded into a N-NW

trending open to close F3 synformal fold (Figures 4 and 9). On the E dipping west limb of the synform there is a small sliver of Brite Valley group (?) pelitic rocks located above the Mountain Park fault and structurally below the Antelope Canyon group quartzites. The contact between these two different lithologies is not exposed, but the contact is inferred to be the Water Canyon fault repeated across the F3 synform. F3 folding of the Water Canyon fault would suggest that it is older than the Mountain Park fault, which largely post dates the F3 folding. The juxtaposition of the Antelope Canyon and Brite Valley group metasedimentary rocks along the Water Canyon fault in conjunction with the intense high temperature ductile deformation fabrics localized adjacent to the fault suggests the fault may be a fundamental tectonic boundary.

OAK CREEK MYLONITE ZONE

In the structurally lowest levels of the eastern Tehachapi gneiss complex close to the Garlock fault near the head of Oak Creek Canyon a NW trending high temperature subsolidus foliation in the quartz diorite locally is transposed by a NE trending shallow NW dipping greenschist grade mylonitic fabric. The quartz diorite adjacent to the alluvium at the mouth of a small canyon between Tylerhorse and Horsethief Canyons is deformed to ortho- and ultramylonite in a zone about ten meters thick which is called the Oak Creek mylonite zone' (Figures 3 and 4). This mylonite could be part of the highly deformed White Oak diorite gneiss unit adjacent to the north branch of the Garlock fault that was mapped by Sharry (1981). There does not appear to be a clear lithologic difference or sharp structural break between the mylonitic rocks and the structurally higher quartz diorite and gabbro, however, so the mylonitic rocks are inferred to be part of the Tehachapi Intrusive Complex gabbro unit. In the single thin section of the mylonite zone examined most of the biotite and hornblende in the rock is replaced by chlorite and epidote and plagioclase hosts abundant fine grained white mica and epidote group minerals. A N-NE trending shallow NE plunging type 2 mineral lineation defined by smeared chlorite and elongate

quartzofeldspathic aggregates is present in the mylonitic foliation. Shear sense in the mylonite is top down to the N based on obliquely recrystallized quartz grains, chlorite fish, and the deflection of recrystallized epidote and chlorite tails on σ -type porphyroclasts of hornblende. Fractures filled with strained and unstrained calcite and zeolite minerals crosscut the mylonitic fabric of the rock.

The top to the N shear sense in the Oak Creek mylonite zone is opposite to the shear sense of the eastern Tehachapi shear zone. The relative timing of the two shear zones is not known although microstructures in a nearby sample of the gneiss complex suggest the top down to the north shearing may have followed the top to the S-SW shearing. In the bottom of Sawmill Canyon between the eastern Tehachapi shear zone and the Oak Creek mylonite zone hornblende gabbro with a well developed shear band fabric records top to the S-SW shearing at greenschist conditions. The margins of hornblende grains intersected by shear surfaces are recrystallized to actinolite and chlorite. This top to the S-SW deformation fabric is crosscut by fractures and tension gashes filled with zeolites and recrystallized quartz. The orientation of the tension gashes relative the deformation fabric in the gneiss suggests top to the N shearing, which is opposite in shear sense to the shear sense indicated by the shear band fabric. The obliquity of recrystallized quartz grains in the quartz filled fractures indicates top to the N shear sense as well.

The significance of the Oak Creek mylonite zone is not clear because alluvium is present between the mylonite zone and Rand schist exposed immediately to the south (Figure 4). Sharry (1981) maps the contact of the Rand schist with the alluvium to the north as the north branch of the high-angle Garlock fault, but during this study the trace of the Garlock fault in the area southeast of the Oak Creek mylonite zone could not be located with any degree of certainty because of poor exposure. An alternate possibility is that the north branch of the Garlock fault locally has Rand schist on both sides of it and that the contact between the Oak Creek mylonite and the Rand schist is northwest of the Garlock

fault buried beneath the alluvium (Figure 4). The irregular shape of the Rand schist-alluvium contact immediately southeast of the Oak Creek mylonite zone, the proximity of the schist to the mylonite zone, and the presence of low-angle N dipping foliation in the Rand schist closest to the mylonite zone suggest that the concealed contact between the mylonite zone and the Rand schist may not be the high-angle north branch of the Garlock fault, but instead might be a primary low-angle tectonic contact.

The location of the Oak Creek mylonite zone at the lowest structural level of the eastern Tehachapi gneiss complex close to exposures of the Rand schist suggests it may be part of a regional low-angle fault system that overlies the Rand schist in the southern Sierra Nevada area. East of the study area in the southeastern Sierra Nevada (Figure 2) and across the Garlock fault in the Rand Mountains the Rand schist underlies mixed ortho- and paragneiss of the Johannesburg gneiss along a low-angle fault contact (Silver et al., 1984; Silver, 1986; Nourse, 1989; Postlethwaite and Jacobson, 1987). The lithologic assemblage, degree of deformation, and grade of metamorphism of the Johannesburg gneiss is remarkably similar to what is observed in the eastern Tehachapi gneiss complex (L. T. Silver, personal communication, 1995). Southwest of the study area, at the west end of the north branch of the Garlock fault diorite gneiss of the Tehachapi gneiss complex overlies Rand schist along a fault contact that dips 25° to the NW (see Figure 26) based on tunnel log and drill-hole data from near the north portal of Tunnel #3 of the Tehachapi aqueduct tunnels (Peters, 1972). Results from a recent Calcrust seismic profile across the western Tehachapi mountains, the location of which is shown in Figure 2, suggest that Rand schist underlies the Tehachapi Mountains along a shallow NW dipping contact (Malin et al., 1995), a conclusion which confirms the observations of Peters (1972).

QUAIL CANYON AND SOUTH RIDGE FAULT ZONES

The Quail Canyon and South Ridge fault zones in the southwestern part of the Oak Creek Pass complex are NW to N trending and E to NE dipping zones of extensive

cataclasis with local areas of well developed protomylonitic foliation (Figures 3 and 4). These fault zones were not studied in detail and their precise location, regional extent, and sense of motion are not well defined. The available field data and observations concerning these fault zones are summarized below. Over most of their length these two fault zones appear to juxtapose different plutonic lithologies across a relatively broad zone of extensive cataclasis and mylonitization. Within the deformed zones it frequently is difficult to distinguish between the different lithologies so the fault zones are shown as broad zones of undifferentiated lithologies in Figure 4. Within the Quail Canyon fault zone on the east side of uppermost Quail Canyon there is, however, a small exposure of protomylonitic hornblende diorite that is compositionally dissimilar to the granodioritic lithologies of the Oak Creek Pass complex.

The rocks in the fault zones are fractured and crosscut by non-penetrative cataclastic shears that vary widely in orientation and shear sense. Mylonitic-cataclastic tectonite zones up to several meters wide are developed locally in the fault zones and tend to have N to NW trends and dip shallowly to steeply to the E. Within these tectonite zones lozenges of fractured granodiorite from several millimeters to several centimeters wide are surrounded by anastomosing bands of proto- to orthomylonite that may be several centimeters in thickness. Feldspar in the mylonite is fractured and broken and quartz in the mylonite is both dynamically recrystallized and fractured. The tectonized granodiorite has a distinct green color that is the result of the alteration of hornblende and biotite in the rock to chlorite and epidote. The shear sense of the Quail Canyon and South Ridge fault zones is not clear at this time. Within any given outcrop of the fault zones there usually are several different shear surfaces each of which frequently has a different sense of shear. A consistent shear sense within a single outcrop was observed only in one location in the Quail Canyon fault zone. The small exposure of protomylonitic diorite in upper Quail Canyon has a well developed moderately NE dipping composite shear band fabric with a NE plunging mineral

lineation and deflection of the foliation into the shear surfaces clearly indicates top to the SW shear.

Consideration of the location and orientation of the Quail Canyon and South Ridge fault zones in relation to nearby structures in the study area suggests they may have formed and/or were reactivated during one or more of several different faulting episodes. First, the overall trend and eastward dip of the fault zones is somewhat similar to the orientation of the Blackburn Canyon detachment fault which suggests that one or both of them may have formed during the time when the Oak Creek Pass complex was being emplaced above the gneiss complex along the Blackburn Canyon fault. As was discussed earlier the Oak Creek Pass complex originally may have been composed of two structural plates separated by a single low-angle fault instead of the five plates shown in Figure 3. Thus, the Quail Canyon fault zone and/or the South Ridge fault zone may be segments of a detachment fault similar to and subparallel to the Blackburn Canyon fault. Another possible interpretation of the Quail Canyon and South Ridge fault zones is that they represent a continuation of the Mountain Park ductile fault across the Blackburn Canyon fault. The Quail Canyon and South Ridge fault zones both have an orientation similar to the Mountain Park fault, they are located along the southeastward projection of that fault, and as mentioned above there is some indication for top to the SW shear along the Quail Canyon fault zone which is similar to the shear sense of the Mountain Park fault. A third possible interpretation of these two fault zones is that they are continuous with the Mendiburu Canyon fault to the north (see Figure 21) and were active as sinistral-oblique ramps during NW directed thrusting along that fault as was discussed earlier.

SLIVER OF GNEISS COMPLEX ABOVE BLACKBURN CANYON FAULT

The Oak Creek Pass complex is everywhere structurally above the eastern Tehachapi gneiss complex along the Blackburn Canyon detachment fault except at one location where a small fault-floored sliver of the gneiss complex locally appears to overlap




the Blackburn Canyon fault and overlie the Witnet Formation and the Bootleg Canyon granodiorite of the lower plate of the Oak Creek Pass complex (Figures 3 and 4). The suite of lithologies in the gneiss sliver is similar to the rocks present in the gneiss complex nearby suggesting the sliver is not far traveled. The base of the gneiss sliver is a low-angle cataclastic fault that has an overall very shallow dip to the NE, subparallel to the local mountain slope. Because of very dense brush and sparse exposure the location of contact between the gneiss sliver and the gneiss complex is largely inferred based on a few scattered outcrops of brecciated gneiss and local abrupt changes in trend of the gneiss. Direct structural evidence for the transport direction of the sliver was not observed because the contacts of the sliver are mostly obscured by brush and colluvium and where exposed the rocks at the contact are fractured and slickensides were not observed.

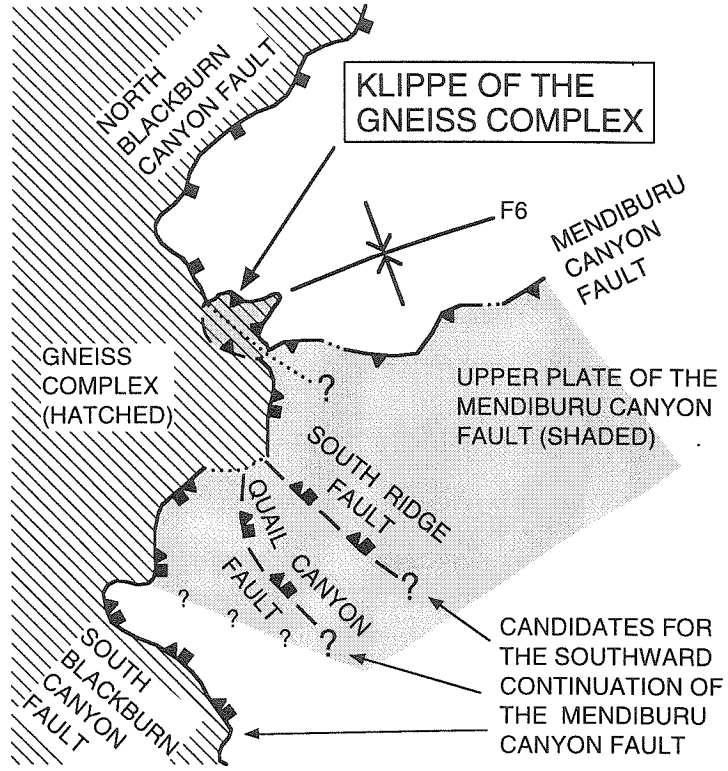
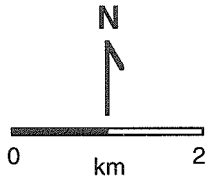
The gneiss sliver obscures the Blackburn Canyon fault at the west end of the Mendiburu Canyon fault (Figures 2, 3, 4, and 14) and may be part of the upper plate of the Mendiburu Canyon fault (Figure 21A). If the sliver of gneiss is bounded by the Mendiburu Canyon fault, then it most likely originated from a position to the southeast of its current location. The size and position of the klippe would require a minimum fault displacement of about 1.5 to 2 km. That distance is about the width of the part of the Witnet Formation where the bedding is discordant to the Mendiburu Canyon fault (Figure 4). Alternatively, the sliver of the gneiss complex may be a large landslide block that was emplaced across the Blackburn Canyon fault and onto the Oak Creek Pass complex either prior to, during, or following motion on the Mendiburu Canyon fault (Figure 21B). While the landslide block hypothesis cannot be ruled out with the available data, it seems more likely that the sliver was emplaced during motion on the Mendiburu Canyon fault for the following reasons. First, based on its trace across the topography the fault at the base of the gneiss sliver appears to be folded into gentle NE trending folds, subparallel to the F6 fold in the Witnet Formation. Second, the position of the sliver at the terminus of the

Figure 21.




Maps illustrating possible relationships among the different faults in the vicinity of the western end of the Mendiburu Canyon fault. The South Ridge, Quail Canyon, and Blackburn Canyon faults are all candidates for the southward continuation of the Mendiburu Canyon fault. A and B show two different hypotheses for the emplacement of eastern Tehachapi gneiss complex rocks above the Oak Creek Pass complex. A) NW directed thrust emplacement of a klippe of the gneiss complex during overriding of the Witnet Formation along the Mendiburu Canyon fault. B) Landslide emplacement of the gneiss complex over the Blackburn Canyon fault either before, during, or after activity along the Mendiburu Canyon fault.

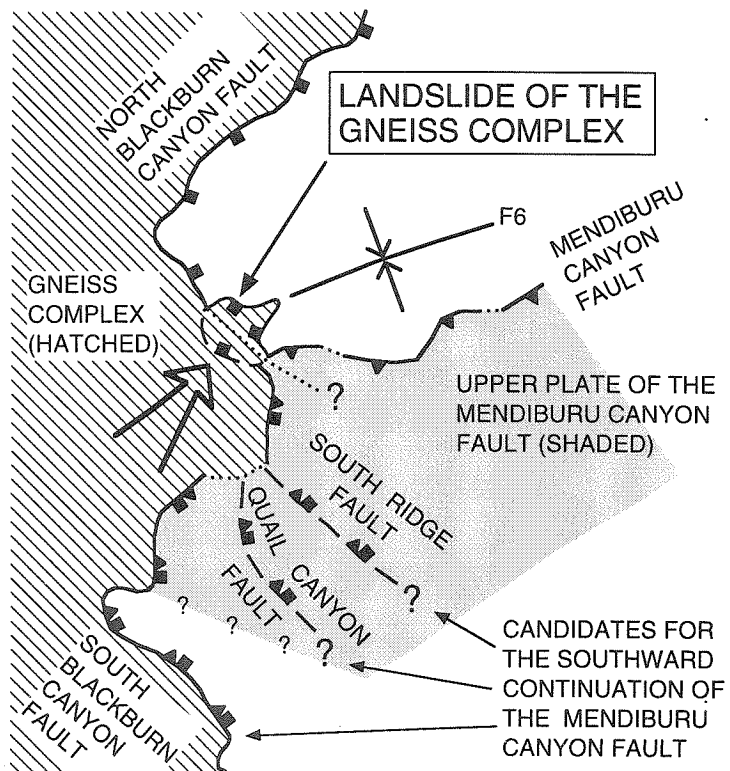
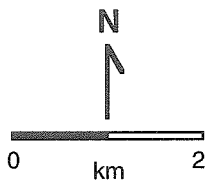
A

-  THRUST FAULT
-  DETACHMENT FAULT
-  DETACHMENT FAULT REACTIVATED (?) AS A THRUST FAULT
- FAULTS DASHED WHERE APPROXIMATE OR INFERRED AND DOTTED WHERE CONCEALED



B

-  THRUST FAULT
-  DETACHMENT FAULT
-  DETACHMENT FAULT REACTIVATED (?) AS A THRUST FAULT
- FAULTS DASHED WHERE APPROXIMATE OR INFERRED AND DOTTED WHERE CONCEALED



Mendiburu Canyon fault suggests the two structures may be related although the position of the sliver at that location could be fortuitous.

TEJON CANYON FAULT

In the southern part of the south structural block the Tejon Canyon fault separates Double Mountain on the north from Bison Peak on the south (Figure 4). The area around this fault was not studied in detail and its location is mostly inferred. Where examined in the saddle between Double Mountain and Bison Peak the fault zone consists of a sliver, several tens of meters wide, of ductilely deformed garnet-bearing dioritic or gabbroic gneiss bounded on either side by what appear to be high-angle cataclastic shear zones. At this locality the fault zone separates mostly biotite poor gabbroic rocks to the north from biotite bearing quartz dioritic rocks underlying Bison Peak to the south. Dibblee and Warne (1970) suggest that the Tejon Canyon fault may be subvertical or steeply NE dipping and they indicate that the northeast side of the fault has moved up relative to the southwest side. North side up motion on the fault is consistent with the presence of gabbro on the north side of the fault since the gabbro appears to structurally underlie tonalite throughout the eastern Tehachapi Mountains. The significance of the Tejon Canyon fault is not clear. The lack of significant ductile deformation in the rocks on either side of the fault where it passes between Bison Peak and Double Mountain suggests that it may be a Cenozoic (?) age reverse (?) fault. It may have been active when the Beno Springs fault of Malin et al. (1995) and/or the Mendiburu Canyon fault of this study were active.

METAMORPHISM

SUMMARY OF METAMORPHIC HISTORY

As discussed earlier it is not known if the earliest deformation events recognized in the study area, the F1AC and F1BV folding and inferred thrust faulting of the metasedimentary rocks, were accompanied by metamorphism because of subsequent high temperature metamorphic events. The second deformation episode in the eastern Tehachapi

gneiss complex, which occurred after and possibly during intrusion of the group I orthogneisses, was accompanied by regional metamorphic recrystallization at amphibolite facies and the formation of NE trending F2 folds and gneissic deformation fabrics. A second regional amphibolite facies deformation fabric, this time with a NW trend, formed in the gneiss complex during and following intrusion and F3 folding of the group II gabbro and tonalite plutons of the Tehachapi Intrusive Complex. A mineral assemblage consisting of quartz, biotite, garnet, sillimanite, plagioclase, potassium feldspar, and muscovite developed in rocks of pelitic composition during these two amphibolite facies metamorphic events. There are no obvious contact metamorphic aureoles developed in the paragneiss adjacent to the group I and II intrusions in the gneiss complex.

Following the second regional amphibolite facies metamorphism the rocks of the gneiss complex locally were retrograded to greenschist facies along the eastern Tehachapi shear zone during top to the S-SW simple shear deformation. Deformation along the Blackburn Canyon, Quail Canyon, and South Ridge fault zones and the ubiquitous cataclasis in the Oak Creek Pass complex also occurred at greenschist facies metamorphic conditions although some of the deformation may have occurred at lower temperatures. There is no evidence in any of the group IV granitic rocks of the Oak Creek Pass complex for metamorphism above greenschist facies. The pendants of Oaks metavolcanic rocks in the Oak Creek Pass complex have local hornfelsic textures inferred to have developed when the adjacent granitic rocks intruded. Overriding of the Witnet Formation along the Mendiburu Canyon fault is inferred to have occurred at low temperature because, in contrast to the rest of the Oak Creek Pass complex, zeolite minerals in this fault zone are deformed and there is abundant growth of what appear to be clay minerals in the fault zone rocks as well.

GARNET BEARING VEINS, MIGMATITES, AND OTHER MOBILIZATES

One of the most distinctive and enigmatic features of the southern Sierra Nevada batholith is the local presence in metamorphosed gabbroic and mafic tonalitic rocks of dark reddish colored garnets that commonly are surrounded by coarse grained haloes of leucocratic minerals and which are scattered throughout leucocratic veins, layers, and pods (Sams and Saleeby, 1988; Ross, 1989b; Pickett and Saleeby, 1993). These garnets are anhedral to euhedral, they commonly are poikilitic, and they range in size up to ~10 centimeters in diameter. Noting that the garnets and their host veins in the western Tehachapi Mountains commonly are discordant to the hot subsolidus gneissic fabrics in the mafic host rocks and that they also frequently are localized along contacts with quartzofeldspathic assemblages that exhibit retrograde paragenetic relations Sams and Saleeby (1988) inferred that the garnets are of retrograde origin and suggested that they may have grown during high-grade autometamorphism following crystallization of wet magmas. Based on the common veinlike paragenesis of the garnets in the metaigneous rocks and thermodynamic estimates of volatile activities in the garnet bearing assemblages of the western Tehachapi Mountains Pickett and Saleeby (1993) suggested that the formation of the garnets may be related to the localized influx of a CO₂-rich fluid phase. These garnet-bearing veins are also found in the eastern Tehachapi Mountains (this study; Ross, 1989b).

The most deformed parts of the Tehachapi Intrusive Complex in the study area locally host veins, layers, and patches of generally medium to coarse grained plagioclase and quartz, ± hornblende, ± garnet that are both concordant and discordant to the high temperature gneissic fabric in both the metamorphosed tonalite and gabbro. The contacts of the leucocratic veins and patches with the host gneisses range from sharp to irregular and diffuse, and commonly the leucocratic-veined and layered orthogneisses have a migmatitic appearance. Most of the garnet-bearing veins and patches crosscut and appear to postdate

much of the high temperature subsolidus fabric development in the Tehachapi Intrusive Complex. The garnets in the leucocratic veins and patches are reddish brown, generally subhedral, commonly poikilitically enclose quartz and plagioclase, and they range from several millimeters up to about 7 centimeters in diameter. The garnets usually are surrounded by a leucocratic halo composed of plagioclase and quartz. The garnets are most common in the fine grained gabbro/amphibolite part of the intrusive complex in the central structural block. Most of the large garnets are found in the southeastern part of the gneiss complex in the vicinity of Astronomy Ridge where the rocks are most deformed and where the structurally deepest parts of the gneiss complex are exposed. In this area the late-tectonic veins and feldspathic patches with abundant garnets commonly are found within a distance of 100 to 200 meters on either side of the two ductile fault zones in the gneiss complex. Garnet-bearing veins with a similar textural setting are also present in the group I Antelope Canyon garnet diorite although some of these garnets may have formed prior to intrusion of the Tehachapi Intrusive Complex which contains few garnets in that area.

The garnet bearing veins in the Tehachapi Intrusive Complex appear to have formed during a transitional period in the deformation history of the study area between the high grade deformation accompanying the F3 folding and the subsequent retrograde greenschist facies mylonitic deformation closely associated with the eastern Tehachapi shear zone. Most of the garnets grow across the moderate to steeply dipping amphibolite facies solid-state fabric that is inferred to have developed during F3 folding, but the garnets are deformed by low-angle top to the S-SW shear bands of the eastern Tehachapi shear zone. The garnets occasionally are elongated in a direction subparallel to the type 2 mineral lineations of the shear zone. The garnet-bearing veins in the metaigneous rocks of the western Tehachapi Mountains also are crosscut by shallow dipping domainal mylonitic fabrics (Pickett and Saleeby, 1993), although the shear sense of those fabrics is unknown. In Tehachapi Intrusive Complex tonalitic rocks the garnets frequently overgrow a gneissic

fabric and in rocks of gabbroic composition the most common host of the garnets is an extensively recrystallized, non- to poorly foliated, massive, fine grained amphibolite. Mylonitic and shear band fabrics commonly deform the garnets in the quartz-bearing diorite and tonalite, but the garnets in the massive fine grained gabbro and amphibolite are largely undeformed and unrotated. The general lack of obvious deformation of the garnets in the gabbro may be because the gabbro better resists plastic deformation since it mostly lacks quartz and biotite.

A possible origin for some of the garnet-bearing veins and patches in the study area is suggested by their local migmatitic appearance and their apparent concentration in the vicinity of the two discrete ductile fault zones in the gneiss complex. The two ductile faults appear to have been a primary locus of fluid flow during much of their existence because the greenschist facies retrograde metamorphism in the gneiss complex is most intense in the vicinity of the faults and massive quartz veins up to several meters thick also are found in and near the faults. These ductile faults may have initiated when the gneiss complex was still at upper amphibolite facies conditions and fluids may have begun to migrate along the faults at this time as well. Deformation of high temperature quartz-poor mafic rocks of the gneiss complex at high strain rates in the vicinity of the ductile faults may have produced fractures into which fault zone fluids migrated. If the fluids were water rich they could have depressed the solidus temperature of the amphibolites in the immediate vicinity of the cracks below the ambient temperature of the rocks such that localized partial melting of the amphibolite occurred.

Veins, migmatitic textures, and mobilizates are also common in the metasedimentary rocks and the group I orthogneisses in the study area. In some well exposed outcrops of these rocks there are multiple generations of mobilizate that cut the fabric of the gneiss and sometimes each other with varying degrees of discordance. In general, however, there appear to be two main groups of veining in the paragneisses and

group I orthogneisses. The earlier generation of mobilizate consists of leucocratic granitic (quartz plus two feldspars) to tonalitic (quartz plus plagioclase) composition veins, layers, and lenses millimeters to centimeters thick that generally are concordant to the compositional layering and gneissic fabric in the rocks although locally the compositional layering is crosscut by the veins. These concordant veins commonly are recrystallized and have a weak fabric subparallel to the host fabric, and locally they are folded by small-scale F3 folds.

Granitic composition concordant veins of the earlier generation usually are found in quartzofeldspathic host rocks and they commonly contain minor amounts of biotite and garnet. Common lit-par-lit layering of the granitic veins with their host and the diffuse character of many of the contacts suggest the veins are the result of partial melting of the host. The concordant veins in mafic host rocks are tonalitic in composition and minor constituents of the veins may include a wide variety of mafic minerals including hornblende, biotite, clinopyroxene, and orthopyroxene. Granulitic textured group I hornblende clinopyroxene biotite diorite gneiss from the southeastern part of the north structural block locally hosts leucocratic medium grained concordant tonalitic (plagioclase and quartz) veins containing hornblende, clinopyroxene, and orthopyroxene in a lit-par-lit textural relationship that is suggestive of a migmatite. The two-pyroxene bearing leucosomes suggest the metamorphic conditions during formation of the veins may have been transitional to granulite facies. The orthopyroxene bearing veins were observed at only one locality. Occurrences of orthopyroxene bearing veins do not appear to be common in southern California although occurrences of possibly similar veins have been reported in the Cone Peak area of the Santa Lucia Range in the Salinian block (Compton, 1960; Hansen and Stuk, 1989).

The second generation of veins in the study area are mostly discordant to the compositional layering in the paragneiss, they crosscut the foliation in the orthogneiss, and

they also crosscut the earlier concordant veins. The discordant veins usually are internally undeformed and lack a discernible deformation fabric although locally the veins may be buckled slightly. In all host lithologies the discordant veins usually are composed mostly of plagioclase and quartz and lack potassium feldspar. Minor constituents of the discordant veins include biotite, muscovite, and garnet.

THERMOBAROMETRIC STUDIES IN THE TEHACHAPI MOUNTAINS REGION

Thermobarometric studies on deformed ~100 to 115 Ma plutonic rocks and their metasedimentary framework rocks in the western Tehachapi Mountains north of the Garlock fault using garnet-hornblende-plagioclase-quartz and garnet-biotite-plagioclase-quartz thermobarometers indicate metamorphic pressures of ~7-9 kilobars and temperatures of ~600°-800°C (Pickett and Saleeby, 1993; Sharry, 1982). A localized area around the Tunis Creek metagabbro in the western Tehachapi Mountains bears evidence for a later metamorphic event occurring at ~4 kilobars and ~580°C which Pickett and Saleeby (1993) interpret as a retrograde event resulting from a localized fluid influx. In contrast to the deep crustal level metamorphic rocks north of the Garlock fault, metasedimentary rocks in pendants within granitic rocks in the Tehachapi Mountains south of the Garlock fault were metamorphosed at pressures of 2-3 kilobars (Haase and Rutherford, 1975; Sharry, 1982). Igneous crystallization pressures calculated from the Al content of hornblende in plutons in the southern Sierra Nevada at the latitude of Walker Basin and Kelso Valley range from 4.0-5.7 kilobars (Ague and Brimhall, 1988a). Thermobarometry on metasedimentary rocks and garnet-bearing granites within and just west of the study area in the eastern Tehachapi Mountains indicates peak conditions of 5-8 kilobars and 770°-800°C and retrograde conditions of 1-3 kilobars and 480°-580°C (Dixon et al., 1994; Dixon, 1995). The upper amphibolite facies metamorphic peak in the study area most likely occurred during the F2 and/or F3 folding events which appear to be coeval with and/or closely

follow the intrusion of the group I orthogneisses and the group II Tehachapi Intrusive Complex, respectively.

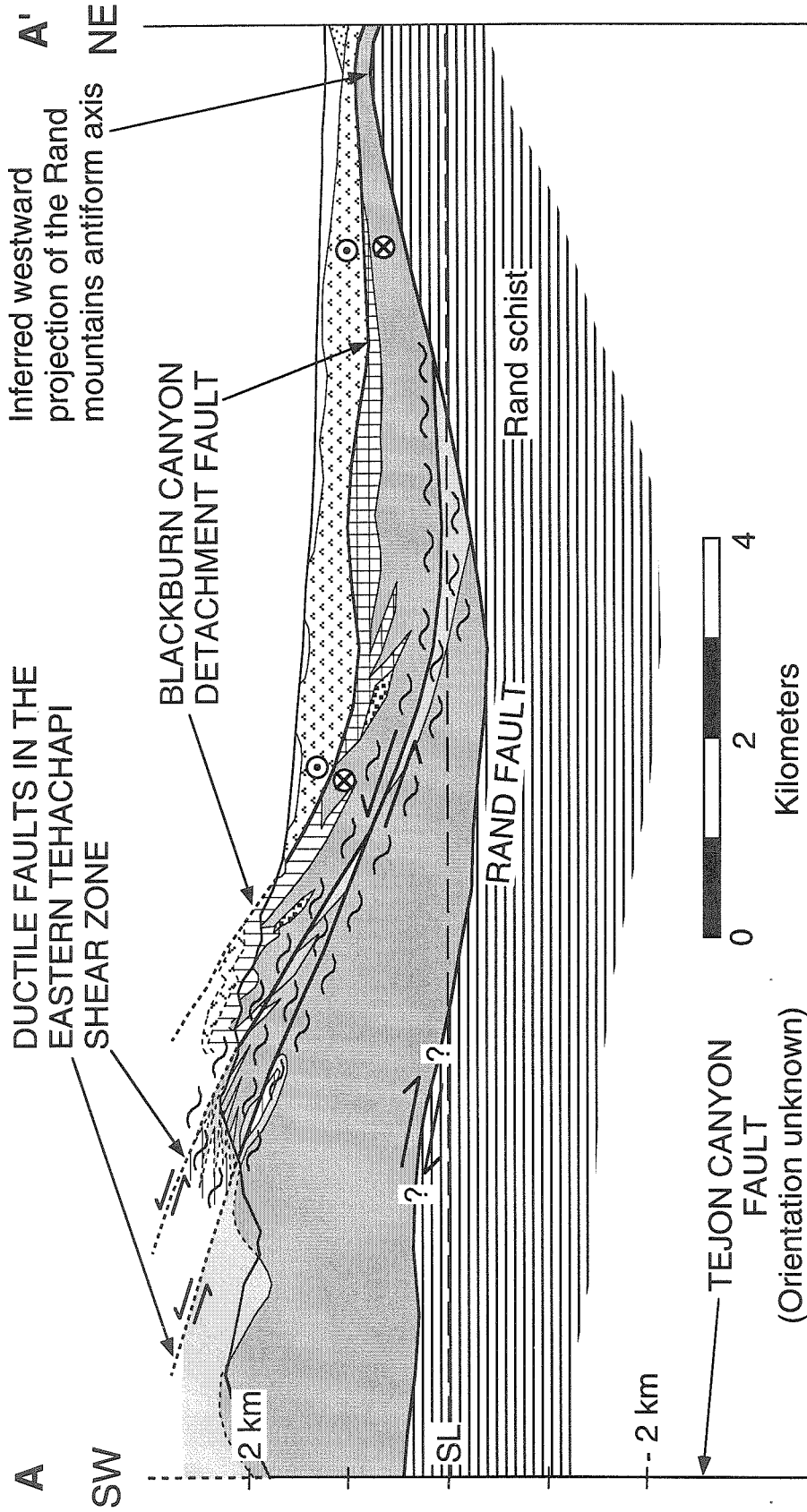
STRUCTURAL CROSS SECTIONS

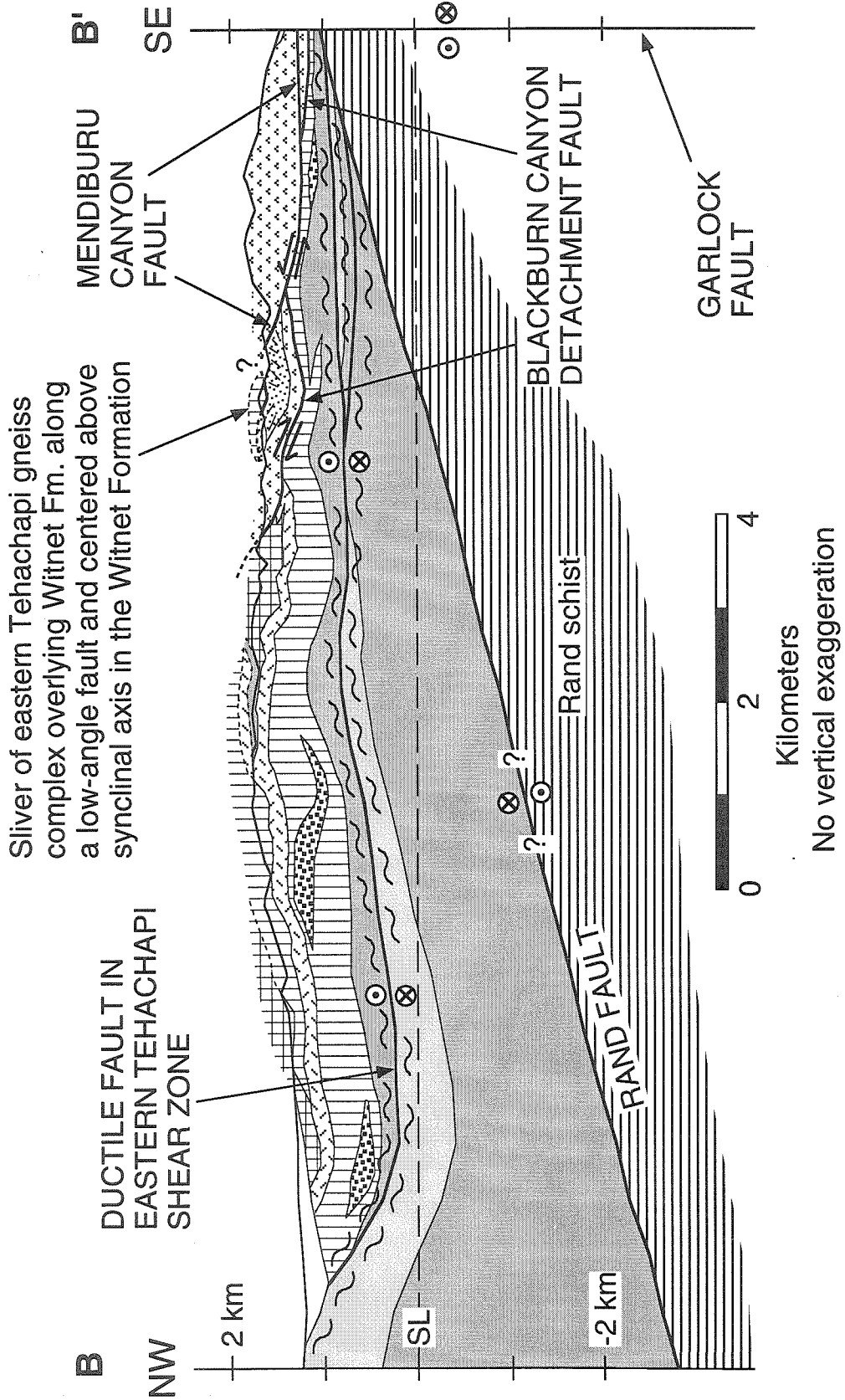
Interpretive geologic cross sections of the study area are shown in Figure 22 and the locations of the sections are marked in Figure 14. Section A-A' is a SW-NE oriented section across the most deformed part of the eastern Tehachapi shear normal to its trend. Features to note in section A-A' include the inferred presence of Rand schist at shallow depth beneath the eastern Tehachapi Mountains, the suspected presence of gabbro structurally beneath tonalite throughout the study area, folding of the gabbro-tonalite contact by F3 folds, the low-angle orientation of the ductile faults in the eastern Tehachapi shear zone, the possible merging of the shear zone with the Rand fault at depth, the top to the southwest shear sense of the shear zone, and the overall low-angle orientation of all the major faults in the study area. The antiformal culmination shown in the Rand schist beneath Tehachapi Valley is drawn assuming that the ~E-W trending axis of the Cenozoic post-metamorphic antiform of the Rand schist in the Rand Mountains (the trend is a compromise between the N60-70°E trend of Silver and Nourse (1986) and the ~NW-SE trend cited by Postlethwaite and Jacobson (1987)) is continuous to the west and has been offset ~45-50 km along the Garlock fault.

Cross section B-B' in Figure 22 is a NW-SE section oriented roughly parallel to the trend of the eastern Tehachapi shear zone. The shear sense of the faults shown in the section are only for the most recent phase of fault motion. Many of the faults may have had earlier movement histories with a different shear sense. Geologic features to note in section B-B' include the thin sheetlike form of the Pine Tree tonalite pluton, the low-angle NW dip of the Rand fault based on the seismic study of Malin et al. (1995), the proximity of the Rand schist to the surface at the Garlock fault suggested by the Oak Creek mylonite zone, the NW directed overriding of the Witnet Formation by granitic rocks along the Mendiburu

Figure 22.

Geologic cross sections, **A-A'** and **B-B'**, of the eastern Tehachapi mountains area. The locations of the cross sections are shown in Figure 14. The map patterns in the cross sections are the same as the patterns in Figure 14. Contacts that are projected above the topographic surface in the cross sections are shown as dotted lines.





Canyon fault, the top to the SE shear sense along the Blackburn Canyon fault, the overall low-angle orientation of the lithologic layering in the study area, the crosscutting of the Blackburn Canyon fault by the Mendiburu Canyon fault, and the sliver of the gneiss complex on top of the Witnet Formation.. The connection between the Mendiburu Canyon fault and the fault between the Witnet Formation and the overlying sliver of gneiss complex is queried because the sliver could have been emplaced either during motion along the Mendiburu Canyon fault or as a landslide block at some other time.

A series of five geologic cross sections through the study area is shown in Plate 3 and the locations of the sections are shown in Plate 1. Sections A-A', B-B', C-C', and D-D' are SW-NE trending and they cross the eastern Tehachapi shear zone at high-angle, while section E-E' is NW-SE trending and parallels the trend of the shear zone. The lithologic units in the cross sections of Plate 3 are same as in the geologic map of Plate 1. Sections C-C' and E-E' of Plate 2 are the same sections as A-A' and B-B' in Figure 22, respectively, but they show greater detail. In addition to the features mentioned above other features to note in the cross sections of Plate 2 include the progressive tightening and attenuation of the F3 folds in the gneiss complex from section A-A' in the northwest part of the study area through section D-D' in the southeast part of the study area. In sections A-A' and B-B' the inferred Tehachapi Valley fault is shown as a concealed low-angle normal fault dipping to the NE beneath rocks exposed north of Tehachapi Valley. The leucogranite shown beneath the north side of the valley is part of the Tehachapi Airport leucogranite of Ross (1989b) and the Brushy Ridge leucogranite south of the valley may correlate with it. The Atlas Formation shown buried beneath the alluvium in section A-A' consists of granitic and metamorphic rubble (Lawson, 1906; Dibblee and Louke, 1970) that may have been deposited while the inferred Tehachapi Valley fault was active as will be discussed later. In section D-D' note the alignment of the Quail Canyon fault zone in the granitic rocks above the Blackburn Canyon fault with the Mountain Park fault in the gneisses below the

Blackburn Canyon fault. The motion sense shown in section D-D' for the Quail Canyon fault zone is assuming the most recent motion along the fault occurred when the Mendiburu Canyon fault was active. As discussed earlier, however, a phase of top to the SW motion along the Quail Canyon fault is indicated and the Quail Canyon fault zone may represent a continuation of the Mountain Park fault into the Oak Creek Pass complex after the Oak Creek Pass complex was emplaced above the gneiss complex along the Blackburn Canyon fault.

CHAPTER IV: DISCUSSION AND INTERPRETATION

INFERRED AGE AND SEQUENCE OF TECTONIC EVENTS

The inferred protolith and emplacement ages of the rock units, the age constraints on the deformation events, and possible correlations between the structures in the study area with other structures of similar age and origin in the southern Sierra Nevada area are discussed in this chapter. Figure 23 is a chart which summarizes the inferred ages and sequence of tectonic events in the study area and it is based on information that will be covered in this chapter.

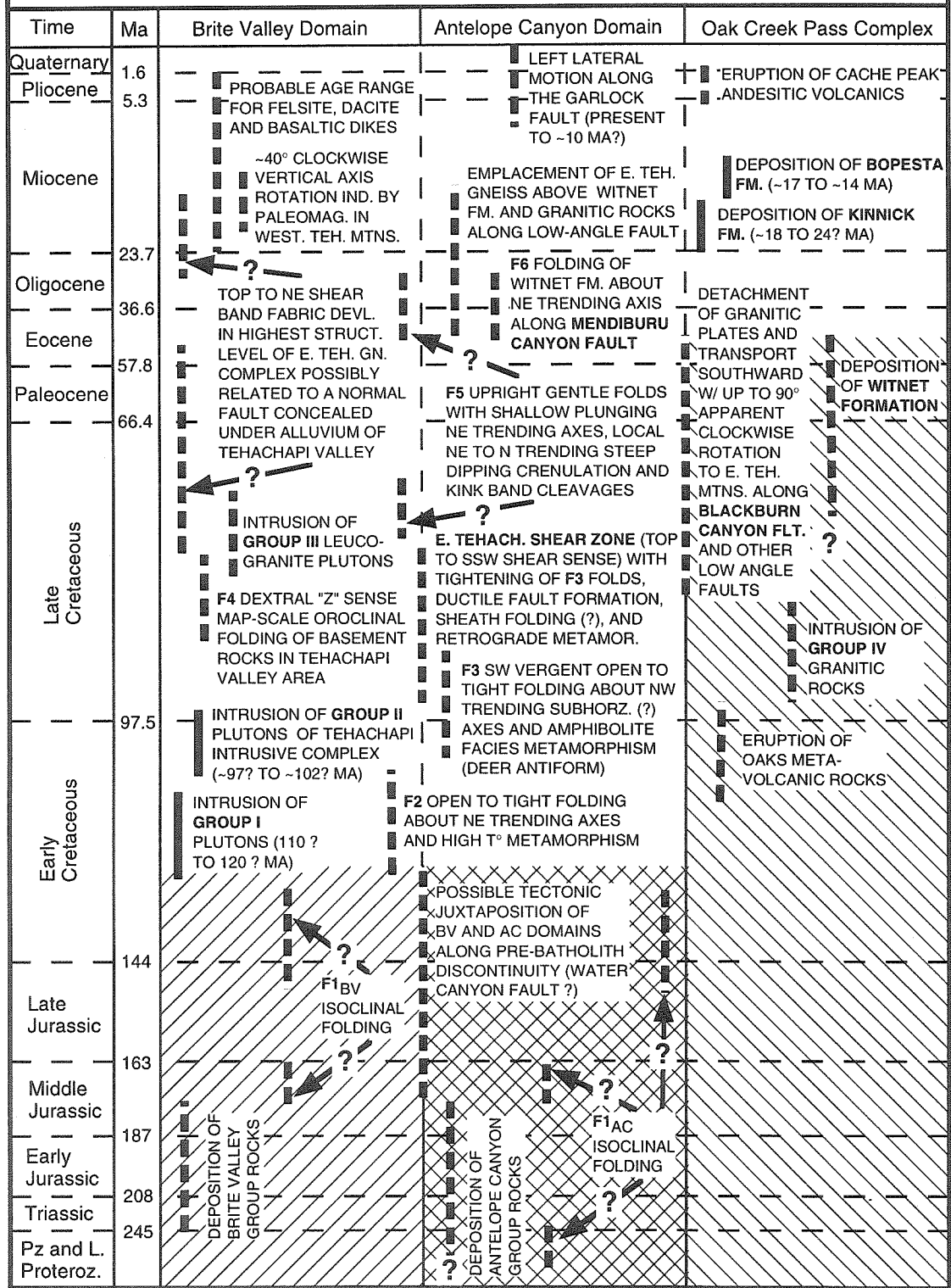
METASEDIMENTARY ROCKS: POSSIBLE CORRELATION, INFERRED AGE, AND PRE-INTRUSIVE DEFORMATION

The protolith ages of the metasedimentary rocks in the Antelope Canyon and Brite Valley sequences are unknown because no fossils have been found in any of the rocks. Dibblee and Louke (1970) and Dibblee and Warne (1970) considered the metasedimentary rocks in the Tehachapi Valley area to be Paleozoic in age based on their lithologic similarity to Paleozoic rocks in the Mojave desert and other nearby area, and Saleeby et al. (1978) correlated the Tehachapi area rocks with the Triassic-Jurassic age Kings sequence rocks exposed to the north in the Lake Isabella area based on similar grounds. Prior to this study the metasedimentary rocks in the Tehachapi area had not been subdivided into different groups although Ross (1987; 1989b) did note that marble appeared to be more abundant in the metasedimentary rocks located north and south of Tehachapi Valley than in the metasedimentary pendants found to the west of the valley. The purpose of this section is to discuss possible correlations of the metasedimentary rocks in the study area by comparing their lithologies, lithologic sequence, and style of deformation with nearby dated and undated sequences of rocks.

Figure 23

Inferred age and sequence of tectonic events in the eastern Tehachapi Mountains region. The ages (Ma) of the epoch and period boundaries shown in the figure are from Palmer (1983). The study area is divided into three domains each of which is inferred to have had a separate history prior to its juxtaposition with the other domains. The pre- to syn-juxtaposition histories of the Brite Valley, Antelope Canyon, and Oak Creek Pass complex domains are indicated by right leaning hatching, crosshatching, and left leaning hatching, respectively. The age constraints on the tectonic events are discussed in the text. Early formed structures may have had their original orientation changed by subsequent deformations. Where the trend, plunge, and/or dip of a structure is listed in the figure that aspect of its current orientation is inferred to be similar to its original orientation as discussed in the text.

INFERRED SEQUENCE AND AGES OF TECTONIC EVENTS IN THE EASTERN TEHACHAPI MOUNTAINS REGION



BRITE VALLEY GROUP

The overall sequence of lithologies in the Brite Valley group is similar to the Triassic-Jurassic age Kings sequence exposed in the Lake Isabella pendant to the north (Saleeby and Busby, 1993). The Brite Valley group rocks consist of a lower section of thinly laminated graphitic quartzite separated from an overlying section of interbedded sillimanite-rich pelite and psammite by a distinctive thin tripartite sequence of marble, calc-silicate rock, and pure quartzite (Figure 6). Uncommon thin layers of amphibolite in the rock sequence may be metamorphosed lenses of basalt, but lithologies that could be interpreted as more siliceous metavolcanic rocks were not observed. Small lenses of microcrystalline quartzite locally present north of Highway 58 may be metachert layers. Saleeby et al. (1978) divided the Kings sequence into two facies, a western basinal facies characterized by pelitic and volcanoclastic turbidites that interfinger westward with chert-rich sediments and mafic volcanic rocks, and an eastern shelfal facies characterized by shallow water limestones and quartz-rich detrital rocks locally interlayered with silicic volcanic rocks.

The Brite Valley group rocks have characteristics of both facies of the Kings sequence and may be transitional between them although they appear to be more similar to the western facies. The abundance of pelites and graphite in the quartzites suggests the sediments were carbonaceous and more basinal and the lack of siliceous volcanics also is suggestive of the western facies. The persistent thin marble layer overlain by a layer of calc-silicate rock in the Brite Valley group section is very similar to a thick (~15-100 meters) Late Triassic-Early Jurassic marble and calc-silicate section found in the eastern facies of the Kings sequence (Saleeby and Busby, 1993). The marble layer in the Brite Valley group rocks, however, is only 1 to 15 meters thick which suggest the Brite Valley group may be transitional between the eastern and western facies of the Kings sequence.

Another possible correlation of the Brite Valley group rocks is with the undated Sur series metasedimentary rocks exposed in the Santa Lucia Range west of the San Andreas fault in the Salinian block of central California (Figure 1). Prior to northwestward transport along the Neogene San Andreas fault system the north end of the Salinian block was adjacent to the Tehachapi Mountains and the southernmost Sierra Nevada (Hill and Dibblee, 1953; Powell and Weldon, 1992). The Sur series metasedimentary rocks consist primarily of thinly layered impure quartzite with local marble and calc-silicate layers that are poly-deformed and intruded by several generations of Cretaceous age plutonic rocks (Ross, 1977; James and Mattinson, 1988; Mattinson, 1990). In the northern Santa Lucia Range Wiebe (1970a) mapped a distinctive lithologic unit composed of graphitic and pyritic quartzite, biotite feldspar quartzite, calc-silicate granofels, and calcite marble which he called the Los Padres unit. Along strike to the SE of the exposures of the Los Padres unit graphitic metasedimentary rocks mapped by Seiders et al. (1983) may be a continuation of the Los Padres unit, and Powell (1993) suggests that the graphite-rich rocks mapped by Seiders et al. (1983) may be part of a regional assemblage of gneiss containing graphite-rich metasedimentary rocks which he calls the Limerock Canyon assemblage.

Wiebe (1970a) notes that ten to twenty percent of the rocks in the Los Padres unit contain at least a few percent of graphite and pyrite. The Los Padres unit dips to the NE, is semicontinuous along strike for about 30 km, and the metamorphic rocks immediately above the unit are dominantly pelitic and lack graphite (Wiebe, 1970a). The graphite and pyrite bearing quartzite lithology of the Los Padres unit appears to be similar to the rusty weathering graphitic quartzite of unit 1 in the study area which contains up to ~2 percent graphite and which is the structurally lowest unit of the Brite Valley group. The thin layers of marble, calc-silicate, and vitreous quartzite of units 2 and 3 of the Brite Valley group (Figure 6) may correlate with the other lithologies that are present in the Los Padres unit. The sillimanite rich pelitic rocks of unit 4 in the study area are the structurally highest

metasedimentary rocks of the Brite Valley group and they may correlate with the pelitic rocks structurally above the Los Padres unit in the Santa Lucia Range.

ANTELOPE CANYON GROUP

The Antelope Canyon group of metasedimentary rocks consists of a siliciclastic dominated lower section and a carbonate dominated upper section (Figure 6). There is much more carbonate and less pelite in the Antelope Canyon group section compared to the Brite Valley group rocks and the overall sequence of lithologies is different as well. It is conceivable that the Brite Valley group is the same lithologic sequence as the Antelope Canyon group minus the upper carbonate units. The Antelope Canyon group rocks may correlate with the lower part of the Triassic-Jurassic Kings sequence exposed in the Lake Isabella area. The two marble layers and the intervening layer of calc-silicate rock at the top of the Antelope Canyon group (units A through C) may correlate with the carbonate layer of inferred Late Triassic age present in the eastern facies of the Kings sequence in the Lake Isabella area (Saleeby and Busby, 1993). The calc-silicate rock/quartzite unit and pelitic unit overlying the marble in the Lake Isabella area, however, are lacking in the Tehachapi study area. Amphibolite lenses are present structurally below the thick marble layers in both the Lake Isabella and Antelope Canyon metasedimentary sections although they are much thicker and more continuous in the Lake Isabella area.

While the Antelope Canyon group rocks may correlate with the Mesozoic Kings sequence rocks they also might correlate with miogeoclinal rocks of late Proterozoic-early Paleozoic age. Pendants containing uppermost Proterozoic to Lower Cambrian miogeoclinal rocks are present in the Mojave desert southeast of the study area at Quartzite Mountain (Stewart and Poole, 1975; Miller, 1981; Miller and Cameron, 1982) and in the northern Shadow Mountains (Brown, 1982; Martin and Walker, 1995). In addition, recent work in the central Sierra Nevada has identified metamorphosed uppermost Proterozoic to Lower Cambrian miogeoclinal rocks in the Snow Lake pendant (Lahren and Schweickert,

1989; Lahren et al., 1990). The stratigraphy of the miogeoclinal rocks exposed at Quartzite Mountain (see Figure 3 of Stewart and Poole (1975) and Figure 2 of Miller (1977) or Figure 8 of Miller and Cameron (1982)) is remarkably similar to the stratigraphy of the Antelope Canyon group rocks shown in Figure 6. There appears to be almost a one to one correlation between units in the two different areas although the units in the Antelope Canyon group are thinner by a factor of 5 to 10 or more than the potentially correlative units at Quartzite Mountain. The difference in thicknesses might be the result of greater tectonic attenuation of the rocks in the study area.

METASEDIMENTARY ROCKS AT MONOLITH

The metasedimentary rocks north of Tehachapi Valley in the vicinity of the Monolith quarry (Figure 14) are called the Monolith group and were examined in reconnaissance in order to compare them with the metasedimentary rocks found south of the valley. The most prominent element of the Monolith group rocks is a 100-250 meter thick marble layer that is being quarried north of Tehachapi Valley (Troxel and Morton, 1962; Dibblee and Louke, 1970). Structurally beneath this thick marble layer is a succession of micaceous and feldspathic quartzites, with scattered local meter-scale layers of marble and amphibolite (D. J. Wood, unpublished mapping). The Monolith group rocks have a thicker marble layer and appear to be less deformed than both the Antelope Canyon and Brite Valley group rocks. The sequence of lithologies exposed in the Monolith area does not resemble either the Antelope Canyon group or the Brite Valley group in detail, but it is somewhat similar to the Kings sequence rocks found in the Lake Isabella area to the north. The sequence of metasedimentary rocks at Monolith resembles the portion of the stratigraphy in the Isabella pendant that immediately underlies calc-silicate rocks where Late Triassic to Early Jurassic fossils were found (Saleeby and Busby, 1993). The Monolith group rocks may be part of the eastern facies of the Triassic-Jurassic Kings sequence as originally suggested by Saleeby et al. (1978).

The contrast in style and degree of deformation between the Monolith group metasedimentary rocks north of Tehachapi Valley and the Antelope Canyon group rocks south of Tehachapi Valley also suggests the Monolith group rocks may be a different sequence from the Antelope Canyon group. The Monolith group rocks appear to be in a shallowly SE dipping homoclinal sequence and while they are locally folded into gentle subhorizontal NE trending folds they do not appear to share the N trending tight to isoclinal F1 folding and faulting that is present in the Antelope Canyon group rocks. There are at least two ways these apparent structural differences might be explained. If the two groups of rocks are different parts of the same metasedimentary sequence then the Antelope Canyon group rocks may have been closer than the Monolith rocks to the area where the F1 deformation event was focused, and thus, were more intensely deformed and attenuated. Alternatively, prior to top down to the NE motion along the inferred shallow NE dipping Tehachapi Valley fault the Antelope Canyon group rocks may have been structurally below the Monolith group rocks. If so, then the Antelope Canyon group may be an entirely different and older sequence than the Monolith group and the F1 deformation event affecting the Antelope Canyon group may have occurred prior to deposition of the Monolith group unconformably above it. Saleeby and Busby (1993) have suggested that Kings sequence rocks in the southern Sierra Nevada may comprise an early Mesozoic overlap sequence deposited on top of a polygenetic basement complex of Paleozoic age.

PRE-INTRUSIVE DEFORMATION OF THE METASEDIMENTARY ROCKS

The earliest deformation events recognized in the metasedimentary rocks of the study area, the F1_{BV} folding and faulting in the Brite Valley group rocks and the F1_{AC} folding and faulting in the Antelope Canyon group rocks, both appear to predate intrusion of the No Name Canyon augen gneiss. The No Name Canyon augen gneiss and the Antelope Canyon garnet diorite are inferred to have intruded along fault discontinuities between F1_{AC} folds, and the augen gneiss appears to intrude and crosscut an F1_{BV} fold.

The age of the Antelope Canyon garnet diorite gneiss is unknown, but the No Name Canyon augen gneiss is compositionally and texturally similar to the augen gneiss of Tweedy Creek which has a U-Pb zircon age of ~117 Ma (Saleeby et al., 1987). The maximum age of the F1 folds is constrained by the age of the metasedimentary sequences since there are no intrusive rocks that are clearly involved in the F1 folds.

If the Brite Valley group rocks correlate with the Middle Triassic to Early Jurassic age Kings sequence (Saleeby and Busby, 1993) then that would suggest the F1_{BV} folding event is Middle Jurassic to mid-Cretaceous in age. Middle-Late Jurassic to Early Cretaceous contractional deformation events have been recognized in the Mojave Desert region to the south of the study area (Martin and Walker, 1995; Boettcher and Walker, 1993) and also in the Sierra Nevada to the north (Saleeby and Busby-Spera, 1992). If the Antelope Canyon group rocks correlate with Late Proterozoic to Early Cambrian miogeoclinal rocks then that would broaden the constraints of F1_{AC} folding to younger than early Paleozoic in age. In addition to the Jurassic deformation events mentioned above the F1 folding of the Antelope Canyon group rocks might correlate with a Permo-Triassic deformation event during which miogeoclinal rocks in the Mojave Desert region were folded (Miller and Cameron, 1982).

JUXTAPOSITION OF THE METASEDIMENTARY ROCK GROUPS

Recent tectonic syntheses have emphasized the possibility that during the late Paleozoic and throughout the Mesozoic multiple generations of strike-slip faults with both dextral and sinistral sense of motion have played a role in truncating the edge of the craton and miogeocline in the southwestern Cordillera and then subsequently shuffling slices/plates of the same along the axis of the Mesozoic batholith (Saleeby and Busby-Spera, 1992; Saleeby and Busby, 1993). Locating these proposed structures is hampered by multiple episodes of Mesozoic deformation and plutonism and extensive Cenozoic extension, but clues such as contrasting assemblages of metasedimentary wallrocks,

discontinuities in the isotopic and chemical character of plutons, and locations of later shear zones are useful in constraining the location of these cryptic structures. The evidence summarized below suggests that a major lithologic and structural discontinuity, possibly a strike-slip fault, existed within the metasedimentary rocks both south and north of Tehachapi Valley prior to intrusion of most or all of the plutonic rocks in the area and prior to the development of the eastern Tehachapi shear zone.

The primary observation which suggests that a major prebatholithic structural discontinuity may have existed in the study area is the relatively sharp transition between the two different sequences of metasedimentary rocks in the study area, the Brite Valley group to the west and the Antelope Canyon group to the east (Figures 4 and 14). The only exposed contact between the two groups of metasedimentary rocks is the Water Canyon fault (Figures 3 and 4). The Water Canyon fault appears to be synformally folded in an F3 fold which suggests it existed prior to the F3 folding event and also prior to the eastern Tehachapi shear zone which postdates the F3 folding. A small mylonitic sliver of the No Name Canyon augen gneiss is exposed on a ridge-top between the W dipping limb of the Water Canyon fault and Water Canyon road where it rests on top of Brite Valley group metasedimentary rocks (Figure 4). The location, orientation, and degree of deformation of this augen gneiss sliver suggests it may have been deformed within the Water Canyon fault and that it may once have been part of the larger N trending body of augen gneiss exposed east of Water Canyon road. The Water Canyon fault east and north of Water Canyon road is not exposed and is inferred to be intruded by several generations of plutons.

The thin sheet-like form of the Pine Tree tonalite pluton, the Highline olivine gabbro pluton, and the bodies of the No Name Canyon and Tweedy Creek augen gneiss in conjunction with the locations of these intrusions in a narrow region of mixed orthogneiss and paragneiss between the two groups of metasedimentary rocks (see Figures 4, 14, and 22) suggests the plutons may have intruded along a preexisting structural discontinuity.

Plutons inferred to have intruded along intrabatholithic faults are present elsewhere in the Sierran Nevada batholith (Bateman et al., 1983; Kistler, 1993). The tabular shape of the augen gneiss may in part be the result of later strain related to deformation along the eastern Tehachapi shear zone, but the sheet-like aspect of the Pine Tree tonalite and the Highline gabbro is interpreted to be primary because most of the Pine Tree tonalite lacks fabrics suggestive of extreme thinning and the Highline gabbro is largely undeformed.

The location of the eastern Tehachapi shear zone between the two groups of metasedimentary rocks and the relatively narrow width of the shear zone also suggest that an older structure may have been present in that location. An older fault most likely would be a weak zone in the crust which would be susceptible to reactivation in later deformation events. The eastern Tehachapi shear zone may represent a Late Cretaceous reactivation of an older fault zone and the inferred older fault may be the structure which originally juxtaposed the Brite Valley and Antelope Canyon groups of metasedimentary rocks.

Another line of evidence suggesting that a significant pre-shear zone structural discontinuity may exist in the area is the relatively abrupt change in a number of isotopic, chemical, lithologic, and zircon inheritance characteristics of the plutonic rocks across the proposed location of the structure. North of Tehachapi Valley the position of the initial Sr 0.706 isopleth (Saleeby et al., 1987; Kistler and Ross, 1990) appears to closely coincide with the transition between the Brite Valley and Antelope Canyon groups of metasedimentary rocks (Figures 14). West of the 0.706 isopleth the Bear Valley Springs tonalite intrudes the Brite Valley group metasedimentary rocks and east of the isopleth a "cupola" of the Bear Valley Springs tonalite (Saleeby et al., 1987) intrudes the metasedimentary rocks of the Antelope Canyon group. In addition, the initial Sr 0.706 isopleth in the region is shown by Kistler and Ross (1990) as truncating the 0.705 isopleth in the southern Sierra Nevada area and the apparent truncation might be tectonic in origin.

While there does not appear to be a sharp discontinuity in oxygen isotopic data across the proposed location of the discontinuity, Saleeby et al. (1987) note that in the Tweedy Creek area samples from the eastern margin of the Bear Valley Springs tonalite (Tehachapi Intrusive Complex tonalite, Figure 14), the Claraville granodiorite, and the Tweedy Creek augen gneiss (No Name Canyon augen gneiss in Figure 14) are enriched in ^{18}O which they attribute to contamination by Kings sequence rocks. The proximity of the enriched samples to the Antelope Canyon group rocks suggests those rocks may be the source of the enrichment. Saleeby et al. (1987) also note that the Claraville granodiorite and the eastern marginal phase of the Bear Valley Springs tonalite are contaminated by Proterozoic zircons in contrast to the plutonic rocks further west where contamination is less apparent. The apparent differences in zircon contamination may reflect the presence of two different source regions that were tectonically juxtaposed. The Water Canyon discontinuity also approximately coincides with the quartz diorite line of Moore (1959).

AGE AND NORTHWARD CONTINUATION OF THE WATER CANYON FAULT

Assuming that metasedimentary rocks on one or both sides of the inferred Water Canyon fault are Triassic to Early Jurassic Kings sequence rocks, as discussed earlier, and assuming that intrusion of the ~117 Ma Tweedy Creek augen gneiss was localized along the discontinuity, then the age of the fault is constrained to be between mid-Jurassic time and the 117 Ma U-Pb zircon age (Saleeby et al., 1987) of the Tweedy Creek augen gneiss.

As noted above the augen gneisses of No Name Canyon and Tweedy Creek are inferred to have intruded along a structural discontinuity between the two different sequences of metasedimentary rocks. In the N trending pendant east and northeast of Walker Basin there is a long narrow body of granitic augen gneiss in the vicinity of Brown Meadow that is compositionally similar to and along strike from the augen gneiss of Tweedy Creek (Ross, 1989b). The Brown Meadow augen gneiss also may have intruded along the discontinuity, but the westward divergence of the 0.706 initial Sr isopleth from

the south end of the Brown Meadow augen gneiss body and the eastward divergence of the proto-Kern Canyon fault zone from the north end of the Brown Meadow augen gneiss (Figure 2) complicate speculation about the position of the discontinuity to the north.

LATE EARLY CRETACEOUS NW-SE DIRECTED INTRA-ARC SHORTENING

Contractional deformation structures in orogenic belts commonly are oriented subparallel to the strike of the belts. Contractional structures oriented transverse to the trend of orogenic belts also occur although they appear to be less common. In the southwestern Cordillera of North America contractional structures oriented at high angle to the trend of the continental margin and the Mesozoic batholith belt have long been noted and have been interpreted as evidence of arc-parallel contractional deformation, but the origin and significance of these mostly NE trending structures is not well understood as will be discussed below. The F2 folds in the study area are NE trending and oriented at high angle to the trend of the Sierra Nevada batholith which suggests that they may have formed as a result of shortening in a direction subparallel to the trend of the batholith. The purpose of this section is to estimate the age of this deformation event, to review the evidence for other arc-parallel contractional deformation events of similar age, and to propose a model which might explain the origin of the arc-parallel shortening.

STYLE AND AGE OF NW-SE SHORTENING IN THE STUDY AREA

Amphibolite facies gneissic fabrics in the paragneiss groups and the group I orthogneisses locally are folded by map-scale and mesoscale open to tight F2 folds that in their current orientation have gently plunging NE trending hinge lines and mostly subvertical to SE dipping axial surfaces (Figures 9, 10, and 11A). Although the current orientation of the F2 folds is not necessarily the same as it was when they formed because of subsequent deformation events the original trend of the F2 fold hinge lines is inferred to have been similar to the current NE trend of the hinge lines as discussed below.

The current F2 fold hinge lines are subparallel with the F5 fold hinge lines so neither their trend nor their plunge are inferred to have been changed significantly by F5 folding. Lithologic layering in the SW limb of the Tehachapi Valley orocline (which includes the study area) locally is inferred to have been rotated or transposed from a moderate NE dip to a shallow NE dip during activity along the eastern Tehachapi shear zone as will be discussed later. This rotation/transposition may have shallowed the plunge of F2 fold axes, but their trends are inferred not to have changed significantly. The F2 folds in the study area may have been rotated about a steep axis during regional-scale F4 oroclinal folding which is reflected by the changing trend of the metasedimentary pendants north of Tehachapi Valley in Figure 2. The NW trend of the pendants in the study area, however, is similar to the regional pendant trends in the Sierra Nevada batholith north of Walker Basin which appear to be unaffected by the F4 folding. This relationship suggests that the current trend of the F2 folds *in the study area* may be similar to their trend prior to the regional F4 folding. Finally, the F2 fold hinge lines may have been rotated about subhorizontal NW trending axes during F3 folding, but the F3 folding event is inferred not to have significantly changed their trend. Since the current trend of the F2 folds in the study area is inferred to be similar to their original trend, their NE orientation suggests that they formed during an episode of NW-SE directed contractional deformation.

The timing of the NE trending open to tight F2 folding in the study area is most clearly constrained between the pre- and possibly syndeformation intrusion of group I biotite hornblende quartz diorite gneiss and the intrusion of the late- to postdeformation Highline olivine gabbro and associated plagiogranite dikes. The Highline olivine gabbro intrudes biotite hornblende quartz diorite gneiss that has a well developed NE trending NW dipping gneissic fabric and it also intrudes metasedimentary rocks that have well developed mesoscale F2 folds. Annealed granoblastic fabrics in the folded paragneiss adjacent to the gabbro and a lack of any NE trending deformation fabric in the gabbro suggest its intrusion

postdates most of the F2 folding and deformation. There are several 1 to 2 meter wide NW trending subvertical plagiogranite dikes which crosscut the gabbro and the wallrocks immediately adjacent to it. The apparent truncation of the NE trending gneissic fabrics and F2 folds by the gabbro in conjunction with emplacement of the NW trending dikes in the gabbro suggests the Highline gabbro and accompanying dikes may have intruded during the waning stages of a NW-SE directed contractional deformation. The ages of the gneiss and gabbro are not known at this time.

The age of the F2 folding is also bracketed by the pre- to syndeformation intrusion of the No Name Canyon augen gneiss and the postdeformation intrusion of the tonalite of the Tehachapi Intrusive Complex. As discussed earlier, the No Name Canyon augen gneiss is similar to the augen gneiss of Tweedy Creek located north of Tehachapi Valley in degree of deformation, composition, and position in the regional tectonic stratigraphy. Because of these similarities the age of the No Name Canyon granite gneiss may be similar to the age of the Tweedy Creek augen gneiss which has a U-Pb zircon age of 117 ± 4 Ma (Saleeby et al., 1987). The tonalite of the Tehachapi Intrusive Complex appears to be continuous with the Bear Valley Springs tonalite exposed to the north and west of the study area and the U-Pb zircon age of the Bear Valley Springs tonalite ranges from ~97 to ~101 Ma (Saleeby et al., 1987). The above relations suggest the deformation and metamorphic event that formed the NE trending F2 folds in the study area occurred in the late Early Cretaceous between about 117 Ma and 100 Ma.

POSSIBLE CORRELATIVE DEFORMATIONS IN THE SOUTHWEST CORDILLERA

A survey of the literature on the southwest Cordillera of North America reveals a number of other localities within the batholith belt of central and southern California and northwestern Mexico where NE trending folds and deformation fabrics of known and possible late Early Cretaceous age are present. Many of these structures have been inferred to have formed in the Early to Middle Jurassic or in latest Jurassic time during the latter

stages of the Nevadan orogeny (Nokleberg and Kistler, 1980), but age constraints on many of the structures are permissive of deformation in late Early Cretaceous time and recent work suggests that many structures formerly thought to be Nevadan in age are Cretaceous in age (Tobisch et al., 1987). The widespread extent of these structures oriented normal to the main trend of the continental margin and the relatively narrow age range in which they were active, as will be outlined below, suggests they all may have formed during a major regional tectonic event. In the following discussion the evidence for late Early Cretaceous continental margin and magmatic arc parallel contractional deformation in the SW Cordillera is summarized. The localities are discussed from north to south starting in the central Sierra Nevada region.

In a summary of deformation events in the central Sierra Nevada region Nokleberg and Kistler (1980) noted that in several locations in the Western Metamorphic Belt and in the Strawberry Mine and Boyden Cave roof pendants there was a generation of NE trending structures which they assigned an Early to Middle Jurassic age to based on regional geologic relations. More recent work suggests that the age of some of the NE trending structures may be late Early Cretaceous. In the Strawberry Mine and Boyden Cave pendants Kings sequence Triassic and Early Jurassic metasedimentary rocks were deformed under amphibolite facies conditions into NE trending folds and fabrics (Girty, 1977; Nokleberg, 1981) prior to the eruption of the Merced Peak volcanic rocks of ~100 Ma (U-Pb zircon age) in the Strawberry Mine pendant area (Peck and Van Kooten, 1983) and volcanic rocks of ~105 Ma (U-Pb zircon age) in the Boyden Cave pendant (Saleeby et al., 1990). Saleeby et al. (1990) indicate that amphibolite facies deformation and intrusion of ~110 Ma plutons preceded eruption of the volcanic rocks in the Boyden Cave pendant which suggests that the NE trending structures may have formed between 105 and 110 Ma.

Local domains of conjugate folds and crenulation cleavages, inferred to have formed during NW-SE directed maximum compression, deform a NW trending steeply

dipping slaty cleavage developed in mid-Cretaceous through Triassic age metavolcanic rocks and Paleozoic metasedimentary rocks in the Ritter Range pendant of the central Sierra Nevada (Tobisch and Fiske, 1976; Tobisch and Fiske, 1982). Formation of the conjugate fabrics in the mid-Cretaceous metavolcanics is constrained to have occurred between ~85 and ~99 Ma based on U-Pb zircon dating of the deformed volcanics and post deformation plutons, but an earlier Late Jurassic to mid-Cretaceous episode of NW-SE contraction and associated conjugate fabric formation in the older rocks cannot be ruled out (Tobisch and Fiske, 1982). Two sets of steeply dipping crenulation cleavages and minor fold axial planes, one set trending N to N-NE and the other set trending E to E-SE, crosscut slaty cleavage developed in 160 to 130 Ma (U-Pb zircon ages) metavolcanic rocks of the Goddard pendant (Tobisch et al., 1986). The two sets of cleavage in the Goddard pendant rocks are inferred to be conjugate and their orientations are similar to the conjugate cleavages developed in the Ritter Range pendant to the north which suggests they may have formed during the same deformation episode. The age of the conjugate cleavages developed in the Goddard pendant rocks is constrained to be between the age of the youngest metavolcanic rocks, ~130 Ma (Tobisch et al., 1986), and the ~90 Ma U-Pb zircon age of undeformed crosscutting plutons (Stern et al., 1981).

There are a few other structures in the central and southern Sierra Nevada area that may have formed in late Early Cretaceous time and which have orientations that suggest a component of contraction oriented subparallel to the continental margin. West vergent thrusting along the NE trending Barcroft structural break in the White Mountains was active in Early Cretaceous time prior to the 100 Ma (U-Pb zircon age) intrusion of the crosscutting McAfee Creek granite (Hanson et al., 1987). Early Mesozoic age Kings sequence rocks in the Kern Canyon pendant north of Lake Isabella in the southern Sierra Nevada record a pre-105 Ma fold and thrust history expressed by E-W trending open to tight folds and a penetrative spaced cleavage which overprint shallow to moderate S dipping bedding

surfaces (Saleeby and Busby-Spera, 1986; Saleeby, 1992; Saleeby and Busby, 1993). In the Sierran foothills south of the western metamorphic belt Bateman et al. (1983) document an episode of deformation in metasedimentary rocks and Early Cretaceous plutons of the Sierran batholith which they infer was synchronous with the emplacement of the 113 Ma leucotonalite of Ward Mountain. They infer that the eastern flank of the leucotonalite pluton was arched symmetrical to an eastward plunging axis during intrusion. E to NE plunging mineral lineations, crenulation axes, and small fold axes are present in the deformed metasedimentary rocks adjacent to the pluton and locally NE trending steeply dipping gneissic fabrics are developed in the adjacent 114 Ma tonalite of Blue Canyon (Bateman et al., 1983).

Well developed NE trending folds and deformation fabrics of known and probable late Early Cretaceous age are present at a number of different localities in the Salinian block of central California west of the San Andreas fault (Figure 1). In the Ben Lomond Mountain area near Santa Cruz Sur series metasedimentary rocks of unknown protolith age were deformed into shallow NE and SW plunging folds and metamorphosed at amphibolite facies (Leo, 1967). Several bodies of granitic orthogneiss are inferred to have intruded the Sur series rocks synkinematic with the deformation because gneissic foliation and mineral lineations in the intrusions are concordant with the folds and mineral lineations in the metasedimentary rocks (Compton, 1966b; Leo, 1967). U-Pb zircon dating of the synkinematic plutons indicates a probable emplacement age range of 103 to 130 Ma, and tonalite and gabbro plutons that truncate the deformation fabrics in the paragneiss have a 99 Ma U-Pb zircon age (James, 1992). E to NE trending folds and amphibolite facies deformation fabrics similar to the dated structures in the Ben Lomond Mountain area are also present in the northern Santa Lucia Mountains (Wiebe, 1970b; Wiebe, 1970a), the western Santa Lucia Mountains (Hall, 1991), and possibly in the northern Gabilan Range (Compton, 1966b; John, 1981) of the Salinian block. Hall (1991) suggests the NE

trending folds in the Sur series rocks formed prior to the emplacement in the western edge of the Salinian block of charnokitic tonalite (Compton, 1960) that has an approximate emplacement age of ~104 Ma based on U-Pb studies on zircons (Mattinson, 1978).

One location in southern California where late Early Cretaceous age structures suggestive of NW-SE crustal shortening occur is in the Peninsular Ranges batholith west of the Cuyamaca-Laguna Mountains shear zone. In this area Todd et al. (1988) report the presence of folds and faults that have orientations suggestive of NW-SE directed contraction and they note that one of the youngest rocks involved in the shortening is a pluton with a 103 Ma K-Ar date on hornblende.

E-NE trending structures of known and probable late Early Cretaceous age are also present in northwestern Mexico. In the southern part of the Mexican state of Sinaloa the strike of foliation and bedding in metamorphosed sedimentary rocks and the strike of foliation in codeformed igneous intrusions is E-NE and the trend of outcrop scale folds is similar (Henry, 1986). The age of the deformation producing the E-NE structures is bracketed by the Aptian-Albian age of deformed carbonate rocks and the 100 Ma U-Pb zircon age of a crosscutting quartz diorite pluton (Henry, 1986). Henry (1986) also summarizes evidence for other E to NE trending structures found in a 300 by 1100 km area along the northwest margin of Mexico that may have formed in Early Cretaceous time.

A MODEL FOR ARC-PARALLEL SHORTENING DEFORMATION

From the results of this study and the preceding review of the literature it appears that a regional episode of NW-SE directed arc-parallel crustal shortening deformation, accompanied locally by amphibolite facies metamorphism, occurred during emplacement of the southwest Cordilleran batholith most likely in late Early Cretaceous time. The origin of these structures which suggest continental margin parallel contraction is enigmatic. Tobisch and Fiske (1976) suggested that the conjugate crenulation cleavages may have formed during an "elastic recovery" phase following cessation of an episode of mountain

belt-normal crustal shortening. Henry (1986) suggested the E-NE structures in northwest Mexico may have formed in response to oblique subduction, but he noted that the orientation of the structures subperpendicular to the paleosubduction zone seemed to require more tangential convergence than what is indicated for that time. Another possibility is that the contractile structures could be transpressional in origin and may have formed alongside strike-slip faults. The difficulty with the structures being transpression in origin, however, is that the trends of transpressional folds are oriented at 45° , and typically much less, to the trend of the adjacent strike slip fault (Sanderson and Marchini, 1984; Sylvester, 1988). If the NE trending contractile structures are transpressional in origin that would imply that the accompanying strike-slip faults have E to N strikes and major strike-slip faults with such orientations have not been observed in the SW Cordillera.

While these structures suggestive of NW-SE contraction appear to be present over a wide geographic region, encompassing the continental margin in central and southern California and northwestern Mexico, they are not pervasively developed in rocks of Early Cretaceous age and older. The domains where the structures are found frequently appear to be of limited areal extent, an observation first made by Tobisch and Fiske (1976). Consideration of the locations where these NE trending structures are found reveals that many of them are developed within or adjacent to known or inferred faults or shear zones that are both older and younger than the structures of interest. For example, as discussed earlier, a pre-batholith structural break may be present in the Tehachapi Mountains study area between the two groups of metasedimentary rocks. In the Lake Isabella area the E trending, N vergent structures are located adjacent to the proto-Kern Canyon fault zone which is inferred to have been active as early as 105 Ma (Busby-Spera and Saleeby, 1988). The zone of ductile deformation associated with the leucotonalite of Ward Mountain lies along strike from the Melones fault zone (Bateman et al., 1983). In the central Sierra

Nevada the NE trending structures in the Strawberry Mine and Boyden Cave pendants are located adjacent to the axial intrabatholithic break of Saleeby and Busby (1993).

The apparent local development of these late Early Cretaceous NE trending contractile structures in the vicinity of known and inferred faults and shear zones that trend subparallel to the continental margin along the axis of the magmatic arc suggests a model for their origin. Data concerning the state of stress of the San Andreas fault system indicates that in the vicinity of the fault the direction of maximum horizontal compression is oriented normal to the trace of the fault (Zoback et al., 1987). Based on these data Zoback et al. (1987) suggest that the San Andreas fault is an extremely weak fault that mostly relieves the shear stresses along the fault with the result that the regional far-field state of stress in the crust is reoriented in the vicinity of the fault such that the directions of the principle horizontal stresses are oriented parallel and perpendicular to the fault. Zoback et al. (1987) note that if the far-field maximum compressive stress is oriented at an angle of greater than 45° to the strike of a weak strike-slip fault then in the vicinity of the fault the maximum compressive stress is reoriented to an orientation nearly perpendicular to the fault. Alternatively, if the direction of the far-field maximum horizontal stress is oriented at less than 45° to the strike of the fault then the direction of maximum horizontal compression adjacent to the fault is reoriented to become almost parallel to the fault (Zoback et al., 1987).

The late Early Cretaceous structures in California and Mexico that are suggestive of regional NW-SE directed crustal shortening may have formed in the vicinity of preexisting and/or coeval steeply dipping generally NW trending weak faults. These hypothesized weak faults locally may have served to reorient the direction of maximum horizontal stress when they were active, or reactivated, during a relatively short lived orogenic event in late Early Cretaceous time. This model requires the presence of weak faults that could reorient stresses in the region where the NE trending contractile structures are found and it also

requires that the regional maximum horizontal compressive stress direction was oriented at less than 45° to the strike of these faults during a relatively short period in late Early Cretaceous time. While there are a number of candidates for faults in the region under consideration, as discussed below, it appears difficult, if not impossible, to directly prove that any of the ancient faults were weak. It does, however, appear to be reasonable to assume that some of the faults were weak by analogy to present day active faults, many of which appear to be weak. Based on stress studies of active strike-slip faults Mount and Suppe (1992) suggest that large-scale strike-slip faults may be inherently weak, and recent studies of shear zones (Janecke and Evans, 1988) and of fluids in fault zones also suggest many faults may be weak (Wintsch et al., 1995; Hickman et al., 1995).

A large number of major strike-slip faults of inferred mid-Cretaceous and older age and having general NW trends are known or have been proposed to exist within the area of the continental margin in California and Mexico where the late Early Cretaceous NE trending contractile structures are found. Assuming these faults were weak the regional principle stresses of the plate margin in late Early Cretaceous time could have been reoriented locally such that the direction of maximum horizontal compressive stress in the vicinity of the faults was NW trending. Some of these known and inferred continental margin and magmatic arc parallel faults of mid-Cretaceous age and older are reviewed below. The purpose of reviewing the faults is not to make a case for or against their existence or proposed location, but merely to illustrate that potentially there are a large number of faults that could have affected the orientation of later or coeval structures that developed nearby.

NW trending structures related to inferred late Paleozoic to early Mesozoic and/or Late Jurassic sinistral-sense strike-slip truncation of the Cordilleran continental margin are postulated to extend from the Sierra Nevada region, through southern California, and into northwestern Mexico. The late Paleozoic-early Mesozoic structures include the

Pennsylvanian-Permian truncation boundary of Walker (1988) and Stevens et al. (1992), the Foothills suture of Saleeby (1990a), and the Permo-Triassic truncation boundary of Burchfiel and Davis (1981). Late Jurassic age continental truncation is inferred to have occurred along the Mojave-Sonora megashear (Silver and Anderson, 1974; Anderson and Silver, 1979; Silver and Anderson, 1983) which may have two strands (Dickinson, 1981; Silver and Anderson, 1983). Other proposed strike-slip faults in western Mexico which may be similar in age to the megashear are the Mexican volcanic belt megashear (Anderson and Schmidt, 1983) and the Walper lineament (Longoria, 1985). In the foothills of the western Sierra Nevada the Bear Mountains and Melones fault zones may have been active as strike-slip faults in Late Jurassic time (Wolf and Saleeby, 1991). A number of different N-NW trending faults, possibly active in Jurassic and/or Early to mid-Cretaceous time, are inferred to exist in the axial region of the Sierra Nevada batholith. These Sierran intrabatholithic faults include the axial and eastern intrabatholithic breaks of Saleeby and Busby (1993) which correspond to intrabatholith breaks 2 and 3 of Kistler (1993); the Mojave-Snow Lake fault of Schweickert and Lahren (1990), and the proto-Kern Canyon fault of Busby-Spera and Saleeby (Busby-Spera and Saleeby, 1988). By analogy with the San Andreas fault system which is composed of multiple strands that have been active at different times, any of the above mentioned faults may have had multiple strands, thus providing more opportunities to potentially influence the orientation of nearby structures.

The requirement of this weak fault model that the regional far-field maximum horizontal compressive stress direction in the southwest Cordillera during late Early Cretaceous time was oriented at less than a 45° angle to the general NW trends of the faults discussed above is difficult to demonstrate since there are few geologic structures that can reliably be used to infer principle stress directions. Dikes, conjugate fractures, and twin gliding in calcite are examples of structures that could be used to infer principle stress directions (Hobbs et al., 1976; Suppe, 1985), but this author is not aware of any studies

using these features that would be relevant for stress directions during the time of interest. Alternatively, if a system of faults is assumed to approximate Coulomb fractures, as in the Anderson theory of faulting, then the orientation and slip of the faults can be used to estimate the directions of the principle stresses (Suppe, 1985; Anderson, 1951). Using this assumption the orientation of the far-field principle stresses during the late Early Cretaceous might be estimated from the orientation and slip of faults active at that time in the back-arc region of the Cordillera. The Luning-Fencemaker thrust belt in western Nevada contains both NW and SE vergent NE trending thrust faults which appear to have been active in late Early Cretaceous time (Burchfiel et al., 1992a; Maher and Saleeby, 1988; Oldow, 1984) which suggests that the direction of maximum horizontal compressive stress at that time may have been approximately NW-SE trending, and at an angle of less than 45° to the strike of the inferred intrabatholithic faults reviewed above.

PROTRACTED MID- TO LATE CRETACEOUS CONTRACTIONAL DEFORMATION IN THE MIDDLE TO LOWER CRUSTAL LEVELS OF THE SOUTHERN SIERRA NEVADA BATHOLITH

CONTRACTIONAL DEFORMATION IN THE STUDY AREA

The F3 folds and accompanying high temperature gneissic fabrics, the F4 oroclinal folds, and the greenschist facies mylonitic fabrics and ductile faults of the eastern Tehachapi shear zone in the eastern Tehachapi gneiss complex portion of the study area are all interpreted to have developed progressively during a protracted and complex episode of contractional deformation in the southernmost Sierra Nevada batholith. Some of the structural and metamorphic features found within the eastern Tehachapi gneiss complex, such as greenschist facies low-angle mylonitic fabrics superimposed on high-grade gneisses and the local overprinting of ductile deformation fabrics by brittle fabrics as evidenced by the cataclastic chloritic breccia development along some faults, commonly are encountered in metamorphic core complexes which form in extensional tectonic settings.

The reasons why the F3 folds, F4 folds, and the eastern Tehachapi shear zone in the study area are interpreted as having progressively developed in a contractional rather than an extensional deformation are discussed below.

As noted by Wheeler and Butler (1994) structures extending the crust should intersect the surface of the earth when traced out in the direction opposite to the direction of hangingwall transport. The structures in the gneiss complex that might be interpreted as extensional structures based on their retrograde metamorphic history include the eastern Tehachapi shear zone and the two ductile faults in the shear zone, the Taco Saddle and the Mountain Park faults. The hangingwall transport of these structures is top to the S-SW. These structures cannot be traced to the southeast because they disappear beneath the Blackburn Canyon fault and the Taco Saddle fault cannot be traced to the northwest because it appears to die out by the time it reaches Brite Valley (Figure 4). The Mountain Park fault and the eastern Tehachapi shear zone both appear to continue to the north across Tehachapi Valley and the shear zone, at least, is inferred to be continuous with the proto-Kern Canyon fault zone to the north in the Lake Isabella area (Busby-Spera and Saleeby, 1990). There is no evidence, however, that the proto-Kern Canyon fault zone intersects the earth's surface to the northeast of the Tehachapi Valley area; it continues northward from the Lake Isabella area. Thus, based on the above criterion the eastern Tehachapi shear zone appears to be a contractional structure and not an extensional structure.

The large-scale NW trending SW vergent F3 folds and the associated NW trending type 1 mineral elongation lineations of the Tehachapi Intrusive Complex suggest the local batholith crust has been shortened in a NE-SW direction during F3 folding. Most fold (\pm thrust fault) dominated terranes traditionally have been interpreted as forming during crustal shortening. Recent studies, however, have documented a number of cases of folds forming in extensional shear zones although the styles of these folds generally are different than the folds encountered in contractional orogens. Some of the ways folds may develop

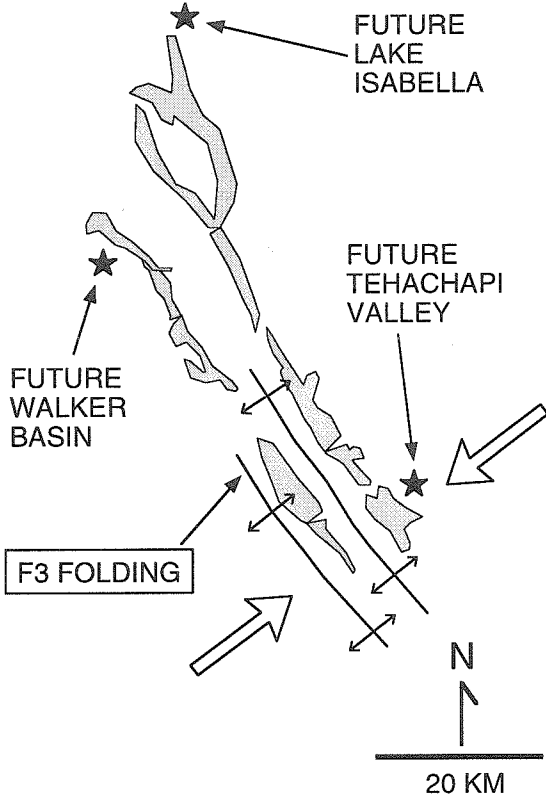
in extensional shear zones is by buckling of previously existing steeply dipping layering (Ramsay, 1980; Froitzheim, 1992), by rotation of earlier fold axes into parallelism with the stretching lineation to form sheath folds (Malavieille, 1987), or by contraction oriented normal to the transport direction (Fletcher and Bartley, 1994). None of the above mechanisms appear to be involved in the formation of the F3 folds in the study area. The F3 folds in the central and southern structural blocks of the study area are best developed in the gabbro-tonalite contact of the Tehachapi Intrusive Complex, and the inferred regional presence of the gabbro structurally beneath the tonalite (Figures 14 and 22) suggests that this contact may have had a low-angle orientation prior to the F3 folding. The second and third mechanisms of fold formation during extensional deformation mentioned above do not appear to apply in this case because the F3 folds are not sheath folds and there is no evidence that they formed in a shear zone with a transport direction parallel to F3 fold axes.

The F3 folds, the F4 folds, and the eastern Tehachapi shear zone are interpreted to have formed more or less sequentially during a protracted period of NE to N-NE directed contractional deformation and the later phases of this deformation are inferred to represent the contractional component of regional dextral transpression. The inferred sequential development of these structures is illustrated in parts A, B, and C of Figure 24. The estimated ages of the different phases of the deformation are discussed in the next section. The current NW trend and SW vergence of the F3 folds located south of Tehachapi Valley are inferred to be similar to their original orientation (Figure 24A) and the folds are inferred to have developed during an episode of NE directed contractional deformation localized in the southernmost part of the batholith (Figure 24A). F4 oroclinal folding of the basement in the southern Sierra Nevada may have formed in response to a component of N to N-NE directed contraction in conjunction with a component of N-NW directed dextral simple shear resulting in overall dextral transpressional deformation (Figure 24B). Synbatholithic dextral transpressional deformation has been documented in the Sierra Nevada to the north

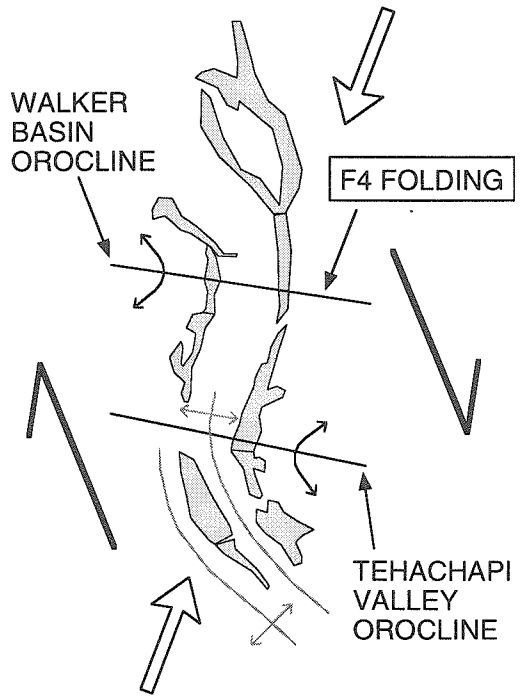
Figure 24.

Schematic diagram illustrating a model for the mid-Cretaceous to Late Cretaceous-early Cenozoic (?) structural evolution of part of the southern Sierra Nevada batholith. Shaded bodies are selected metasedimentary screens and pendants found between the Lake Isabella and Tehachapi areas. Prior to Late Cretaceous deformation the metasedimentary rocks in the southernmost part of the Sierra Nevada batholith are assumed to have had a trend subparallel to the ~N-NW trend of pendants found in the batholith to the north. The metasedimentary pendants shown in the figure are assumed to have steep to moderate dips, mostly to the east, unless otherwise noted. A) Initiation of originally NW to N-NW trending F3 folds with subhorizontal plunges in the southernmost of part of the batholith during ~arc-normal NE directed contractional deformation. B) Change from arc-normal contraction to dextral transpression resulting in initiation of regional-scale dextral-sense F4 oroclinal folding. The earlier F3 folds are folded around the F4 folds resulting in trend changes but not plunge changes. A component of N-NE directed contraction is inferred to have contributed to tightening and continued development of the F3 folds. C) N-NE directed thrust (?) emplacement of the Rand schist beneath the southernmost Sierra Nevada batholith resulting in the localized transposition of the moderately NE dipping southwest limb of the Tehachapi Valley orocline into a shallowly NE dipping orientation along the eastern Tehachapi shear zone. The dextral-sense N trending proto-Kern Canyon fault zone is inferred to be continuous with the top to the S-SW shear sense eastern Tehachapi shear zone. D) The eastern Tehachapi shear zone is folded by NE trending shallowly NE plunging F5 folds which may have developed during intrusion of several Late Cretaceous (?) age leucogranite plutons. A NE dipping fault hypothesized to be concealed beneath the alluvium of Tehachapi Valley may have accommodated NE directed extension during intrusion of the leucogranite plutons. The structures shown in the Tehachapi Valley area are from a structural level below the Blackburn Canyon fault which is not shown in D or C.

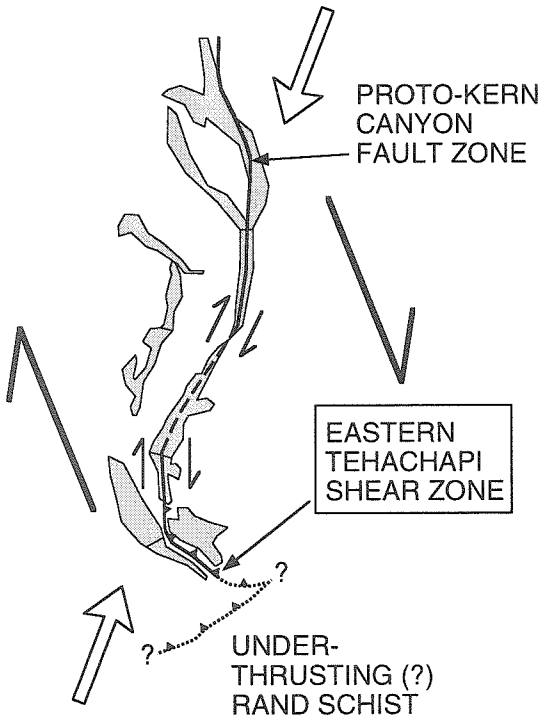
A ~100-90 MA



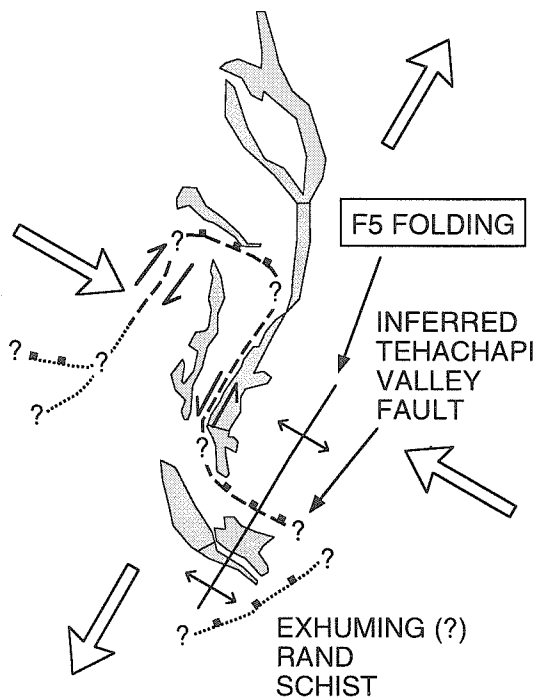
B ~90-85 MA



C ~85-80 MA



D POST ~80 MA



(Tikoff and Teyssier, 1992; Greene and Schweickert, 1995). Finally, the S-SW slip direction and upper plate transport direction of the eastern Tehachapi shear zone suggests that lower levels of the southern Sierra Nevada batholith were shortened in a N-NE direction possibly during underthrusting of Rand schist at lower structural levels (Figure 24C). The eastern Tehachapi shear zone may represent the contractional component and the N trending dextral-sense proto-Kern Canyon fault zone may represent the dextral simple shear component of regional dextral transpressional deformation.

During the protracted period of deformation discussed above the grade of metamorphism in the eastern Tehachapi gneiss complex decreased. The F3 folds initiated and developed during amphibolite facies conditions which may have persisted through the F4 folding and formation of the Tehachapi Valley orocline. Deformation fabrics of the subsequent eastern Tehachapi shear zone are dominated by greenschist facies metamorphic mineral assemblages and in the latest stages of the shear zone activity brittle fracturing of quartz and cataclasite development along the Taco Saddle fault suggest deformation locally may have continued into subgreenschist metamorphic conditions.

AGE OF THE CONTRACTIONAL DEFORMATION IN THE EASTERN TEHACHAPI MOUNTAINS

The overall timing of this protracted deformation event appears to be approximately constrained between the time of intrusion of the gabbro and tonalite of the Tehachapi Intrusive Complex and the time of intrusion of the Brushy Ridge leucogranite. Initial deformation and recrystallization of the gabbro and tonalite of the Tehachapi Intrusive Complex at amphibolite facies was accompanied by the formation of the NW trending SW vergent F3 folds. High temperature subsolidus gneissic fabrics in the gabbro and tonalite of the Tehachapi Intrusive Complex generally are subparallel to and locally superimposed on possible magmatic flow textural features such as flattened mafic enclaves, schlieren layers, and aligned plagioclase lathes which suggests the intrusions may have been

emplaced syntectonically (Paterson et al., 1989). The Tehachapi Intrusive Complex appears to be continuous with the tonalite of Bear Valley Springs which has an age of ~100 Ma based on multiple U-Pb zircon dates (Saleeby et al., 1987).

The latest phase of the contractional deformation in the study area is represented by the top to the S-SW simple shearing associated with the shallowly NE dipping eastern Tehachapi shear zone. The Brushy Ridge leucogranite and other leucogranite bodies in the study area appear to have intruded at or near the end of shear zone activity. Pine Tree tonalite with top to the N-NE shear zone fabrics that is exposed on Brushy Ridge (Figure 4) is intruded by leucogranite that is penetratively deformed by an S-C fabric with the opposite sense of shear, top to the NE. Leucogranite on Pine Tree Ridge, in contrast, locally is deformed by top to the S-SW shear band fabrics, but it also intrudes along and crosscuts top to the S-SW shear bands in the augen gneiss of No Name Canyon. In the vicinity of the Brushy Ridge leucogranite the Pine Tree tonalite locally exhibits top to the NE shear fabrics. The only place a crosscutting relationship was observed between these two sets of shear fabrics with opposite shear sense is in the No Name Canyon augen gneiss where the top to the S-SW shear zone fabric is crosscut by top to the NE shear bands. The above observations in aggregate suggest that intrusion of the Brushy Ridge leucogranite occurred near the end of eastern Tehachapi shear zone activity. Preliminary results of U-Pb zircon geochronological studies of the Brushy Ridge leucogranite suggest it has an age in the range of ~70 to 80 Ma (J. B. Saleeby, personal communication, 1996).

The ages of the F3 folding, the F4 folding, and the shear zone within this 20 to 30 My period of deformation between ~100 and 70-80 Ma are only loosely constrained. While the structural evidence presented earlier suggests a sequential development for these structures they appear to be part of a more or less continuous progressive deformation and the structures most likely overlap in age to some degree. Much of the high temperature subsolidus deformation and accompanying F3 folding of the Tehachapi Intrusive Complex

probably occurred at temperatures greater than $\sim 500^{\circ}\text{C}$ which suggests that hornblende K-Ar or $^{40}\text{Ar}/^{39}\text{Ar}$ ages might provide a minimum age bound for this phase of the deformation since the approximate closure temperature for Ar in hornblende is $\sim 500^{\circ}\text{C}$ (Harrison, 1981). $^{40}\text{Ar}/^{39}\text{Ar}$ hornblende apparent ages of 91, 88, 86, and 84 Ma have been determined on amphibolite layers in metasedimentary rocks of the study area (Dixon et al., 1994; Dixon, 1995), and a sample of tonalite just west of the study area yields a K-Ar hornblende apparent age of 88 Ma (J. L. Morton, written communication, 1979, in Ross, 1989b). The two youngest $^{40}\text{Ar}/^{39}\text{Ar}$ hornblende apparent ages of 86 and 84 Ma are from rocks within the eastern Tehachapi shear zone and their younger age may reflect some disturbance related to the shear zone, possibly Ar loss. Thus, much of the F3 folding is inferred to have occurred between ~ 100 and $\sim 85\text{-}90$ Ma (Figure 24A).

The ~ 90 Ma Claraville granodiorite (Saleeby et al., 1987) appears to be folded by the F4 Tehachapi Valley orocline (Figure 14) which suggests the folding, at least in part, postdates intrusion of the granodiorite. If motion along the eastern Tehachapi shear zone is synchronous with and/or postdates formation of the F4 fold, as suggested earlier, then the time shear zone activity ceased would provide an approximate minimum age for formation of the F4 fold. As discussed below, the eastern Tehachapi shear zone may have been active between ~ 90 Ma and $\sim 80\text{-}70$ Ma, with the most likely time of activity at ~ 85 Ma (Figure 24B).

Paleomagnetic data suggesting $\sim 45^{\circ}$ of vertical axis clockwise rotation of the Bear Valley Springs tonalite pluton immediately northeast of Tehachapi Valley (Kanter and McWilliams, 1982) is compatible with the amount of apparent rotation of the F4 Tehachapi Valley orocline at that location. However, formation of the F4 Tehachapi orocline between ~ 90 and ~ 80 Ma as suggested above does not appear to be compatible with the suggestion of Kanter and McWilliams (1982) that magnetization of the Bear Valley Springs pluton was acquired during a transition from reversed to normal polarity in the earth's magnetic field at

~80 Ma since magnetization of the pluton at 80 Ma would imply it was rotated after that time. A potential unresolved problem with the inferred ~80 Ma age of magnetization for the pluton above stems from the fact that biotite from virtually the same location as the paleomagnetic samples yields a K-Ar apparent age of ~81 Ma (Evernden and Kistler, 1970). If the closure temperature for Ar in biotite is assumed to be ~300° C and if the magnetization of the tonalite is assumed to occur in a temperature range of ~400-500°C then it is difficult to see how the magnetization of the tonalite could have occurred at ~80 Ma.

The end of shear zone deformation appears to coincide with intrusion of the Brushy Ridge leucogranite, as described earlier, and the leucogranite appears to have a U-Pb zircon age of 70-80 Ma (J. B. Saleeby, personal communication, 1996). Most of the top to the S-SW mylonitic and shear band fabrics observed south of Tehachapi Valley are associated with retrograde greenschist facies metamorphic mineral assemblages. In the deformed rocks both hornblende and biotite are extensively replaced by chlorite and epidote and plagioclase is fractured and altered to fine grained sericite and epidote group minerals. Most of this greenschist facies phase of deformation in the shear zone probably occurred at temperatures below the ~500° C closure temperature for Ar in hornblende so much of the shear zone deformation probably is younger than the 84 and 86 Ma $^{40}\text{Ar}/^{39}\text{Ar}$ apparent ages on hornblende from amphibolites within the shear zone (Dixon et al., 1994; Dixon, 1995). The above observations suggest the most likely time of peak activity along the shear zone was from ~85 Ma to ~80 Ma (Figure 24C).

POSSIBLE REGIONAL CORRELATION OF DEFORMATIONS IN THE EASTERN TEHACHAPI GNEISS COMPLEX

Southernmost Sierra Nevada Region

High temperature gneiss terranes, possibly correlative with the eastern Tehachapi gneiss complex, are present in a number of locations in the southernmost Sierra Nevada region. Ross (1989b) noted that the suite of ortho- and paragneisses present in the

Tehachapi Mountain Park region of the study area is lithologically similar to the gneissic rocks present in the western Tehachapi Mountains and exposed along the Garlock fault east of Tehachapi Valley. L. T. Silver (personal communication) has suggested that the gneissic rocks in the study area may correlate with the Johannesburg gneiss in the Rand Mountains south of the Garlock fault, and Silver (1986) also correlated the gneisses along the Garlock fault with the Johannesburg gneiss. The Johannesburg gneiss was complexly deformed and metamorphosed at upper amphibolite facies after intrusion of ~100 Ma orthogneiss and prior to a superimposed greenschist facies mylonitic deformation which is older than ~79 Ma (Silver and Nourse, 1991; Nourse and Silver, 1986; Nourse, 1989). This early high temperature deformation of the Johannesburg gneiss is similar to the amphibolite facies metamorphism and deformation that accompanied the F3 folding in the eastern Tehachapi gneiss complex. The early high temperature deformation and accompanying F3 folding in the study area probably is part of a regional ~100 to ~94-90 Ma synplutonic and subsolidus deformation event recognized in the Tehachapi Mountains (Saleeby et al., 1987; Sams and Saleeby, 1988).

The continuation of the eastern Tehachapi shear zone south of the study area is uncertain because it disappears to the southeast beneath the Oak Creek Pass complex along the Blackburn Canyon fault (Figure 3). The shear zone might be sinistrally offset 45-60 km along the Neogene Garlock fault to the Rand Mountains region and/or it may merge at depth with the Rand fault (Figure 22), which regional geologic and seismic data suggest is present beneath the southernmost Sierra Nevada (Malin et al., 1995). The possible merging at depth of the eastern Tehachapi shear zone with the Rand fault is not meant to imply, however, that the most recent sense of motion along the two faults is the same.

The map-scale F3 folds found in the Tehachapi Intrusive Complex south of Tehachapi and Brite Valleys appear to be less well developed along strike to the north and the intensity of subsolidus fabric development in the plutonic rocks appears to decrease to

the north as well. Antiformal F3 folds in the Tehachapi Intrusive Complex generally are cored by gabbro and exposures of gabbro north of Brite Valley are rare. A swarm of mafic inclusions northwest of Tehachapi Valley and south of Highway 58 (Figure 14) mapped by Ross (1989b) may be exposed along the crest region of an open regional-scale F3 antiformal fold. A region of strongly deformed Bear Valley Springs tonalite surrounds the metasedimentary pendants around Brite Valley (Ross, 1989b). This area of deformed tonalite west of Tehachapi Valley is continuous with the area of intense deformation and F3 folding south of Tehachapi Valley in the study area, but it dies out well south of Highway 58 which suggests that the intensity of the deformation decreases to the north.

While the intensity of the regional high temperature subsolidus deformation fabrics in the plutonic rocks of the batholith appears to decrease to the north the locus of greenschist facies simple shear deformation of the eastern Tehachapi shear zone appears to continue to the north across Tehachapi Valley (Figure 14). North of Tehachapi Valley the eastern Tehachapi shear zone is coincident with a zone of "cataclastic" deformation mapped by Ross (1989b) that is continuous along strike to the north with the proto-Kern Canyon fault zone of Busby-Spera and Saleeby (1990). The shear sense of the proto-Kern Canyon fault zone is reverse-dextral (Busby-Spera and Saleeby, 1990; Gazis and Saleeby, 1991) and the shear sense of the eastern Tehachapi shear zone south of Tehachapi Valley is top to the S-SW. Mylonitic mineral lineations in both shear zones have similar northerly trends and shallow N plunges suggesting they may have formed in the same deformation. The presence of both dextral-sense strike-slip shear bands and top to the S-SW oblique thrust-sense shear bands with similar lineation directions in the ductilely deformed rocks in the vicinity of Highway 58 (Figure 15D) is consistent with the area being a transition zone between the proto-Kern Canyon fault zone to the north and the eastern Tehachapi shear zone south of Tehachapi Valley. The apparent continuity between the proto-Kern Canyon fault zone and the eastern Tehachapi shear zone, the similar orientation of mylonitic mineral

lineations in the two structures, and the similar ~85 Ma age of activity for both structures suggest the latter structure is an oblique ramp of the former structure.

Central Sierra Nevada and White-Inyo Mountains Region

While there is widespread evidence in the southernmost Sierra Nevada batholith for pervasive hot subsolidus contractional deformation from ~100 to 90 Ma which produced NW trending structures (Saleeby et al., 1987; Sams and Saleeby, 1988) studies in the Sierra Nevada to the north indicate that contractional deformation of this age is minor and generally limited to discrete shear zones in the batholith and scattered localities in the metasedimentary wallrocks. The NW trending steeply dipping Courtright/Wishon, Quartz Mountain, Kaiser Pear, and Bench Canyon solid-state ductile shear zones in granitic rocks of the central Sierra Nevada batholith (Figure 1) all have steeply dipping mineral lineations and exhibit some evidence for a minor phase of contractional deformation between ~90 and 100 Ma (Tobisch et al., 1995). An upper greenschist to amphibolite facies deformation episode in the Strawberry Mine pendant that formed folds and faults with average trends of N25°W occurred contemporaneously with intrusion of the granodiorite of Jackass Lakes (Nokleberg, 1981) which has a U-Pb zircon age of 98 Ma (Stern et al., 1981). Similar N-NW trending structures in a number of other central Sierra Nevada pendants may have formed coevally with the structures in the Strawberry Mine pendant (Nokleberg and Kistler, 1980).

N-NE directed displacement along the eastern Tehachapi shear zone at ~80-85 Ma appears to be coeval with a number of structural features in the central Sierra Nevada and White-Inyo Mountains that have been or might be interpreted as forming during N-NE directed contractional deformation. Folds and faults with N65-90°W trends deform 98 Ma granodiorite, but not Late Cretaceous plutons in the Strawberry Mine pendant (Nokleberg, 1981), and there is a N80°W trending mineral foliation in the ~90 Ma Tuolumne Intrusive Suite and adjacent older rocks (Bateman, 1992). Steeply dipping joints and fractures in

granitic rocks of the central Sierra Nevada formed when the maximum horizontal compressive stress was oriented at $\sim N60^{\circ}E$ and upon rotation of the maximum horizontal stress direction to $\sim N35^{\circ}E$ some of the joints evolved into sinistral-sense faults, and dilatant fractures reflecting the new stress orientation formed at the tips of some of the sinistral faults (Segall and Pollard, 1983). The timing of the above fracture and fault formation is constrained to be between ~ 90 Ma which is the U-Pb zircon age of the host granodiorite, and ~ 79 Ma which is the mean $^{40}Ar/^{39}Ar$ and K-Ar age of hydrothermal muscovite growing in two of the left-slip faults (Segall et al., 1990; Stern et al., 1981).

In the White-Inyo Mountains (Figure 1) a system of conjugate strike-slip faults which cut the margin of the Papoose Flat quartz monzonite pluton are interpreted to have formed during a deformation during which the horizontal maximum principle stress had a N-NE orientation (Sylvester, 1969; Sylvester et al., 1978). These faults are healed in the interior of the pluton by muscovite and K-feldspar mineralization which led Sylvester (1969) to suggest that the pluton was deformed while its interior was still hot, perhaps within 1-2 My of emplacement. K-Ar biotite apparent ages of ~ 78 Ma (Evernden and Kistler, 1970) and a U-Pb monazite apparent age of 83 Ma (Miller, 1996) on the Papoose Flat pluton suggest the N-NE directed contractional deformation of the pluton occurred between ~ 78 Ma and 83 Ma.

DISCUSSION AND INTERPRETATION OF THE MID- TO LATE CRETACEOUS AGE DEFORMATION

The transition from the F3 folding to the F4 folding and the possibly coeval eastern Tehachapi shear zone appears to mark a major change in the structural and metamorphic evolution of the gneiss complex. Prior to this transition NE directed shortening in the gneiss complex appears to have occurred through the development of NW trending and NE dipping high temperature subsolidus gneissic fabrics and SW vergent F3 folds. After this transition the direction of shortening appears to have changed to a more northerly trend, as

suggested by the N-NE trend of the shear zone slip lineations, and shortening in the gneiss complex appears to have occurred predominantly by non-coaxial simple shear along the shear zone. It is during this structural transition that many of the coarse grained leucocratic veins which frequently host large garnets appear to have formed. The large garnets with haloes of leucocratic minerals commonly are observed to grow across the amphibolite facies subsolidus gneissic foliation in the Tehachapi Intrusive Complex rocks, yet the garnets locally are crosscut by top to the S-SW greenschist facies shear bands of the eastern Tehachapi shear zone. This tectonic transition appears to mark the onset of extensive greenschist facies retrograde metamorphism in the study area.

The change in the study area from F3 folding to F4 folding and initiation of the eastern Tehachapi shear zone at ~90 to 85 Ma appears to coincide temporally with a change in the central Sierra Nevada from a tectonic regime characterized by alternating weak extension and contraction to a regime dominated by dextral transcurrent shear at ~90 Ma (Tobisch et al., 1995), and also with a change in the orientation of the maximum horizontal compressive stress from ~N60°E to ~N35°E between 90 Ma and 79 Ma (Segall and Pollard, 1983). Following this regional tectonic change the maximum horizontal compressive stress in both the central Sierra Nevada and the White-Inyo Mountains at ~80 Ma appears to be N-NE directed, as discussed in the previous section. The significance of the approximate correspondence of the N-NE slip direction of the eastern Tehachapi shear zone at ~85 to 80 Ma with the direction of the maximum horizontal principle stress direction is not clear. The slip direction of the shear zone may reflect the direction of relative plate motion at ~80 Ma.

Recent studies of magmatic arcs suggest that emplacement of the batholithic rocks commonly occurs in a neutral to weakly extensional deformational regime (Tobisch et al., 1995; Busby-Spera, 1988; Hamilton, 1988). In contrast, during emplacement of the Sierra Nevada batholith the deep crustal levels of the southernmost part of the batholith appear to

have experienced a protracted episode of contractional deformation from ~100 Ma to ~80 Ma. One possible interpretation of the top to the S-SW motion along the eastern Tehachapi shear zone at ~85 Ma to ~80 Ma is that it reflects the northeastward underthrusting of Rand schist beneath the batholith at a deeper structural level in response to inferred shallowing of the subducting oceanic plate in the early stages of the Laramide orogeny (Saleeby et al., 1993; Malin et al., 1995). Fluids from underthrust Rand schist may have migrated up the shear zone and contributed to the extensive retrograde metamorphism observed in the study area. The above model, however, does not take into account the earlier (~100 Ma to 90 Ma) phase of high temperature contractional deformation or the inferred regional change in the direction of contraction at ~90 to ~85 Ma.

It has been suggested that the shallowing of the subducting oceanic plate that is inferred to be responsible for the Laramide orogeny may have been caused by the subduction of an oceanic plateau or an aseismic ridge, possibly the conjugate counterpart to the Hess Rise located in the central Pacific (Livaccari et al., 1981; Henderson et al., 1984). The Permanente terrane in the Franciscan assemblage southeast of San Francisco Bay, a remnant of Cretaceous age oceanic crust overlain by cherts and limestones, may be part of the conjugate of the Hess Rise based on stratigraphic and paleontological similarities (Saleeby et al., 1994). Collision of an oceanic plateau with the mid- to Late Cretaceous paleosubduction zone at the current latitude of southern California might have produced major contractional deformation in the southernmost part of the Sierra Nevada batholith without significantly deforming the central and northern parts of the batholith, and if the colliding plateau was large enough the collision might affect relative plate motions. Collision of an oceanic ridge has also been suggested by Barth (1996) as a means of producing the mid- to Late Cretaceous regional uplift in southern California that is suggested by thermobarometric studies. The work of Cloos (1993) suggests that subduction of a basaltic oceanic plateau ≥ 30 km thick would likely result in collisional

orogenesis and might alter plate motion patterns. A number of studies (Dickinson and Snyder, 1978; Keith, 1978; George and Dokka, 1994) have inferred that shallowing of the subducting oceanic slab at the start of the Laramide orogeny began in Late Cretaceous time at ~80-75 Ma. The 100 Ma to 90 Ma phase of contractional deformation in the southernmost Sierra Nevada area, however, may record the early stages of collision of an oceanic plateau or aseismic ridge which may have initiated shallowing of the downgoing slab. The regional change in deformation style and contraction direction at ~90 to 85 Ma may reflect a minor change in relative plate motions caused by such a collision.

SIGNIFICANCE OF RETROGRADE METAMORPHISM DURING CONTRACTION

The contractional deformation history described above appears to have been ongoing during a period of waning temperature as evidenced by the retrograde metamorphic history of the gneiss complex. There are several mechanisms that may have lowered temperatures and contributed to the retrograde metamorphism of the gneiss complex during the contractional deformation. First, emplacement of relatively cold Rand schist beneath the southernmost Sierra Nevada batholith by underthrusting (Malin et al., 1995) coupled with ongoing low-angle Laramide subduction may have served to refrigerate the lower levels of the batholith crust (Peacock, 1988; Dumitru et al., 1991). Finite difference thermal modeling of the Sierra Nevada crust during shallow subduction by Dumitru (1990) indicates that rocks at a depth of ~20 km in crust that is floored by a cold subducting plate at a depth ranging from 35 to 50 km would have cooled to greenschist facies temperatures (~300°-500°C) in ~3 to 4 My after the beginning of shallow subduction. Initiation of the eastern Tehachapi shear zone may correspond to the beginning of low-angle subduction and prior to shear zone activity the study area most likely was at mid-crustal levels based on the geobarometric data of Dixon et al. (1994) and Dixon (1995) which indicates pressures of 5-8 kilobars. Thus, the greenschist facies retrograde

metamorphism accompanying the eastern Tehachapi shear zone deformation may result from cooling associated with shallow subduction.

A second way the temperature in the gneiss complex may have been lowered is by the migration of relatively cool fluids from underthrust Rand schist through the gneiss complex and along the eastern Tehachapi shear zone. Finally, cooling of the gneiss complex during the contractional deformation also may have been accomplished by heat conduction to the surface of the earth resulting from rapid erosional and/or tectonic (extensional) unroofing. Unroofing the southernmost part of the Sierra Nevada, however, requires the removal of 20 to 30 km of crust by ~50 Ma (Pickett and Saleeby, 1993) and a major problem is where all this eroded or tectonically removed material went. The most likely resting place for sediments eroded from the Sierra Nevada is the adjacent Great Valley forearc basin, but it only contains ~15 km of sedimentary deposits at its deepest point (Moxon, 1988). The alternative to erosional unroofing of the batholith is tectonic removal of the upper crust (Saleeby et al., 1993; Malin et al., 1995) and as will be discussed in the next section the Blackburn Canyon fault in the study area is a likely candidate for a major exhumational structure.

REGIONAL LOW-ANGLE DUCTILE-CATACLASTIC FAULTS IN THE SOUTHERN SIERRA NEVADA - POSSIBLE LATE CRETACEOUS-PALEOCENE AGE EXTENSIONAL STRUCTURES

The thesis of this section is that part of the southernmost Sierra Nevada batholith was unroofed by extensional faulting in Late Cretaceous time along a regional system of low-angle faults. First, the evidence that suggests that the southernmost part of the Sierra Nevada batholith has been exhumed to a greater depth than the batholith to the north is reviewed. Second, the Blackburn Canyon fault and a number of other previously identified low-angle faults which may have been involved in the inferred tectonic unroofing of the southeastern part of the batholith are discussed. Third, a number of possible correlations

between distinctive features in the footwall and hangingwall rocks of the fault system are suggested. Fourth, the possible relationship between the Witnet Formation and the extensional fault system is discussed. In the last parts of this section a number of other aspects of this inferred extensional faulting event are discussed including the age, direction, and rate of faulting along with the possible relationship of the faulting to the contractional deformation in the deeper levels of the batholith.

EXPOSURE DEPTH OF ROCKS IN THE SOUTHERN SIERRA NEVADA

Regional geobarometric and geologic studies in the Sierra Nevada (Ague and Brimhall, 1988a; Saleeby, 1990b) indicate that most of the batholithic and framework rocks currently exposed south of about the latitude of Lake Isabella were intruded and/or metamorphosed at a deeper level in the crust than were the rocks that are exposed north of Lake Isabella. Estimates of the crustal depth represented by the current level of exposure in the central Sierra Nevada batholith north of the Lake Isabella area range from about 5 to 15 km as summarized by Ross (1985) and Bateman (1992). North of Lake Isabella the crystallization pressures of plutons determined from amphibole barometry are mostly 3-4 kilobars along the western margin of the batholith and the calculated pressures systematically decrease eastward across the batholith to values of 1-2 kilobars along the east side of the batholith (Ague and Brimhall, 1988a). The low pressures indicated for the eastern side of the batholith are consistent with the presence in that area of upper crustal level calderas and vent phases of the batholith (Saleeby, 1990b).

In contrast, much of the batholith and its metasedimentary wallrocks south of the Lake Isabella area and north of the Garlock fault appears to have been emplaced and metamorphosed at pressures greater than about 3-4 kilobars (Ague and Brimhall, 1988a; Saleeby, 1990b; Pickett and Saleeby, 1993; Dixon et al., 1994; Dixon, 1995). The deepest exposures of rocks in the Sierra Nevada are found in the southernmost part of batholith in the western Tehachapi Mountains where the rocks were intruded and metamorphosed at

pressures of 7-9 kilobars based on geobarometric studies (Pickett and Saleeby, 1993; Sharry, 1981; Sharry, 1982). Based on a synthesis of the available geobarometric and geologic data Saleeby (1990b) suggested that the exposure depth of the Sierra Nevada batholith increases progressively in a southward direction from shallow crustal levels north of Lake Isabella to deep crustal levels in the western Tehachapi Mountains, thus defining an apparent northward tilted section of the batholithic crust. In contrast, the results of recent geobarometric studies in the southern Sierra Nevada suggest that the rocks from the Lake Isabella area southward to the Tehachapi Valley area were uplifted from ~5-8 kilobars to ~1-4 kilobars without appreciable tilting (Dixon et al., 1994; Dixon, 1995).

Examination of geobarometric data for the southern Sierra Nevada region (Ague and Brimhall, 1988a; Pickett and Saleeby, 1993; Dixon et al., 1994; Dixon, 1995) suggests that both of the above interpretations may be correct. There appears to be a longitudinal discontinuity or step in the observed pressures that approximately coincides with the N trending proto-Kern Canyon fault zone (Figure 25) which is a subvertical dextral-sense ductile shear zone (Busby-Spera and Saleeby, 1990). West of the proto-Kern Canyon fault zone the calculated pressures appear to increase southward more or less progressively from ~2-4 kilobars near Lake Isabella to ~5-8 kilobars in the vicinity of Tehachapi, while east of the fault zone peak pressures in the batholith appear to be moderately high, ~5-8 kilobars, throughout most of the region from Lake Isabella southward to the Tehachapi area. This apparent pattern in the regional geobarometric data is consistent with the observation of Saleeby and Busby-Spera (1986) and Busby-Spera and Saleeby (1990) that there is an abrupt eastward increase in depth of exposure across the proto-Kern Canyon fault zone in the Lake Isabella area. They noted that peperitic textures in the ~100 Ma Erskine Canyon hypabyssal volcanic rocks west of the fault zone indicated near surface emplacement while contact metamorphism in the aureole of a ~100 Ma pluton on the east side of the fault zone occurred at pressures of ~3 kilobars based on the work of Elan (1985).

The distribution of aluminosilicate minerals in the wallrocks of the southern Sierra Nevada batholith is generally consistent with the regional geobarometric data in the sense that andalusite appears to be restricted primarily to the areas of lowest pressure. If the upper stability limit of andalusite is taken to be ~4 kilobars (Holdaway, 1971) then the presence of andalusite in the wallrocks implies metamorphic pressures of ~4 kilobars or less. East of the proto-Kern Canyon fault zone andalusite is found only in the Lake Isabella region where it coexists with sillimanite (Ross, 1990), and west of that fault zone andalusite is found only as far south as the latitude of Walker Basin where it mostly occurs in the Pampa schist exposed directly west of Walker Basin (Dibblee and Chesterman, 1953; Ross, 1989b). Everywhere else in the wallrocks of the southern Sierra Nevada batholith sillimanite is the only aluminosilicate mineral found except for one locality in the western Tehachapi Mountains where white mica appears to have pseudomorphed after kyanite (Pickett and Saleeby, 1993).

From the above review of geobarometric data it is apparent that most of the southern Sierra Nevada batholith south of the Lake Isabella region has been exhumed to a greater degree than has the batholith to the north and there is mounting evidence suggesting that much of this unroofing took place in Late Cretaceous time. Pickett and Saleeby (1993) infer that ~15 km of unroofing took place in the western Tehachapi Mountains between ~100 Ma and ~87 Ma, and fission track ages of ~70 Ma on apatite and ~80 Ma on zircon from granitic basement in the western Tehachapi Mountains (Naeser et al., 1990) suggest that the rocks at the surface today were within several km of the surface by the end of the Cretaceous assuming a geothermal gradient of ~30°C/km and a closure temperature of ~100°C for fission tracks in apatite. In addition, Dixon (1995) suggests that the entire region of the Cretaceous batholith between Lake Isabella and Tehachapi may have been uplifted from ~5-8 kilobars to ~1-4 kilobars before the rocks cooled below about ~500°C. If the 85-92 Ma ^{40}Ar - ^{39}Ar apparent ages of hornblende in the rocks of the Lake Isabella

and Tehachapi areas represent the time the rocks cooled through $\sim 500^{\circ}\text{C}$, which is the approximate closure temperature for Ar in hornblende (Harrison, 1981), then that would suggest that the region had begun to decompress between 85 and 92 Ma (Dixon, 1995).

This apparent rapid Late Cretaceous unroofing in the southern Sierra Nevada could have been accomplished by erosional and/or tectonic removal of the upper crust. As discussed in the following sections the Blackburn Canyon fault along with several other previously recognized low-angle faults in the southern Sierra Nevada region are suggested to be part of a regional system of upper crustal extensional faults along which a large portion of the eastern side of the southern part of the Sierra Nevada batholith was unroofed.

EXTENSIONAL ORIGIN FOR THE BLACKBURN CANYON FAULT

As described earlier the Blackburn Canyon fault is a N to NE trending shallowly SE dipping fault in the eastern part of the study area that juxtaposes cataclastically deformed granitic rocks of the Oak Creek Pass complex in the hangingwall against rock of the eastern Tehachapi gneiss complex in the footwall (Figure 3). Kinematic indicators in this fault zone indicate that the latest direction of shearing along the fault was top to the S or SE.

The Blackburn Canyon fault exhibits a number of characteristics that suggest it is an extensional fault. First, the Blackburn Canyon fault intersects the surface of the earth when traced out in a direction opposite to the direction of hangingwall transport which is a characteristic of extensional faults according to the criteria of Wheeler and Butler (1994). Second, the fault places dominantly cataclastically deformed granitic rocks that locally have been deformed at greenschist facies and lower temperatures structurally above severely ductilely deformed gneisses that have been metamorphosed at upper amphibolite facies and subsequently retrograded to greenschist facies. It is reasonable to interpret a fault that juxtaposes low-grade rocks above high-grade rocks as an extensional fault although this should be considered as evidence and not as proof as noted by Hodges and Walker (1992).

Third, there is some suggestion that the granitic and metavolcanic rocks in the Oak Creek Pass complex may have been emplaced and deformed at a higher level in the crust than the rocks in the eastern Tehachapi gneiss complex. Some of the Oaks silicic metavolcanic rocks in the lower plate of the Oak Creek Pass complex have a black colored aphanitic groundmass with a glassy appearance which appears to be composed mostly of microcrystalline quartz grains less than 0.01 millimeters in diameter. The extremely fine grain size of the matrix in these rocks suggests that they cooled relatively rapidly after emplacement and have not been subjected to extensive metamorphic recrystallization since then. Rapid cooling of these metavolcanic rocks most likely would occur at a relatively shallow level in the batholithic crust. Elsewhere in the Sierra Nevada batholith pendants of silicic metavolcanic rocks commonly are found in regions where geobarometric data indicate that 1-3 kilobar levels of the batholith are exposed (Saleeby and Busby-Spera, 1986; Saleeby, 1990b). A somewhat higher crystallization pressure of 5.1 kilobars is indicated for the Bootleg Canyon granodiorite (sample 90-TH-49) in the south middle plate of the Oak Creek Pass complex based on hornblende barometry (Dixon, 1995). In contrast, geobarometric data on the rocks of the eastern Tehachapi gneiss complex indicate they crystallized and/or were metamorphosed in the mid- to lower crust at pressures of 5-8 kilobars (Dixon, 1995).

In summary, the orientation and transport direction of the Blackburn Canyon fault, the juxtaposition of low to moderate-grade cataclastically deformed rocks above high-grade ductilely deformed rocks by the fault, and the evidence suggesting that the hangingwall rocks were deformed at a generally shallower crustal level than the footwall rocks all suggest that the Blackburn Canyon Fault is an extensional fault.

AGE OF THE BLACKBURN CANYON FAULT

The youngest rock type crosscut by the Blackburn Canyon fault is either the gabbro and tonalite of the Tehachapi Intrusive Complex or the Bootleg Canyon granodiorite in the

Oak Creek Pass complex. Thus, the maximum age of the Blackburn Canyon fault is no older than the inferred ~100 Ma age of the Tehachapi Intrusive Complex, and the maximum age of the fault may be as young as 90-87 Ma if the age of the Bootleg Canyon granodiorite is comparable to the 90 Ma U-Pb age of the Claraville granodiorite north of Tehachapi Valley (Saleeby et al., 1987) or to the 87 Ma U-Pb age of the Atolia quartz monzonite south of the Garlock fault in the Rand Mountains (Silver and Nourse, 1991). Some, or all, of the activity along the Blackburn Canyon fault might be younger than the depositional age of the Witnet Formation. The Witnet Formation is exposed close to the Blackburn Canyon fault at the surface, but it is not known if the fault crosscuts the Witnet Formation at depth.

The minimum age of the Blackburn Canyon fault is not directly constrained by crosscutting intrusions, but there are a number of indirect lines of evidence for its minimum age. Most activity along the fault is almost certainly older than the dacite and felsite dikes in the study area which are probably Miocene in age (Dibblee and Louke, 1970). While none of the volcanic dikes that were examined in detail could be clearly traced completely across the fault, several of the dikes intrude the granodiorite breccia within a few meters of the fault and those dikes are undeformed. The gneiss complex and the Oak Creek Pass complex in the southern part of the study area both host large E-W trending groups of felsite dikes that lie along strike from each other (Figure 4). These two groups of dikes may be part of a single swarm that is not appreciably offset across the Blackburn Canyon fault. Some structural evidence suggests that the Blackburn Canyon fault is older than the Mendiburu Canyon fault. At one location in the gneiss complex mylonitic fabrics of the Blackburn Canyon fault are crosscut and offset by brittle shears inferred to be related to the Mendiburu Canyon fault. As was discussed earlier the Mendiburu Canyon fault most likely was active prior to Early Miocene time which suggests that the Blackburn Canyon fault is older than the Early Miocene as well.

The Blackburn Canyon fault also may be older than the age of the latest phase of top to the S-SW motion along the eastern Tehachapi shear zone. As was described earlier the Quail Canyon fault zone and/or the South Ridge fault zone in the hangingwall of the Blackburn Canyon fault may be the along-strike continuation of the Mountain Park fault in the footwall of the Blackburn Canyon fault, and there is some evidence that the Quail Canyon fault underwent a phase of top to the S-SW shearing. If the top to the S-SW shearing along the eastern Tehachapi shear zone ended at about 80 Ma, as discussed earlier, then the Oak Creek Pass complex may have been in place structurally above the gneiss complex by ~80 Ma as well. In summary, the Blackburn Canyon fault appears to have been active between ~100 Ma and Early Miocene time, and there is the possibility that much of the displacement along the fault may have occurred between 87-90 Ma and ~80 Ma.

REGIONAL CORRELATION OF THE BLACKBURN CANYON FAULT

The low-angle Blackburn Canyon detachment fault represents a significant petrologic, metamorphic, isotopic, and structural break in the southern Sierra Nevada. Rocks in the footwall are upper amphibolite grade ductilely deformed paragneiss and mostly gabbroic to tonalitic orthogneiss while the rocks in the hangingwall are greenschist and lower grade dominantly cataclastically deformed rocks of mostly granodiorite composition. The Blackburn Canyon fault also corresponds locally to the 0.706 initial Sr isopleth of Kistler and Ross (1990). Consideration of the regional geology of the southern Sierra Nevada area (Figure 25) suggests that the Blackburn Canyon fault may correlate with a number of nearby previously recognized low-angle faults.

Geologic studies of the Rand Mountains region south of the Garlock fault have documented a series of low-angle faults separating several thin plates of crystalline rock (Silver et al., 1984; Silver and Nourse, 1986; Nourse and Silver, 1986; Nourse, 1989). The structurally lowest fault of this Rand fault complex ("thrust" I of Silver and Nourse (1986) and Fault I of Nourse (1989)) is the Rand thrust which separates mafic schist and

Figure 25

Geologic map of the southern Sierra Nevada region showing rocks that are inferred to be out of place relative to regional geologic trends. Most of these allochthonous rocks appear to be underlain by a complex system of low-angle faults (Silver, 1982; Silver, 1983; Silver et al., 1984; Silver, 1986; Silver and Nourse, 1986; Silver and Nourse, 1991; Silver, 1993). The Blackburn Canyon fault of this study appears to be part of this family of faults and the contrast in lithologies and metamorphic grade across it suggests it correlates most closely with fault II of the fault complexes in the Rand Mountains and the southeastern Sierra Nevada (Silver and Nourse, 1986; Silver, 1986). The Blackburn Canyon fault also may correlate with the Jawbone Canyon fault zone of Samsel (1962) and Dibblee (1967). In the figure the low-angle faults are shown by heavy lines with square teeth in the hangingwall. Data from this study indicate an episode of S to SE directed transport for rocks in the upper plate of the Blackburn Canyon detachment fault which suggests that the source region for the hangingwall rocks may be in the Sierra Nevada batholith to the north. As discussed in the text, certain geologic features of the inferred allochthonous hangingwall rocks, labeled with bold primed letters in the figure, may correlate with similar features exposed in the southern Sierra Nevada batholith that are labeled with the same bold letters. Cretaceous plutonic rocks with $Sr_i \geq 0.706$, from Kistler and Ross (1990), are shown by NE trending hatching. The granitic rocks above fault II in the Rand Mountains are assumed to have $Sr_i \geq 0.706$ based on their correlation with similar rocks in the southeastern Sierra Nevada (Silver, 1986). The locations of Cretaceous plutonic rocks with magnetic susceptibilities $\leq 200 \times 10^{-5}$ siu are from Ross (1989a) and indicated by NW trending hatching. The discontinuous wavy lines in the figure indicate the location of ductile shear zones. Sources for the geology in this figure are the same as for figure 2 with the additions noted below. Geology north of latitude $35^\circ 30'$ N from Ross (1990). Geology of the Rand Mountains and location of fault II of the Rand

fault complex from Silver and Nourse (1986) and Nourse (1989). Location of fault II of the southern Sierra detachment fault system from Silver (1986) and Silver (personal communication, 1991). Abbreviations are ATP, aqueduct tunnel pendant; BC, Back Canyon pendant; BCP, Bean Canyon pendant; BVP, Brite Valley pendants; CCP, Cottonwood Creek pendant; CV, Cummings Valley; IP, Isabella pendant; KCP, Kern Canyon pendant; KV, Kelso Valley; M, Monolith pendant; QRP, Quinn Ranch pendant; SFV, South Fork Valley; TCP, Tylerhorse Canyon pendant; TV, Tehachapi Valley; WB, Walker Basin.

metagraywacke in the footwall from multiply deformed amphibolite grade ortho- and paragneiss of the Johannesburg gneiss in the hangingwall (Ehlig, 1968; Silver et al., 1984; Postlethwaite and Jacobson, 1987). Structurally above the Rand thrust fault is Fault II of the Rand fault complex which is a low-angle cataclastic and locally mylonitic fault which juxtaposes high-grade Johannesburg gneiss in its footwall against hangingwall rocks composed of cataclastic hornblende biotite granodiorite deformed under greenschist facies (Nourse, 1989; Nourse and Silver, 1986; Silver and Nourse, 1986).

Kinematic analysis of structures and fabrics associated with Fault II in the Rand Mountains indicate the upper plate granodiorite was transported in a south to southeastward direction (Nourse, 1989; Nourse and Silver, 1986; Postlethwaite and Jacobson, 1987). Nourse (1989) infers that the granodiorite, the Johannesburg gneiss, and the Rand schist were juxtaposed along Faults II and I during the same S vergent deformation event. Based on this interpretation the age of Fault II in the Rand fault complex is constrained between the ~87 Ma age of the upper plate granodiorite and the ~79 Ma age of an undeformed post-tectonic granodiorite stock which intrudes the Rand schist and contains xenoliths of Johannesburg gneiss (Silver and Nourse, 1991; Nourse, 1989).

The Blackburn Canyon fault is inferred to correlate across the Garlock fault with Fault II of the Rand fault complex for several reasons. First, both faults place largely brittlely deformed greenschist facies granodioritic rocks above high-grade paragneiss and orthogneiss. Second, the lower plate orthogneiss in the eastern Tehachapi Mountains and in the Rand Mountains both appear to have components with ages of ~100 Ma (Saleeby et al., 1987; Silver and Nourse, 1991). Third, the S to SE direction of hangingwall transport of the Blackburn Canyon fault is similar to the southward directed upper plate transport along Fault II in the Rand Mountains. Finally, both the Blackburn Canyon fault and Fault II in the Rand Mountains may have been active at the same time.

Silver (1986) correlated the system of low-angle faults in the Rand Mountains with a similar sequence of low-angle faults exposed along the Garlock fault in the southeastern Sierra Nevada. As in the Rand Mountains Fault II of the southern Sierra Nevada detachment fault system (Figure 2) juxtaposes cataclastic granodiorite structurally above high-grade Cretaceous age gneiss that is lithologically similar to the Johannesburg gneiss (Silver, 1986; Nourse, 1989). The Blackburn Canyon fault is inferred to correlate with Fault II of the detachment fault system in the southeastern Sierra Nevada based on lithologic similarities between the upper and lower plate rocks in both areas.

The Blackburn Canyon fault also may correlate with a major fault zone exposed in lower Jawbone Canyon in the southeastern Sierra Nevada (Samsel, 1962; Dibblee, 1967) which is referred to as the Jawbone Canyon fault zone (Figures 2 and 25). Samsel (1962) first mapped the fault zone as a series of N-NE trending E dipping high-angle faults in lower Jawbone Canyon while in a later study Dibblee (1967) shows the fault zone as a relatively wide interval of crushed granodiorite hosting numerous E dipping faults one of which has a dip of 30° to the E. Silver (1986) suggested that this zone of faulting in the Jawbone Canyon area may be part of the system of low-angle faults exposed adjacent to the Garlock fault discussed above. The Jawbone Canyon fault zone juxtaposes hangingwall granitic and granodioritic rocks that are locally overlain by Miocene (?) age sedimentary and volcanic rocks above footwall rocks composed of mafic hornblende diorite (locally garnet bearing) and tonalite (Dibblee, 1967; Ross, 1989b). Reconnaissance examination of the fault zone in Jawbone Canyon indicates that it is similar to the Blackburn Canyon fault. The hangingwall granitic rocks in Jawbone Canyon are extensively cataclasized and hydrothermally altered and the footwall is composed of gneissic gabbro and tonalite some of which has a subhorizontal foliation.

The location of the Jawbone Canyon fault zone westward of its intersection with Jawbone Canyon is unknown, but similarities between the geology in the Jawbone Canyon

area and the geology in the vicinity of the Blackburn Canyon fault suggest that the two faults may be continuous and buried beneath the Kinnick, Bopesta, and Cache Peak Formations (Figure 2). In upper Jawbone Canyon the fault may correspond to the contact between hornblende diorite and granodiorite shown by Dibblee (1967) and Ross (1989b). Like the location of the Witnet Formation in the upper plate of the Blackburn Canyon fault the Witnet Formation exposed in upper Jawbone Canyon (Dibblee, 1967) may be located close to the possible western continuation of the Jawbone Canyon fault and it may be deposited on top of the hangingwall of the fault. As will be discussed later the deposition of the Witnet Formation may have been in a structural basin formed by the Blackburn Canyon and Jawbone Canyon faults.

The Pastoria fault in the western Tehachapi and San Emigdio Mountains (Figures 2 and 25) is similar to the Blackburn Canyon fault in that it is a low-angle fault which juxtaposes cataclastically deformed granitic and granodioritic rocks structurally above high-grade predominantly dioritic to tonalitic orthogneiss (Crowell, 1952; Ross, 1989b; Davis and Lagoe, 1988). Also like the Blackburn Canyon fault the Pastoria fault represents an isotopic discontinuity and it corresponds to the initial Sr 0.706 isopleth (Kistler and Ross, 1990). Sharry (1981, 1982) suggested that the Pastoria fault may represent an older splay and westward continuation of the south branch of the Garlock fault that has only recently been reactivated as a thrust fault because both faults appear to be a boundary between exposures of deep crust to the north and shallow crust to the south. South of the south branch of the Garlock fault metasedimentary roof pendants in granitic rocks were metamorphosed at pressures of 2.5 kilobars (Haase and Rutherford, 1975; Sharry, 1981) while north of the south branch of the Garlock fault Rand schist and mafic orthogneiss both were metamorphosed at pressures of ~8 kilobars (Pickett and Saleeby, 1993; Sharry, 1982). In contrast to Sharry, Silver (1983, 1986) correlated the Pastoria fault with pre-

Garlock fault age low-angle faults in the Rand Mountains and the southeastern Sierra Nevada.

The Pastoria fault dips to the south at about 20° towards the Garlock fault (Crowell, 1952) which suggests that the Pastoria fault might be truncated at depth and sinistrally offset along the Neogene Garlock fault at depth. The total slip on the west end of the Garlock fault is not well constrained, but similarities between the granodiorite of Lebec north of the fault and the granodiorite of Gato-Montes south of the fault led Ross (1989b) to suggest that the two units may correlate. This would imply that the granodiorites have been sinistrally offset from one another along the Garlock fault by about 45-50 km. If the Pastoria fault also has been sinistrally offset 45-50 km along the Garlock fault then that would suggest that the granitic and metamorphic rocks south of the Garlock fault at the west end of the Mojave Desert in the southern Tehachapi Mountains might be underlain at depth by a low-angle fault. There is some evidence that suggests such a low-angle fault exists beneath the southern Tehachapi Mountains as discussed next.

Low-angle faults have not been identified at the surface in the southern Tehachapi Mountains, but in a study of the geology in and around two tunnels of the California Aqueduct in the western Tehachapi Mountains Peters (1972) suggested that a low-angle fault underlies the Tehachapi Mountains south of the Garlock fault. The location of the aqueduct tunnels is shown in Figure 25 and Figure 26 is a cross section of the geology along the tunnel lines modified from Peters (1972). Peters (1972) documents a moderate to shallow SE dipping fault zone in granite that is exposed in two test adits near the north portal of the C. V. Porter aqueduct tunnel and he interprets this fault zone as a thrust that flattens with depth to the south because the upper contact of the zone dips more shallowly to the south in the structurally lower of the two adits. In addition, based on study of drill logs from along the C. V. Porter tunnel line Peters (1972) notes that fresh granite encountered along the tunnel appears to be underlain by hydrothermally altered granite that

Figure 26.

Geologic cross section of the western Tehachapi Mountains along the line of the California aqueduct tunnels (figure modified from Peters (1972)). Location of the cross section is shown in Figure 25 and the lithologic patterns of the cross section are the same as in Figure 25. The crosshatch pattern indicates granite that is weathered or hydrothermally altered. The short near-vertical heavy black lines in the cross section are scattered steeply dipping fault zones. Peters (1972) suggested that a low-angle fault may underlie the Tehachapi Mountains south of the south branch of the Garlock fault based on the geology exposed in the C. V. Porter aqueduct tunnel and in adjacent test adits, and data from drill logs along the tunnel line. The hypothetical southern Tehachapi detachment fault shown in the figure is an inference of the current study that is based on the observations of Peters (1972) in conjunction with regional geologic relations. See text for discussion.

CROSS SECTION THROUGH THE WESTERN TEHACHAPI MOUNTAINS ALONG THE CALIFORNIA AQUEDUCT TUNNELS

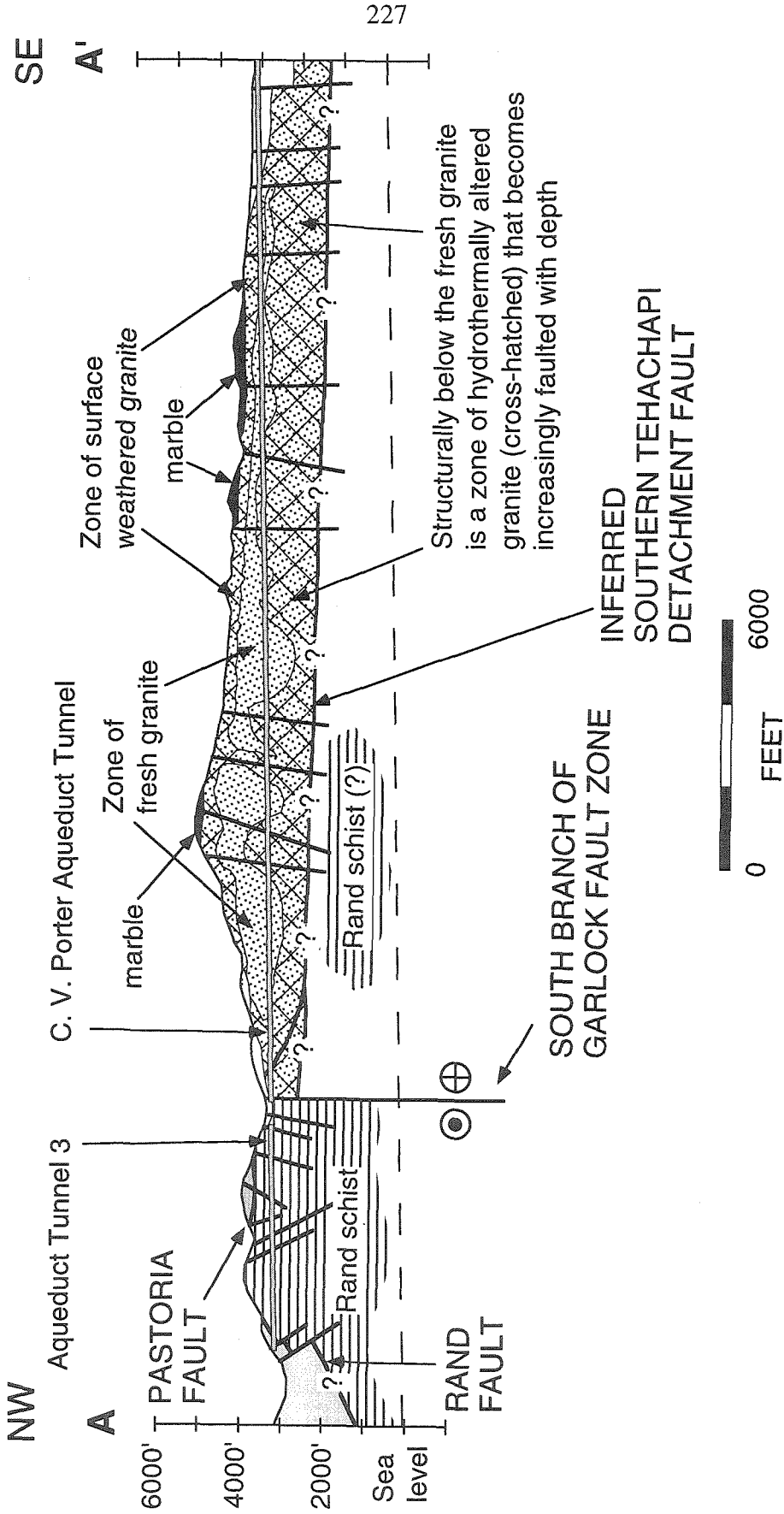


Figure modified from Peters (1972)

becomes increasingly altered and faulted with depth. Peters (1972) suggests that the alteration could be the result of hot fluids ascending along faults and shear surfaces developed after intrusion of the granite.

The increasing degree of fracturing and alteration with depth suggests that a post-batholith low-angle detachment fault may underlie the southern Tehachapi Mountains south of the south branch of the Garlock fault (Figure 26). As noted above, this inferred low-angle fault may be the sinistrally offset continuation of the Pastoria fault. While the Pastoria fault may have been a thrust fault during part of its motion history, as will be discussed later, the contrast in level of crustal exposure across the Pastoria fault with low pressure rocks structurally above high pressure rocks (Sharry, 1981; Sharry, 1982) is consistent with an interpretation of the Pastoria fault as an extensional fault similar to the Blackburn Canyon fault.

POSSIBLE SOURCE LOCATION FOR ALLOCHTHONOUS ROCKS IN THE SOUTHERN SIERRA NEVADA REGION

The crystalline rocks in the southern Sierra Nevada region that are underlain by many of the low-angle faults discussed above appear to be out of place relative to regional geologic trends (Silver, 1982; Silver, 1983). The granitic and metavolcanic rocks of the Oak Creek Pass complex in the hangingwall of the Blackburn Canyon fault are inferred to be part of this regional terrane of allochthonous rocks. Rocks of the southern Sierra Nevada batholith and its metasedimentary framework that are in the hangingwall of the low-angle faults discussed in the previous section and which are inferred to be out of place are shown in Figure 25. The possible location of the source region for these inferred allochthonous rocks is the subject of the following discussion.

Based on the apparent offset of petrologic, age, isotopic, and chemical zonation patterns in the batholithic rocks Silver (1982, 1983) inferred that the upper plate rocks were emplaced by W vergent overthrusting which suggests that the source region for the

allochthonous rocks may lie to the east. In contrast, the kinematic and structural data from this study indicate an episode of S to SE directed transport for rocks in the upper plate of the Blackburn Canyon detachment fault which suggests that the source region for the hangingwall rocks may be in the Sierra Nevada batholith to the north. The transport direction of upper plate rocks along Fault II in the Rand Mountains also appears to be to the south or southeast (Nourse, 1989; Nourse and Silver, 1986). While a source to the east for the allochthonous rocks cannot be ruled out at this time there is additional geologic evidence which appears to support a source location to the north as discussed below.

The source area for the rocks in the upper plate of the Pastoria fault and the inferred allochthonous rocks in the southern Tehachapi Mountains south of the Garlock fault is suggested to be the region in the southern Sierra Nevada east of the proto-Kern Canyon fault zone, west of Kelso Valley, south of the Isabella pendant, and north of Tehachapi Valley. Most of the Cretaceous plutonic rocks in those areas are characterized by $Sr_i \geq 0.706$ (Kistler and Ross, 1990) and magnetic susceptibilities $\leq 200 \times 10^{-5}$ siu (International standard units) (Ross, 1989a) as indicated by the cross hatch pattern in Figure 25. The inferred allochthonous rocks in the southeastern Sierra Nevada and Rand Mountains are suggested to have originated from the area in the southern Sierra Nevada northeast of Kelso Valley, southwest of Walker Pass, and mostly southeast of South Fork Valley. Both the footwall and hangingwall Cretaceous plutonic rocks in those areas have $Sr_i \geq 0.706$ (Kistler and Ross, 1990) and most of the plutonic rocks in those areas also have magnetic susceptibilities $> 200 \times 10^{-5}$ siu (Ross, 1989a).

There also are a number of specific geologic features in the allochthonous upper plate rocks, labeled with bold primed letters in Figure 25, that may correlate with similar features exposed in the autochthonous rocks of the southern Sierra Nevada batholith, which are labeled with the same bold letters without the prime mark. A'-A: the metasedimentary rocks in the Aqueduct Tunnel and Quinn Ranch pendants may correlate

with the metasedimentary rocks of the *Monolith and Back Canyon* pendants. All four of these pendants are characterized by thick layers of marble and they also are distinctive compared to other pendants in the southern Sierra Nevada batholith because most of their contacts are subhorizontal to shallow dipping as is much of the compositional layering of the rocks in the pendants (Wiese, 1950; Crowell, 1952; Troxel and Morton, 1962; Kim, 1972; Ross, 1989b). In addition, these four pendants are intruded by relatively large bodies of leucocratic (Color Index ≤ 5) biotite (\pm garnet, \pm muscovite) granite (Ross, 1989b; Kim, 1972), and the granite of *Tejon Lookout* at A' may correlate with the granite of *Tehachapi Airport* at A. The rare-earth-element abundances of the *Tejon Lookout* and *Tehachapi Airport* granites are similar (see Figure 75 in Ross, 1989b).

B'-B: the steeply dipping *Cottonwood Creek*, *Tylerhorse Canyon*, and *Bean Canyon* metasedimentary pendants along the south edge of the southern Tehachapi Mountains may have formerly occupied the gap between the *Isabella* pendant and the pendant south of *Kelso Valley* in the southern Sierra Nevada. The metasedimentary rocks in the *Bean Canyon* and *Tylerhorse Canyon* pendants lithologically resemble Late Triassic rocks in the *Mineral King* pendant (Dunne et al., 1975; Rindosh, 1977) and more recent work indicates that the metasedimentary rocks in both the *Mineral King* and *Isabella* pendants are part of the Triassic-Jurassic age *Kings* sequence (Saleeby and Busby, 1993). Ross (1989b) considered all of the rocks in the different pendants of the southern Tehachapi mountains to be part of the *Bean Canyon Formation* although Rindosh (1977), in a more detailed study, noted that most of the sequence of rocks in the *Tylerhorse Canyon* pendant did not correlate with the type locality of the *Bean Canyon Formation* in the *Bean Canyon* pendant (Dibblee, 1963).

The *Bean Canyon Formation* in the *Tylerhorse Canyon* and *Bean Canyon* pendants includes a prominent marble layer that ranges up to ~300 meters in thickness, thick intervals of psammitic and pelitic schist, calc-silicate hornfels, and various metamorphosed

volcanic rocks including basalt, andesite, and dacite (Simpson, 1934; Dibblee, 1963; Dunne et al., 1975; Rindosh, 1977; Ross, 1989b). The age of the Bean Canyon Formation is poorly constrained. The metasedimentary rocks are intruded by plutons of presumed Cretaceous (?) age (Dunne et al., 1975), and Rb/Sr ages on dacitic metavolcanic rocks in the Bean Canyon pendant average ~150 Ma (R. A. Fleck, written communication, 1976, in Ross (1989b)). Poorly preserved macrofossils in the Bean Canyon Formation are not age diagnostic (Dunne et al., 1975). Map-scale fold axes or fold closures have not been observed in the Tylerhorse Canyon and Bean Canyon pendants and fault repetition of section cannot be ruled out (Rindosh, 1977) so there is no clear stratigraphic or structural up direction in the Bean Canyon Formation which makes correlation difficult. There do, however, appear to be a number of lithologic similarities between the Bean Canyon Formation and the Triassic-Jurassic age Kings sequence rocks in the Isabella pendant.

The Bean Canyon Formation and the Kings Sequence rocks in the Isabella pendant both are characterized by abundant marble with some layers ranging up to ~300 meters in thickness (Rindosh, 1977; Saleeby and Busby, 1993). Metamorphosed basalt layers up to ~100 meters thick are present in the Bean Canyon pendant (Dibblee, 1963) and a layer of amphibolitic mafic volcanic rocks several hundred meters thick is present in the Kings sequence rocks north of Lake Isabella (Saleeby and Busby, 1993). Both the Bean Canyon Formation and the Kings sequence rocks in the Kern Canyon pendant also host a distinctive marble horizon containing lenses and boudins of amphibolite that is adjacent to a section of white and gray quartz-rich gneiss (Rindosh, 1977; Saleeby and Busby-Spera, 1986). Finally, Late Triassic to Early Jurassic Weyla fossils that have been found in the Isabella pendant are from a calcareous quartzite unit immediately adjacent to a thick Late Triassic (?) marble, and the localities of the poorly preserved fossils in the Tylerhorse Canyon pendant are in a calc-silicate hornfels, quartzite, and marble bearing unit that is adjacent to a 300 meter thick marble layer (Rindosh, 1977; Saleeby and Busby, 1993).

C'-C: between the Cottonwood Creek and Tylerhorse Canyon pendants at C' there are small bodies of mafic granodiorite and hornblende diorite that are engulfed in the granodiorite of Gato Montes (Dibblee, 1963; Ross, 1989b). A localized exposure of dark granodiorite, gabbro, and mafic-inclusion rich granodiorite within the Claraville granodiorite at C (Ross, 1989b) in the autochthonous rocks of the Sierra Nevada is suggested to correlate with the mafic rocks in the upper plate at C'.

D'-D: the small body of felsic coarse grained biotite granite of Tejon Lookout located near the east end of the basement rock exposures south of the Garlock fault and which intrudes metasedimentary rocks of the Bean Canyon Formation (Ross, 1989b) at D' may correlate with the felsic coarse grained biotite granite of Bob Rabbit Canyon (Ross, 1990) which is located adjacent to the Isabella pendant southeast of Lake Isabella at D.

E'-E: the Oaks silicic metavolcanic rocks at E' in the Oak Creek Pass complex in the upper plate of the Blackburn Canyon fault may correlate with the ~100 Ma Erskine Canyon and related rhyolitic volcanic rocks exposed west of the proto-Kern Canyon fault in the Lake Isabella area at E (Busby-Spera and Saleeby, 1990; Saleeby and Busby-Spera, 1986). The lack of exposures of the mid-Cretaceous Erskine Canyon series silicic volcanic rocks east of the proto-Kern Canyon fault zone in the Lake Isabella area may be because they were removed by upper crustal detachment faulting. Samples of the ~100 Ma metavolcanic rocks from the Piute Lookout area south of Lake Isabella in sample collections at Caltech resemble the Oaks metavolcanic rocks from the study area in the eastern Tehachapi Mountains although the age of the Oaks metavolcanic rocks is not known.

F'-F: the small plug of the granite of Lone Tree Canyon which intrudes the granodiorite of Claraville (Ross, 1989b) in the allochthonous upper plate rocks at F' may be the offset equivalent of the granite of Onyx (Ross, 1990) located at F. Ross (1989b) describes the granite of Lone Tree Canyon near the Garlock fault as a fine grained aplitic-textured biotite granite and notes that it is very similar in appearance and composition to the

small body of Onyx granite which is located about 50 km to the north, east of Lake Isabella in South Fork valley.

G'-G: within the granitic rocks in the southern Rand Mountains at G' there is a small exposure of gneissic rocks as well as several larger exposures of hornblende diorite (Dibblee, 1967). The hornblende diorite and the gneiss in the Rand Mountains may correlate with the Summit gabbro and the locally strongly foliated quartz diorite of Walker Pass, respectively, in the vicinity of Walker Pass at location G (Miller and Webb, 1940; Ross, 1990). The Summit gabbro and Walker Pass quartz diorite are probable Jurassic to Triassic age plutonic rocks in the dominantly Cretaceous age southern Sierra Nevada batholith (Ross, 1990). The Jurassic and Triassic rocks also may be present along strike from the exposures in the Sierra Nevada beneath the alluvium southeast of the Sierran frontal fault so the potential source area for the possibly correlative rocks in the Rand Mountains is relatively large.

The evidence reviewed above support the hypothesis that the allochthonous rocks in the southern Sierra Nevada region originated from a position structurally above the current southeastern Sierra Nevada batholith. Removal of the upper crust in this area by extensional faulting also is consistent with the geobarometric evidence reviewed above which suggests that the southern Sierra Nevada batholith east of the proto-Kern Canyon fault zone has been exhumed to a deeper level than has the batholith to the north and the batholith to the west although to a lesser degree. I speculate that formation of the relatively broad E-NE trending South Fork Valley which is restricted to the area east of Lake Isabella (Figure 25) may be indirectly related to extensional removal of the upper crust to the southeast. The valley may be located in the area where a mid-crustal subhorizontal detachment in the southeastern Sierra Nevada ramped up to the north to a breakaway zone at the surface located just north of the valley. Isostatic rebound of the footwall in the vicinity of the breakaway zone à la Wernicke and Axen (1988) may have caused

fragmentation of the rocks along steeply dipping faults and cataclastic cleavages, thus making the rocks more susceptible to later erosion. Late E to NE trending steeply dipping non-penetrative cleavage and fractures locally present in basement rocks north of Lake Isabella (D. J. Wood, unpublished mapping, 1994) may be structures that formed in response to footwall uplift.

REGIONAL SIGNIFICANCE OF THE WITNET FORMATION

The Witnet Formation, a continentally derived arkosic sandstone interbedded with conglomerate and locally with shaley layers, is exposed in three separate areas in the southern Sierra Nevada (Figures 2 and 25). The type locality of the Witnet Formation is located in the lower part of the Cache Creek drainage. The sedimentary rocks of the Cache Creek area were first described by Lawson (1906), and the Witnet Formation was defined and named by Buwalda (1934). The Witnet Formation in the Cache Creek region has been mapped and described in a number of subsequent studies (Smith, 1951; Buwalda, 1954; Michael, 1960; Dibblee, 1967; Dibblee and Louke, 1970; Quinn, 1987). Arkosic and conglomeratic sedimentary rocks found in upper Jawbone Canyon and south of Tehachapi Valley are lithologically similar to and have been correlated with the Witnet Formation in the Cache Creek type location (Dibblee, 1959; Dibblee, 1967; Dibblee and Louke, 1970).

The age of the Witnet Formation is unknown but it has been suggested to correlate with the Goler Formation in the El Paso Mountains (Dibblee and Louke, 1970) part of which is Paleocene to Early Eocene in age based on marine and terrestrial fossil evidence (Cox, 1987; McKenna et al., 1987; McDougall, 1987). Fossils have not been found in the Witnet Formation although during the course of this study a resident living in the study area reported to me that seashells had been found in an area of the Witnet Formation exposed south of Tehachapi Valley and Squires et al. (1988) have reported the presence of Late Paleocene to Early Eocene age marine mollusks in the upper part of the Goler Formation. A limited search was made for these reported seashells in the Witnet Formation but none

were found. The lower parts of the Goler Formation, and by inference the Witnet Formation as well, may be as old as Late Cretaceous age, but probably not much older than ~91 Ma which is the biotite K-Ar apparent age of a clast of silicic metavolcanic rock collected from near the base of the formation (Cox, 1987). Both the Witnet Formation in the Tehachapi Valley area and the Goler Formation in the El Paso Mountains are no younger than ~18 Ma which is the radiometric age of volcanic rocks interbedded in sedimentary and volcanic sections that unconformably overlie them (Cox, 1987).

The Witnet Formation exposed both south and north of Tehachapi Valley is folded into a NE trending NW vergent syncline and locally the strata of the SE limb are overturned as was described earlier. The contact between the Witnet Formation of the SE limb of the syncline and the adjacent granitic rocks has been interpreted as a SE dipping thrust fault called the Oil Canyon thrust (Smith, 1951; Buwalda, 1954; Michael, 1960) and as a folded depositional contact (Dibblee and Louke, 1970). Michael (1960) suggests that displacement across the fault probably is not great because locally there appear to be small remnants of Witnet Formation in depositional contact on the granitic rocks of the hangingwall of the fault. Further to the northeast in upper Jawbone Canyon Dibblee (1967) maps all the Witnet Formation-granitic basement contacts as being depositional in origin and not faults. The conflicting observations and interpretations of the Oil Canyon "thrust" northeast of Tehachapi Valley, the apparent lack of a correlative tectonic contact further to the northeast in upper Jawbone Canyon (Dibblee, 1967), and the lack of a well defined SE dipping fault surface associated with the Mendiburu fault south of Tehachapi Valley, as discussed in Chapter 3, all suggest that the Oil Canyon and Mendiburu Canyon faults are local faults that have not accommodated a large amount of displacement.

Prior to this study the two primary hypotheses regarding the origin and tectonic significance of the Witnet and Goler Formations were 1) that the formations were deposited in strike-slip basins that formed adjacent to a proto-Garlock fault (Nilsen and Clarke, 1975;

Nilsen, 1987; Nilsen, 1978), and 2) that the formations were deposited in a tectonic trough that subsided as the Mojave block was uplifted and possibly thrust to the northwest over the rocks of the southern Sierra Nevada (Cox, 1987). Based on the parallel alignment of the exposures of the Witnet and Goler Formations close to the Garlock fault and the coarseness, composition, and thickness of the formations Nilsen and Clarke (1975) suggested that the sediments may have been deposited in a fault-bounded basin that formed during activity along the Garlock fault in the early Tertiary. Cox (1987) suggests, however, that the estimated long-term subsidence rate of 0.3 meters/1000 years for the Goler basin might be less than expected for a strike-slip basin.

Hewett (1954; 1955) suggested that the Mojave Desert region underwent major uplift in the early Tertiary. Cox (1987) proposed that the Witnet and Goler Formations may have been deposited in a NE trending tectonic basin that was located along the northern margin of this uplifted region and he suggested that subsidence of the basin may have resulted from northward overthrusting of the Mojave Desert block. Silver (1982; 1983) has suggested that the Mojave Desert and southern Sierra Nevada regions were the site of early Tertiary westward directed overthrusting. The Witnet and Goler sediments might have been eroded from a northwestward advancing thrust sheet which then locally deformed and overrode the deposits along the Oil Canyon and Mendiburu Canyon faults (Silver, 1995, personal communication) in a manner similar to the molasse deposits that have been deformed and overridden by alpine nappes (Trumpy, 1960). In this case, however, one might expect to find overridden Witnet Formation exposed beneath the low-angle faults that traverse the mountain front immediately northwest of the Garlock fault (Silver, 1986), but no such deposits have been observed (Dibblee, 1959; Dibblee, 1967; Dibblee and Louke, 1970; Ross, 1989b; L. T. Silver, personal communication, 1995).

The proximity of the Witnet Formation sediments to the Blackburn Canyon and Jawbone Canyon faults leads to speculation that the faults might have created the basin into

which the sediments were deposited. The Witnet Formation was deposited on the hangingwall of the Blackburn Canyon fault. Both the Blackburn Canyon and Jawbone Canyon faults are inferred to be part of a major regional extensional fault system.

Sedimentary basins formed in the hangingwall adjacent to detachment faults, sometimes referred to as supradetachment basins, commonly are characterized by a half-graben geometry, basin elongation normal to the hangingwall transport direction, and the presence of coarse grained high gradient alluvial fan deposits and rock-avalanche or gravity slide-block deposits (Fillmore et al., 1994; Friedmann et al., 1994; Fedo and Miller, 1992).

The Witnet basin exhibits some of the characteristics of a supradetachment basin. While the Witnet Formation is not now in contact with the Blackburn Canyon fault, so it cannot unequivocally be demonstrated that it was deposited in a half-graben basin, it may have been in contact with the fault in the past and has been subsequently removed by erosion for which there is ample evidence in the unconformity between the Witnet and Kinnick Formations (Dibblee and Louke, 1970). The Witnet Formation in upper Jawbone Canyon may be in contact with the inferred westward continuation of the Jawbone Canyon fault zone (Figure 2), but an attempt to examine this area was hindered by property access restrictions. The NE trend of the Witnet basin does appear, however, to be oriented normal to the approximate SE direction of transport for the upper plate of the Blackburn Canyon detachment fault (Figure 18B) which is one of the characteristics of a supradetachment basin (Fillmore et al., 1994). Finally, the local coarse grained conglomeratic character of the Witnet Formation (Michael, 1960; Dibblee and Louke, 1970), is consistent with the formation being a supradetachment basin deposit.

The timing of the Witnet Formation deposition relative to activity on the Blackburn Canyon fault currently is not directly constrained. Deposition of the Witnet Formation in the study area at least locally appears to postdate cataclastic deformation and chloritic alteration of the Bootleg Canyon granodiorite that may have occurred during activity along

the Blackburn Canyon fault. At one locality in Mendiburu Canyon close to the contact between the Bootleg Canyon granodiorite and the overlying basal conglomerate of the Witnet Formation the granodiorite is altered and cataclastically deformed while the nearby Witnet Formation appears to be undeformed and unaltered.

There is other evidence that suggests the Witnet Formation was deposited after deformation of the nearby basement rocks. North of Tehachapi Valley Smith (1951) noted that at most localities adjacent to the Oil Canyon fault the granitic rocks of the hangingwall were considerably more shattered and brecciated than the Witnet Formation adjacent to the fault in the footwall. He suggested the difference in degree of deformation of the two units may have been because the granular nature of the Witnet Formation allowed its constituent grains to rotate and flow to absorb the strain while the granitic rocks were too brittle to do so and were fractured. Another possible interpretation is that the granitic rocks adjacent to the Oil Canyon fault were cataclastically deformed prior to both deposition of the Witnet Formation and motion along the Oil Canyon fault. This interpretation is supported by the observation of Michael (1960) who notes that many of the granitic boulders in the basal conglomerate of the Witnet Formation in the Oil Canyon area are "sheared" which suggests they may have been derived from nearby basement that was already deformed by faulting. In a possibly analogous situation, chloritic brecciated granitic clasts are present in a syntectonic sedimentary basin above the Chemehuevi detachment fault and their appearance in the sediments was interpreted by Miller and John (1988) as recording the unroofing of the detachment fault zone as extension progressed.

Clearly more work on the Witnet Formation needs to be done in order to better document its proposed syntectonic relationship with the Blackburn Canyon and Jawbone Canyon faults, but the available evidence reviewed above suggests that the model of the Witnet Formation as a supradetachment basin deposit is a viable one. Better age control on the Witnet Formation is also needed to see if its age is compatible with the age constraints

on the proposed regional extensional faulting in the southern Sierra Nevada which are discussed in the next section. Since fossils have not been found in the Witnet Formation an estimate of its age might be obtained palynology (pollen dating) or through paleomagnetic study to try to date it by correlation with the geomagnetic reversal time scale.

OVERVIEW OF INFERRED REGIONAL EXTENSIONAL FAULTING

Age of Extensional Faulting

As discussed earlier the Blackburn Canyon fault is clearly younger than ~100 Ma and possibly younger than ~90 Ma. The fault locally may have been reactivated to a minor extent in Miocene time. The allochthonous hangingwall rocks of the Oak Creek Pass complex most likely were transported to their current position along the Blackburn Canyon fault prior to the time when the Mendiburu Canyon fault was active. The Mendiburu Canyon fault is inferred to crosscut and locally coincide with the Blackburn Canyon fault (Figure 21) and it most likely was active in pre-Miocene time. An older minimum age of ~80 Ma may be indicated for the Blackburn Canyon fault if the Mountain Park fault in the footwall of the Blackburn Canyon fault correlates with either the Quail Canyon fault or the South Ridge fault in the hangingwall of the Blackburn Canyon fault. Fault II of the Rand fault complex in the Rand Mountains, located between the Johannesburg gneiss and structurally overlying cataclastically deformed granodiorite, was active between 87 Ma and 79 Ma (Silver and Nourse, 1991; Nourse, 1989). The Pastoria fault in the San Emigdio Mountains is younger than the 98 Ma U-Pb zircon age of the Brush Mountain granite in the upper plate of the fault (James, 1986) and the fault is older than the Middle to Late Eocene age of sedimentary rocks which unconformably overlap it (Davis and Lagoe, 1988).

There is also indirect control on the age of extension/exhumation in the southern Sierra Nevada. Dixon et al. (1994) and Dixon (1995) document a decompression event from 5-8 kilobars to 1-4 kilobars in the Lake Isabella and Tehachapi regions of the southern Sierra Nevada batholith that occurred at temperatures \geq ~500°C. Assuming that the

Blackburn Canyon and allied extensional faults are responsible for this exhumation of the southeastern Sierra Nevada batholith as suggested above, and if the hornblende $^{40}\text{Ar}/^{39}\text{Ar}$ apparent ages of 83-91 Ma on amphibolites and plutons east of the proto-Kern Canyon fault zone (Dixon, 1995) are interpreted as the time the rocks cooled through $\sim 500^\circ\text{C}$ then the extensional unroofing of the batholith most likely began sometime between 83 and 91 Ma. As summarized earlier there is a ~ 3 kilobar difference in the level of exposure of rocks metamorphosed at ~ 100 Ma across the proto-Kern Canyon fault in the Lake Isabella area with the deeper rocks exposed to the east. Since there is little evidence along the proto-Kern Canyon fault zone for major vertical uplift since ~ 85 Ma, the time when it clearly was active as a dextral strike-slip fault, that would suggest that the differential uplift across the fault occurred between 85 and 100 Ma (Busby-Spera and Saleeby, 1990). If the apparent uplift of the rocks east of the proto-Kern Canyon fault zone occurred during extensional unroofing then the extension may have begun prior to ~ 85 Ma.

Extensional unroofing of the southeastern Sierra Nevada batholith also may have been largely completed by the time part of the garnet bearing Tehachapi Airport leucogranite was intruded. Intrusion of the Tehachapi Airport leucogranite into the center of the Back Canyon pendant (Figure 25) was accompanied by the localized retrograde metamorphism of higher grade sillimanite bearing pelitic rocks adjacent to the pluton (Kim, 1972). Garnet thermobarometry on a pelitic sample from the contact aureole of the leucogranite pluton in the Back Canyon pendant yields a metamorphic pressure and temperature of ~ 1 kilobar and $\sim 500^\circ\text{C}$ (Dixon, 1995) and Dixon (1995) suggests that the compositions of the minerals in the sample may have been reset during intrusion of the pluton. This low retrograde (?) metamorphic pressure in the contact aureole of the leucogranite suggests that it intruded after much of the unroofing of the region and the Tehachapi Airport leucogranite may have an emplacement age similar to the ~ 70 -80 Ma U-Pb zircon age of the Brushy Ridge granite with which it may correlate.

Regional Extension Direction

Determination of the regional Late Cretaceous-early Cenozoic extension direction of the upper crust in the southern Sierra Nevada region is difficult because other coeval or younger tectonic events may have contributed to the apparent displacement of some of the allochthonous rocks. The kinematic data from this study and from Nourse (1989), and Nourse and Silver (1986) indicate that the allochthonous rocks in the upper plates of the Blackburn Canyon fault and Fault II of the Rand fault complex were transported in a southeastward to southward direction, at least during part of the time these faults were active. Upon restoration of ~45-50 km of sinistral displacement along the Garlock fault this generally southward transport direction is more or less consistent with the inferred source location in the Sierra Nevada to the north for these out of place rocks. In contrast, the inferred allochthonous rocks of the batholith found in the upper plate of both the Pastoria fault and the inferred correlative fault beneath the Tehachapi Mountains south of the Garlock fault clearly are displaced relatively westward from potentially correlative rocks located in the east side of the Cretaceous batholith in southern California, as noted in previous studies (Silver, 1982; Silver, 1983), as well as being displaced in a southward direction from their suggested source region (Figure 25). The apparent westward component of displacement of these rocks may be the result of a different deformation episode which will be discussed later.

The S to SE direction of extension for the inferred Late Cretaceous and possibly younger extension along the Blackburn Canyon fault is similar to Late Cretaceous extension directions documented in a number of localities east of the southern Sierra Nevada batholith (Figure 1). Late Cretaceous age extension in the Funeral Mountains which was ongoing at ~72 Ma and over by 70 Ma was NW directed (Applegate and Hodges, 1995; Applegate et al., 1992; Hodges and Walker, 1990). Hodges and Walker (1992) suggest that some N-NW directed extension in the Panamint Mountains may have

occurred in Late Cretaceous time based on a summary of geologic studies in that area. In an overview of the geologic history of the southern Inyo, Argus, and Slate Ranges Dunne (1986) summarized the regional evidence for Late Cretaceous Laramide age deformation and concluded that it involved a component of NW-SE directed crustal extension based on the orientation of conjugate strike-slip faults and subhorizontal NW trending stretching lineations in moderate grade gneisses in the Panamint Range.

Paterson et al. (1991) suggest that the Papoose Flat pluton and a number of other Late Cretaceous age granitic plutons in the White-Inyo Mountains all were intruded during a regional Late Cretaceous deformation event which resulted in ballooning of the plutons in a westward to northwestward direction. This west to northwest ballooning of the plutons may reflect the regional direction of extension in Late Cretaceous time. The Papoose Flat pluton, which has been dated at 83 Ma by the U-Pb method on monazite (Miller, 1996), locally contains a penetrative deformation fabric with well developed NW-SE trending shallowly plunging stretching lineations, and shear sense along the lineation direction is top to the SE or sinistral (Law et al., 1992; Paterson et al., 1991). Law et al. (1992) suggest that the Papoose Flat pluton may have intruded during SE directed thrusting based on the kinematic data. Given the regional evidence for Late Cretaceous NW-SE extension outlined above, however, the top to the SE shearing may be due to crustal extension.

Apparent Rotation of Hangingwall Rocks

The location and trend of the metasedimentary pendants and the orientation of igneous foliation in the hangingwall rocks of the regional detachment system suggests that some of them may have been rotated up to 90° clockwise relative to the autochthonous rocks in the southern Sierra Nevada batholith. Igneous foliation in the granitic rocks of the Oak Creek Pass complex in the study area, which is inferred to be magmatic based on its parallelism to schlieren and mafic enclaves, has mostly E to NE trends and the small pendants of Oaks metavolcanic rocks also have NE trends. In the region east and southeast

of Lake Isabella where the Oak Creek Pass complex is inferred to have originated the pendants have NW trends and the plutons have a primary foliation that is generally NW to N-NW trending (Ross, 1990). The NE trending Tylerhorse Canyon and Bean Canyon pendants south of the Garlock fault appear to have been rotated about 90° clockwise relative to the Isabella pendant in the Sierra Nevada. Paleomagnetic results from the Cretaceous Lebec granodiorite in the upper plate of the Pastoria fault indicate that it has been rotated clockwise by more than 90° (McWilliams and Li, 1983) which is consistent with the above estimates of rotation that are based on geologic data.

A puzzling contrast to the apparent rotations described above is that the Aqueduct Tunnel pendant, the Quinn Ranch pendant, and Tejon Lookout granite do not appear to be substantially rotated relative to their inferred correlatives the Monolith pendant, the Back Canyon pendant, and the Tehachapi Airport granite north of Tehachapi Valley (Figure 25). One possible explanation of this observation is that the pendants and granite body north of Tehachapi Valley also originally had a NW trend and were rotated during F4 oroclinal folding of the footwall rocks around the Walker Basin orocline. Oroclinal F4 folding in the lower crust may have been coeval with extension and rotation of the upper crust as will be discussed in a later section.

Rate of Extensional Faulting

Even though the current position of some of the out of place rocks in the southern Sierra Nevada most likely is the result of more than one episode of low-angle fault transport it is instructive to try to estimate the rate of extensional faulting, assuming a single episode of faulting, to see if it is reasonable compared to the rates of extension documented in other areas. After restoring 45 km of sinistral displacement along the Neogene Garlock fault the straight-line displacement between correlative features offset along the low-angle fault system in the southern Sierra Nevada region ranges from ~90-100 km for the upper plate rocks in the western and southern Tehachapi Mountains, and ~50-60 km for most of

the offset features in the allochthonous rocks of the southeastern Sierra Nevada and Rand Mountains. If all of the regional extension occurred during the time interval 87-79 Ma, the age constraints for low-angle faulting in the Rand Mountains (Silver and Nourse, 1991; Nourse, 1989), then the calculated rate of extension ranges from about 6 to 13 millimeters per year. These rates of extensional faulting are comparable to the estimated rates of Cenozoic regional extension in the Basin and Range province which range from 5-8 to 10-20 millimeters per year (Wernicke, 1992).

POSSIBLE COEVAL LATE CRETACEOUS AGE EXTENSION AND CONTRACTION

The progressive contractional deformation in the eastern Tehachapi gneiss complex is inferred to have been ongoing from ~100 Ma until ~80 Ma as was discussed earlier. Most of the age constraints on the possible extensional exhumation of the southeastern Sierra Nevada batholith along the regional detachment system indicate it may have occurred between ~90-85 Ma and ~80 Ma as outlined above. Thus, the latter phases of the ongoing contractional deformation in the lower to mid-levels of the batholith may have been accompanied by coeval extensional deformation in the upper crustal levels of the southern Sierra Nevada batholith. The possible 90-85 Ma initiation age for the upper crustal detachment faulting in the southern Sierra Nevada is similar to the time when folding in the eastern Tehachapi gneiss complex changed from NW trending subhorizontal F3 folds to dextral-sense F4 oroclinal folds. In addition to the apparent temporal similarity between the F4 folding and the inferred upper crustal detachment the two deformations appear to be spatially related as well. The metasedimentary pendants in the central and southern Sierra Nevada begin to deviate from their regular N-NW trend south of the Lake Isabella area and this deviation in trend becomes more pronounced further to the south where the rocks are folded in the F4 Walker Basin and Tehachapi Valley oroclines (Figure 25). The area of regional-scale F4 folding south of the latitude of Lake Isabella approximately corresponds

to the area in the batholith that is inferred to have been unroofed along the regional detachment system.

OTHER POSSIBLE EXTENSIONAL FAULTS IN THE STUDY AREA

Inferred Tehachapi Valley Fault

As discussed in the previous chapter the NW trending moderately NE dipping shear fabrics with top to the NE shear sense which are localized in the upper structural levels of the north block of the gneiss complex may be related to a NE dipping normal fault buried beneath the alluvium of Tehachapi Valley (Figure 14 and Plate 3). The eastern Tehachapi gneiss complex in the study area may comprise the footwall to this inferred Tehachapi Valley fault and the rocks exposed north of Tehachapi Valley may be part of the hangingwall of this fault. The Tehachapi Airport leucogranite (\pm biotite, \pm garnet, \pm muscovite) exposed along the north margin of Tehachapi Valley (Figure 14) is compositionally similar to the Brushy Ridge leucogranite exposed near the south margin of Tehachapi Valley (Figure 4) and may correlate with it. The metasedimentary rocks surrounding the body of Brushy Ridge leucogranite located adjacent to Antelope Canyon dip beneath it suggesting that it has no root and may have been emplaced from above, possibly when it was beneath the north side of the valley. If the Brushy Ridge granite formerly was adjacent to and/or beneath the Tehachapi Airport granite that would suggest the inferred Tehachapi Valley fault may have accommodated 5-8 km of top to the NE extensional displacement.

Assuming the Tehachapi Valley fault exists it must continue outside of Tehachapi Valley, but where it might be located is not clear. At the east end of Tehachapi Valley the relationship between the inferred Tehachapi Valley fault and the Blackburn Canyon fault is not known (Figure 14), although the difference in transport direction of the two faults suggests that they are not the same structure. At the west end of Tehachapi Valley the fault does not appear to continue northwest of Tehachapi Valley parallel to Highway 58 along

the course of Tehachapi Creek where Dibblee and Louke (1970) indicated there is a fault because distinctive lithologic units in the basement rocks can be traced across the creek without significant deflection (Figure 14) (D. J. Wood, unpublished mapping, 1993). The fault may skirt to the southwest of the prong of metasedimentary rocks extending south into the northwest corner of Tehachapi Valley and then continue to the north parallel the pendant as a strike-slip fault with an oblique sinistral shear sense (Figure 24D).

There is some evidence suggesting that the Tehachapi Valley fault may be located within and/or along the western margin of the mixed gneiss pendant that trends north from the northwest corner of Tehachapi Valley. First, the western contact of the pendant with the tonalite of the Tehachapi Intrusive Complex (Bear Valley Springs tonalite) is extensively tectonized, much more so than the adjacent lithologies. Second, locally within the paragneiss along the west side of the pendant there are garnets with asymmetric tails suggesting sinistral shearing. Finally, there is a small intrusion of gneissic biotite leucogranite in the paragneiss north of Highway 58 that resembles the Brushy Ridge granite south of Tehachapi Valley. This granite gneiss exhibits NW trending shallowly NW plunging mineral lineations and a well developed S-C fabric clearly indicating sinistral shear. In contrast, all of the other igneous rocks within and adjacent to the pendant north of Tehachapi Valley have deformation fabrics indicating dextral or top to the SW shear (Figure 15D). Like the relationship between the deformation fabrics in much of the Brushy Ridge granite and the Tehachapi Intrusive Complex in the eastern Tehachapi gneiss complex, the leucogranite north of Tehachapi Valley has the opposite sense of shear than nearby gneisses. The leucogranite in both areas may have intruded syntectonically with motion along the inferred Tehachapi Valley fault.

North of the Tweedy Creek area the hypothetical fault might jog to the west along a ramp to become a low-angle NE dipping normal fault buried beneath the alluvium in Walker Basin (Figures 2 and 24D). Walker Basin may have extended in a N-NE direction

in a manner analogous to the inferred extensional opening Tehachapi Valley. The metasedimentary pendants immediately north and south of Walker Basin (Louke, 1966; Ross, 1989b) originally may have been more or less continuous and separation along an intervening shallowly NE dipping fault is one way to account for their separation. West of Walker Basin the possible continuation of the inferred Tehachapi Valley fault may merge with either the Kern Canyon fault to the north or the Breckenridge fault to the south. Located near the south end of the Breckenridge fault along the west side of the San Joaquin Basin is the Edison fault (Figure 2) which is a NW trending normal fault that dips 30-60° to the NE (Dibblee and Warne, 1988; Dibblee and Chesterman, 1953). The orientation and motion sense of the Edison fault is similar to that inferred for the hypothetical fault in Walker Basin and the Breckenridge fault might have served as a dextral-sense transfer fault between those two faults.

The age of activity of the inferred Tehachapi Valley fault is not well constrained since the fault is not exposed, but regional geologic relations suggest the fault might have been active in Late Cretaceous time and also possibly during the early to middle Cenozoic as well. The fault may have been active in Late Cretaceous time during and immediately following intrusion of the Brushy Ridge granite since the structurally highest granite body in the gneiss complex is penetratively deformed by a top to the NE shear fabric while the adjacent rocks that it intrudes are undeformed or only weakly deformed as discussed in the previous chapter. Intrusion of the granite may in fact have facilitated or initiated movement along the fault through a process of melt-enhanced deformation (Hollister and Crawford, 1986). The inferred Tehachapi Valley fault also may have been active during Oligocene-Miocene time if it correlates with the Edison fault which was active at that time (Dibblee and Warne, 1988).

A well cemented but decomposed rubble composed of cobble to boulder size angular clasts of granitic and metasedimentary rocks, called the Atlas Formation by Lawson

(1906) and mapped as granitic and metamorphic rubble by Dibblee and Louke (1970), is exposed locally in the northwestern part of Tehachapi Valley and may be a hangingwall syntectonic breccia deposited during activity along the inferred Tehachapi Valley fault. The Atlas formation may be pre-Miocene in age because it is positionally overlain by the Tank volcanics of Lawson (1906) which Buwalda (1954) considered to be part of the Kinnick Formation of Early Miocene age (Quinn, 1987). The Atlas Formation contains abundant clasts of leucocratic garnet and biotite bearing granitic rocks which resemble the granites of Tehachapi Airport and Brushy Ridge so its depositional age most likely is younger than the possible Late Cretaceous age of those granites.

Oak Creek Mylonite Zone

The Oak Creek mylonite zone is a NE trending NW dipping zone of greenschist facies ortho- and ultramylonite exposed at the lowest structural level of the eastern Tehachapi gneiss complex (Figure 3) and limited evidence for top to the N shearing in the mylonite suggests it may be part of an extensional shear zone. As discussed in the previous chapter the Oak Creek mylonite zone may be part of a regional system of low-angle faults that overlie the Rand schist and it may correlate with the Rand fault across the Garlock fault in the Rand Mountains. Based on a study of the Rand fault and on similar studies (Silver et al., 1984; Nourse and Silver, 1986) Postlethwaite and Jacobson (1987) suggested that part of the Rand fault exposed in the southwestern Rand Mountains may be a low-angle normal fault.

If the Oak Creek mylonite zone is part of the regional low-angle fault system overlying Rand schist then K-Ar and $^{40}\text{Ar}/^{39}\text{Ar}$ apparent ages from nearby areas also are consistent with an extensional origin for the mylonite zone. Assuming that isothermal surfaces in the crust were parallel to the Earth's surface prior to faulting then extensional faulting would juxtapose rocks with older cooling ages in the hangingwall against footwall rocks with younger cooling ages (Wheeler and Butler, 1994). Jacobson (1990) determined

several $^{40}\text{Ar}/^{39}\text{Ar}$ apparent ages on muscovite and hornblende from Rand schist exposed in the Rand Mountains which he interpreted as cooling ages and noted that they were younger than K-Ar ages in inferred upper plate rocks of the Rand fault exposed north of the Garlock fault in the Tehachapi Mountains. Recent hornblende $^{40}\text{Ar}/^{39}\text{Ar}$ apparent ages of 84-91 Ma from amphibolites and plutons structurally above the Oak Creek mylonite zone in the eastern Tehachapi Mountains (Dixon, 1995) also are older than the ~74 Ma hornblende $^{40}\text{Ar}/^{39}\text{Ar}$ apparent age of the Rand schist in the Rand Mountains (Jacobson, 1990).

Possible Late Extension Along the Mountain Park and Taco Saddle Faults

The Mountain Park and Taco Saddle faults in the eastern Tehachapi gneiss complex are NW trending shallowly NE dipping ductile faults with top to the S-SW shear sense that were active primarily during greenschist facies metamorphic conditions. While these faults are interpreted to have accommodated crustal shortening during most of their history there is limited evidence suggesting they may have been reactivated as extensional faults late in their history. The steeply dipping orientation of some late tension cracks present locally in orthogneiss near the faults appears to be more compatible with top to the NE shear than top to the S-SW shear. In addition, at one or two localities in sheared Tehachapi Intrusive Complex tonalite close to the Mountain Park fault kinematic evidence for top to the NE shearing predominates over evidence for top to the S-SW shearing.

APPARENT DEXTRAL-SENSE OFFSET AND WESTWARD DISPLACEMENT OF PRE-CENOZOIC GEOLOGIC FEATURES IN THE SOUTHERN SIERRA NEVADA-MOJAVE DESERT REGION

The inferred allochthonous granitic and metamorphic rocks scattered across the width of the southernmost Sierra Nevada region are suggested to have originated from a position structurally above the southeastern part of the current Sierra Nevada as was discussed earlier. After unslipping ~45 km of sinistral offset along the Garlock fault the position of some of these allochthonous rocks is well to the west of their inferred area of

origin which implies that their translation included a westward component of displacement in addition to a southward component of displacement (Figure 25). The simplest way to transport them to their current position would be by a single stage episode of upper plate motion in a southwest direction. A southwest direction of transport, however, is inconsistent with the evidence discussed in the previous section for regional NW-SE directed upper crustal extension and the S to SE directed transport of the rocks in the upper plate of the Blackburn Canyon fault. An alternate model for the transport of the upper plate rocks might involve a two stage path, the first stage involving S to SE directed extensional transport as indicated by the shear sense and direction along the Blackburn detachment, and a second stage involving local westward or northwestward tectonic transport. This inferred second phase of displacement to the west for the allochthonous rocks in the southern Sierra Nevada is consistent with the results of previous studies in the region as described below.

It has been noted by Silver (1982; 1983) and Burchfiel and Davis (1981), as well as in a number of other studies which are reviewed below, that various structural, lithologic, geochemical, and isotopic zones or boundaries which trend more or less parallel to the Cordilleran continental margin in California appear to have been displaced to the west and/or deflected in a dextral sense at the approximate latitude of the southern Sierra Nevada-Mojave Desert region prior to the initiation of right-lateral strike-slip motion along the Neogene San Andreas fault system (Powell, 1993). Much of the evidence for this apparent pre-San Andreas fault system disruption of the Cordilleran continental margin comes from the correlation of geologic features in the southern Sierra Nevada region with similar features present in the Salinian block which appear to have been displaced relatively westward.

The Salinian block is the region in the Coast Ranges of central California bounded by the San Andreas fault on the east, the Sur-Nacimiento-Rinconada faults on the west, and the Big Pine fault on the south (Figure 1). The Salinian block consists of polydeformed

crystalline basement composed primarily of Sur series metasedimentary rocks of unknown ages which are intruded by several generations of Cretaceous age plutons as summarized by James (1992). A small sliver of the basement rocks in the southeastern Salinian block is composed of Precambrian age gneiss (Mattinson, 1983). The metamorphic and igneous basement rocks of the Salinian block locally are depositionally overlain by Late Cretaceous to Quaternary age sedimentary rocks (Grove, 1993). Grove (1993) has suggested that the Late Cretaceous age sedimentary rocks in the Salinian block were deposited in an extensional forearc basin analogous to the Sunda Straight in Indonesia. Located outboard of the San Andreas fault in west-central California the Salinian block is slivered by dextral strike-slip faults of the Neogene San Andreas fault system (Powell, 1993).

The place of origin of the Salinian block has been a matter of some controversy. Some paleomagnetic studies of Cretaceous sedimentary rocks in the Salinian block suggest that it is a far-traveled terrane originating thousands of km to the south (McWilliams and Howell, 1982; Page, 1982; Champion et al., 1984; Kanter and Debiche, 1985) while other studies focusing on the geology, isotopic character, and age of the crystalline basement rocks in the Salinian block, Mojave Desert area, and the southern Sierra Nevada east of the San Andreas fault (Silver, 1982; Silver, 1983; Ross, 1984; Silver and Mattinson, 1986; Pickett and Saleeby, 1991; James, 1992) have suggested that the Salinian block originated from a location adjacent to the Mojave Desert and the southern Sierra Nevada. See Hall (1991) for an extended review of the different hypotheses for the origin of the Salinian block. Recent paleomagnetic studies of Late Cretaceous age sedimentary rocks deposited on the granitic basement of the Salinian block suggest, however, that the block is not far-traveled and may have originated at the latitude of the Mojave Desert region (Whidden et al., 1991; Grove, 1993).

The discussion which follows is divided into three parts. First, since the possible westward displacement and clockwise rotation of the rocks in the upper plate of the

Blackburn detachment fault may be part of a larger regional-scale deformation event (Silver, 1982; Silver, 1983; Burchfiel and Davis, 1981) the previously documented evidence for westward displacements and dextral deflections is reviewed below. Second, while a number of studies have documented similarities between the ages, isotopic properties, and lithologies of the Salinian block and the southern Sierra Nevada there has not been a detailed comparison of the structural histories of the two areas. The second section below is a comparison between the structural histories of the eastern Tehachapi gneiss complex and the northern Salinian block. In the final section below the different tectonic models which have been proposed to account for the westward displacement and dextral-sense offset of the geologic features in the southern Sierra Nevada-Mojave-Salinian region are reviewed and discussed relative to the results of this study.

PREVIOUSLY DOCUMENTED DISPLACEMENTS AND DEXTRAL DEFLECTIONS

A number of lithologic belts and structures in the southern Sierra Nevada-western Mojave Desert region appear to be displaced westward and/or deflected in a right-lateral sense. Early on Locke et al. (1940) noted that the N-NW trending outcrop pattern of the Sierran basement curved to the west at its southern end as a "great westward hook, convex southward" which they attributed to drag resulting from dextral shearing along the San Andreas fault zone. In a later study, Hill and Dibblee (1953) recognized that the San Andreas fault zone had accumulated 300 km of dextral displacement since early Miocene time and they also suggested that Sierran-type basement rocks west of the fault may have been dextrally offset from the southern end of the Sierra Nevada by an additional 300 km prior to post Early Miocene activity along the fault.

The boundary between plutons of dominantly quartz dioritic composition and plutons of mostly granodioritic composition in the southern California region, the quartz diorite boundary line of Moore (1959), is deflected westward at the latitude of the southern Sierra Nevada. Ross (1978) noted that the granitic rocks in the Salinian block are

compositionally similar to granitic rocks located to the east in the east-central Sierra Nevada, and Silver (1982) suggested that the granitic rocks in the northern Salinian block had been displaced on low-angle faults from the east side of the southern Sierra Nevada. Burchfiel and Davis (1981) summarized a number of pre-Cenozoic features in the western Mojave region which they suggest had been oroclinally deflected in a dextral sense, including the western boundary of the Sierran batholith, the initial $^{87}\text{Sr}/^{86}\text{Sr}$ 0.706 line, a belt of Paleozoic rocks inferred to have been emplaced during a Permo-Triassic truncation of the continental margin, the pre-latest Jurassic terranes of the Sierran foothills, the Great Valley and Franciscan terranes, and windows in the Rand-Pelona-Orocopia low-angle fault system. The N-NW trending Late Jurassic age Independence dike swarm apparently is offset ~70 km in a dextral-sense in the central Mojave Desert area (James, 1989; Glazner et al., 1989; Martin et al., 1993). Martin et al. (1993) also suggested that a zone of distinctive Jurassic-Triassic age volcanic and sedimentary rocks as well as deformation belts of Permo-Triassic and Jurassic age have been offset in the same sense and a comparable distance as the Independence dike swarm.

Other studies have documented apparent westward displacements or dextral sense deflections in geochronologic and isotopic patterns present in the batholithic rocks of California in the southern Sierra Nevada and Mojave Desert regions. A regional compilation of biotite K-Ar apparent age data from Mesozoic igneous rocks in central and southern California (Evernden and Kistler, 1970; Armstrong and Suppe, 1973; Krummenacher et al., 1975) by Krummenacher et al. (1975) reveals that N-NW trending 100 Ma and 85 Ma isochrons of K-Ar biotite apparent ages are deflected westward at the southern end of the Sierra Nevada. The contact between Cretaceous plutonic rocks with U-Pb zircon ages ≥ 105 Ma and < 105 Ma shown in Figure 1 (sources of data for the figure are listed in the caption) appears to be offset to the west in the vicinity of the Garlock fault. The $\text{Sr}_1 = 0.706$ isopleth in plutonic rocks of the southern Sierran-Mojave-Salinian region

is clearly displaced to the west relative to its location in the Sierra Nevada to the north (Kistler and Ross, 1990; Kistler and Peterman, 1978; Kistler and Peterman, 1973) as noted by Burchfiel and Davis (1981). Initial Pb isotopic patterns in the plutonic rocks of the Salinian block, Mojave Desert, and the Sierra Nevada also are consistent with westward displacement of the Salinian block from the southern Sierra Nevada area (Silver and Mattinson, 1986; Doe and Delevaux, 1973; Mattinson, 1990; Chen and Tilton, 1991).

STRUCTURAL CORRELATION OF THE EASTERN TEHACHAPI MOUNTAINS WITH THE NORTHERN SALINIAN BLOCK

While a number of studies have suggested lithologic, geochronologic, and geochemical ties between the southern Sierra Nevada region and the Salinian block (Ross, 1984; Silver and Mattinson, 1986; Pickett and Saleeby, 1991; James, 1992) there has not been a detailed structural comparison between the two areas since detailed information on the structural history of the southern Sierra Nevada has been lacking. The results from this study, however, suggest that the Cretaceous deformation history of the eastern Tehachapi Mountains region is remarkably similar to the Cretaceous deformation history of the crystalline basement rocks of the northern Salinian block as outlined below. The following comparison of structures in the eastern Tehachapi gneiss complex with previously documented structures in the crystalline basement rocks of the northern Salinian block is made assuming that the rocks in both areas have not undergone significant vertical axis rotation since the Late Cretaceous. Upper Cretaceous strata in the Lake Nacimiento area of the Salinian block appear to have been rotated clockwise $\sim 38^\circ$ since the Cretaceous (Grove, 1993), but this locality is ~ 60 km southeast of the areas discussed below and the observed rotation in that area is not necessarily indicative of rotation elsewhere in the Salinian block.

The geology of different areas of the basement in the Salinian block has been studied by different workers and in most of the different locations that have been studied two major generations of folds were recognized in the Sur series metasedimentary rocks, as

will be summarized below. Some literature on the Salinian block is somewhat confusing regarding the deformation history of the crystalline basement rocks because it seems to imply that the same two episodes of folding occurred in all of the different exposures of Sur series metasedimentary rocks in the Salinian block. A close review and comparison of the literature on the geology and structure of the Salinian basement rocks (Compton, 1960; Compton, 1966b; Compton, 1966a; Leo, 1967; Wiebe, 1970b; Wiebe, 1970a; John, 1981), however, suggests that the Sur series metasedimentary rocks of the Salinian block may have experienced three major episodes of folding followed by the localized formation of recrystallized and mylonitic fabrics as described in the following sections.

Northeast Trending Shallow Plunging Folds

The earliest deformation structures recognized in the metasedimentary rocks of the Salinian block are NE to E trending open to tight map-scale and mesoscale folds that have gentle plunges to the NE and steeply dipping axial planes. These early folds appear to be developed best in the northern Santa Lucia Range (Wiebe, 1970b; Wiebe, 1970a) and in the Ben Lomond Mountain area (Leo, 1967), but they also may be present in the northern Gabilan Range (Compton, 1966b; John, 1981). In descriptions of the geology of the southern Santa Lucia Range Compton (1966b; 1966a) does not mention a generation of NE trending shallow plunging folds which suggests that in this area these early folds either were not present, were transposed by later deformation, or were not identified. Wiebe (1970a) suggested that the first generation NE trending folds present in the northern Santa Lucia Range might be present elsewhere in the Salinian basement, but may not be recognized because of voluminous intrusions, tightly appressed later folds, and poor stratigraphic control in the basement rocks.

Development of these early NE trending folds was preceded and/or accompanied by amphibolite facies metamorphism, and several orthogneiss bodies are inferred to have intruded coevally with the folding because the foliation and lineations in the orthogneiss are

parallel to the fabrics in the metasedimentary rocks (Compton, 1966b; Leo, 1967; Wiebe, 1970a). The ages of some of the synkinematic orthogneisses in the Ben Lomond Mountain area are bracketed between about 103 Ma and 130 Ma (James, 1992). The age, grade of metamorphism, and orientation of these early folds in the Salinian block are similar to the age, metamorphic grade, and orientation of the NE trending F2 generation of folds in the eastern Tehachapi Mountains documented in this study.

Northwest Trending Shallow Plunging Folds

A second major deformation in the basement rocks of the northern Santa Lucia Range of the Salinian block produced a set of N-NW trending map-scale and mesoscale folds that have steeply dipping axial surfaces and wavelengths that are smaller than the wavelengths of the earlier northeast trending folds (Wiebe, 1970b; Wiebe, 1970a). The N-NW trending folds in the northern Santa Lucia Range developed during amphibolite facies metamorphism as indicated by associated sillimanite and hornblende lineations and most of the plutons in the area appear to have been emplaced during the second folding event (Wiebe, 1970a). Wiebe (1970b) notes that some of these second folds are tightly appressed and that the plunges of the second folds are variable, but he does not elaborate on the plunges of the folds. Inspection of the geologic maps in Wiebe (1970b; 1970a), however, reveals that about two thirds of the mineral lineations and minor fold axes with trends in the northwest and southeast quadrants of the compass have plunges of 30° or less. This suggests that most of the N-NW trending folds formed in the second deformation event have shallow to subhorizontal plunges.

The orientation of the second folds in the northern Santa Lucia Range described above appears to be similar in orientation to the first of two generations of folds documented by Compton (1966b; 1966a) in the basement rocks of the Junipero Serra area of the southern Santa Lucia Range. Compton (1966b) notes that the first major folds in the Junipero Serra area are isoclinal with subhorizontal axes and that high temperature minerals

such as sillimanite lie parallel to the fold axes, but he does not specifically state the trend of the first folds in this area. In a geologic map of the Junipero Serra area, however, Compton (1966b) shows a group of "older" lineations, presumably subparallel to the first fold axes, that are generally NW trending and have mostly subhorizontal to shallow plunges. In another study of the geology of the Santa Lucia Range Compton (1966a) reports that the axes of folds formed in the first episode of deformation and metamorphism of the basement rocks are subhorizontal and trend parallel to the Santa Lucia Range, which has a NW trend. The metamorphic rocks along the main coastal ridge on the west side of the Santa Lucia Range have SE trending fold hinges and aligned linear crystals of sillimanite, biotite, and hornblende that plunge at low angles (Compton, 1960).

Based on the above structural relations the second folding episode recognized by Wiebe (1970b; 1970a) in the northern Santa Lucia Range is inferred to correlate with the first folding episode in the southern Santa Lucia Range documented by Compton (1966b; 1966a). This generation of NW trending subhorizontal to shallow plunging tight to isoclinal folds appears to be pervasively developed only in the Santa Lucia Range of the northern Salinian block since folds of this orientation have not been reported in the Ben Lomond Mountain or Gabilan Range areas (Leo, 1967; Compton, 1966b; John, 1981). Formation of these NW trending folds appears to have been accompanied by the emplacement of tonalitic and granodioritic plutons in the northern Santa Lucia Range (Wiebe, 1970b) and emplacement of adamellite and granite in the southern Santa Lucia Range (Compton, 1966b). The U-Pb zircon ages of plutonic rocks in these areas of the Santa Lucia Mountains range from 83-95 Ma (Mattinson and James, 1985) which suggests that these folds and the accompanying amphibolite facies metamorphism are of Late Cretaceous age. The orientation and style, common map-scale size, age, and amphibolite metamorphic grade of these second generation folds in the Salinian block are very similar to

the NW trending F3 folds developed in the Tehachapi Intrusive Complex and metasedimentary rocks of the eastern Tehachapi Mountains.

Steep-axis Folds

In an apparent third major deformation of the crystalline rocks in the Salinian block the granitic and metasedimentary rocks in the southern Santa Lucia Range, and also possibly the basement rocks in the northern Gabilan Range and Ben Lomond Mountain area, were deformed by steep-axis map- and mesoscale folds. This deformation corresponds to the second folding episode recognized by Compton (1966b; 1966a) in the Junipero Serra area of the southern Santa Lucia Range in which the layered basement rocks were repeated across several open to tight loops that have steeply plunging axes. These steep-axis folds trend at about right angles to the Santa Lucia Range and a number of quartz dioritic and granitic plutons emplaced before and/or during the folding have curving contacts that parallel the folds, and lineations in some of the plutons that are from the earlier NW trending folding event are deflected in these second folds as well (Compton, 1966b; Compton, 1966a). Compton (1966b) notes that large-scale steeply plunging folds like those present in the Junipero Serra area appear to be absent elsewhere in the Santa Lucia Range. The map-scale steep-axis folds in the southern part of the Junipero Serra quadrangle (Compton, 1966b; Compton, 1966a) appear to fold the lithologic layering of the basement rocks into the form of a large "z" which suggests the folds have a dextral sense of vergence (Bell, 1981).

Steeply plunging mesoscale and map-scale folds also are present in the metasedimentary rocks in the northern Gabilan Range (Compton, 1966b; John, 1981). The E-W trending metasedimentary pendant at Fremont Peak in the Gabilan Range changes trend at its west end to a N-NW trend and defines a map-scale steeply plunging fold (Compton, 1966b). The second deformation in the Fremont Peak area of the northern Gabilan Range, coeval with intrusion of the Fremont Peak quartz monzonite, produced

small-scale open folds with axes that plunge 40° to 70° to the N or S and also a local crenulation cleavage (John, 1981). John (1981) notes that these small folds are similar in orientation to the second generation steep-axis folds of Compton (1966b) which suggests they may correlate with the third generation of folds in the Salinian block as a whole. These late steep-axis folds in the Salinian block basement are younger than the N-NW trending subhorizontal folds in the Junipero Serra area which formed sometime between 95-83 Ma, and the steep-axis folds are older than Campanian age (84-74.5 Ma on DNAG time scale (Palmer, 1983)) fossiliferous marine strata deposited on top of the metamorphosed basement rocks (Compton, 1966b). The steep plunges, local dextral-sense vergence, and age of these late folds in the Salinian block are similar to the F4 oroclinal folds in the eastern Tehachapi Mountains region.

Late Recrystallized and Mylonitic Fabrics

The metasedimentary rocks in the Junipero Serra quadrangle and nearby areas of the Santa Lucia Range exhibit evidence in thin section for widespread recrystallization and cataclasis of probable Late Cretaceous age (Compton, 1966b; Compton, 1966a). Compton notes that the marbles commonly are crushed or extensively recrystallized and also that the degree of deformation of the metasedimentary rocks apparently increases to the southwest where quartzofeldspathic rocks locally are blastomylonitic. Foliation in the southwest corner of the Junipero Serra quadrangle dips mostly shallowly to the NE (Compton, 1966a). Minor folds in the mylonitic rocks have NW trends and subhorizontal plunges, and stress analyses of twinned calcite grains in the marbles and quartz deformation lamellae in quartz-bearing rocks indicate that the axis of maximum compressive stress plunged moderately to steeply to the SW (Compton, 1966b). Local zones of fine grained porphyroclastic marble are also present in the northern Gabilan Range (Compton, 1966b).

Compton (1966b; 1966a) infers that these post-granitic zones of mylonite and cataclasis formed during or immediately prior to large-scale uplift of the high-grade

metamorphic rocks of the Salinian block in the Late Cretaceous. While there are no published kinematic data on these mylonitic rocks in the Salinian block their apparent concentration along the southwest margin of the Santa Lucia Range, the NW trends and shallow plunges of folds in the mylonite, and the observation that they are the latest major structures in the metamorphic rocks all suggest that they may be part of a major NW trending zone of ductile shearing possibly similar to the eastern Tehachapi shear zone.

James (1992) suggested that prior to Late Cretaceous and Cenozoic tectonism in southern California that the Ben Lomond Mountain area of the Salinian block may have been located along strike to the south of the Tehachapi area in the southernmost Sierra Nevada based on similarities in U-Pb ages, discordance characteristics, and inheritance patterns of the plutonic rocks in both areas. The remarkable similarity between the sequence of F2, F3, and F4 folding followed by the eastern Tehachapi ductile shear zone in the Tehachapi Valley area with the sequence of Cretaceous deformation structures in the northern Salinian block described above lends support to the suggestion of James (1992) that the two areas may have evolved adjacent to one another.

POSSIBLE MECHANISMS FOR WESTWARD/DEXTRAL OFFSETS

A number of different tectonic models have been proposed to account for the pre-San Andreas fault system apparent westward displacement and/or dextral deflection of geologic features in the southern Sierra Nevada-Mojave Desert-Salinian region. The proposed models are divided into five different groups based on their underlying tectonic mechanism: 1) Late Cretaceous to Oligocene age dextral-sense offset along either a proto-San Andreas fault (Suppe, 1970; Nilsen, 1978) or other NW trending strike-slip faults (Howell, 1975; Howell, 1976), 2) a major Late Cretaceous to Eocene age right-lateral intraplate oroclinal bend (Burchfiel and Davis, 1981), 3) early Cenozoic and/or Late Cretaceous west-vergent thrusting along low-angle faults (Silver, 1982; Silver, 1983; May, 1989; Hall, 1991), 4) early Miocene age localized extension (Glazner et al., 1989) and/or

extension-related right-lateral transfer faulting in the central Mojave Desert (Martin et al., 1993), and 5) regional Late Cretaceous age west-directed extension (Malin et al., 1995). While the model(s) invoking early Miocene extension as the mechanism for the apparent dextral-sense displacements do not address offset features outside the central Mojave Desert area they are included above because Burchfiel and Davis (1981) considered the apparent dextral deflection of features in the central Mojave Desert, in addition to deflected features in the Sierra Nevada and Salinia, as evidence for their orocline model.

The results of this study may shed some light on the possible mechanism(s) of the regional deformation which resulted in the apparent westward displacement and dextral offset of the continental margin in the southern Sierra Nevada-Mojave Desert region. The presence of possible Late Cretaceous age extensional faulting in the southern Sierra Nevada region suggests that some of the apparent westward displacement of batholithic rocks in the region may be due to extension of the crust at the latitude of the Mojave Desert, as has been suggested by Malin et al. (1995), even though the inferred extension direction in the southern Sierra Nevada is not west directed. The expanded width of the exposures of Cretaceous plutonic rocks in the Mojave Desert-Salinian region relative to the width of the exposures of presumably correlative plutonic rocks in the Sierra Nevada batholith to the north is consistent with extension of the former region as was noted by Malin et al. (1995). Miocene age extension must account for some of this apparent westward displacement (Glazner et al., 1989; Dokka, 1989; Tennyson, 1989), but not all of it. Martin et al. (1993) suggested that displacement along the Early Miocene Waterman Hills detachment fault in the central Mojave Desert may be 60-70 km based on the apparent offset of a number of regional geologic features, but Fillmore et al. (1994) suggested that there is only ~24 km of Early Miocene age extension along the fault based on the offset of synextensional sedimentary deposits. The 36-46 km difference between the Early Miocene estimate for

displacement along the fault and the inferred total displacement may have resulted from Late Cretaceous age extension.

The possibly coeval contractional deformation of the lower to middle crust and extensional deformation of the upper crust in Late Cretaceous time in the study area as discussed above suggests that both thrust faulting, as proposed by Silver (1982; 1983), and low-angle normal faulting, as proposed by Malin et al. (1995) and suggested above, may have played a role in the overall westward displacement of the rocks in the region. Slabs or wedges of middle and lower crustal gneisses in the southern Sierran-Mojave-Salinian region, bounded below by thrust faults and above by generally E dipping extensional faults may have been extruded westward relative to correlative rocks to the north in the Sierra Nevada and also westward relative to Rand schist being underthrust to the east. This possible mechanism for the regional deformation is analogous to the model proposed for Miocene deformation in the Himalayas where a sliver of the middle crust appears to have been extruded to the south relative to the adjacent lower and upper crust along coeval thrust and low-angle normal faults, respectively (Burchfiel and Royden, 1985; Hodges et al., 1992; Burchfiel et al., 1992b). Some of the apparent westward displacement of upper crustal rocks, such as the rocks in the hangingwall of the Pastoria fault and the rocks in the southern Tehachapi Mountains, may be partly the result of their being carried along, piggy-back-style, on top of mid- or lower crustal rocks extruding relatively westward.

While much of the apparent westward displacement of out-of-place rocks in the southern Sierra-Mojave-Salinian region may have occurred along low-angle thrust and extensional faults some of the results of this study also indicate that dextral-sense oroclinal folding similar to what was proposed by Burchfiel and Davis (1981) also may have been an important element in the regional deformation. As outlined in the previous section the structural histories of the northern Salinian block and the southern Sierra Nevada are

remarkably similar. Perhaps the most significant structural similarity between these two areas is the presence of the late steep-axis folds, some of which appear to have dextral vergence, in the metamorphosed basement rocks. In the Cretaceous batholith belt of California large-scale relatively steep-axis basement folds of known or suspected Late Cretaceous age have, to this author's knowledge, only been recognized in the southernmost Sierra Nevada, the Salinian block, and in local areas of the central Mojave Desert at Iron Mountain (Boettcher and Walker, 1993) and in the area around Fremont Peak and the Buttes (Miller et al., 1992; Dibblee, 1968). The coincidence of these occurrences of suspected Late Cretaceous age steep-axis basement folds with the disrupted region of the continental margin suggests that the formation of the folds may be related to the disruption.

The displacement to the NW of the geologic features in the region suggests a dextral component of shearing during the deformation as noted by Burchfiel and Davis (1981). Decoupling of the lower and upper crust along low-angle faults may have allowed the lower crust to accommodate the dextral component of shearing by dextral ductile oroclinal folding while brittle plates of upper crustal rocks responded by wholesale clockwise rotation. Part of the apparent westward displacement of the rocks in the upper plate of the Pastoria fault may have resulted from piggy-backing on top of lower crustal rocks that are being deflected to the west by large-scale F4 dextral oroclinal folds. For example, if the Tehachapi Valley and Walker Basin oroclines are unfolded such that the pendants are restored to an inferred original N-NW trend while keeping the hangingwall rocks above the Pastoria fault fixed above the western Tehachapi gneiss complex then the Pastoria fault upper plate rocks are restored to a position eastward of their current position. The dextral vergence of some of the lower crustal steep-axis folds and the clockwise rotation of the upper crustal plates in the southern Sierran-Mojave-Salinian region is consistent with the presence of Late Cretaceous age right-lateral strike-slip faults in the Sierra Nevada, e.g., (Busby-Spera and Saleeby, 1990), and also with plate tectonic evidence for relatively rapid

oblique dextral convergence between the North American and Farallon plates in the Late Cretaceous (Engebretson et al., 1985).

CENOZOIC DEFORMATION IN THE SOUTHERN SIERRA NEVADA REGION

MENDIBURU CANYON FAULT AND POSSIBLE RELATED STRUCTURES

The Mendiburu Canyon fault is interpreted to be a shallow SE dipping thrust fault along which granitic rocks hangingwall moved to the northwest over Witnet Formation and other granitic rocks in the footwall. Folding and local overturning of the Witnet Formation along the Mendiburu Canyon fault most likely occurred prior to deposition of the Early Miocene age Kinnick Formation across the probably correlative Oil Canyon fault northeast of Tehachapi Valley. The age of the Witnet Formation is unknown but it may correlate with the Goler Formation in the El Paso Mountains some of which is Early Eocene in age. Thus, the fault appears to have been active sometime between Early Eocene and Early Miocene time. Activity along the Mendiburu Canyon fault may be related to the inferred early Cenozoic age W vergent thrusting in the Mojave Desert-southern Sierra Nevada region proposed by Silver (Silver, 1982; Silver, 1983). Alternatively, it may be related to a late Eocene to middle Oligocene age uplift and crustal shortening event called the Ynezan orogeny which has been recognized in the southern San Joaquin Valley (Davis and Lagoe, 1988; Goodman and Malin, 1992) and elsewhere in southern and central California (White and Davis, 1989). The Caballo Canyon fault in the San Emigdio Mountains (Figure 2) is a SW vergent thrust fault that was active during the Oligocene (Davis and Lagoe, 1988). The Beno Springs and El Paso faults of Malin et al. (1995) in the western Tehachapi Mountains have a similar orientation to the Mendiburu Canyon fault and may have been active at the same time.

POSSIBLE MIOCENE EXTENSION AND CRUSTAL ROTATIONS IN THE SOUTHERN SIERRA NEVADA

Northeast directed early Miocene extension is well documented in the central Mojave Desert (Dokka, 1986; Glazner et al., 1989; Dokka, 1989; Walker et al., 1990; Fletcher et al., 1995; Walker et al., 1995) and late Oligocene-early Miocene age extension is documented in the southern San Joaquin Basin (Goodman et al., 1989; Goodman and Malin, 1992). The presence of early Miocene age extensional faulting east and west of the Tehachapi Mountains suggests that the fault systems may continue through the Tehachapi Mountains region. The best candidate in the study area for a normal fault with a NE extension direction is the inferred Tehachapi Valley fault, but as discussed earlier there is no direct evidence for the age of activity along this fault. Indirect evidence such as the penetrative top to the NE shearing in part of the Brushy Ridge leucogranite suggests the inferred Tehachapi Valley fault may have been active during intrusion of the probable Late Cretaceous age Brushy Ridge granite. On the other hand, the possible correlation of the Tehachapi Valley fault with the Edison fault mapped by Dibblee and Warne (1988) suggests it also may have been active in late Oligocene-early Miocene time. If the Waterman Hills detachment fault in the central Mojave Desert does not continue northwest across the Garlock fault into the Tehachapi Mountains then early Miocene displacement along the fault might have been accommodated by a right-lateral transfer fault in the approximate position of the current Garlock fault as suggested by Dokka (1989).

Data from paleomagnetic studies on both Miocene age sedimentary and volcanic rocks and Cretaceous age crystalline basement rocks in the Tehachapi-San Emigdio Mountains have been interpreted as indicating that some parts of the southernmost part of the Sierra Nevada have been rotated in a clockwise sense about a vertical axis. The sites where paleomagnetic data have been gathered are shown in Figure 2. Miocene age rocks north and northeast of Tehachapi Valley and southeast of the Jawbone Canyon fault show

no vertical axis rotation, but tonalite immediately northwest of Tehachapi Valley is interpreted to be rotated 45° clockwise about a vertical axis (Kanter and McWilliams, 1982). Cretaceous plutonic rocks south of Kelso Valley and northwest of the Breckenridge fault do not appear to be rotated, but Cretaceous orthogneiss east of Interstate 5 in the western Tehachapi Mountains is interpreted to be rotated 59° clockwise (McWilliams and Li, 1985), and McWilliams and Li (1983) report paleomagnetic data suggesting that the Lebec granodiorite in the western Tehachapi Mountains is rotated clockwise by more than 90°. Miocene volcanic rocks in the San Emigdio Mountains appear to be rotated clockwise 44° (Graham et al., 1990). Plescia and Calderone (1986) reported that Miocene volcanic rocks in the western Tehachapi Mountains appear to be rotated clockwise 40°, but in a later study of the Miocene volcanic rocks in the same area Plescia et al. (1994) reported that the paleomagnetic data set probably does not adequately average secular variation and they conclude that the data do not support vertical axis clockwise rotation of the Miocene rocks.

Given the conflicting evidence for clockwise rotation of the Miocene age rocks noted above it is difficult to assess the significance of possible Miocene and younger rotations of the crust in parts of the southern Sierra Nevada relative to inferred earlier clockwise rotations of the Cretaceous basement rocks as suggested by Kanter and McWilliams (1982) and McWilliams and Li (1985). It does not appear likely, however, that there has been any differential rotation between the eastern Tehachapi gneiss complex and the Oak Creek Pass complex along the Blackburn Canyon fault since the Miocene. The major swarms of inferred Miocene age volcanic dikes in the granitic rocks of the hangingwall and the gneissic rocks of the footwall have generally E-W trends and lie along strike from each other which suggests that since the emplacement of the dikes that the plates have not rotated relative to each other.

GARLOCK FAULT

The Garlock fault is a major NE to E trending sinistral strike-slip fault zone that separates the Sierra Nevada and Basin and Range region to the north from the Mojave Desert to the south and it has accumulated as much as 48 to 64 km of displacement along the section of the fault east of the Sierra Nevada (Hill and Dibblee, 1953; Smith, 1962; Davis and Burchfiel, 1973). As was mentioned previously the displacement along the western part of the Garlock fault is not well constrained, but based on correlation of similar granitic rocks north and south of the fault Ross (1989b) suggested that left-lateral displacement along the fault was ~45-50 km. Loomis and Burbank (1988) suggest that activity along the Garlock fault began about 9-10 Ma. The Garlock fault in the eastern Tehachapi Mountains area has been mapped by a number of different workers (Clark, 1973; Dibblee and Louke, 1970; Sharry, 1981), but it was not examined in detail in this study.

CHAPTER V: SUMMARY AND CONCLUSIONS

Two sequences of metasedimentary rocks in the Tehachapi Valley area, the Antelope Canyon group and the Brite Valley group, were defined and mapped in this study. The boundary between these two metasedimentary sequences closely coincides with the initial Sr 0.706 isopleth in the batholithic rocks (Kistler and Ross, 1990), it occurs along a major change in the composition of the batholithic rocks (Ross, 1989b), and it also appears to be located between plutons that have different zircon inheritance characteristics (Saleeby et al., 1987). The form of several tabular or sheetlike plutons, which intrude along (?) or close to the boundary between the two groups of metasedimentary rocks, may have been controlled by a preexisting structure. Juxtaposition of the two groups of paragneiss along this hypothetical structural (?) discontinuity is inferred to have occurred prior to intrusion of the plutons which have known and suspected mid- to Early Cretaceous ages of ~100-117 Ma (Saleeby et al., 1987). The Water Canyon fault may be a transposed remnant of this inferred cryptic pre-mid-Cretaceous discontinuity and the eastern Tehachapi shear zone may be a Late Cretaceous reactivation of the discontinuity.

The eastern Tehachapi gneiss complex is interpreted to have experienced a protracted episode of contractional deformation from ~100 Ma to ~80 Ma. Following and possibly synchronous with intrusion of the Tehachapi Intrusive Complex the gneiss complex was deformed during amphibolite facies metamorphism by map-scale NW trending SW vergent F3 folds. In the late stages of the F3 folding the gneiss complex and a large portion of the southernmost Sierra Nevada batholith were folded in a series of regional-scale oroclinal F4 folds which appear to have dextral vergence. The eastern Tehachapi shear zone is a NW trending shallow NE dipping greenschist grade ductile shear zone ~1 km wide which traverses the gneiss complex and has top to the S-SW shear sense. The shear zone is inferred to have been active between ~85 Ma and ~80 Ma coeval with the later stages of F4 folding. The shear zone also appears to be coeval and continuous with

the subvertical and dextral-sense proto-Kern Canyon fault zone located in the Lake Isabella region to the north (Busby-Spera and Saleeby, 1990).

Structurally overlying the eastern Tehachapi gneiss complex along the SE dipping low-angle Blackburn Canyon detachment fault is the Oak Creek Pass complex. The Oak Creek Pass complex is composed of greenschist and lower grade cataclastically deformed upper crustal granodioritic rocks of inferred Late Cretaceous age that locally are nonconformably overlain by arkosic sandstones and conglomerates of the Witnet Formation. The Blackburn Canyon fault and other nearby previously recognized low-angle faults are all interpreted to be part of a major regional extensional fault system along which the southeastern part of the Sierra Nevada batholith was exhumed. The Witnet Formation is hypothesized to have been deposited in a supradetachment basin adjacent to the fault system while it was active. Indirect age constraints for the inferred extensional faulting suggest it occurred during the Late Cretaceous and possibly during the early Cenozoic (?) as well. Lower crustal contraction and upper crustal extension may have been coeval in the southernmost Sierra Nevada during the Late Cretaceous and might be analogous to the simultaneous shortening and extension documented in the Himalayan orogen (Hodges et al., 1992).

The mid- to Late Cretaceous deformation history of the eastern Tehachapi gneiss complex is remarkably similar to the deformation history of the northern Salinian block of coastal central California. The sequence of NE trending F2 folds, NW trending F3 folds, and dextral-sense oroclinal F4 folds followed by the eastern Tehachapi shear zone is similar to a sequence of Cretaceous age folding and shearing episodes that appears to be present in the Salinian block. This structural correlation supports the results of previous workers (Silver, 1982; Ross, 1984; Silver and Mattinson, 1986; James, 1992) who have suggested, based on petrologic, isotopic, and geochronologic data, that the northern Salinian block was tectonically displaced from the southernmost Sierra Nevada-Mojave Desert region.

REFERENCES

- Ague, J. J., and Brimhall, G. H., 1987, Granites of the batholiths of California: Products of local assimilation and regional-scale crustal contamination: *Geology*, v. 15, p. 63-66.
- Ague, J. J., and Brimhall, G. H., 1988a, Magmatic arc asymmetry and distribution of anomalous plutonic belts in the batholiths of California: Effects of assimilation, crustal thickness, and depth of crystallization: *Geological Society of America Bulletin*, v. 100, p. 912-927.
- Ague, J. J., and Brimhall, G. H., 1988b, Regional variations in bulk chemistry, mineralogy, and the compositions of mafic and accessory minerals in the batholiths of California: *Geological Society of America Bulletin*, v. 100, p. 891-911.
- Allmendinger, R. W., 1995, unpublished, Manual for Stereonet Plotting Program-Version 4.9 for Macintosh Computers, 45 p.
- Anderson, E. M., 1951, *The Dynamics of Faulting and Dyke Formation with Applications for Great Britain*: London, Oliver and Boyd, 206 p.
- Anderson, T. H., and Schmidt, V. A., 1983, The evolution of Middle America and the Gulf of Mexico-Caribbean Sea region during Mesozoic time: *Geological Society of America Bulletin*, v. 94, p. 941-966.
- Anderson, T. H., and Silver, L. T., 1979, The role of the Mojave-Sonora megashear in the tectonic evolution of northern Sonora, *in* Anderson, T. H., and Roldan-Quintana, J., eds., *Geology of Northern Sonora: Geological Society of America Annual Meeting Guidebook - Fieldtrip #27*, p. 59-68.
- Applegate, J. D. R., and Hodges, K. V., 1995, Mesozoic and Cenozoic extension recorded by metamorphic rocks in the Funeral Mountains, California: *Geological Society of America Bulletin*, v. 107, p. 1063-1076.
- Applegate, J. D. R., Walker, J. D., and Hodges, K. V., 1992, Late Cretaceous extensional unroofing in the Funeral Mountains metamorphic core complex, California: *Geology*, v. 20, p. 519-522.
- Armstrong, R. L., and Suppe, J., 1973, Potassium-argon geochronometry of Mesozoic igneous rocks in Nevada, Utah, and southern California: *Geological Society of America Bulletin*, v. 84, p. 1375-1392.
- Barth, A. P., 1996, Episodic uplift in the central Transverse Ranges and a model for Cretaceous - Eocene orogenesis in southern California: *Geological Society of America Abstracts with Programs*, v. 28, p. 47.
- Bateman, P. C., 1992, Plutonism in the central part of the Sierra Nevada batholith, California: U. S. Geological Survey Professional Paper 1483, 186 p.
- Bateman, P. C., Busacca, A. J., and Sawka, W. N., 1983, Cretaceous deformation in the western foothills of the Sierra Nevada, California: *Geological Society of America Bulletin*, v. 94, p. 30-42.
- Bateman, P. C., and Dodge, F. C. W., 1970, Variations of major chemical constituents across the central Sierra Nevada batholith: *Geological Society of America Bulletin*, v. 81, p. 409-420.
- Bell, A. M., 1981, Vergence: an evaluation: *Journal of Structural Geology*, v. 3, p. 197-202.
- Berthé, D., Choukroune, P., and Jegouzo, P., 1979, Orthogneiss, mylonite and non coaxial deformation of granites: the example of the South Armorican Shear Zone: *Journal of Structural Geology*, v. 1, p. 31-42.
- Boettcher, S. S., and Walker, J. D., 1993, Geologic evolution of Iron Mountain, central Mojave Desert, California: *Tectonics*, v. 12, p. 372-386.

- Brown, H. J., 1982, Possible Cambrian miogeoclinal strata, northern Shadow Mountains, western Mojave Desert, *in* Fife, D. L., and Minch, J. A., eds., *Geology and Mineral Wealth of the California Transverse Ranges [Mason Hill Volume]*: Santa Ana, California, South Coast Geological Society, Inc., p. 355-365.
- Bucher, K., and Frey, M., 1994, *Petrogenesis of Metamorphic Rocks*: Berlin, Springer-Verlag, 318 p.
- Burchfiel, B. C., Cowan, D. S., and Davis, G. A., 1992a, Tectonic overview of the Cordilleran orogen in the western United States, *in* Burchfiel, B. C., Lipman, P. W., and Zoback, M. L., eds., *The Cordilleran Orogen: Conterminous U. S.: The Geology of North America*: Boulder, Colorado, Geological Society of America, p. 407-479.
- Burchfiel, B. C., and Davis, G. A., 1972, Structural framework and evolution of the southern part of the Cordilleran orogen, western United States: *American Journal of Science*, v. 272, p. 97-118.
- Burchfiel, B. C., and Davis, G. A., 1981, Mojave Desert and environs, *in* Ernst, W. G., ed., *The Geotectonic Development of California [Rubey Volume I]*: Englewood Cliffs, New Jersey, Prentice-Hall, Inc., p. 217-252.
- Burchfiel, B. C., and Royden, L. H., 1985, North-south extension within the convergent Himalayan region: *Geology*, v. 13, p. 679-682.
- Burchfiel, B. C., Zhiliang, C., Hodges, K. V., Yuping, L., Royden, L. H., Changrong, D., and Jiene, X., 1992b, The south Tibetan detachment system, Himalayan orogen: Extension contemporaneous with and parallel to shortening in a collisional mountain belt: *Geological Society of America Special Paper* 269, 41 p.
- Busby-Spera, C. J., 1988, Speculative tectonic model for the early Mesozoic arc of the southwest Cordilleran United States: *Geology*, v. 16, p. 1121-1125.
- Busby-Spera, C. J., and Saleeby, J. B., 1988, An intrabatholithic strike-slip fault: evidence for a Cretaceous movement history of the Kern Canyon fault, southern Sierra Nevada, California: *Geological Society of America Abstracts with Programs*, v. 20, p. A272.
- Busby-Spera, C. J., and Saleeby, J. B., 1990, Intra-arc strike-slip fault exposed at batholithic levels in the southern Sierra Nevada, California: *Geology*, v. 18, p. 255-259.
- Buwalda, J. P., 1916, New mammalian faunas from Miocene sediments near Tehachapi Pass in the southern Sierra Nevada: *University of California Publications Bulletin of the Department of Geology*, v. 10, p. 75-85.
- Buwalda, J. P., 1920, Fault system at the southern end of the Sierra Nevada, California: *Geological Society of America Bulletin*, v. 31, p. 127.
- Buwalda, J. P., 1934, Tertiary tectonic activity in Tehachapi region: *The Pan-American Geologist*, v. 61, p. 309-310.
- Buwalda, J. P., 1935, Tertiary tectonic activity in the Tehachapi region, California: *Proceedings of the Geological Society of America for 1934*, p. 312.
- Buwalda, J. P., 1954, Geology of the Tehachapi mountains, California, part 9 of chapter 2, *in* Jahns, R. H., ed., *Geology of Southern California*: California Division of Mines Bulletin 170, p. 131-142.
- Champion, D. E., Howell, D. G., and Gromme, C. S., 1984, Paleomagnetic and geologic data indicating 2500 km of northward displacement for the Salinian and related terranes, California: *Journal of Geophysical Research*, v. 89, p. 7736-7752.
- Chen, J. H., and Moore, J. G., 1982, Uranium-lead isotopic ages from the Sierra Nevada batholith, California: *Journal of Geophysical Research*, v. 87, p. 4761-4784.
- Chen, J. H., and Tilton, G. R., 1991, Applications of lead and strontium isotopic relationships to the petrogenesis of granitoid rocks, central Sierra Nevada batholith, California: *Geological Society of America Bulletin*, v. 103, p. 439-447.

- Clark, M. M., 1973, Map showing recently active breaks along the Garlock and associated faults, California: U. S. Geological Survey Miscellaneous Geologic Investigations Map I-741, scale 1:24,000.
- Cloos, M., 1993, Lithospheric buoyancy and collisional orogenesis: subduction of oceanic plateaus, continental margins, island arcs, spreading ridges, and seamounts: *Geological Society of America Bulletin*, v. 105, p. 715-737.
- Cobbold, P. R., and Quinquis, H., 1980, Development of sheath folds in shear regimes: *Journal of Structural Geology*, v. 2, p. 119-126.
- Compton, R. R., 1960, Charnockitic rocks of Santa Lucia range, California: *American Journal of Science*, v. 258, p. 609-636.
- Compton, R. R., 1966a, Analyses of Pliocene-Pleistocene deformation and stresses in northern Santa Lucia Range, California: *Geological Society of America Bulletin*, v. 77, p. 1361-1380.
- Compton, R. R., 1966b, Granitic and metamorphic rocks of the Salinian block, California Coast Ranges: *California Division of Mines and Geology Bulletin* 190, p. 277-287.
- Cox, B. F., 1987, Stratigraphy, depositional environments, and paleotectonics of the Paleocene and Eocene Goler formation, El Paso mountains, California---geologic summary and roadlog, in Cox, B. F., ed., *Basin Analysis and Paleontology of the Paleocene and Eocene Goler Formation, El Paso Mountains, California*: Los Angeles, California, Pacific Section, Society of Economic Paleontologists and Mineralogists, p. 1-29.
- Crowell, J. C., 1952, Geology of the Lebec quadrangle, California: *California Division of Mines and Geology Special Report* 24, 23 p.
- Davis, G. A., and Burchfiel, B. C., 1973, Garlock fault: An intracontinental transform structure, southern California: *Geological Society of America Bulletin*, v. 84, p. 1407-1422.
- Davis, T. L., and Lagoe, M. B., 1988, A structural interpretation of major tectonic events affecting the western and southern margins of the San Joaquin valley, California, in Graham, S. A., ed., *Studies of the Geology of the San Joaquin basin*: Los Angeles, California, Pacific Section, Society of Economic Paleontologists and Mineralogists, p. 65-87.
- Dibblee, T. W., Jr., 1952, Geology of the Saltdale quadrangle: *California Division of Mines Bulletin* 160, p. 1-43.
- Dibblee, T. W., Jr., 1959, Preliminary geologic map of the Mojave Quadrangle, California: U. S. Geological Survey Mineral Investigations Field Studies Map MF-219, scale 1:62,000.
- Dibblee, T. W., Jr., 1963, Geology of the Willow Springs and Rosamond quadrangles, California, *Geologic Investigations of Southern California Deserts*: U. S. Geological Survey Bulletin 1089-C, p. 141-253.
- Dibblee, T. W., Jr., 1967, Areal geology of the western Mojave Desert, California: U. S. Geological Survey Professional Paper 522, 153 p.
- Dibblee, T. W., Jr., 1968, Geology of the Fremont Peak and Opal Mountain quadrangles, California: *California Division of Mines and Geology Bulletin* 188, 64 p.
- Dibblee, T. W., Jr., and Chesterman, C. W., 1953, Geology of the Breckenridge Mountain quadrangle: *California Division of Mines and Geology Bulletin* 168, 56 p.
- Dibblee, T. W., Jr., and Louke, G. P., 1970, Geologic Map of the Tehachapi quadrangle, Kern County, California: U. S. Geological Survey Miscellaneous Geologic Investigations Map I-607, scale 1:62,500.
- Dibblee, T. W., Jr., and Warne, A. H., 1970, Geologic Map of the Cummings Mountain quadrangle, Kern County, California: U. S. Geological Survey Miscellaneous Geologic Investigations Map I-611, scale 1:62,500.

- Dibblee, T. W., Jr., and Warne, A. H., 1988, Inferred relation of the Oligocene to Miocene Bealville fanglomerate to the Edison fault, Caliente canyon area, Kern County, California, *in* Graham, S. A., ed., *Studies of the Geology of the San Joaquin basin: Los Angeles, California*, Pacific Section, Society of Economic Paleontologists and Mineralogists, p. 223-231.
- Dickinson, W. R., 1981, Plate tectonic evolution of the southern Cordillera, *in* Dickinson, W. R., and Payne, W. D., eds., *Relations of tectonics to ore deposits in the southern Cordillera: Arizona Geological Society Digest 14*, p. 113-135.
- Dickinson, W. R., and Snyder, W. S., 1978, Plate tectonics of the Laramide orogeny, *in* Matthews, V., III, ed., *Laramide Folding Associated with Basement Block Faulting in the Western United States: Geological Society of America Memoir 151*, p. 355-366.
- Dillon, J. T., and Ehlig, P. L., 1993, Displacement on the southern San Andreas fault, *in* Powell, R. E., Weldon, R. J., II, and Matti, J. C., eds., *The San Andreas Fault System: Displacement, Palinspastic Reconstruction, and Geologic Evolution: Geological Society of America Memoir 178*, p. 199-216.
- Dixon, E. T., 1995, $^{40}\text{Ar}/^{39}\text{Ar}$ hornblende geochronology and evaluation of garnet and hornblende barometry, Lake Isabella to Tehachapi area, southern Sierra Nevada, California [M.S. thesis]: Ann Arbor, Michigan, University of Michigan, 63 p.
- Dixon, E. T., Essene, E. J., and Halliday, A. N., 1994, Critical tests of hornblende barometry, Lake Isabella to Tehachapi area, southern Sierra Nevada, California: EOS (American Geophysical Union Transactions), v. 75, p. 744.
- Doe, B. R., and Delevaux, M. H., 1973, Variations in lead-isotopic compositions in Mesozoic granitic rocks of California: A preliminary investigation: Geological Society of America Bulletin, v. 84, p. 3513-3526.
- Dokka, R. F., 1986, Patterns and modes of early Miocene crustal extension, central Mojave Desert, California, *in* Mayer, L., ed., *Extensional tectonics of the southwestern United States: A perspective on processes and kinematics: Geological Society of America Special Paper 208*, p. 75-95.
- Dokka, R. K., 1989, The Mojave extensional belt of southern California: Tectonics, v. 8, p. 363-390.
- Dumitru, T. A., 1990, Subnormal Cenozoic geothermal gradients in the extinct Sierra Nevada magmatic arc: Consequences of Laramide and post-Laramide shallow-angle subduction: Journal of Geophysical Research, v. 95, p. 4925-4941.
- Dumitru, T. A., Gans, P. B., Foster, D. A., and Miller, E. L., 1991, Refrigeration of the western Cordilleran lithosphere during Laramide shallow-angle subduction: Geology, v. 19, p. 1145-1148.
- Dunne, G. C., 1986, Geologic evolution of the southern Inyo range, Darwin plateau, and Argus and Slate ranges, east-central California-an overview, *in* Dunne, G. C., ed., *Mesozoic and Cenozoic Structural Evolution of Selected Areas, East-Central California: Geological Society of America, Cordilleran Section Fieldtrip Guidebook: Los Angeles, California, California State University*, p. 3-21.
- Dunne, G. C., Moore, J. N., Anderson, D., and Galbraith, G., 1975, The Bean Canyon formation of the Tehachapi mountains, California: An early Mesozoic arc-trench gap deposit?: Geological Society of America Abstracts with Programs, v. 7, p. 314.
- Ehlig, P. L., 1968, Causes of distribution of Pelona, Rand, and Orocopia schists along the San Andreas and Garlock faults: Proceedings of Conference on Geologic Problems of San Andreas Fault System, p. 294-306.
- Elan, R., 1985, High grade contact metamorphism at the Lake Isabella north shore roof pendant, southern Sierra Nevada, California [M.S. thesis]: Los Angeles, University of Southern California, 202 p.

- Engebretson, D. C., Cox, A., and Gordon, R. G., 1985, Relative motions between oceanic and continental plates in the Pacific basin: Geological Society of America Special Paper 206, 59 p.
- Evernden, J. F., and Kistler, R. W., 1970, Chronology of emplacement of Mesozoic batholithic complexes in California and western Nevada: U. S. Geological Survey Professional Paper 623, 42 p.
- Fedo, C. M., and Miller, J. M. G., 1992, Evolution of a Miocene half-graben basin, Colorado River extensional corridor, southeastern California: Geological Society of America Bulletin, v. 104, p. 481-493.
- Fillmore, R. P., Walker, J. D., Bartley, J. M., and Glazner, A. F., 1994, Development of three genetically related basins associated with detachment-style faulting: Predicted characteristics and an example from the central Mojave Desert, California: *Geology*, v. 22, p. 1087-1090.
- Fletcher, J. M., and Bartley, J. M., 1994, Constrictional strain in a non-coaxial shear zone: implications for fold and rock fabric development, central Mojave metamorphic core complex, California: *Journal of Structural Geology*, v. 16, p. 555-570.
- Fletcher, J. M., Bartley, J. M., Martin, M. W., Glazner, A. F., and Walker, J. D., 1995, Large-magnitude continental extension: an example from the central Mojave metamorphic core complex: Geological Society of America Bulletin, v. 107, p. 1468-1483.
- Fleuty, M. J., 1964, The description of folds: Proceedings of the Geologists' Association, London, v. 75, p. 461-492.
- Friedmann, S. J., Davis, G. A., Fowler, T. K., Brudos, T., Parke, M., Burbank, D. W., and Burchfiel, B. C., 1994, Stratigraphy and gravity-glide elements of a Miocene supradetachment basin, Shadow Valley, east Mojave Desert, *in* McGill, S. F., and Ross, T. M., eds., Geological Investigations of an Active Margin: Geological Society of America Cordilleran Section Guidebook, 27th Annual Meeting, p. 302-318.
- Froitzheim, N., 1992, Formation of recumbent folds during synorogenic crustal extension (Austroalpine nappes, Switzerland): *Geology*, v. 20, p. 923-926.
- Gapais, D., 1989, Shear structures within deformed granites: Mechanical and thermal indicators: *Geology*, v. 17, p. 1144-1147.
- Gazis, C., and Saleeby, J. B., 1991, Southward continuation of the proto-Kern Canyon fault zone (PKF) to the upper Caliente Creek area, southern Sierra Nevada: Geological Society of America Abstracts with Programs, v. 23, p. 28.
- George, P. G., and Dokka, R. K., 1994, Major Late Cretaceous cooling events in the eastern Peninsular Ranges, California, and their implications for Cordilleran tectonics: Geological Society of America Bulletin, v. 106, p. 903-914.
- Girty, G. H., 1977, Multiple regional deformation and metamorphism of the Boyden Cave roof pendant, central Sierra Nevada, California [M. A. thesis]: Fresno, California, California State University, 82 p.
- Glazner, A. F., Bartley, J. M., and Walker, J. D., 1989, Magnitude and significance of Miocene crustal extension in the central Mojave Desert, California: *Geology*, v. 17, p. 50-53.
- Glazner, A. F., Walker, J. D., Bartley, J. M., Fletcher, J. M., Martin, M. W., Schermer, E. R., Boettcher, S. S., Miller, J. S., Fillmore, R. P., and Linn, J. K., 1994, Reconstruction of the Mojave block, *in* McGill, S. F., and Ross, T. M., eds., Geological Investigations of an Active Margin: Geological Society of America Cordilleran Section Guidebook, 27th Annual Meeting, p. 3-30.
- Goodman, E. D., and Malin, P. E., 1992, Evolution of the southern San Joaquin Basin and mid-Tertiary "transitional" tectonics, central California: *Tectonics*, v. 11, p. 478-498.

- Goodman, E. D., Malin, P. E., Ambos, E. L., and Crowell, J. C., 1989, The southern San Joaquin Valley as an example of Cenozoic basin evolution in California, *in* Price, R. A., ed., *Origin and Evolution of Sedimentary Basins and their Energy and Mineral Resources: Geophysical Monograph 48, IUGC Series 4*: Washington, American Geophysical Union, p. 87-107.
- Goodyear, W. A., 1888, Kern county: California State Mining Bureau Report, v. 8, p. 309-324.
- Graham, S. A., Decelles, P. G., Carroll, A. R., and Goodman, E. D., 1990, Middle Tertiary contractile deformation, uplift, extension, and rotation in the San Emigdio range, southern California: *American Association of Petroleum Geologists Bulletin*, v. 74, p. 665.
- Greene, D. C., and Schweickert, R. A., 1995, The Gem Lake shear zone: Cretaceous dextral transpression in the northern Ritter Range pendant, eastern Sierra Nevada, California: *Tectonics*, v. 14, p. 945-961.
- Grove, K., 1993, Latest Cretaceous basin formation within the Salinian terrane of west-central California: *Geological Society of America Bulletin*, v. 105, p. 447-463.
- Haase, C. S., and Rutherford, M. J., 1975, The effect of pressure and temperature on the compositions of biotite and cordierite coexisting with sillimanite+quartz+sanidine (muscovite): *Geological Society of America Abstracts with Programs*, v. 7, p. 1094-1095.
- Hall, C. A., Jr., 1991, Geology of the Point Sur-Lopez Point region, Coast Ranges, California: A part of the southern California allochthon: *Geological Society of America Special Paper 266*, 40 p.
- Hamilton, W., 1988, Tectonic setting and variations with depth of some Cretaceous and Cenozoic structural and magmatic systems of the western United States, *in* Ernst, W. G., ed., *Metamorphism and Crustal Evolution of the Western United States [Rubey Volume VII]*: Englewood Cliffs, New Jersey, Prentice-Hall, Inc., p. 1-40.
- Hansen, E. C., and Stuk, M. A., 1989, Devolitization reactions in the amphibolite to granulite facies transitional terrane around Cone Peak, Santa Lucia Range, California: *Geological Society of America Abstracts with Programs*, v. 21, p. A277.
- Hanson, R. B., Saleeby, J. B., and Fates, D. G., 1987, Age and tectonic setting of Mesozoic metavolcanic and metasedimentary rocks, northern White Mountains, California: *Geology*, v. 15, p. 1074-1078.
- Harrison, T. M., 1981, Diffusion of ^{40}Ar in hornblende: *Contributions to Mineralogy and Petrology*, v. 78, p. 324-31.
- Henderson, L. J., Gordon, R. G., and Engebretson, D. C., 1984, Mesozoic aseismic ridges on the Farallon plate and southward migration of shallow subduction during the Laramide orogeny: *Tectonics*, v. 3, p. 121-132.
- Henry, C. D., 1986, East-northeast-trending structures in western Mexico: evidence for oblique convergence in the late Mesozoic: *Geology*, v. 14, p. 314-317.
- Hewett, D. F., 1954, General geology of the Mojave Desert region, California, part 1 of chapter 2, *in* Jahns, R. H., ed., *Geology of Southern California*: California Division of Mines Bulletin 170, p. 5-20.
- Hewett, D. F., 1955, Structural features of the Mojave Desert region: *Geological Society of America Special Paper 62*, p. 377-390.
- Hickman, S., Sibson, R., and Bruhn, R., 1995, Introduction to special section: Mechanical involvement of fluids in faulting: *Journal of Geophysical Research*, v. 100, p. 12,831-12,840.
- Hill, M. L., and Dibblee, T. W., Jr., 1953, San Andreas, Garlock and Big Pine faults, California - A study of the character, history, and tectonic significance of their displacements: *Geological Society of America Bulletin*, v. 64, p. 443-458.

- Hobbs, B. E., Means, W. D., and Williams, P. F., 1976, An outline of structural geology: New York, John Wiley & Sons, 571 p.
- Hodges, K. V., Parrish, R. R., Housh, T. B., Lux, D. R., Burchfiel, B. C., Royden, L. H., and Chen, Z., 1992, Simultaneous Miocene extension and shortening in the Himalayan orogen: *Science*, v. 258, p. 1466-1470.
- Hodges, K. V., and Walker, J. D., 1990, Petrologic constraints on the unroofing history of the Funeral Mountain metamorphic core complex, California: *Journal of Geophysical Research*, v. 95, p. 8437-8445.
- Hodges, K. V., and Walker, J. D., 1992, Extension in the Cretaceous Sevier orogen, North American Cordillera: *Geological Society of America Bulletin*, v. 104, p. 560-569.
- Holdaway, M. J., 1971, Stability of andalusite and the aluminum silicate phase diagram: *American Journal of Science*, v. 271, p. 97-131.
- Hollister, L. S., and Crawford, M. L., 1986, Melt-enhanced deformation: a major tectonic process: *Geology*, v. 14, p. 558-561.
- Howell, D. G., 1975, Hypothesis suggesting 700 km of right slip in California along northwest-oriented faults: *Geology*, v. 3, p. 81-83.
- Howell, D. G., 1976, Hypothesis suggesting 700 km of right slip in California along northwest-oriented faults: Reply: *Geology*, v. 4, p. 632-633.
- Jacobson, C. E., 1990, The $40\text{Ar}/39\text{Ar}$ geochronology of the Pelona schist and related rocks, southern California: *Journal of Geophysical Research*, v. 95, p. 509-528.
- Jacobson, C. E., Dawson, M. R., and Postlethwaite, C. E., 1988, Structure, metamorphism, and tectonic significance of the Pelona, Orocoxia, and Rand schists, southern California, in Ernst, W. G., ed., *Metamorphism and Crustal Evolution of the Western United States [Rubey Volume VII]*: Englewood Cliffs, New Jersey, Prentice-Hall, Inc., p. 976-997.
- Jacobson, C. E., Oyarzabal, F. R., and Haxel, G. B., 1996, Subduction and exhumation of the Pelona-Orocoxia-Rand schists, southern California: *Geology*, v. 24, p. 547-550.
- James, E. W., 1986, U/Pb age of the Antimony Peak tonalite and its relation to Rand schist in the San Emigdio Mountains: *Geological Society of America Abstracts with Programs*, v. 18, p. 121.
- James, E. W., 1989, Southern extension of the Independence dike swarm of eastern California: *Geology*, v. 17, p. 587-590.
- James, E. W., 1992, Cretaceous metamorphism and plutonism in the Santa Cruz mountains, Salinian block, California, and correlation with the southernmost Sierra Nevada: *Geological Society of America Bulletin*, v. 104, p. 1326-1339.
- James, E. W., and Mattinson, J. M., 1988, Metamorphic history of the Salinian block: An isotopic reconnaissance, in Ernst, W. G., ed., *Metamorphism and Crustal Evolution of the Western United States [Rubey Volume VII]*: Englewood Cliffs, New Jersey, Prentice-Hall, Inc., p. 938-952.
- Janecke, S. U., and Evans, J. P., 1988, Feldspar-influenced rock rheologies: *Geology*, v. 16, p. 1064-1067.
- John, D., 1981, Structure and petrology of pelitic schist in the Fremont peak pendant, northern Gabilan range, California: *Geological Society of America Bulletin*, Part 1, v. 92, p. 237-246.
- Kanter, L. R., and Debiche, M., 1985, Modeling the motion histories of the Point Arena and central Salinia terranes, in Howell, D. G., ed., *Tectonostratigraphic Terranes of the Circum-Pacific Region*: Houston, Circum-Pacific Council for Energy and Mineral Resources, p. 227-238.
- Kanter, L. R., and McWilliams, M. O., 1982, Rotation of the southernmost Sierra Nevada, California: *Journal of Geophysical Research*, v. 87, p. 3819-3830.

- Karish, C. R., Miller, E. L., and Sutter, J. F., 1987, Mesozoic tectonic and magmatic history of the central Mojave Desert, *in* Dickinson, W. R., and Klute, M. A., eds., *Mesozoic Rocks of Southern Arizona and Adjacent Areas: Arizona Geological Society Digest 18*, p. 15-32.
- Keith, S. B., 1978, Paleosubduction geometries inferred from Cretaceous and Tertiary magmatic patterns in southwestern North America: *Geology*, v. 6, p. 516-521.
- Kim, H. S., 1972, *Polymetamorphism of metasedimentary rocks in the southern Sierras, California [Ph.D. thesis]: Cleveland, Ohio, Case Western Reserve University, 199 p.*
- Kistler, R. E., and Peterman, Z. E., 1973, Variations in Sr, Rb, K, Na and initial $^{87}\text{Sr}/^{86}\text{Sr}$ in Mesozoic granitic rocks and intruded wall rocks, central California: *Geological Society of America Bulletin*, v. 84, p. 3489-3511.
- Kistler, R. W., 1974, Phanerozoic batholiths in western North America: A summary of some recent work on variations in time, space, chemistry, and isotopic composition: *Annual Reviews of Earth and Planetary Science*, v. 2, p. 403-418.
- Kistler, R. W., 1993, Mesozoic intrabatholithic faulting, Sierra Nevada, California, *in* Dunne, G. C., and McDougall, K. A., eds., *Mesozoic Paleogeography of the Western United States-II: Los Angeles, California, Pacific Section, Society of Economic Paleontologists and Mineralogists*, p. 247-262.
- Kistler, R. W., and Peterman, Z. E., 1978, Reconstruction of crustal blocks of California on the basis of initial strontium isotopic compositions of Mesozoic granitic rocks: *U. S. Geological Survey Professional Paper 1071*, 17 p.
- Kistler, R. W., and Ross, D. C., 1990, A strontium isotopic study of plutons and associated rocks of the southern Sierra Nevada and vicinity, California: *U. S. Geological Survey Bulletin 1920*, 20 p.
- Krummenacher, D., Gastil, R. G., Bushee, J., and Doupont, J., 1975, K-Ar apparent ages, Peninsular Ranges batholith, southern California and Baja California: *Geological Society of America Bulletin*, v. 86, p. 760-768.
- Lahren, M. M., and Schweickert, R. A., 1989, Proterozoic and Lower Cambrian miogeoclinal rocks of Snow Lake pendant, Yosemite-Emigrant Wilderness, Sierra Nevada, California: *Geology*, v. 17, p. 156-160.
- Lahren, M. M., Schweickert, R. A., Mattinson, J. M., and Walker, J. D., 1990, Evidence of uppermost Proterozoic to lower Cambrian miogeoclinal rocks and the Mojave-Snow Lake fault: Snow Lake pendant, central Sierra Nevada, California: *Tectonics*, v. 9, p. 1585-1608.
- Law, R. D., Morgan, S. S., Casey, M., Sylvester, A. G., and Nyman, M., 1992, The Papoose Flat pluton of eastern California: a reassessment of its emplacement history in the light of new microstructural and crystallographic fabric observations: *Transactions of the Royal Society of Edinburgh: Earth Sciences*, v. 83, p. 361-375.
- Lawson, A. C., 1906, The geomorphology of the Tehachapi valley system: *University of California Publications Bulletin of the Department of Geology*, v. 4, p. 431-462.
- Leo, G. W., 1967, The plutonic and metamorphic rocks of the Ben Lomond mountain area, Santa Cruz county, California: *California Division of Mines and Geology Special Report 91*, 27-43 p.
- Lin, S., and Williams, P. F., 1992a, The geometrical relationship between the stretching lineation and the movement direction of shear zones: *Journal of Structural Geology*, v. 14, p. 491-497.
- Lin, S., and Williams, P. F., 1992b, The origin of ridge-in-groove slickenside striae and associated steps in an S-C mylonite: *Journal of Structural Geology*, v. 14, p. 315-321.

- Lindgren, W., 1915, The igneous geology of the Cordilleras and its problems, *in* Rice, W. N., Adams, F. D., Coleman, A. P., Walcott, C. D., and others, eds., *Problems of American geology*: New Haven, Connecticut, Yale University Press, p. 234-286.
- Lister, G. S., and Snoke, A. W., 1984, S-C mylonites: *Journal of Structural Geology*, v. 6, p. 617-638.
- Livaccari, R. F., Burke, K., and Sengor, A. M. C., 1981, Was the Laramide orogeny related to subduction of an oceanic plateau?: *Nature*, v. 289, p. 276-278.
- Locke, A., Billingsley, P., and Mayo, E. B., 1940, Sierra Nevada tectonic pattern: *Geological Society of America Bulletin*, v. 51, p. 513-539.
- Longoria, J. F., 1985, Tectonic transpression in the Sierra Madre Oriental, northeastern Mexico: An alternative model: *Geology*, v. 13, p. 453-456.
- Loomis, D. P., and Burbank, D. W., 1988, The stratigraphic evolution of the El Paso basin, southern California: Implications for the Miocene development of the Garlock fault and uplift of the Sierra Nevada: *Geological Society of America Bulletin*, v. 100, p. 12-28.
- Louke, G. P., 1966, Geologic map of the Emerald Mountain Quadrangle, California, Unpublished map on file with the California Department of Conservation, Division of Mines and Geology, scale 1:62,500.
- MacKenzie, W. S., and Guilford, C., 1980, *Atlas of Rock-forming Minerals in Thin Section*: New York, John Wiley & Sons, 98 p.
- Maher, K. A., and Saleeby, J., 1988, Age constraints on the geologic evolution of the Jackson Mountains, NW Nevada: *Geological Society of America Abstracts with Programs*, v. 20, p. 177.
- Malavielle, J., 1987, Extensional shearing deformation and kilometer-scale "a" type folds in a Cordilleran metamorphic core complex (Raft River Mountains, northwestern Utah): *Tectonics*, v. 6, p. 423-448.
- Malin, P. E., Goodman, E. D., Henyey, T. L., Li, Y. G., Okaya, D. A., and Saleeby, J. B., 1995, Significance of seismic reflections beneath a tilted exposure of deep continental crust, Tehachapi mountains, California: *Journal of Geophysical Research*, v. 100, p. 2069-2087.
- Martin, M. W., Glazner, A. F., Walker, J. D., and Schermer, E. R., 1993, Evidence for right-lateral transfer faulting accommodating an echelon Miocene extension, Mojave Desert, California: *Geology*, v. 21, p. 355-358.
- Martin, M. W., and Walker, J. D., 1995, Stratigraphy and paleogeographic significance of metamorphic rocks in the Shadow Mountains, western Mojave Desert, California: *Geological Society of America Bulletin*, v. 107, p. 354-366.
- Mattinson, J. M., 1978, Age, origin, and thermal histories of some plutonic rocks from the Salinian block of California: *Contributions to Mineralogy and Petrology*, v. 67, p. 233-245.
- Mattinson, J. M., 1983, Basement rocks of the southeastern Salinian block, California: U-Pb isotopic relationships: *Geological Society of America Abstracts with Programs*, v. 15, p. 414.
- Mattinson, J. M., 1990, Petrogenesis and evolution of the Salinian magmatic arc, *in* Anderson, J. L., ed., *The Nature and Origin of Cordilleran Magmatism*: *Geological Society of America Memoir* 174, p. 237-250.
- Mattinson, J. M., and James, E. W., 1985, Salinian block U/Pb age and isotopic variations: Implications for origin and emplacement of the Salinian terrane, *in* Howell, D. G., ed., *Tectonostratigraphic Terranes of the Circum-Pacific Region*: Houston, Circum-Pacific Council for Energy and Mineral Resources, p. 215-226.
- May, D. J., 1989, Late Cretaceous intra-arc thrusting in southern California: *Tectonics*, v. 8, p. 1159-1173.

- May, D. J., and Walker, N. W., 1989, Late Cretaceous juxtaposition of metamorphic terranes in the southeastern San Gabriel Mountains, California: *Geological Society of America Bulletin*, v. 101, p. 1246-1267.
- McClay, K. R., 1987, *The Mapping of Geological Structures*, Geological Society of London Handbook Series: Milton Keynes, Open University Press, 161 p.
- McDougall, K., 1987, Foraminiferal biostratigraphy and paleoecology of marine deposits, Goler Formation, California, *in* Cox, B. F., ed., *Basin Analysis and Paleontology of the Paleocene and Eocene Goler Formation*, El Paso Mountains, California: Los Angeles, California, Pacific Section, Society of Economic Paleontologists and Mineralogists, p. 43-67.
- McKenna, M. C., Hutchison, J. H., and Hartman, J. H., 1987, Paleocene vertebrates and nonmarine mollusca from the Goler Formation, California, *in* Cox, B. F., ed., *Basin Analysis and Paleontology of the Paleocene and Eocene Goler Formation*, El Paso Mountains, California: Los Angeles, California, Pacific Section, Society of Economic Paleontologists and Mineralogists, p. 31-41.
- McWilliams, M., and Li, Y., 1983, A paleomagnetic test of the Sierran orocline hypothesis: EOS (American Geophysical Union Transactions), v. 64, p. 686.
- McWilliams, M., and Li, Y., 1985, Oroclinal bending of the southern Sierra Nevada batholith: *Science*, v. 230, p. 172-175.
- McWilliams, M. O., and Howell, D. G., 1982, Exotic terranes of western California: *Nature*, v. 297, p. 215-217.
- Michael, E. D., 1960, *The Geology of the Cache Creek Area, Kern County, California* [Master of Arts thesis]: Los Angeles, California, University of California, 141 p.
- Miller, E. L., 1981, *Geology of the Victorville region, California: Summary: Geological Society of America Bulletin, Part I*, v. 92, p. 160-163.
- Miller, E. L., and Cameron, C. S., 1982, Late Precambrian to late Cretaceous evolution of the southwestern Mojave Desert, California, *in* Cooper, J. P., Troxel, B. W., and Wright, L. A., eds., *Geology of selected areas in the San Bernardino Mountains, western Mojave Desert, and southern Great Basin, California: Field Trip Guidebook, 78th meeting of the Cordilleran Section, Geological Society of America*, p. 21-34.
- Miller, J. M. G., and John, B. E., 1988, Detached strata in a Tertiary low-angle normal fault terrane, southeastern California: a sedimentary record of unroofing, breaching, and continued slip: *Geology*, v. 16, p. 645-648.
- Miller, J. S., 1996, Pb/U crystallization age of the Papoose Flat pluton, White-Inyo Mountains, California: *Geological Society of America Abstracts with Programs*, v. 28, p. 91.
- Miller, J. S., Fletcher, J. M., Boettcher, S. S., Martin, M. W., and Glazner, A. F., 1992, Late Cretaceous deformation, plutonism and cooling around Fremont peak, central Mojave Desert, California: EOS (American Geophysical Union Transactions), v. 73, p. 574.
- Miller, J. S., Glazner, A. F., and Crowe, D. E., 1996, Muscovite-garnet granites in the Mojave Desert: relation to crustal structure of the Cretaceous arc: *Geology*, v. 24, p. 335-338.
- Miller, J. S., Glazner, A. F., Walker, J. D., and Martin, M. M., 1995, Geochronologic and isotopic evidence for Triassic-Jurassic emplacement of the eugeoclinal allochthon in the Mojave Desert region, California: *Geological Society of America Bulletin*, v. 107, p. 1441-1457.
- Miller, W. J., and Webb, R. W., 1940, Descriptive geology of the Kernville quadrangle, California: *California Journal of Mines and Geology*, v. 36, p. 343-378.
- Moore, J. G., 1959, The quartz diorite boundary line in the western United States: *Journal of Geology*, v. 67, p. 198-210.

- Mount, V. S., and Suppe, J., 1992, Present-day stress orientations adjacent to active strike-slip faults: California and Sumatra: *Journal of Geophysical Research*, v. 97, p. 11,995-12,013.
- Moxon, I. W., 1988, Sequence stratigraphy of the Great Valley basin in the context of convergent margin tectonics, *in* Graham, S. A., ed., *Studies of the Geology of the San Joaquin basin: Los Angeles, California*, Pacific Section, Society of Economic Paleontologists and Mineralogists, p. 3-28.
- Naeser, N. D., Naeser, C. W., and McCulloh, T. H., 1990, Thermal history of rocks in southern San Joaquin valley, California: Evidence from fission-track analysis: *American Association of Petroleum Geologists Bulletin*, v. 74, p. 13-29.
- Nilsen, T. H., 1978, Late Cretaceous geology of California and the problem of the proto-San Andreas fault, *in* Howell, D. G., and McDougall, K. A., eds., *Mesozoic Paleogeography of the Western United States: Pacific Coast Paleogeography Symposium: Los Angeles, California*, Pacific Section, Society of Economic Paleontologists and Mineralogists, p. 559-573.
- Nilsen, T. H., 1987, Paleogene tectonics and sedimentation of coastal California, *in* Ingersoll, R. V., and Ernst, W. G., eds., *Cenozoic Basin Development of Coastal California [Rubey Volume VI]: Englewood Cliffs, New Jersey*, Prentice-Hall, Inc., p. 81-123.
- Nilsen, T. H., and Clarke, S. H., 1975, Sedimentation and tectonics in the early Tertiary continental borderland of central California: *U. S. Geological Survey Professional Paper 925*, 64 p.
- Nokleberg, W. J., 1981, Stratigraphy and structure of the Strawberry Mine roof pendant central Sierra Nevada, California: *U. S. Geological Survey Professional Paper 1154*, 18 p.
- Nokleberg, W. J., and Kistler, R. W., 1980, Paleozoic and Mesozoic deformations in the central Sierra Nevada, California: *U. S. Geological Survey Professional Paper 1145*, 24 p.
- Nourse, J. A., 1989, Geologic evolution of two crustal scale shear zones, Part I: The Rand thrust complex, northwestern Mojave desert, California, Part II: The Magdalena metamorphic core complex, north central Sonora, Mexico [Ph.D. thesis]: Pasadena, California, California Institute of Technology, 394 p.
- Nourse, J. A., and Silver, L. T., 1986, Structural and kinematic evolution of sheared rocks in the Rand "Thrust" complex, northwest Mojave Desert, California: *Geological Society of America Abstracts with Programs*, v. 18, p. 165.
- Oldow, J. S., 1984, Evolution of a late Mesozoic back-arc fold and thrust belt, northwestern Great Basin, U.S.A.: *Tectonophysics*, v. 102, p. 245-274.
- Page, B. M., 1982, Migration of Salinian composite block, California, and disappearance of fragments: *American Journal of Science*, v. 282, p. 1694-1734.
- Palmer, A. R., compiler, 1983, The decade of North American geology 1983 geologic time scale: *Geology*, v. 11, p. 503-504.
- Passchier, C. W., and Simpson, C., 1986, Porphyroclast systems as kinematic indicators: *Journal of Structural Geology*, v. 8, p. 831-843.
- Paterson, S. R., Brudos, T., Fowler, K., Carlson, C., Bishop, K., and Vernon, R. H., 1991, Papoose Flat pluton: Forceful expansion or post-emplacement deformation: *Geology*, v. 19, p. 324-327.
- Paterson, S. R., Vernon, R. H., and Tobisch, O. T., 1989, A review of criteria for the identification of magmatic and tectonic foliations in granitoids: *Journal of Structural Geology*, v. 11, p. 349-363.
- Peacock, S. M., 1988, Inverted metamorphic gradients in the westernmost Cordillera, *in* Ernst, W. G., ed., *Metamorphism and Crustal Evolution of the Western United*

- States [Rubey Volume VII]: Englewood Cliffs, New Jersey, Prentice-Hall, Inc., p. 953-975.
- Peck, D. L., and Van Kooten, G. K., 1983, Merced Peak quadrangle, central Sierra Nevada—Analytic data: U. S. Geological Survey Professional Paper 1170-D, p. 29.
- Peters, C. M. F., 1972, A structural interpretation of the Garlock fault zone at the Tehachapi crossing, *in* Lane, K. S., and Garfield, L. A., eds., Proceedings North American Rapid Excavation and Tunneling Conference, Chicago, Illinois, June 5-7, 1972, Volume 1: New York, The American Institute of Mining, Metallurgical and Petroleum Engineers, Inc., p. 133-155.
- Pickett, D. A., and Saleeby, J. B., 1991, The Cretaceous gneissic rocks of the Tehachapi mountains, southern Sierra Nevada batholith—correlatives of Salinia?: Geological Society of America Abstracts with Programs, v. 23, p. 89.
- Pickett, D. A., and Saleeby, J. B., 1993, Thermobarometric constraints on the depth of exposure and conditions of plutonism and metamorphism at deep levels of the Sierra Nevada batholith, Tehachapi Mountains, California: Journal of Geophysical Research, v. 98, p. 609-629.
- Plescia, J. B., and Calderone, G. J., 1986, Paleomagnetic constraints on the timing and extent of rotation of the Tehachapi Mountains, California: Geological Society of America Abstracts with Programs, v. 18, p. 171.
- Plescia, J. B., Calderone, G. J., and Snee, L. W., 1994, Paleomagnetic analysis of Miocene basalt flows in the Tehachapi Mountains, California: U. S. Geological Survey Bulletin 2100, 11 p.
- Postlethwaite, C. E., and Jacobson, C. E., 1987, Early history and reactivation of the Rand thrust, southern California: Journal of Structural Geology, v. 9, p. 195-205.
- Powell, R. E., 1993, Balanced palinspastic reconstruction of pre-late Cenozoic paleogeology, southern California: Geologic and kinematic constraints on the evolution of the San Andreas fault system, *in* Powell, R. E., Weldon, R. J., II, and Matti, J. C., eds., The San Andreas Fault System: Displacement, Palinspastic Reconstruction, and Geologic Evolution: Geological Society of America Memoir 178, p. 1-106.
- Powell, R. E., and Weldon, R. J., II, 1992, Evolution of the San Andreas fault: Annual Reviews of Earth and Planetary Science, v. 20, p. 431-468.
- Quinn, J. P., 1987, Stratigraphy of the Middle Miocene Bopesta Formation, Southern Sierra Nevada, California, Contributions in Science, Number 393: Los Angeles, California, Natural History Museum of Los Angeles County, 31 p.
- Ramsay, J. G., 1967, Folding and Fracturing of Rocks: New York, McGraw-Hill, 568 p.
- Ramsay, J. G., 1980, Shear zone geometry: A review: Journal of Structural Geology, v. 2, p. 83-99.
- Ramsay, J. G., and Graham, R. H., 1970, Strain variation in shear belts: Canadian Journal of Earth Sciences, v. 7, p. 786-813.
- Rindosh, M. C., 1977, Geology of the Tylerhorse canyon pendant, southern Tehachapi mountains, Kern County, California [Masters thesis]: Los Angeles, California, University of Southern California, 80 p.
- Ross, D. C., 1977, Pre-intrusive metasedimentary rocks of the Salinian block, California—a paleotectonic dilemma, *in* Stewart, J. H., Stevens, C. H., and Fritsche, A. E., eds., Paleozoic Paleogeography of the Western United States: Pacific Coast Paleogeography Symposium 1: Los Angeles, California, Pacific Section, Society of Economic Paleontologists and Mineralogists, p. 371-380.
- Ross, D. C., 1978, The Salinian block—a Mesozoic granitic orphan in the California Coast ranges, *in* Howell, D. G., and McDougall, K. A., eds., Mesozoic Paleogeography of the Western United States: Pacific Coast Paleogeography Symposium 2: Los

- Angeles, California, Pacific Section, Society of Economic Paleontologists and Mineralogists, p. 509-522.
- Ross, D. C., 1984, Possible correlations of basement rocks across the San Andreas, San Gregorio-Hosgri, and Rinconada-Reliz-King City faults, California: U. S. Geological Survey Professional Paper 1317, 37 p.
- Ross, D. C., 1985, Mafic gneissic complex (batholithic root?) in the southernmost Sierra Nevada, California: *Geology*, v. 13, p. 288-291.
- Ross, D. C., 1987, Metamorphic framework rocks of the southern Sierra Nevada, California: U. S. Geological Survey Open-File Report 87-81, 74 p.
- Ross, D. C., 1989a, Magnetic susceptibilities of modally analyzed granitic rocks from the southern Sierra Nevada, California: U. S. Geological Survey Open-File Report 89-204, 53 p.
- Ross, D. C., 1989b, The metamorphic and plutonic rocks of the southernmost Sierra Nevada, California, and their tectonic framework: U. S. Geological Survey Professional Paper 1381, 159 p.
- Ross, D. C., 1990, Reconnaissance geologic map of the southern Sierra Nevada, Kern, Tulare, and Inyo counties, California: U. S. Geological Survey Open-File Report 90-337, 163 p.
- Saleeby, J., and Sharp, W., 1980, Chronology of the structural and petrologic development of the southwest Sierra Nevada foothills, California: *Geological Society of America Bulletin*, Part II, v. 91, p. 1416-1535.
- Saleeby, J. B., 1990a, Geochronological and tectonostratigraphic framework of Sierran-Klamath ophiolitic assemblages, *in* Harwood, D. S., and Miller, M. M., eds., *Paleozoic and Early Mesozoic Paleogeographic Relations: Sierra Nevada, Klamath Mountains, and Related Terranes*: Geological Society of America Special Paper 255, p. 93-114.
- Saleeby, J. B., 1990b, Progress in tectonic and petrogenetic studies in an exposed cross-section of young (~100 Ma) continental crust, southern Sierra Nevada, California, *in* Salisbury, M. H., and Fountain, D. M., eds., *Exposed Cross-Sections of the Continental Crust*: Dordrecht, Holland, D. Reidel Publishing Co., p. 137-158.
- Saleeby, J. B., 1992, Structure of the northern segment of the proto-Kern canyon fault zone (PKCFZ), southern Sierra Nevada: *Geological Society of America Abstracts with Programs*, v. 24, p. 80.
- Saleeby, J. B., and Busby, C., 1993, Paleogeographic and tectonic setting of axial and western metamorphic framework rocks of the southern Sierra Nevada, California, *in* Dunne, G., and McDougall, K., eds., *Mesozoic Paleogeography of the Western United States-II: Los Angeles, California, Pacific Section, Society of Economic Paleontologists and Mineralogists*, p. 197-226.
- Saleeby, J. B., and Busby-Spera, C., 1992, Early Mesozoic tectonic evolution of the western U. S. Cordillera, *in* Burchfiel, B. C., Lipman, P. W., and Zoback, M. L., eds., *The Cordilleran Orogen: Conterminous U. S.: The Geology of North America*: Boulder, Colorado, Geological Society of America, p. 107-168.
- Saleeby, J. B., and Busby-Spera, C. J., 1986, Fieldtrip guide to the metamorphic framework rocks of the Lake Isabella area, southern Sierra Nevada, California, *in* Dunne, G. C., ed., *Mesozoic and Cenozoic Structural Evolution of Selected Areas, East-Central California*: Geological Society of America, Cordilleran Section Fieldtrip Guidebook: Los Angeles, California, California State University, p. 81-94.
- Saleeby, J. B., Goodin, S. E., Sharp, W. D., and Busby, C. J., 1978, Early Mesozoic paleotectonic-paleogeographic reconstruction of the southern Sierra Nevada region, *in* Howell, D. E., and McDougall, K. A., eds., *Mesozoic Paleogeography of the Western United States: Pacific Coast Paleogeography Symposium 2*: Los Angeles,

- California, Pacific Section, Society of Economic Paleontologists and Mineralogists, p. 311-336.
- Saleeby, J. B., Kistler, R. W., Longiaru, S., Moore, J. G., and Nokleberg, W. J., 1990, Middle Cretaceous silicic metavolcanic rocks in the Kings Canyon area, central Sierra Nevada, California, *in* Anderson, J. L., ed., *The nature and origin of Cordilleran magmatism: Geological Society of America Memoir 174*, p. 251-270.
- Saleeby, J. B., Sams, D. B., and Kistler, R. W., 1987, U/Pb zircon, strontium, and oxygen isotopic and geochronological study of the southernmost Sierra Nevada batholith, California: *Journal of Geophysical Research*, v. 92, p. 10,443-10,466.
- Saleeby, J. B., Silver, L. T., Wood, D. J., and Malin, P. E., 1993, Late Cretaceous tectonics of the southern Sierra Nevada batholith (SNB) viewed from the Tehachapi mountains (TM), California: *Geological Society of America Abstracts with Programs*, v. 25, p. 141.
- Saleeby, J. B., Speed, R. C., and Blake, M. C., 1994, Tectonic evolution of the central U. S. cordillera: a synthesis of the C1 and C2 continent-ocean transects, *in* Speed, R. C., ed., *Phanerozoic Evolution of North American Continent-Ocean Transitions: DNAG Continent-Ocean Transect Volume: Boulder, Colorado, Geological Society of America*, p. 315-356.
- Sams, D. B., 1986, U/Pb zircon geochronology, petrology, and structural geology of the crystalline rocks of the southern Sierra Nevada and Tehachapi mountains, Kern County, California: Pasadena [Ph.D. thesis]: Pasadena, California, California Institute of Technology, 315 p.
- Sams, D. B., and Saleeby, J. B., 1988, Geology and petro-tectonic significance of crystalline rocks of the southernmost Sierra Nevada, California, *in* Ernst, W. G., ed., *Metamorphism and Crustal Evolution of the Western United States [Rubey Volume VII]: Englewood Cliffs, New Jersey, Prentice-Hall, Inc.*, p. 865-893.
- Samsel, H. S., 1962, Geology of the southeast quarter of the Cross Mountain quadrangle, Kern County, California: California Division of Mines and Geology Map Sheet 2, scale 1:48,000.
- Sanderson, D. J., and Marchini, W. R. D., 1984, Transpression: *Journal of Structural Geology*, v. 6, p. 449-458.
- Schweickert, R. A., and Lahren, M. M., 1990, Speculative reconstruction of the Mojave-Snow Lake fault: Implications for Paleozoic and Mesozoic orogenesis in the western United States: *Tectonics*, v. 9, p. 1609-1629.
- Segall, P., McKee, E. H., Martel, S. J., and Turrin, B. D., 1990, Late Cretaceous age of fractures in the Sierra Nevada batholith, California: *Geology*, v. 18, p. 1248-1251.
- Segall, P., and Pollard, D. D., 1983, Nucleation and growth of strike-slip faults in granite: *Journal of Geophysical Research*, v. 88, p. 555-568.
- Seiders, V. M., Joyce, J. M., Leverett, K. A., and McLean, H., 1983, Geologic map of part of the Ventana Wilderness and the Black Butte, Bear Mountain, and Bear Canyon roadless areas, Monterey County, California: U. S. Geological Survey Miscellaneous Field Studies Map MF-1559-B, scale 1:50,000.
- Sharry, J., 1981, The geology of the western Tehachapi Mountains, California [Ph.D. thesis]: Boston, Massachusetts, Massachusetts Institute of Technology, 215 p.
- Sharry, J., 1982, Minimum age and westward continuation of the Garlock fault zone, Tehachapi Mountains, California: *Geological Society of America Abstracts with Programs*, v. 14, p. 233.
- Silver, L. T., 1982, Evidence and a model for west-directed early to mid-Cenozoic basement overthrusting in southern California: *Geological Society of America Abstracts with Programs*, v. 14, p. 234.

- Silver, L. T., 1983, Paleogene overthrusting in the tectonic evolution of the Transverse Ranges, Mojave and Salinian regions, California: Geological Society of America Abstracts with Programs, v. 15, p. 438.
- Silver, L. T., 1986, Evidence for Paleogene low-angle detachment of the southern Sierra Nevada: Geological Society of America Abstracts with Programs, v. 18, p. 750.
- Silver, L. T., 1993, Observations on the extended tectonic history of the southern Sierra Nevada: Geological Society of America Abstracts with Programs, v. 25, p. 147.
- Silver, L. T., and Anderson, T. H., 1974, Possible left-lateral early to middle Mesozoic disruption of the southwestern North American craton margin: Geological Society of America Abstracts with Programs, v. 6, p. 955-956.
- Silver, L. T., and Anderson, T. H., 1983, Further evidence and analysis of the role of the Mojave-Sonora megashear(s) in Mesozoic Cordilleran tectonics: Geological Society of America Abstracts with Programs, v. 15, p. 273.
- Silver, L. T., and Hill, R. T., 1986, U-Th-Pb microdiscordance in young zircons; a case study in the San Jacinto Mountains, California: EOS (American Geophysical Union Transactions), v. 67, p. 339-340.
- Silver, L. T., and Mattinson, J. M., 1986, "Orphan Salinia" has a home: EOS (American Geophysical Union Transactions), v. 67, p. 1215.
- Silver, L. T., and Nourse, J. A., 1986, The Rand Mountains thrust complex in comparison with the Vincent thrust-Pelona schist relationship, southern California: Geological Society of America Abstracts with Programs, v. 18, p. 185.
- Silver, L. T., and Nourse, J. A., 1991, Timing of the Rand thrust and its implication for late Cretaceous tectonics in southern California: Geological Society of America Abstracts with Programs, v. 23, p. A480.
- Silver, L. T., Sams, D. B., Bursik, M. I., Graymer, R. W., Nourse, J. A., Richards, M. A., and Salyards, S. L., 1984, Some observations of the tectonic history of the Rand Mountains, Mojave Desert, California: Geological Society of America Abstracts with Programs, v. 16, p. 333.
- Silver, L. T., Taylor, H. P., Jr., and Chappell, B., 1979, Some petrological, geochemical and geochronological observations of the Peninsular Ranges batholith near the international border of the U.S.A. and Mexico, *in* Abbott, P. L., and Todd, V. R., eds., Mesozoic Crystalline Rocks: Peninsular Ranges Batholith and Pegmatites Point Sal Ophiolite: Geological Society of America Guidebook: San Diego, CA, San Diego State University, p. 83-110.
- Simpson, C., 1985, Deformation of granitic rocks across the brittle-ductile transition: Journal of Structural Geology, v. 7, p. 503-511.
- Simpson, C., 1986, Determination of movement sense in mylonites: Journal of Geological Education, v. 34, p. 246-261.
- Simpson, C., and Schmid, S. M., 1983, An evaluation of criteria to deduce the sense of movement in sheared rocks: Geological Society of America Bulletin, v. 94, p. 1281-1288.
- Simpson, E. C., 1934, Geology and mineral deposits of the Elizabeth Lake quadrangle, California: California Journal of Mines and Geology, v. 30, p. 371-415.
- Smith, A. R., compiler, 1964, Bakersfield sheet of the geologic map of California: Sacramento, California, California Division of Mines and Geology, scale 1:250,000.
- Smith, G. I., 1951, The geology of the Cache Creek region, Kern County, California [Masters thesis]: Pasadena, California, California Institute of Technology, 72 p.
- Smith, G. I., 1962, Large lateral displacement on Garlock fault, California, as measured from offset dike swarm: American Association of Petroleum Geologists Bulletin, v. 46, p. 85-104.

- Snow, J. K., 1992, Large-magnitude Permian shortening and continental-margin tectonics in the southern Cordillera: *Geological Society of America Bulletin*, v. 104, p. 80-105.
- Squires, R. L., Cox, B. F., and Powell, C. L., 1988, Late Paleocene or Early Eocene mollusks from the uppermost part of the Goler Formation, California, *in* Filewicz, M. V., and Squires, R. L., eds., *Paleogene Stratigraphy, West Coast of North America: West Coast Paleogene Symposium: Los Angeles, California, Pacific Section, Society of Economic Paleontologists and Mineralogists*, p. 183-187.
- Stern, T. W., Bateman, P. C., Morgan, B. A., Newell, M. F., and Peck, D. F., 1981, Isotopic U-Pb ages of zircon from the granitoids of the central Sierra Nevada, California: *U. S. Geological Survey Professional Paper 1185*, 17 p.
- Stevens, C. H., Stone, P., and Kistler, R. W., 1992, A speculative reconstruction of the middle Paleozoic continental margin of southwestern North America: *Tectonics*, v. 11, p. 405-419.
- Stewart, J. H., and Poole, F. G., 1975, Extension of the Cordilleran miogeosynclinal belt to the San Andreas fault, southern California: *Geological Society of America Bulletin*, v. 86, p. 205-212.
- Streckeisen, A. L., 1973, Plutonic rocks: Classification and nomenclature recommended by the IUGS subcommission on the systematics of igneous rocks: *Geotimes*, p. 26-30.
- Suppe, J., 1970, Offset of late Mesozoic basement terrains by the San Andreas fault system: *Geological Society of America Bulletin*, v. 81, p. 3253-3258.
- Suppe, J., 1985, *Principles of structural geology*: Englewood Cliffs, New Jersey, Prentice-Hall, Inc., 537 p.
- Sylvester, A. G., 1969, A microfabric study of calcite, dolomite, and quartz around Papoose Flat Pluton, California: *Geological Society of America Bulletin*, v. 80, p. 1311-1328.
- Sylvester, A. G., 1988, Strike-slip faults: *Geological Society of America Bulletin*, v. 100, p. 1666-1703.
- Sylvester, A. G., Oertel, G., Nelson, C. A., and Christie, J. M., 1978, Papoose Flat pluton: A granitic blister in the Inyo Mountains, California: *Geological Society of America Bulletin*, v. 89, p. 1205-1219.
- Tennyson, M. E., 1989, Pre-transform early Miocene extension in western California: *Geology*, v. 17, p. 792-796.
- Tikoff, B., and Teyssier, C., 1992, Crustal-scale, en echelon "P-shear" tensional bridges: A possible solution to the batholithic room problem: *Geology*, v. 20, p. 927-930.
- Tobisch, O. T., and Fiske, R. S., 1976, Significance of conjugate folds and crenulations in the central Sierra Nevada, California: *Geological Society of America Bulletin*, v. 87, p. 1411-1420.
- Tobisch, O. T., and Fiske, R. S., 1982, Repeated parallel deformation in part of the eastern Sierra Nevada, California and its implications for dating structural events: *Journal of Structural Geology*, v. 4, p. 177-195.
- Tobisch, O. T., Paterson, S. R., Longiaru, S., and Bhattacharyya, T., 1987, Extent of the Nevadan orogeny, central Sierra Nevada, California: *Geology*, v. 15, p. 132-135.
- Tobisch, O. T., Paterson, S. R., Saleeby, J. B., and Geary, E. E., 1989, Nature and timing of deformation in the Foothills terrane, central Sierra Nevada, California: Its bearing on orogenesis: *Geological Society of America Bulletin*, v. 101, p. 401-413.
- Tobisch, O. T., Saleeby, J. B., and Fiske, R. S., 1986, Structural history of continental volcanic arc rocks, eastern Sierra Nevada, California: A case for extensional tectonics: *Tectonics*, v. 5, p. 65-94.
- Tobisch, O. T., Saleeby, J. B., Renne, P. R., McNulty, B., and Tong, W., 1995, Variations in deformation fields during development of a large-volume magmatic

- arc, central Sierra Nevada, California: *Geological Society of America Bulletin*, v. 107, p. 148-166.
- Todd, V. R., Erskine, B. G., and Morton, D. M., 1988, Metamorphic and tectonic evolution of the northern Peninsular ranges batholith, southern California, *in* Ernst, W. G., ed., *Metamorphism and Crustal Evolution of the Western United States [Rubey Volume VII]*: Englewood Cliffs, New Jersey, Prentice-Hall, Inc., p. 895-937.
- Troxel, B. W., and Morton, P. K., 1962, Mines and mineral resources of Kern County California: California Division of Mines and Geology County Report 1, 370 p.
- Trumpy, R., 1960, Paleotectonic evolution of the central and western Alps: *Geological Society of America Bulletin*, v. 71, p. 843-908.
- Tucker, W. B., 1929, Kern County: California Division of Mines and Mining Report of the State Mineralogist, v. 25, p. 20-73.
- Tullis, J., and Yund, R. A., 1977, Experimental deformation of dry Westerly granite: *Journal of Geophysical Research*, v. 82, p. 5705-5718.
- Walker, J. D., 1988, Permian and Triassic rocks of the Mojave Desert and their implications for timing and mechanisms of continental truncation: *Tectonics*, v. 7, p. 685-709.
- Walker, J. D., Bartley, J. M., and Glazner, A., 1990, Large-magnitude Miocene extension in the central Mojave Desert: Implications for Paleozoic to Tertiary paleogeography and tectonics: *Journal of Geophysical Research*, v. 95, p. 557-569.
- Walker, J. D., Fletcher, J. M., Fillmore, R. P., Martin, M. W., Taylor, W. J., Glazner, A. F., and Bartley, J. M., 1995, Connection between igneous activity and extension in the central Mojave metamorphic core complex, California: *Journal of Geophysical Research*, v. 100, p. 10,477-10,494.
- Wernicke, B., 1992, Cenozoic extensional tectonics of the U.S. Cordillera, *in* Burchfiel, B. C., Lipman, P. W., and Zoback, M. L., eds., *The Cordilleran Orogen: Conterminous U. S.*: Boulder, Colorado, Geological Society of America, p. 553-581.
- Wernicke, B., and Axen, G. A., 1988, On the role of isostasy in the evolution of normal fault systems: *Geology*, v. 16, p. 848-851.
- Wheeler, J., and Butler, R. W. H., 1994, Criteria for identifying structures related to true crustal extension in orogens: *Journal of Structural Geology*, v. 16, p. 1023-1027.
- Whidden, K. J., Lund, S. P., Bottjer, D. J., Champion, D., and Howell, D., 1991, Paleomagnetic evidence from upper Cretaceous strata for autochthoneity of the central block of Salinia: *Geological Society of America Abstracts with Programs*, v. 23, p. 109.
- White, L. A., and Davis, T. L., 1989, Temporal correspondence between the onset of Ynezan-age uplift and crustal shortening, California, and the change in motion of the Farallon plate approximately 40 Ma: *Geological Society of America Abstracts with Programs*, v. 21, p. 159.
- White, S. H., Bretan, P. G., and Rutter, E. H., 1986, Fault-zone reactivation: kinematics and mechanisms: *Philosophical Transactions of the Royal Society of London*, v. 317, p. 81-97.
- Wiebe, R. A., 1970a, Pre-Cenozoic tectonic history of the Salinian block, western California: *Geological Society of America Bulletin*, v. 81, p. 1837-1842.
- Wiebe, R. A., 1970b, Relations of granitic and gabbroic rocks, northern Santa Lucia range, California: *Geological Society of America Bulletin*, v. 81, p. 105-116.
- Wiese, J. H., 1950, Geology and mineral resources of the Neenach quadrangle, California: California Division of Mines Bulletin 153, 53 p.

- Wintsch, R. P., Christoffersen, R., and Kronenberg, A. K., 1995, Fluid-rock reaction weakening of fault zones: *Journal of Geophysical Research*, v. 100, p. 13,021-13,032.
- Wise, D. U., Dunn, D. E., Engelder, J. T., Geiser, P. A., Hatcher, R. D., Kish, S. A., Odom, A. L., and Schamel, S., 1984, Fault-related rocks: suggestions for terminology: *Geology*, v. 12, p. 391-394.
- Wolf, M. B., and Saleeby, J. B., 1991, Tectonics of Late Jurassic dike emplacement in the Sierra Nevada region: *Geological Society of America Abstracts with Programs*, v. 23, p. A248.
- Wood, D. J., Saleeby, J. B., and Silver, L. T., 1993, Structure and tectonic setting of the eastern Tehachapi range, California: *Geological Society of America Abstracts with Programs*, v. 25, p. 165.
- Zoback, M. D., Zoback, M. L., Mount, V. S., Suppe, J., Eaton, J. P., Healy, J. H., Oppenheimer, D., Reasenber, P., Jones, L., Raleigh, C. B., Wong, I. G., Scotti, O., and Wentworth, C., 1987, New evidence on the state of stress of the San Andreas fault system: *Science*, v. 238, p. 1105-1111.